To the Graduate Council:

I am submitting here with a thesis written by David Jonathan Settles entitled "Defining the Hayesville–Soque River and Allatoona faults and an Ordovician arc assemblage within the central Blue Ridge northwest of Dahlonega, Georgia." I have examined the final electronic copy of this thesis for form and content and recommend that it be accepted in partialful fillment of the requirements for the degree of Master of Science, with a major in Geology.

Robert D. Hatcher, Jr.,
Major Professor

We have read this thesis and
recommend its acceptance:

William M. Dunne

Theodore C. Labotka

Accepted for the Council:

Dr. Anne Mayhew
Vice Provost and Dean of Graduate Studies

(Original signatures are on file in the Graduate Student Services Office.)

Defining the Hayesville–Soque River and Allatoona faults and an Ordovician arc assemblage within the central Blue Ridge northwest of Dahlonega, Georgia

A Thesis
Presented for the
Master of Science
Degree
The University of Tennessee, Knoxville

David J. Settles
May, 2002

This thesis is dedicated to my parents,
Bill and Gail Settles,
for their unending support and encouragement.
THANK YOU

ACKNOWLEDGMENTS

First and foremost I'd like to give a special thanks to my advisor, Professor Robert D. Hatcher, Jr., both for providing unrivaled facilities at the University of Tennessee for the continued advancement of field-oriented geology and for his individual guidance and patience. Bob has provided both personal and professional support, in the field, office and at professional meetings, allowing for substantial advancement in my personal abilities to recognize and solve complex geologic problems. Numerous faculty members at the University of Tennessee deserve my up most gratitude including committee members, Drs. Bill Dunne and Ted Labotka, for their reviews, assistance, and guidance; Marvin Bennett for assisting with teaching duties and his help under the microscope; and Hap McSween for taking time to provide an informal review. I would also like to thank John Costello and Ken Gillon for their willingness to visit the field, listen to ideas, and provide encouragement and constructive criticism. A special thanks to Dr. Randy Kath at the State University of West Georgia for sparking my interest in both field geology and structure as an undergraduate, his continued support throughout my graduate career, and his continued assistance and advice in the advancement of my professional career.

I would also like to thank all past and present student members of the Tectonics and Structural Geology Research Group at Tennessee for continued positive criticism and motivation with a touch of humor. Scott Giorgis for taking time to get me up-to-speed upon arriving at Tennessee; Chris and Jen Whisner for providing a haven for distraction in their home; Camilo Montes for both his positive outlook and his assistance with all things Mac and Adobe; and the new crew of Arthur, Jay, and Milan for their constant reminder to finish. I would also like to give a special thanks to office mate and coauthor Brendan Bream for agreeing assist in my endeavors outside the scope of his personal research, providing a roof over my head, and for providing a positive outlook when thesis completion seemed out of reach. And last but not least, Nancy “Damama” Meadows for providing the glue that keeps the Hatchery afloat and making me feel at home.

To my friends and family I owe continued gratitude for unyielding support and encouragement. A special thanks to my closest friend and father, Bill Settles, for helping me keep work and life in perspective and guide me through the difficult times. For someone who knows little of geology, his advice played a crucial role in keeping me motivated. I’d like to equally thank my mother, Gail Settles, who has continued to provide love, strength, and support. I would also like to give a special thanks to my partners in crime, Dave Riestenberg, Mark Pollock, and Steve Tavernier for the constant reminder “Simple Life = Simple Pleasures” and for memories that I will never forget, GO BIG ORANGE.

Funding for my research at Tennessee was provided by the EDMAP component of the National Cooperative Geologic Mapping Program administered by the U. S. Geological Survey. Support was also provided by the University of Tennessee Science Alliance Center for Excellence.

ABSTRACT

The goal of this research within the central Blue Ridge northwest of Dahlonega, Georgia, is to provide new information toward better understanding of the Allatoona(?)/ Hayesville/Gossan Lead fault and terrane boundary, and to provide convincing evidence of Ordovician arc-related igneous activity. The Hayesville-Soque River and Allatoona faults separate three distinct tectonostratigraphic assemblages in this area: the Coweeta Group, Great Smoky Group, and Dahlonega gold belt. The gold belt here contains metasandstone, pelitic schist, and mafic rocks of the Otto Formation and the Sally Free mafic complex, while the Great Smoky Group contains metasandstone and pelitic schist with abundant calc-silicate. The abundance of calc-silicate and apparent lack of mafic rocks in the Great Smoky Group versus the apparent lack of calc-silicate and presence of abundant mafic rocks in the gold belt support the delineation of the Allatoona fault. Inequigranular, biotite-dominant (over trace muscovite), often migmatitic gneiss and schist of the Coweeta Group, Coleman River Formation, versus two-mica, nonmigmatitic, often equigranular metasandstone and schist of the Great Smoky Group and Otto Formation constitute the principal criteria for the delineation of the Hayesville and Soque River faults. Delineation of the Hayesville and Soque River faults here confirms that they are equivalent, and that the area northwest of Dahlonega marks the southwestern terminus of the Hayesville-Soque River thrust sheet.

Fault geometries observed within the study area indicate that a pre- to synmetamorphic ancestral Allatoona fault exists, which was later truncated by the pre- to synmetamorphic Hayesville-Soque River fault approximately 10 km west of Dahlonega. Thus, the postmetamorphic Allatoona fault observed to the southwest of Dahlonega possibly represents reactivation along the ancestral Allatoona fault mapped here. This observation indicates that the Hayesville and Allatoona faults do not represent a continuous Blue Ridge terrane boundary, as previously hypothesized.

The fault-emplaced Sally Free mafic complex (Etowah River fault) within the Dahlonega gold belt contains amphibolite, metagabbro, hornblende gneiss, Cane Creek felsic gneiss, and locally abundant migmatitic intermediate gneiss. Geochemical analyses and comparison of mafic and felsic samples from the Sally Free mafic complex, mafic samples from within the Otto Formation, and a $^{206}Pb/^{238}U$ age of 482 ± 7 Ma for the Cane Creek felsic gneiss reveal a complex Early Ordovician volcanic arc assemblage of gabbro/diorite cumulates (hornblende gneiss), tholeiitic arc basalt/andesite (amphibolite), and arc felsite/rhyodacite (felsic gneiss). The interlayered relationship of the amphibolite (arc basalt) and metasedimentary rocks of the Otto Formation indicative extrusive basalt flows, shallow sills, or mafic tuff emplacement coeval with Otto Formation deposition related to a syndepositional Early Ordovician volcanic arc and/or back-arc basin. The interpreted Early Ordovician age for both igneous activity and sediment deposition for the Dahlonega gold belt implies that faulting (Hayesville-Soque River and Allatoona), metamorphism, and deformation within this portion of the southern Appalachian Blue Ridge is related to the Acadian rather than the Taconic orogeny.

CONTENTS

LIST OF FIGURES

PART I

PART II

LIST OF TABLES

PART I

PART II

LIST OF PLATES

OVERVIEW

This thesis summarizes the results of research conducted during the past three years within portions of the Nimblewill, Campbell Mountain, and Dahlonega quadrangles northwest of Dahlonega, Georgia (Plate 1). The study area was originally chosen to resolve unanswered tectonic questions within the central Blue Ridge, specifically the relationship between the Allatoona, Hayesville, and Soque River faults. Detailed geologic mapping (1:12,000 compiled at 1:24,000 scale) provided new information concerning the Allatoona and Hayesville-Soque River faults and also led to the delineation of a large suite of metaigneous rocks, including the Sally Free mafic complex (defined here) and associated mafic rocks within the Dahlonega gold belt, Otto Formation (Plate 1).

This work is divided into two parts with appendices. Each part is intended to be a future publication that contains individual abstracts, figures, conclusions, and references. Part I consists of a petrographic, geochemical, and geochronological investigation of metaigneous occurrences within the Campbell Mountain quadrangle including the Sally Free mafic complex and associated mafic rocks of the Dahlonega gold belt (Plate 1). That part provides new information concerning the pre-orogenic tectonic setting and subsequent evolution for this portion of the Dahlonega gold belt. Brendan Bream at the University of Tennessee performed U-Pb sensitive high resolution ion microprobe zircon age dating of the Cane Creek felsic gneiss as well as assisted in organization and interpretation of geochemical data for this study.

Part II concentrates on the structural and stratigraphic relationships defining the Hayesville-Soque River and Allatoona faults northwest of Dahlonega (Plate 1), including a detailed examination of stratigraphic units, metamorphism, deformation, and relative timing of faulting. This part provides new information concerning the hypothesized Allatoona/Hayesville/Gossan Lead fault and terrane boundary, and the tectonic evolution of this area.

Plate 1 presents the new detailed geologic map and cross sections (1:24,000 scale) for portions of the Nimblewill, Campbell Mountain, and Dahlonega, Georgia, quadrangles. Plate 2 depicts mapped stations, sample localities, and domains used to rationalize structural analysis for this study. Plate 3 is a 1:250,000 scale geologic map of a portion of the southern Appalachian Blue Ridge in northeastern Georgia, northwestern South Carolina, and southwestern North Carolina used to create tectonic figures and interpret regional structure. Plate 4 is a summary of the methodology used in this study to construct a detailed geologic map with the use of Adobe® Illustrator and Photoshop software.

Appendix A is a summary of the methodology used in this study to sort station numbers into structural domains (Plate 2) for domain analysis with the use of Adobe® Illustrator and Microsoft® Excel software. Appendix B contains structural and stratigraphic information obtained from within the study area corresponding to the station map (Plate 2).

PART I

The Sally Free mafic complex and associated mafic rocks of the Dahlonega gold belt: Evidence of Ordovician arc volcanism and intrusion northwest of Dahlonega, Georgia

ABSTRACT

Recent detailed geologic investigation within the central Blue Ridge northwest of Dahlonega, Georgia, provides convincing evidence of Ordovician, arc-related igneous activity. The Dahlonega area contains three distinct stratigraphic assemblages: the Dahlonega gold belt, Coweeta Group, and the Great Smoky Group, bounded by three crustal-scale faults (Hayesville-Soque River, Chattahoochee, and Allatoona faults). Mafic to felsic metaigneous rocks occur within rocks of the Dahlonega gold belt, which includes mixed mafic rocks within metasedimentary rocks of the Otto Formation and mafic to felsic rocks within the Sally Free mafic complex. The fault-emplaced Sally Free mafic complex (Etowah River fault) contains amphibolite, metagabbro, hornblende gneiss, Cane Creek felsic gneiss, and locally abundant, migmatitic, intermediate gneiss. Geochemical analyses of mafic and felsic samples from the Sally Free mafic complex and mafic samples from within the Otto Formation reveal a complex assemblage of gabbro/diorite cumulates (hornblende gneiss), tholeiitic arc basalt/andesite (amphibolite), and arc felsite/rhyodacite (felsic gneiss). The age of the Sally Free mafic complex is Early Ordovician delimited by the $^{206}Pb/^{238}U$ age of 482 ± 7 Ma for the Cane Creek felsic gneiss. Chemical similarities between amphibolite within the mafic complex and amphibolite from within the Otto Formation indicate probable synchronous igneous activity within the Dahlonega gold belt. The interlayered relationship of the amphibolite (arc basalt) and metasedimentary rocks of the Otto Formation is indicative of extrusive basalt flows, shallow sills, or mafic tuff emplacement coeval with Otto Formation deposition (Early Ordovician). Observed stratigraphic relationships within the Dahlonega gold belt here, combined with chemical characterization of mafic and felsic rocks within the Sally Free mafic complex and mafic rocks within the Otto Formation have provided new information concerning the tectonic evolution of a syndepositional volcanic arc within the north Georgia central Blue Ridge.

INTRODUCTION

The Sally Free mafic complex, located northwest of Dahlonega, Georgia, is one of two large mafic complexes in the southern Appalachian Dahlonega gold belt and one of several large mafic-ultramafic complexes in the central/eastern Blue Ridge of northern Georgia and western North Carolina (Fig. 1). The Sally Free complex, defined here, contains amphibolite, metagabbro, hornblende gneiss, the Cane Creek felsic gniess, and locally migmatitic intermediate gneiss (Fig. 2). Mafic and felsic metaigneous rocks are common throughout the Dahlonega gold belt, both as large complexes and as interlayers within gold belt metasedimentary rocks. The area northwest of Dahlonega, within portions of the Nimblewill, Campbell Mountain, and Dahlonega, Georgia, 7.5-minute quadrangles, contains three distinct stratigraphic assemblages: the Dahlonega gold belt, Coweeta Group, and the Great Smoky Group, which are bounded by three crustal-scale faults (Hayesville-Soque River, Chattahoochee, and Allatoona faults; Fig. 1). The Dahlonega gold belt here contains mixed mafic rocks interlayered with metasandstone and schist of the Otto Formation and mafic to felsic rocks of the Sally Free complex. Although metaigneous rocks northwest of Dahlonega occur predominantly within the gold belt, amphibolite and hornblende gneiss also occur within biotite gneiss, metasandstone, and schist of the Coweeta Group, Coleman River Formation, in the Hayesville-Soque River thrust sheet, as large continuous bodies (Fig. 2), lenses, and mesoscale boudins. Petrographic and whole-rock chemical analyses of metaigneous rocks from the Hayesville-Soque River thrust sheet and Dahlonega gold belt (Sally Free mafic complex and Otto Formation), combined with a magmatic U-Pb sensitive high resolution ion microprobe (SHRIMP) zircon age of the Cane Creek felsic gneiss (Bream, unpublished data) provide new information concerning the tectonic setting and subsequent evolution of this part of the central Blue Ridge.

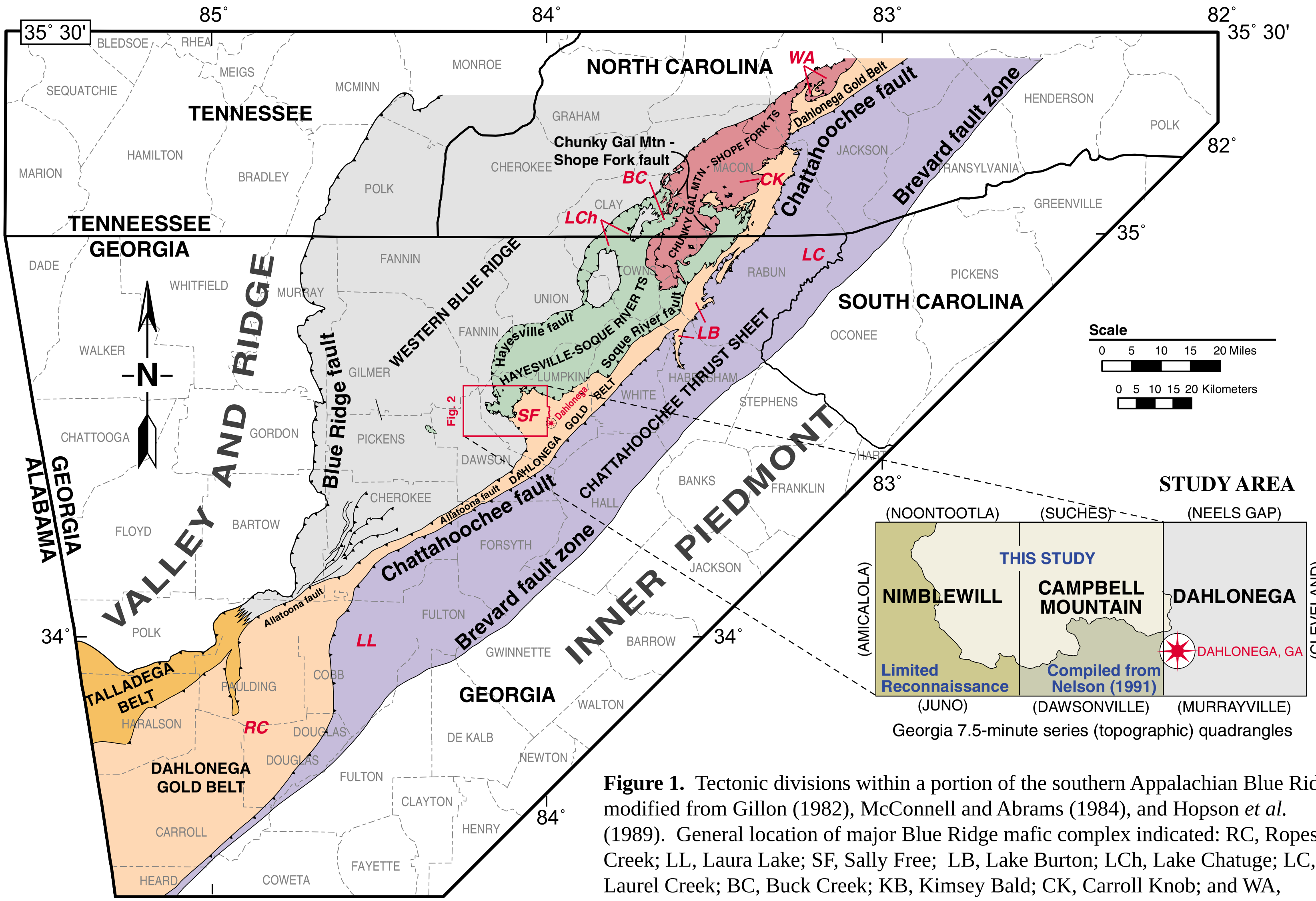

Figure 1. Tectonic divisions within a portion of the southern Appalachian Blue Ridge modified from Gillon (1982), McConnell and Abrams (1984), and Hopson *et al.* (1989). General location of major Blue Ridge mafic complex indicated: RC, Ropes Creek; LL, Laura Lake; SF, Sally Free; LB, Lake Burton; LCh, Lake Chatuge; LC, Laurel Creek; BC, Buck Creek; KB, Kimsey Bald; CK, Carroll Knob; and WA, Webster Addie. Study area reference figure and area shown in Figure 2 indicated.

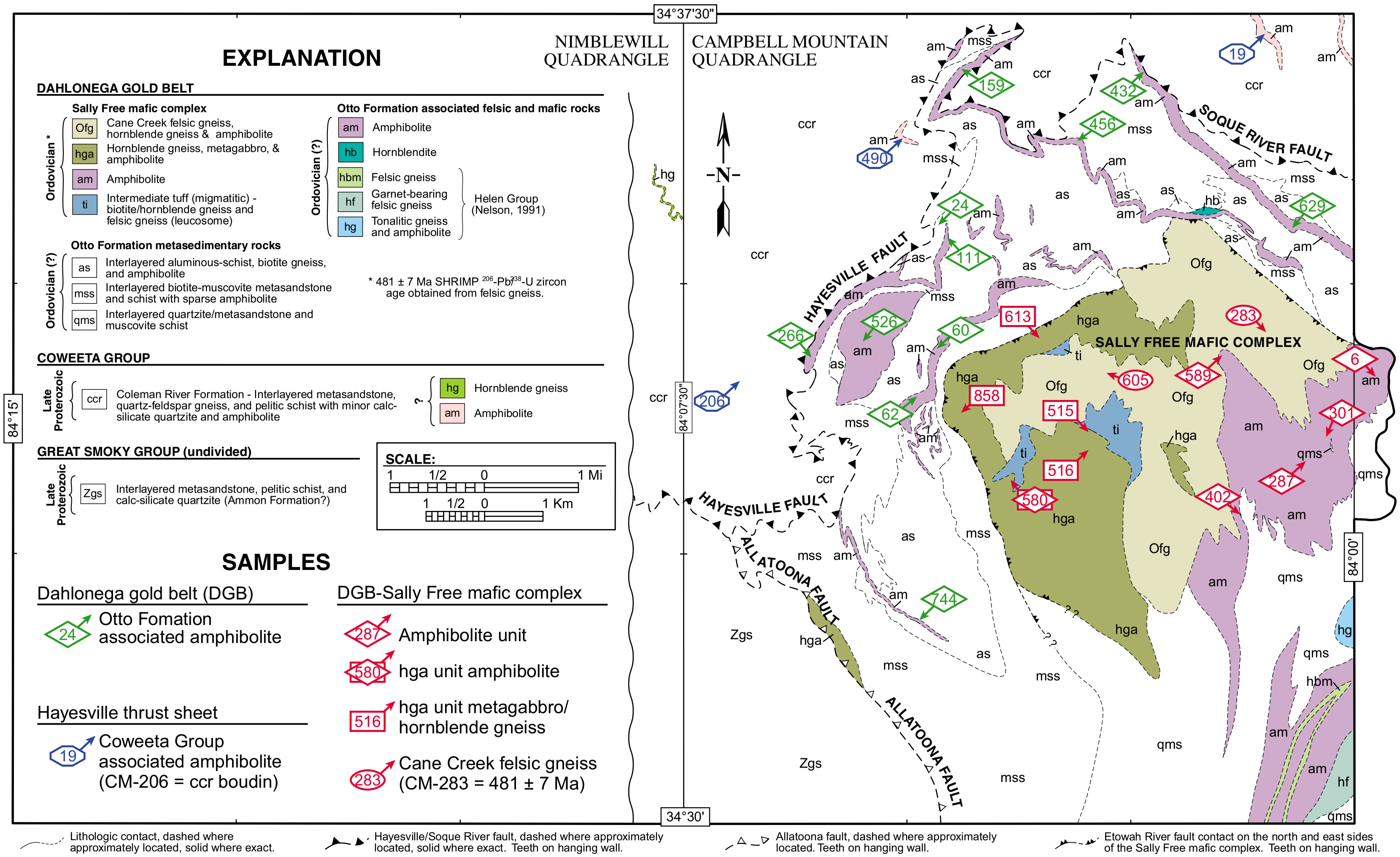

Figure 2. Detailed geologic map of portions of the Nimblewill, Campbell Mountain, and Dahlonega, Georgia, 7.5-minute quadrangles (Settles and Hatcher, *in preparation*) depicting sample localities of mafic and felsic metaigneous rocks (in color) selected for geochemical analysis. Geology within the southern portion of the Campbell Mountain quadrange was complied from Nelson (1991) and geology within the northern portion was mapped in detail for this study (1999 and 2000 field seasons). Regional location and geologic mapping reference indicated on Figure 1.

The term Dahlonega gold belt, originally used in reference to a belt of gold occurrences traceable from the Alabama-Georgia line to the Georgia-North Carolina line (e.g., Yeates *et al.*, 1896; Jones, 1909; German, 1985), is used here in reference to a unique stratigraphic assemblage traceable from Carroll County, Georgia, into southwestern North Carolina (Fig. 1). The gold belt outcrops as a fault-bounded, complex lithotectonic assemblage of highly deformed ortho- and paragneisses including metasandstone, schist, amphibolite, hornblende gneiss, and subordinate ultramafic rocks (Hopson *et al.*, 1989). Due to the presence of gold mineralization, interest in the Dahlonega gold belt can be traced back to the late 1800s when Mackintosh (1879) investigated gold deposits near the city of Dahlonega. Since Mackintosh (1879), there were numerous investigations into the gold-bearing districts throughout the southern Appalachians (e.g., Becker, 1894; Blake and Jackson, 1895; Brewer, 1895; Yeates *et al.*, 1896; Jones, 1909, Cook and Burnell, 1985; German, 1985).

In addition to the origin of gold mineralization, the Dahlonega gold belt has been the focus of numerous debates concerning its tectonic evolution and its role in the orogenic history of the southern Appalachians. Correct determination of protoliths and tectonic setting for crystalline rocks of the southern Appalachians, including the central Blue Ridge gold belt, is difficult due to alteration and pervasive deformation associated with the Taconian and Acadian orogenies. The igneous, often volcanic, nature of mafic and felsic rocks in the Dahlonega area and throughout the southern Appalachian gold belt is texturally and chemically evident. Locally occurring relict volcanic textures within amphibolite, such as pillows and amygdules, have been recognized in numerous areas within the north Georgia gold belt (Hurst and Jones, 1973; McConnell and Abrams, 1984; German, 1985; Higgins *et al.*, 1988; Spell and Norrell, 1990).

Chemical discrimination has also been used variably to indicate the tectonic setting for the Dahlonega gold belt. McConnell (1980) and McConnell and Abrams (1984) interpreted the rocks of the New Georgia Group (Dahlonega gold belt equivalent extending from the Bremen area northwest into the Canton, Georgia, area) to represent back-arc basin volcanic rocks that formed on attenuated (rifted) continental crust. Spell and Norrell (1990) identified the Ropes Creek assemblage (Dahlonega gold belt near New Georgia and Villa Rica, Georgia; Fig. 1) as a possible ophiolite remnant containing island-arc tholeiites to mid-ocean ridge basalts (northwest to southeast) and leucocratic volcanic arc granites. Spell and Norrell (1990) further concluded that the Ropes Creek assemblage initially formed in a back-arc basin over an eastward-dipping subduction zone and was later intruded by volcanic arc granites while being thrust over an associated arc. Burnell and Cook (1984) interpreted the sequence of rocks in the Dahlonega area to represent a back-arc basin environment where basaltic (abyssal tholeiite) volcanism was accompanied by felsic tuff deposition and seafloor hydrothermal activity. German (1989) also concluded that rocks of the Dahlonega gold belt were deposited in a back-arc basin environment in close proximity to a primitive arc system on the basis of the chemical affinity of metavolcanic rocks and the presence of abundant interlayered metasedimentary rocks (Fig. 3). Although numerous authors have noted evidence for the presence of an arc and a subsequent back-arc basin within the southern Appalachian central and eastern Blue Ridge (e.g., Burnell and Cook, 1984; McConnell and Abrams, 1984; German, 1989; Spell and Norrell, 1990), no large well-developed arc magmatic belt has been recognized. Thomas *et al.* (2001) interpreted that either the subduction-arc margin was discontinuous or that the resulting rock assemblage is hidden or removed.

Careful consideration of metaigneous rock composition, lithologic associations, and metamorphism in the study area provides new information concerning both the pre-orogenic tectonic environment and tectonic evolution of the north Georgia Dahlonega gold belt and the southern Appalachian central Blue Ridge.

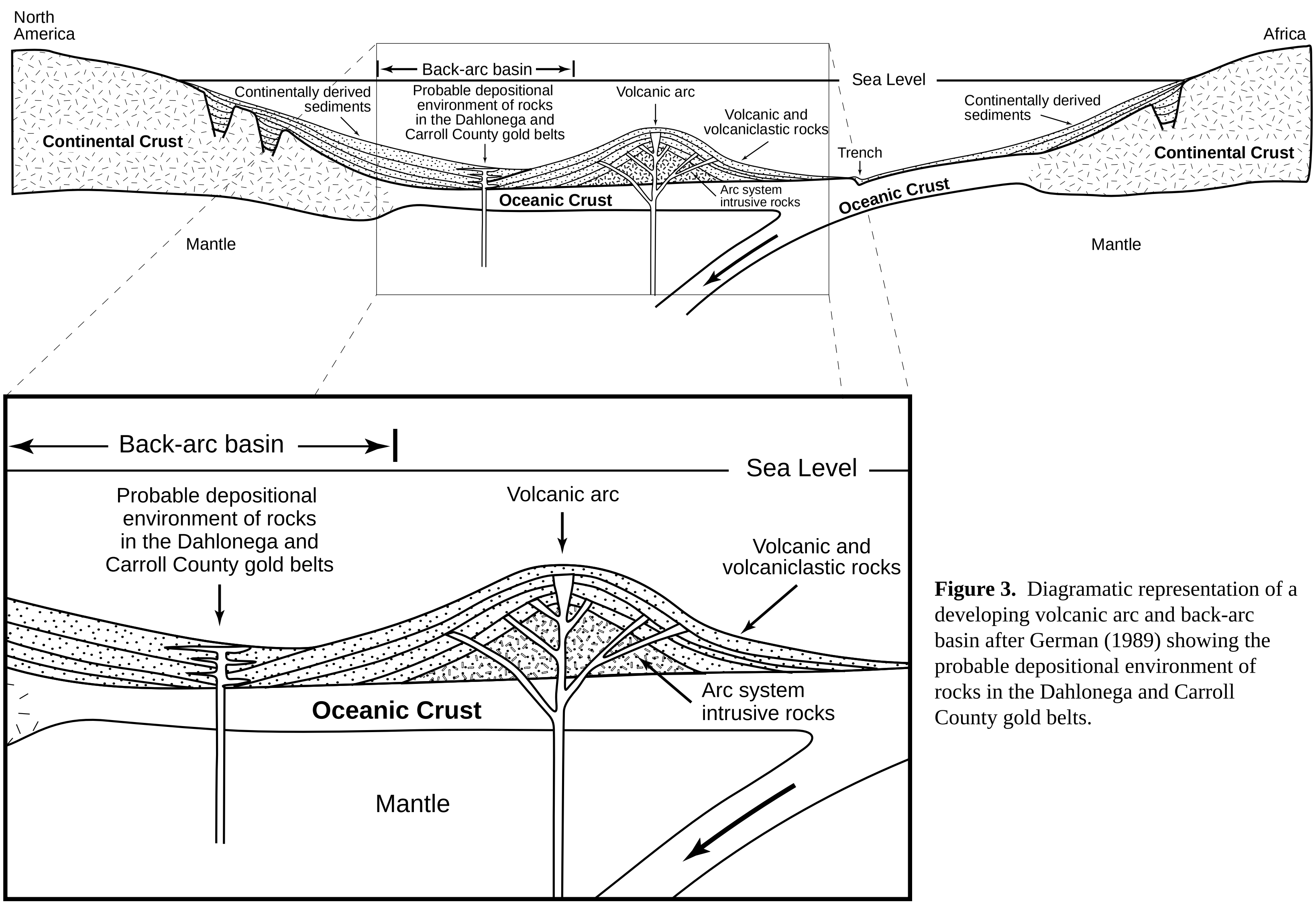

Figure 3. Diagramatic representation of a developing volcanic arc and back-arc basin after German (1989) showing the probable depositional environment of rocks in the Dahlonega and Carroll County gold belts.

GEOLOGIC SETTING

The southern Appalachian Blue Ridge geologic province is separated from the Valley and Ridge to the northwest by the Blue Ridge fault, which thrust Grenville basement and lower Paleozoic rocks of the Appalachian crystalline core over the Paleozoic sedimentary rocks of the Valley and Ridge (Fig. 1). It is separated from the Inner Piedmont to the southeast by the Brevard fault zone (Fig. 1). The Blue Ridge province, part of the Blue-Green-Long axis of Rankin (1976) traceable from Alabama to Newfoundland, is divisible into eastern and western subprovinces on the basis of lithostratigraphic differences between the two distinct assemblages. The western Blue Ridge contains continentally derived rifted-margin succession (slope-and-rise) metasedimentary rocks (Ocoee Supergroup, Mt. Rogers Formation, Grandfather Mountain Formation, and Murphy belt). These metasedimentary rocks were deposited along the Laurentian margin on 1.0 to 1.2 Ga Grenville basement during the Late Proterozoic and early Paleozoic (Williams and Hatcher, 1983; Hatcher, 1989; Hopson *et al.,* 1989; Horton *et al.*, 1989; Hatcher and Goldberg, 1991). The western Blue Ridge also contains abundant external massifs of allochthonous 1.1 Ga Grenville basement and only sparse mafic and ultramafic rocks (Hopson *et al*., 1989).

The Allatoona/Hayesville/Gossan Lead fault separates the rift-drift facies rocks of the western Blue Ridge from the distal, deep water, ocean floor and slope-and-rise metasedimentary rocks of the eastern Blue Ridge (Hatcher, 1978; McConnell and Costello, 1980; Hopson *et al.*, 1989; Hatcher and Goldberg, 1991). The eastern Blue Ridge also contains all the major granitoid bodies and the majority of the mafic and ultramafic rocks of the Blue Ridge (Hatcher, 1978, 1989). Limited Grenville (Laurentian) basement is present in the eastern Blue Ridge as isolated massifs (in the Tallulah Falls and Toxaway domes; Hopson *et al*., 1989).

The Allatoona fault west of Dahlonega, Georgia, thrust rocks of the Dahlonega gold belt (Otto Formation and associated metaigneous rocks) to the northwest over the western Blue Ridge Great Smoky Group (Figs. 1 and 2). The Otto Formation nomenclature used in this study, previously defined by Hatcher (1988) near Otto, North Carolina, is correlative with the New Georgia Group of Higgins and McConnell (1978) to the southwest and the Helen Group (Gillon, 1982; Nelson and Gillon, 1985) to the east and northeast. The Great Smoky Group, originally defined by King (1949), contains metasandstone and pelitic schist with abundant calc-silicate quartzite. The Great Smoky Group, undivided in this study, is subdivided in other parts of the western Blue Ridge (e.g., Hurst, 1955; Ausburn *et al.*, 1998). The abundance of calc-silicate and apparent lack of mafic rocks in the Great Smoky Group versus the apparent lack of calc-silicate and presence of abundant mafic rocks in the Dahlonega gold belt support their separation by the Allatoona fault (Fig. 1).

The Hayesville-Soque River thrust sheet, containing rocks of the Coweeta Group, is bounded to the northwest by the Hayesville fault (Coweeta Group over Great Smoky Group) and to the southeast by the Soque River fault (Coweeta Group over Dahlonega gold belt; Fig. 1). Inequigranular, biotite-dominant (over trace muscovite), often migmatitic gneiss and schist of the Coleman River Formation (Coweeta Group) versus two-mica, nonmigmatitic, often equigranular metasandstone and schist of the Great Smoky Group and Otto Formation (Dahlonega gold belt) is the principal criterion for delineation of the Hayesville-Soque River fault.

Truncation of contacts and presence of mylonite along the northwestern perimeter of the Sally Free mafic complex indicates fault emplacement (thrust) to the northwest over the metasandstone-and-schist and the aluminous-schist units of the Otto Formation (Fig. 2; Settles and Hatcher, *in progress*). Detailed mapping for this study only defines the northern and western fault contacts of the mafic complex; thus, it is unclear whether this fault, termed the Etowah River fault, bounds the complex as a klippe or continues to the south and east into the Dahlonega gold belt (Fig. 2). Compilation of the southern portion of the Campbell Mountain quadrangle from Nelson (1991) with mapping from this study (Figs. 1 and 2) and careful observation of published geologic maps of the Dahlonega (east of Campbell Mountain.; Nelson, 1991) and Dawsonville (south of Campbell Mountain; German, 1985) 7.5 minute quadrangles indicate the size and extent of the Sally Free mafic complex but do not clearly indicate a fault relationship to the south and/ or east of the complex.

Mafic rocks within the field area are present within two of the three stratigraphic assemblages delineated, predominantly within the Dahlonega gold belt, as discussed previously, and sparsely within the Hayesville thrust sheet (Fig. 2). Mafic rocks within the Hayesville thrust sheet predominantly occur as fine- to medium-grained amphibolite with only minor coarse-grained hornblende gneiss. Rare garnet-bearing amphibolite boudins occur within the Coweeta Group, Coleman River Formation. No mafic rocks were observed within the Great Smoky Group in this area (Fig. 2). A mafic occurrence within the Great Smoky Group appears on the Georgia state geologic map (Pickering and Murray, 1976) approximately 28 km west of Dahlonega, Georgia (Pickens County). Costello (per. comm.) tentatively associates this occurrence with a newly delineated Hayesville fault klippe (Burnt Mountain, Georgia) of Coleman River Formation (Coweeta Group), in which mafic rocks are common. Mafic occurrences within the Great Smoky Group, such as the Newtown sill near Mineral Bluff, Georgia (Hurst, 1955), are particularly rare.

SAMPLING AND PETROGRAPHY

Representative metaigneous rock samples, predominantly mafic in composition, were collected across the defined study area depicted in Figure 2 (categorized in Table 1). A total of 26 samples were collected for whole-rock chemical analyses: three amphibolite

Table 1. Sample subdivisions including number of analyses for each subdivision (in parentheses), sample numbers, and symbols used in plotting data. Samples are divided according to thrust sheet, mapped units, and rock type.

Dahlonega gold belt				***Hayesville thrust sheet***
Sally Free mafic complex (SFMC)			**Otto Formation associated mafic rocks**	**Coweeta Group associated mafic rocks**
Cane Creek felsic gneiss	Amphibolite unit	Hornblende gneiss-metagabbro-amphibolite (hga) unit		
✳ CM-283 × CM-605	◇ amphibolite (5) - DG-6, CM-287, -301, -402, and CM-589	◆ amphibolite (1) - CM-580 ⊗ metagabbro/hornblende gneiss (4) - CM-515, -516, -613 and CM-858	• amphibolite (11) CM-24, -60, -62, -111, -159, -266, -432, -456, -526, -629, and CM-744	○ amphibolite (2) - CM-19 and CM-490 ☼ Coleman River Formation amphibolite boudin (1) - CM-209

samples from within the Coweeta Group in the Hayesville-Soque River thrust sheet, eleven amphibolite samples from within the Otto Formation in the Dahlonega gold belt and six amphibolite, four metagabbro/hornblende gneiss, and two Cane Creek felsic gneiss samples from the Sally Free mafic complex in the Dahlonega gold belt (Fig. 2 and Table 1). The migmatitic intermediate gneiss unit within the mafic complex was not selected for chemical analysis due to excessive metamorphic alteration. A single sample of the Cane Creek felsic gneiss (CM-283) was chosen for Nd-Sr isotopic analysis and U-Pb age dating. Numerous thin sections were made for petrographic characterization of mapped and collected metaigneous rocks. Percent anorthite content within plagioclase for several samples was determined by petrographic analysis of thin sections.

Samples from the gold belt have been subdivided into two groups based on occurrence: Otto Formation, which includes mafic rock occurrences within metasedimentary rock of the Otto Formation of various scales (m to km), and Sally Free mafic complex, which includes both mafic and felsic rocks within the complex (Fig. 2 and Table 1).

Samples: Dahlonega Gold Belt - Sally Free Mafic Complex

The Sally Free mafic complex covers an area of approximately 34 km^2 and is divided into four lithologic units: Cane Creek felsic gneiss; hornblende gneiss-metagabbro-amphibolite; amphibolite; and intermediate gneiss. The intermediate gneiss unit occurs in limited exposure and discontinuously between the hornblende gneiss-metagabbro-amphibolite and Cane Creek felsic gneiss units (Fig. 2). The gneiss is both highly sheared and migmatitic (Fig. 4). The Cane Creek felsic gneiss unit contains felsic gneiss with some hornblende gneiss and amphibolite. The felsic gneiss is named here for an exposure in a small abandoned quarry approximately 0.5 km northwest of the township of Cane Creek, just north of the confluence of Little Cane Creek and West Cane Creek to become Cane Creek proper (Lat./Long. - 34° 24’ 33” N / 84° 00’ 59” W).

Two samples of felsic gneiss were collected from the Cane Creek felsic gneiss unit (CM-283 and CM-605; Fig. 2 and Table 1). Cane Creek felsic gneiss is well foliated, strongly lineated, medium- to coarse-grained (equigranular), and contains quartz, plagioclase (An_{28}), biotite, epidote, muscovite, clinozoisite, and garnet (< 1 mm diameter) with trace amounts of apatite and zircon (Fig. 5). Sample CM-283, collected from the previously mentioned abandoned quarry, was used for petrographic and whole-rock chemical analysis, and U-Pb geochronology. Sample CM-605, collected from a large overhang outcrop along Clay Creek (Fig. 5), was selected for petrographic and whole-rock chemical analysis to confirm the lateral extent of the Cane Creek felsic gneiss. Numerous weathered outcrops within the felsic gneiss unit contain mylonitic felsic gneiss interlayered with amphibolite and hornblende gneiss (not sampled here).

A large amphibolite body marks the eastern limit of the Sally Free mafic complex. Five representative samples (DG-6, CM-287, -301, -402, and CM-589) were collected from the amphibolite body (Fig. 2 and Table 1). The amphibolite is dark gray to black, well foliated, medium- to fine-grained, and contains hornblende, epidote, plagioclase, biotite, and quartz with trace amounts of opaque minerals, clinozoisite, sphene, apatite, and retrograde sericite (Fig. 6). Outcrops, such as the excellent exposure at Cane Creek Falls (CM-287, Camp Glisson), are defined by both a prominent foliation (parallel to compositional layering) and extensive jointing (Fig. 6).

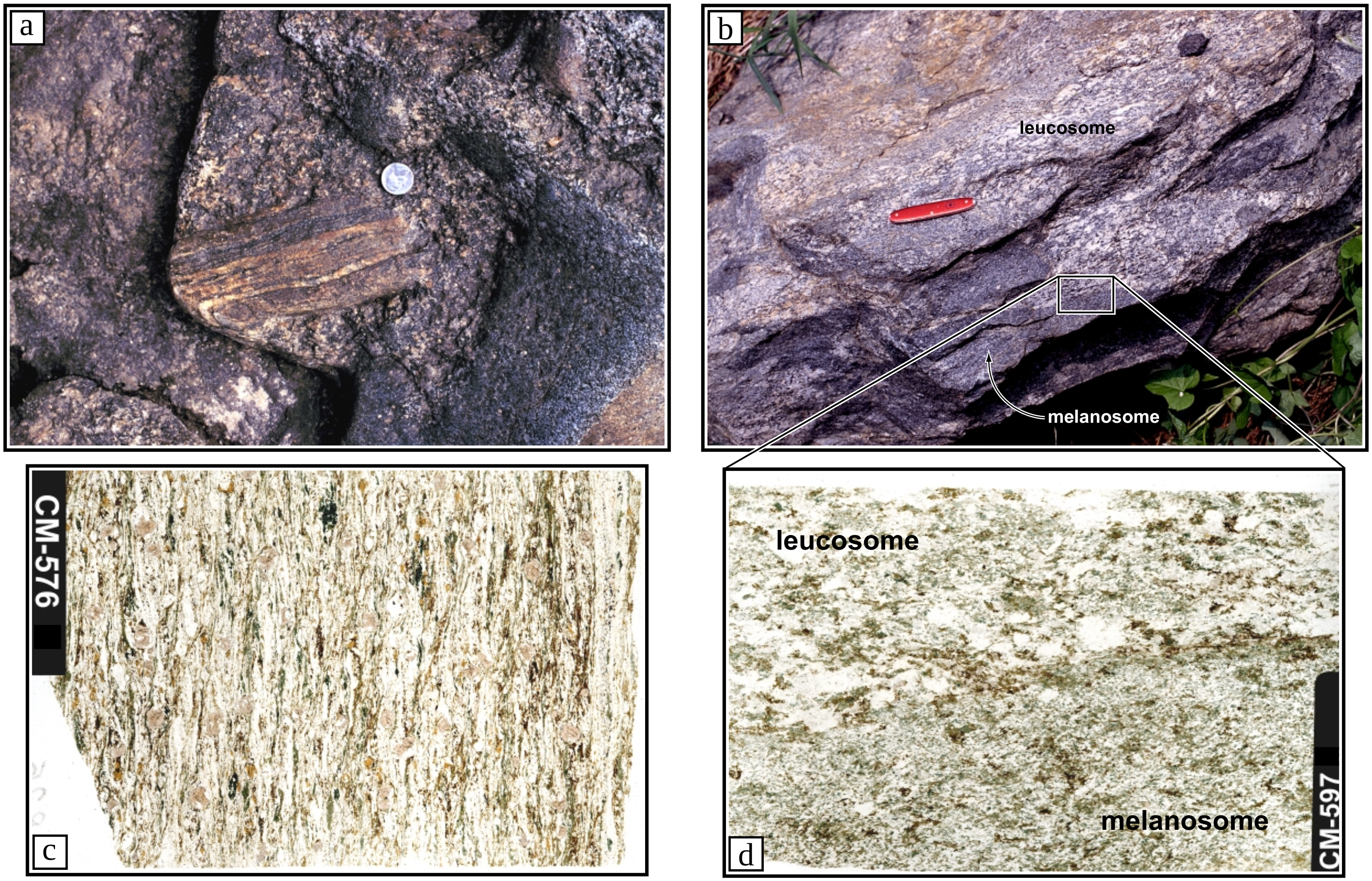

Figure 4. Sally Free mafic complex intermediate gneiss unit. a) Biotite gneiss xenolith within felsic gneiss leucosome at map station CM-592 (Rock Acres Farm). b) Migmatitic intermediate gneiss at map station CM-701 with dark, hornblende/biotite gneiss melanosome and light felsic gneiss leucosome. c) Plane-polarized thin section of intermediate gneiss mylonite from map station CM-576 (long axis = 7.62 cm). d) Plane-polrized migmatitic intermediate gneiss thin section with fine grained, hornblende/biotite gneiss melanosome and coarse grained, felsic gneiss leucosome (long axis = 7.62 cm).

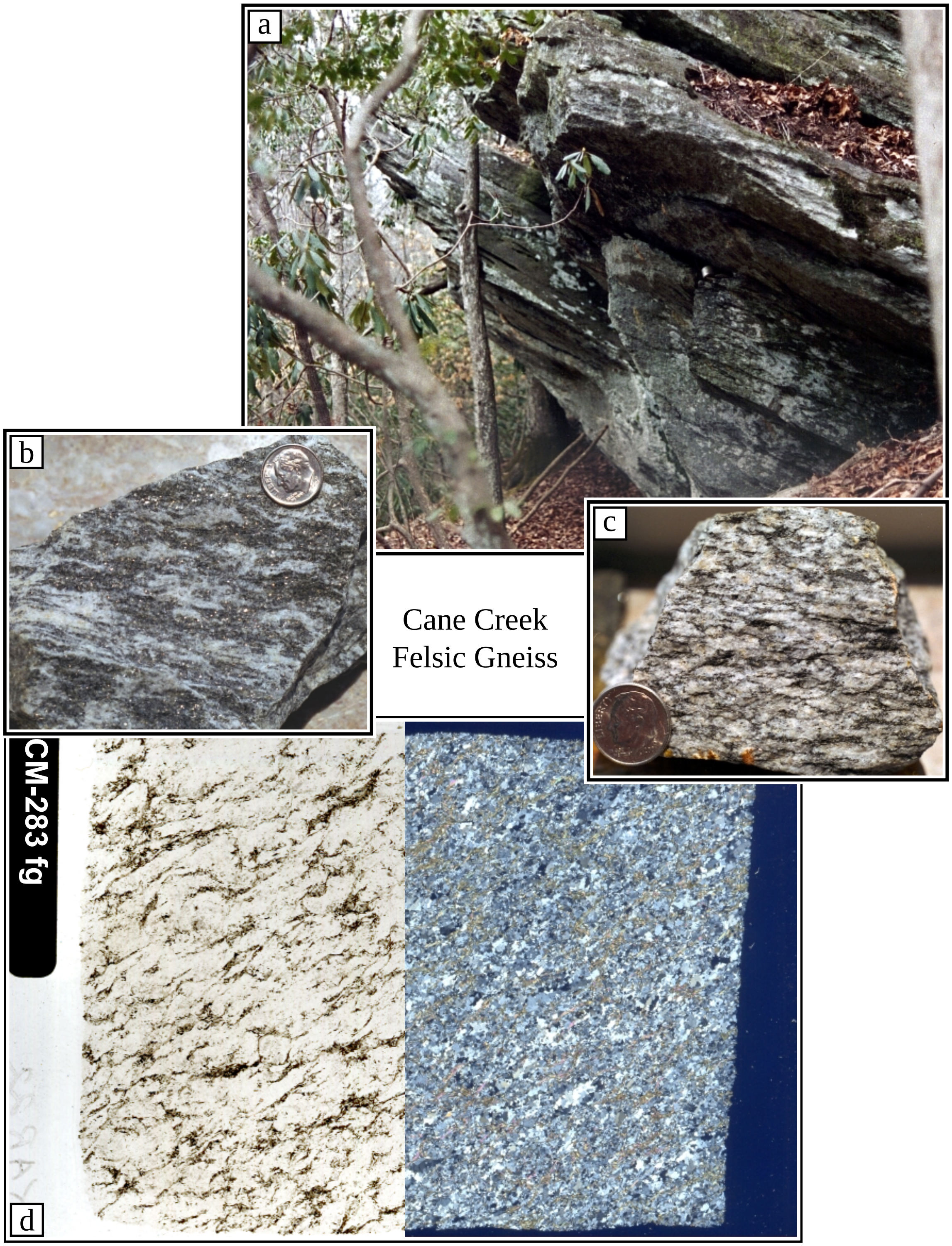

Figure 5. Cane Creek felsic gneiss. a) CM-605 well foliated felsic gneiss outcrop (photo normal to S_2). Outcrop approximately 4.5 meters in height. b) CM-283 felsic gneiss hand sample depicting medium grained, well foliated, strongly lineated texture. c) CM-283 felsic gneiss hand sample depicting medium grained, equigranular texture normal to prominent foliation (S_2) and lineation (L_2). d) CM-283 felsic gneiss thin section shown in plane-polarized (left) and cross-polarized (right) light. Thin section scale: long axis = 3.4cm.

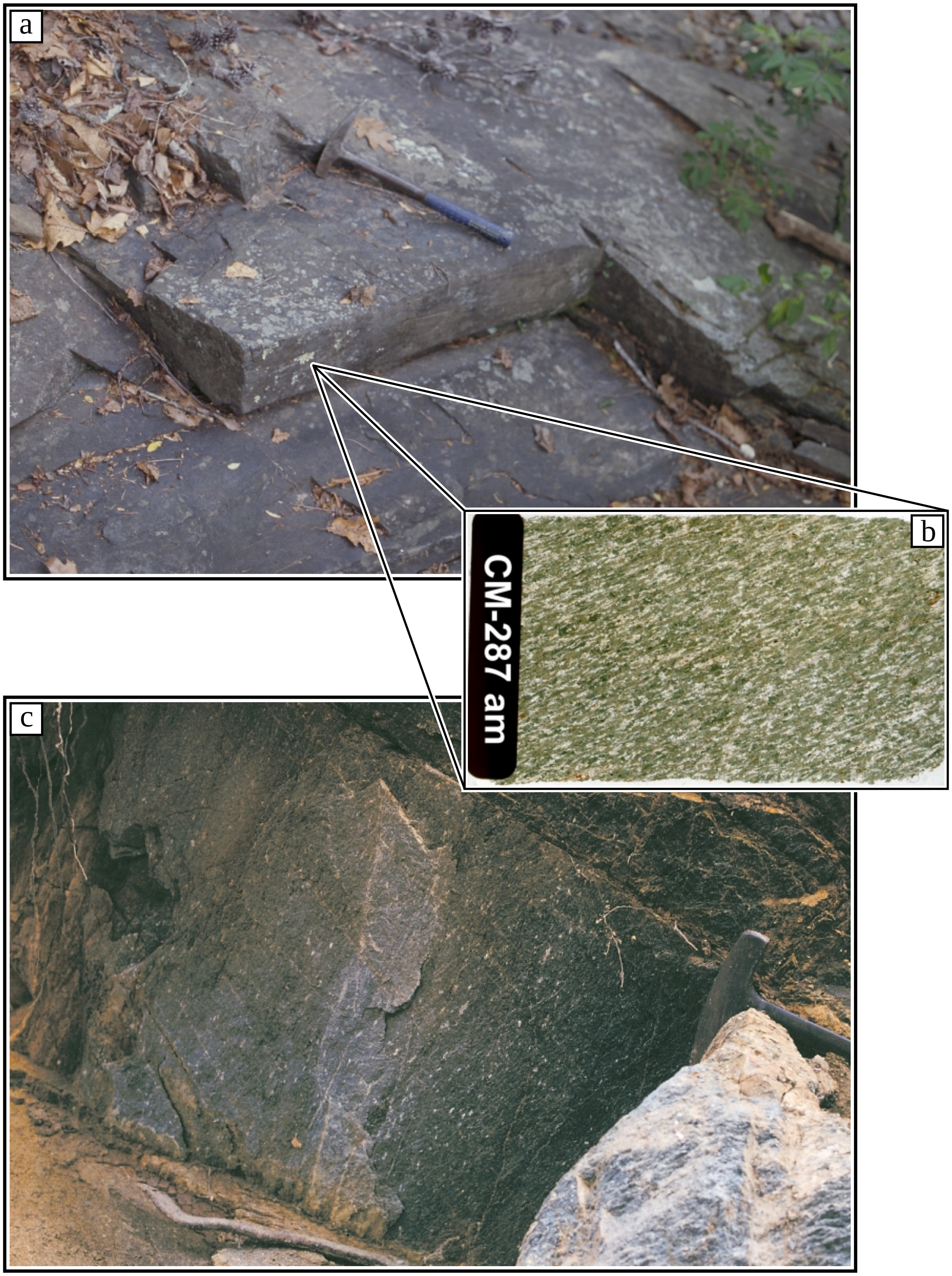

Figure 6. Sally Free mafic complex amphibolite unit. a) Well foliated and highly jointed amphibolite at Cane Creek falls (CM-287). b) Plane-polarized thin section of amphibolite from sample station CM-287 (long axis = 3.4cm). c) Amygdules(?) within a fine grained amphibolite outcrop at sample station CM-301.

The western edge of the Sally Free mafic complex is dominated by a hornblende gneiss-metagabbro-amphibolite unit (Fig. 2). Five samples (CM-515, -516, -580, -613, and CM-858) were collected from this unit (Fig. 2 and Table 1). Samples CM-515 (metagabbro) and CM-516 (hornblende gneiss) were collected from an excellent exposure at Rock Acres Farm, located at the intersection of Oak Grove and Rock Acres roads (Fig. 2). Sample CM-858 (hornblende gneiss) and CM-613 (metagabbro) were collected along the western and northern edges of the complex, respectively (Fig. 2). One amphibolite sample (CM-580) was also collected from the hornblende gneiss-metagabbro-amphibolite unit.

Hornblende gneiss (metadiorite) is well foliated, medium- to coarse-grained and porphyroclastic containing hornblende, plagioclase, epidote, quartz, apatite, and clinozoisite with trace amounts of opaque minerals and sphene (Fig. 7). Hornblende commonly occurs as porphyroclasts and as distinct bands (Fig. 7). Hornblende gneiss is the dominant rock type with sparse poorly foliated metagabbro also present. Metagabbro is dark green to dark gray, medium grained, and equigranular containing hornblende, plagioclase, and epidote with trace amounts of sphene, quartz, and opaque minerals (Fig. 8). Plagioclase is dark blue to gray (calcic) giving fresh rock a dark appearance versus a "salt and pepper" appearance where slightly weathered (Fig. 8). Minor amphibolite also occurs throughout the unit.

Samples: Dahlonega Gold Belt - Mafic rocks within the Otto Formation

Amphibolite occurs within metasedimentary rocks of the Otto Formation as inliers (e.g., Stations CM-24 and CM-111; Fig. 2) and as large bodies (e.g., Station CM-526; Fig. 2). The majority of amphibolite occurs within the aluminous schist unit, with lesser amounts occurring within the metasandstone and schist unit (Fig. 2). Eleven amphibolite samples were collected from various localities within the Otto Formation. Ten samples were collected from mappable occurrences (CM-60, -62, -111, -159, -266, -432, -456, -

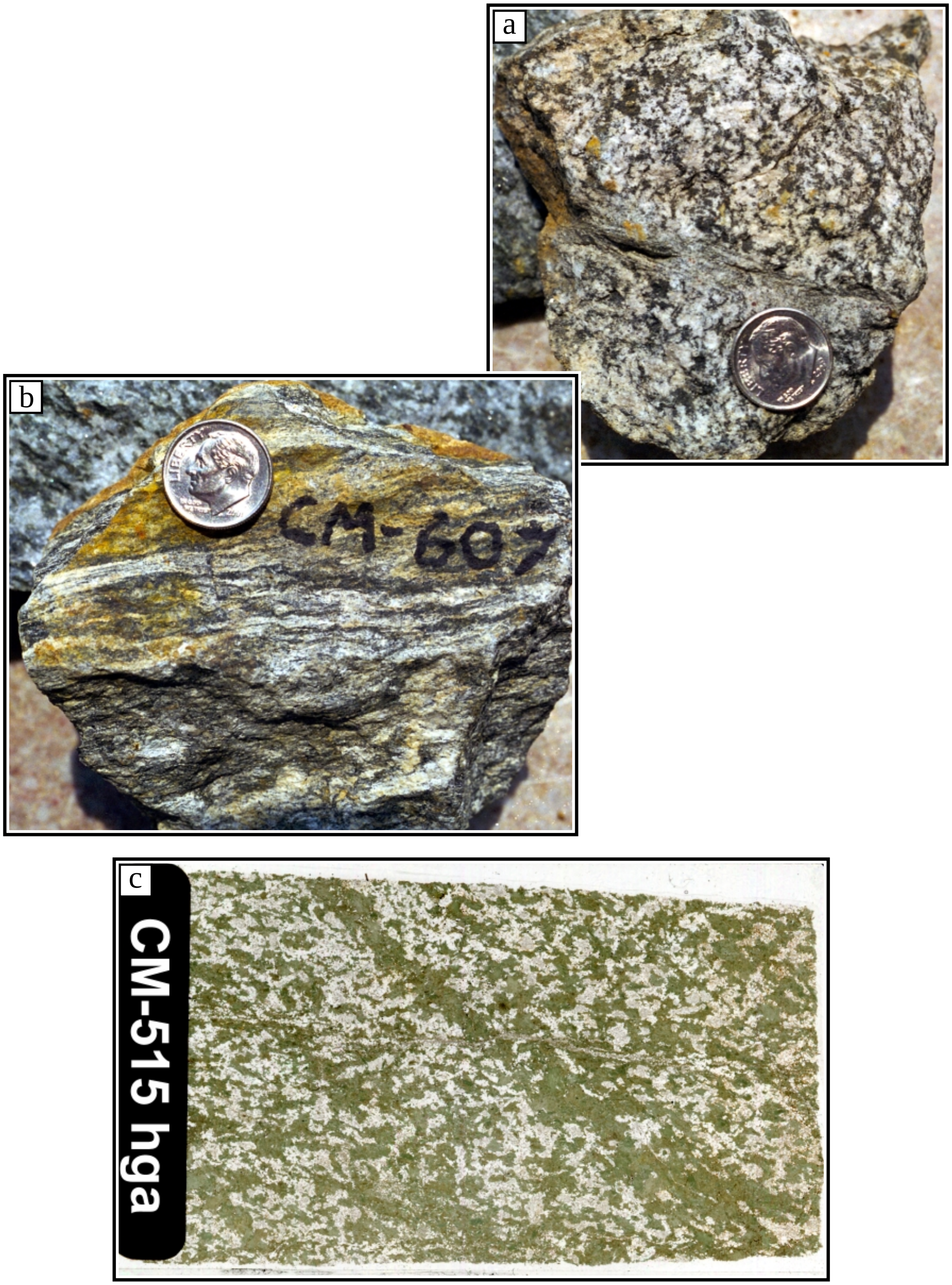

Figure 7. Sally Free mafic complex hornblende gneiss from the hornblende gneiss-metagabbro-amphibolite unit. a) Hornblende gneiss hand sample from map station CM-607 depicted normal to dominant foliation (S_2); and (b) parallel to dominant foliation (S_2). c) Plane-polarized thin section of hornblende gneiss from sample locality CM-515 (long axis = 3.4cm).

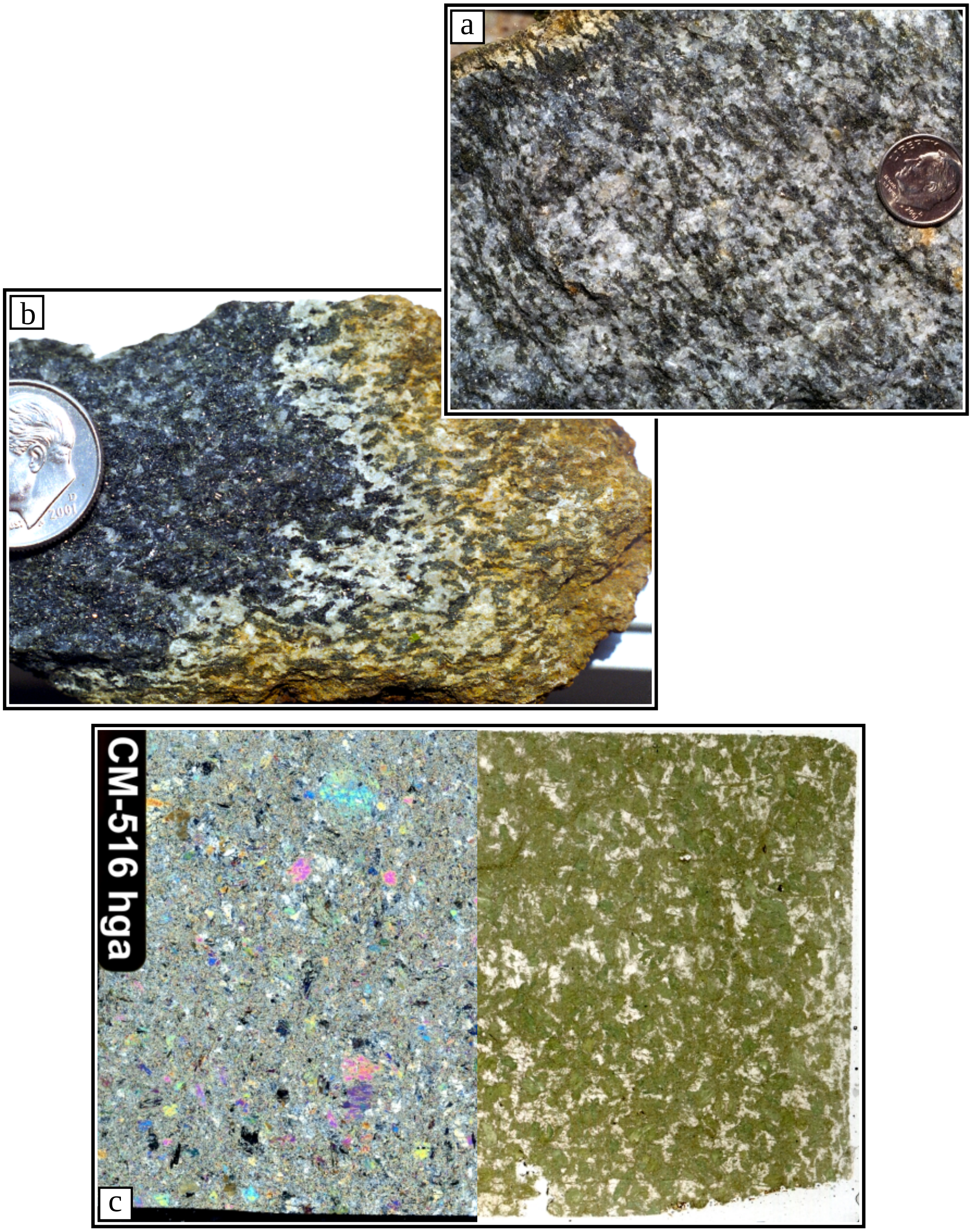

Figure 8. Sally Free mafic complex metagabbro/metadiorite from the hornblende gneiss-metagabbro-amphibolite unit. Metagabbro/metadiorite hand samples from sample station CM-613 (dime for scale) depicting (a) coarse grained, poorly foliated texture characteristic of metagabbro within the complex; and (b) dark, fresh metagabbro (left), composed of blue-to-white plagioclase (calcic) and dark green hornblende, and “salt and pepper” weathering rind (right). c) Metagabbro thin section (cross-polarized on the left and plane-polarized on the right) from sample station CM-516 depicting poorly foliated texture (long axis = 7.62 cm).

526, -629, and CM-743) and one sample was collected from a 0.5-meter thick occurrence within an aluminous schist of the Otto Formation (CM-24; Fig. 2 and Table 1). Amphibolite is well foliated, dark green to black, and fine- to medium-grained containing hornblende, plagioclase (An_{38}), epidote, sphene, quartz, and opaque minerals with trace amounts of apatite and locally abundant clinozoisite, biotite, and retrograde sericite (Fig. 9). Discontinuous gneissic texture, defined by amphibole, epidote, and plagioclase, is prevalent in outcrop. Foliation is parallel to compositional layering.

Samples: Coweeta Group associated mafic rocks

Mafic rocks occur within the Coweeta Group both as large bodies and as boudins within the Coleman River Formation (Fig. 10). Amphibolite is the dominant mafic rock type, although highly weathered hornblende gneiss was observed in outcrop and as float along the eastern edge of the Nimblewill quadrangle (Fig. 2). Three samples were collected from within the Coweeta Group: two from amphibolite bodies (CM-490 and CM-19) and one from an amphibolite boudin (Fig. 10) within the Coleman River Formation (CM-206; Fig. 2 and Table 1). Amphibolite of the Coweeta Group is well-foliated, dark green to black, medium- to fine-grained, containing hornblende, plagioclase, epidote, quartz, opaque minerals (magnetite?) and ± garnet (Fig. 10).

ANALYTICAL TECHNIQUES

Fresh samples were collected with a sledge hammer, cut into thin slabs on a trim saw, washed, broken by hand, and powdered in an alumina ceramic mill. All samples analyzed for whole-rock chemical and isotopic analyses were prepared in this manner. Multi-element whole-rock analyses were performed by ACTLABS (Tucson, AZ) using lithium metaborate/tetraborate fusion inductively coupled plasma emission spectroscopy and inductively coupled plasma (ICP) mass spectrometry for trace elements. Analytical results with detection limits and CIPW normative mineralogy are presented in Tables 2 through 7. Additional trace elements (S, Se, Br, Cd, Ir, Au, and Hg), lower detection

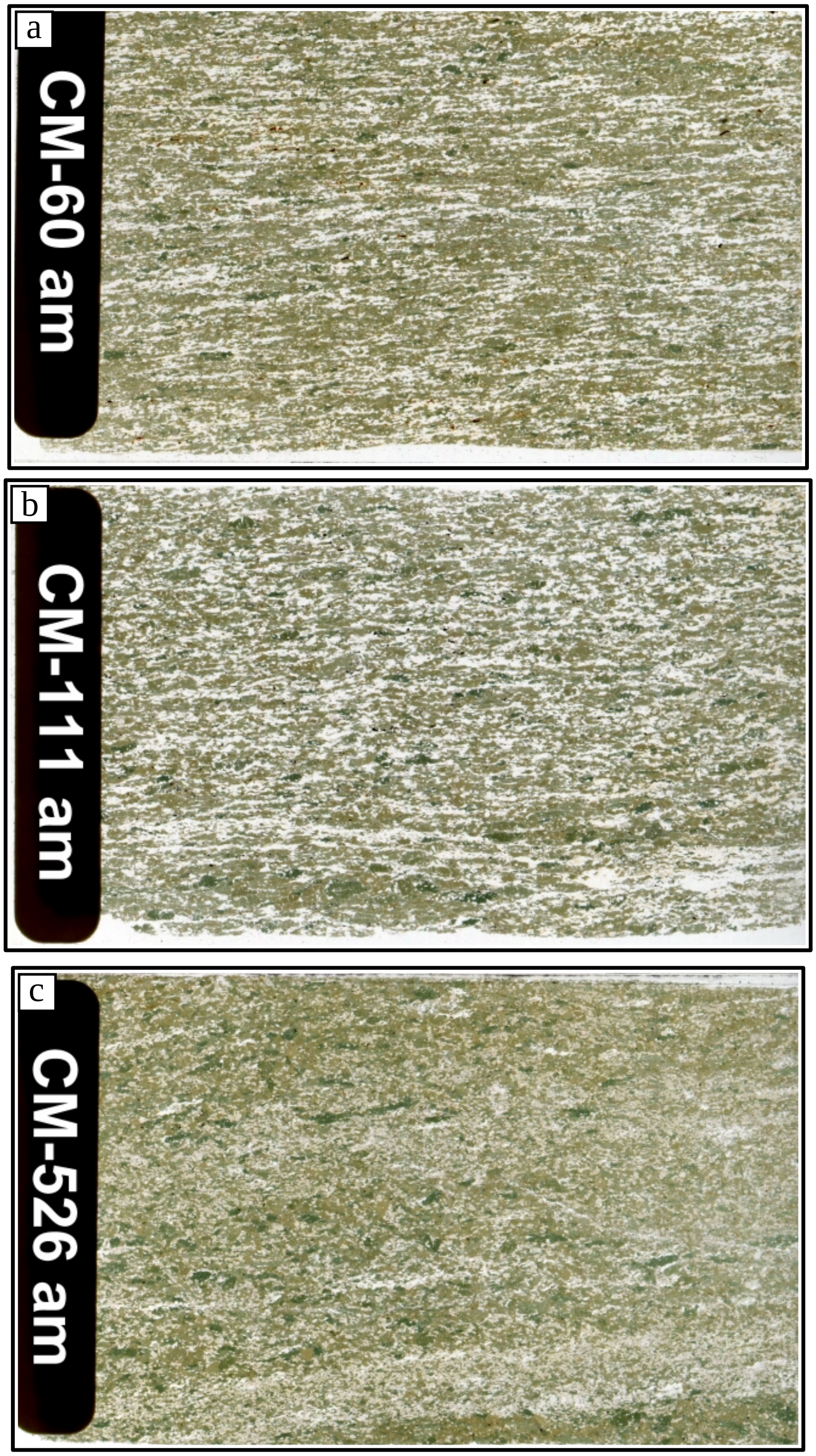

Figure 9. Plane-polarized thin section images of amphibolite from within the Dahlonega gold belt, Otto Formation. Hornblende is blue-green to pale green; epidote is tan to light green; and plagioclase is white (long axis = 3.4 cm).

Figure 10. Amphibolite from within the Coweeta Group in the Hayesville-Soque River thrust sheet. Amphibolite boudin from within the Coweeta Group, Coleman River Formation, at sample station CM-206 depicted (a) parallel to boudin long axis and (b) normal to boudin long axis. c) Plane-polarized thin section of garnet amphibolite boudin from sample station SM-206. d) Plane-polarized thin section of crenulated epidote-amphibolite thin section from sample station CM-490. Thin section scale: long axis = 3.4cm.

Table 2. Dahlonega gold belt, Sally Free mafic complex, amphibolite and hornblende gneiss-metagabbro-amphibolite units: Major element oxides and normative minerals.

	DAHLONEGA GOLD BELT - SALLY FREE MAFIC COMPLEX										
	Amphibolite Unit					hg-metagabbro-amphibolite unit					
Sample Number	DG-6	CM-287	CM-301	CM-402	CM-589	CM-515	CM-516	CM-580	CM-613	CM-858	
Rock Type	am	am	am	am	am	hg	hg	am	hg	hg	ICP
Major Oxide (wt. %)											Detec. Limits
SiO_2	48.27	48.30	46.79	47.17	49.18	50.13	47.30	53.12	46.99	49.67	0.01
Al_2O_3	14.81	14.89	13.73	15.14	13.26	15.81	17.99	17.55	18.27	15.54	0.01
Fe_2O_3	11.91	12.20	16.30	11.52	16.98	8.69	6.30	10.46	6.04	8.85	0.01
MnO	0.18	0.18	0.20	0.20	0.25	0.14	0.11	0.13	0.10	0.16	0.001
MgO	7.74	7.58	5.98	9.66	4.66	9.41	11.14	5.14	11.73	9.00	0.01
CaO	12.63	11.82	9.57	10.49	8.42	11.61	13.96	8.53	13.96	13.04	0.01
Na_2O	2.30	2.28	3.15	2.17	2.47	2.77	1.30	1.20	1.20	1.63	0.01
K_2O	0.14	0.43	0.39	0.23	0.22	0.12	0.19	0.24	0.18	0.22	0.01
TiO_2	1.28	1.27	2.28	1.13	2.87	0.36	0.21	1.12	0.15	0.36	0.001
P_2O_5	0.11	0.11	0.21	0.08	0.26	nd	nd	0.15	nd	nd	0.01
LOI	0.94	1.26	1.38	2.47	1.04	1.36	1.50	2.11	1.64	1.56	0.01
TOTAL	100.31	100.32	99.98	100.25	99.60	100.40	100.00	99.75	100.26	100.04	
Normative Minerals (wt. %)											
Quartz	3.32	0	0	0	5.15	0	0	14.43	0	0	
Plagioclase (total)	37.39	49.62	49.50	49.74	46.05	54.20	54.00	52.03	54.40	48.60	
Anorthite	29.99	29.47	22.51	31.21	24.81	30.59	42.92	41.79	44.16	34.72	
Albite	7.40	20.15	26.99	18.53	21.24	23.61	11.08	10.24	10.24	13.88	
Orthoclase	1.89	0.83	2.36	1.36	1.30	0.71	1.12	1.42	1.06	1.30	
Nepheline	0	0	0	0	0	0	0	0	0	0	
Corundum	0	0	0	0	0	0	0	0.14	0	0	
Diopside	25.99	26.69	20.24	16.97	13.41	22.22	21.37	0	20.3	24.68	
Hypersthene	22.61	8.44	4.56	12.48	22.78	7.79	6.55	24.81	5.78	19.97	
Olivine	0	8.45	13.46	12.43	0	11.55	13.66	0	15.47	1.28	
Ilmenite	3.59	2.45	4.39	2.17	5.53	0.68	0.42	2.15	0.28	0.70	
Magnetite	4.20	2.61	3.60	2.54	3.74	1.9	1.38	2.29	1.32	1.94	
Apatite	0.35	0.25	0.49	0.19	0.6	0	0	0.35	0	0	
Zircon	0.01	0.01	0.03	0.01	0.04	0	0	0.04	0	0	
Chromite	0.01	0.06	0.01	0.09	0	0.04	0.15	0.01	0.12	0.07	
TOTAL	99.36	99.41	98.64	97.98	98.60	99.09	98.65	97.67	98.73	98.54	

Abbreviations: DG - Dahlonega Quad., CM - Campbell Mtn. Quad., am - amphibolite, and hg - hornblende gneiss

Table 3. Dahlonega gold belt, Sally Free mafic complex, amphibolite and hornblende gneiss-metagabbro-amphibolite units: Trace elements.

	DAHLONEGA GOLD BELT - SALLY FREE MAFIC COMPLEX										
	Amphibolite Unit					hg-metagabbro-amphibolite unit					
Sample Number	DG-6	CM-287	CM-301	CM-402	CM-589	CM-515	CM-516	CM-580	CM-613	CM-858	ICP-MS
Rock Type	am	am	am	am	am	hg	hg	am	hg	hg	Detec. Limits
Element (ppm)											ppm
Sc*	49	48	46	52	41	49	34	20	24	51	1
Be*	nd	nd	nd	nd	nd	nd	nd	nd	nd	nd	1
V	306	299	417	307	458	280	103	227	75	195	5
Cr	305	276	82	387	30	172	654	98	513	331	20
Co	44	41	48	53	39	46	39	34	43	39	1
Ni	110	71	51	835	nd	113	251	38	315	121	20
Cu	150	75	27	30	nd	62	77	nd	61	52	10
Zn	92	100	61	149	87	45	49	71	50	94	30
Ga	16	17	19	17	22	15	12	18	12	14	1
Ge	1	1	2	2	2	1	1	1	1	1	1
As	nd	nd	nd	nd	nd	nd	nd	nd	nd	nd	5
Rb	nd	11	4	nd	4	6	nd	4	nd	3	2
Sr	114	128	124	104	148	139	117	138	98	123	2
Y	29	27	51	22	63	4	5	14	3	11	1
Zr	70	69	155	65	203	nd	7	205	7	9	5
Nb	2	2	6	3	8	nd	nd	9	nd	nd	1
Mo	nd	nd	nd	nd	nd	nd	nd	nd	nd	nd	2
Ag	nd	nd	nd	nd	nd	nd	nd	nd	nd	nd	0.5
In	nd	nd	nd	nd	nd	nd	nd	nd	nd	nd	0.2
Sn	nd	nd	2	nd	2	nd	nd	1	nd	nd	1
Sb	nd	nd	nd	nd	nd	nd	nd	nd	nd	nd	0.5
Cs	nd	nd	nd	nd	nd	0.8	nd	nd	nd	nd	0.2
Ba	59	80	46	50	72	34	36	36	14	38	3
La	4.3	3.6	9.5	5.7	16.3	0.6	0.5	16.1	0.5	1.3	0.1
Ce	11.0	9.9	22.9	12.2	32.4	0.6	1.3	26.9	1.2	2.1	0.05
Pr	1.61	1.45	3.45	1.85	5.40	0.12	0.21	3.37	0.18	0.45	0.05
Nd	8.9	8.0	18.3	9.5	26.6	0.7	1.3	13.7	1.1	2.5	0.1
Sm	2.8	2.5	5.5	2.8	7.4	0.3	0.5	2.6	0.3	0.9	0.1
Eu	1.09	1.02	1.86	1.04	2.13	0.22	0.27	0.85	0.24	0.49	0.05
Gd	3.9	3.5	7.1	3.5	9.2	0.5	0.6	2.4	0.5	1.3	0.1
Tb	0.7	0.6	1.2	0.6	1.5	nd	0.1	0.3	nd	0.3	0.1
Dy	4.9	4.4	8.6	4.3	10.6	0.7	0.9	2.4	0.6	1.8	0.1
Ho	1.1	1.0	1.9	0.9	2.4	0.2	0.2	0.5	0.1	0.4	0.1
Er	3.1	2.8	5.7	2.7	6.6	0.5	0.6	1.5	0.4	1.3	0.1
Tm	0.44	0.41	0.82	0.39	0.96	0.07	0.08	0.23	0.05	0.18	0.05
Yb	3.0	2.7	5.5	2.6	6.4	0.5	0.5	1.7	0.4	1.3	0.1
Lu	0.46	0.44	0.86	0.42	0.99	0.07	0.08	0.28	0.05	0.20	0.04
Hf	2.0	1.9	4.1	1.8	5.4	nd	0.2	5.1	0.2	0.3	0.2
Ta	0.2	0.2	0.5	0.2	0.6	nd	nd	0.6	nd	nd	0.1
W	nd	nd	nd	nd	nd	nd	nd	3	nd	nd	1
Tl	nd	nd	nd	nd	nd	0.1	nd	0.3	nd	nd	0.1
Pb	nd	nd	nd	18	nd	nd	nd	7	nd	nd	5
Bi	nd	nd	nd	nd	nd	nd	nd	nd	nd	nd	0.4
Th	0.9	0.3	0.8	0.6	1.5	nd	nd	2.8	nd	nd	0.1
U	nd	nd	0.2	0.2	0.4	nd	nd	0.7	nd	nd	0.1

Abbreviations: DG - Dahlonega Quad., CM - Campbell Mtn. Quad., am - amphibolite, and hg - hornblende gneiss

Table 4. Dahlonega gold belt, Sally Free mafic complex, Cane Creek felsic gneiss unit: Major element oxides, normative mineral, and trace elements.

DAHLONEGA GOLD BELT - SALLY FREE MAFIC COMPLEX
Cane Creek felsic gneiss unit

Major Oxide and Normative Mineralogy

Sample Number	CM-283	CM-605	
Rock Type	fg	fg	Detec. Limits wt. %
Major Oxide (wt. %)			
SiO2	72.13	71.20	0.01
Al2O3	13.59	13.95	0.01
Fe2O3	3.70	3.83	0.01
MnO	0.07	0.08	0.01
MgO	0.92	1.13	0.01
CaO	3.78	3.18	0.01
Na2O	3.32	2.47	0.01
K2O	1.57	2.20	0.01
TiO2	0.22	0.39	0.005
P2O5	0.05	0.09	0.01
LOI	0.93	1.41	0.01
TOTAL	100.28	99.92	

Normative Minerals (wt. %)	CM-283	CM-605
Quartz	35.79	38.21
Plagioclase (total)	45.78	36.34
Anorthite	17.61	15.36
Albite	28.17	20.98
Orthoclase	9.28	13.06
Corundum	0	1.90
Hypersthene	6.25	7.24
Ilmenite	0.42	0.74
Magnetite	0.81	0.84
Apatite	0.12	0.21
Pyrite	0.15	0
Total	98.60	98.54

Abbreviations: CM - Campbell Mtn. Quad. and fg - felsic gneiss

Trace Elements

Sample Number	CM-283	CM-605	
Rock Type	fg	fg	Detec. Limits ppm
Element (ppm)			
S**	712	25	10
Sc*	12	15	0.01
Be	1	2	1
V	50	58	5
Cr*	4	14	0.5
Co*	8	9	0.1
Ni**	16	8	1
Cu**	32	12	1
Zn**	38	52	1
Ga	12	14	1
Ge	1	2	0.5
As	nd	nd	1
Se*	nd	nd	0.5
Br*	nd	nd	0.5
Rb	51	89	2
Sr	84	114	2
Y	15	23	1
Zr	106.5	160.4	1
Nb	5.4	9.5	0.5
Mo*	3	3	2
Ag**	nd	nd	0.5
Cd**	nd	nd	0.5
In	nd	nd	0.1
Sn	1	3	1
Sb*	0	0	0.1
Cs	0.5	2.5	0.1
Ba	356.0	419.0	1
La	17	27	0.05
Ce	30.6	54.7	0.1
Pr	3.4	6.0	0.02
Nd	12	24	0.05
Sm	2.2	4.7	0.01
Eu	0.5	0.9	0.005
Gd	2.00	4.29	0.02
Tb	0.4	0.7	0.01
Dy	2.5	4.0	0.02
Ho	0.55	0.74	0.01
Er	1.7	2.2	0.01
Tm	0.3	0.4	0.005
Yb	2.0	2.2	0.01
Lu	0.3	0.3	0.002
Hf	2.8	4.0	0.1
Ta	0.49	0.92	0.1
W**	nd	nd	1
Ir*	nd	nd	0.001
Au*	nd	nd	0.001
Hg*	nd	nd	5
Tl	0	1	0.05
Pb**	7.2	19.7	5
Bi**	nd	0	0.06
Th	6.0	9.5	0.05
U	1.9	2.4	0.05

* - INAA
** - "Near Total" Digestion ICP

Table 5. Dahlonega gold belt, amphibolite within the Otto Formation: Major element oxides and normative minerals.

	DAHLONEGA GOLD BELT — Amphibolites within the Otto Formation											
Sample Number	CM-24	CM-60	CM-62	CM-111	CM-159	CM-266	CM-432	CM-456	CM-526	CM-629	CM-744	
Rock Type	am	am	am	am	am	am	am	am	am	am	am	ICP Detec. Limits
Major Oxide (wt. %)												
SiO_2	50.41	49.88	50.43	52.39	47.86	45.43	46.34	48.53	45.93	44.18	54.80	0.01
Al_2O_3	15.19	15.25	14.34	13.82	15.20	16.65	13.42	15.51	15.66	14.52	14.48	0.01
Fe_2O_3	10.92	12.74	12.08	13.22	12.28	12.25	18.08	11.57	12.93	18.07	11.51	0.01
MnO	0.17	0.20	0.19	0.20	0.20	0.22	0.25	0.19	0.23	0.26	0.16	0.001
MgO	7.90	6.89	7.43	6.04	8.84	5.73	6.26	8.98	7.87	6.98	5.17	0.01
CaO	11.24	10.52	11.23	9.94	11.08	16.33	8.95	10.09	12.85	8.52	8.23	0.01
Na_2O	1.72	1.52	1.87	2.08	2.45	0.64	2.32	2.97	1.60	1.57	3.35	0.01
K_2O	0.42	0.34	0.36	0.42	0.39	0.34	0.20	0.38	0.19	0.19	0.38	0.01
TiO_2	0.89	1.13	1.07	1.29	0.78	1.04	1.69	0.84	1.05	2.11	1.75	0.001
P_2O_5	0.09	0.10	0.09	0.12	0.05	0.08	0.13	0.06	0.06	0.16	0.11	0.01
LOI	1.37	1.88	1.08	0.96	1.04	1.63	1.52	1.25	1.33	2.54	0.48	0.01
TOTAL	100.32	100.45	100.18	100.48	100.18	100.34	99.16	100.36	99.70	99.10	100.42	
Normative Minerals (wt. %)												
Quartz	2.26	4.32	2.39	6.51	0	0	0	0	0	0	6.99	
Plagioclase (total)	47.50	47.19	45.98	45.25	50.61	47.50	46.00	53.55	49.10	46.07	52.20	
Anorthite	32.78	34.16	29.99	27.48	29.63	42.00	26.03	28.17	35.39	32.53	23.60	
Albite	14.72	13.03	15.99	17.77	20.98	5.50	19.97	25.38	13.71	13.54	28.60	
Orthoclase	2.48	2.01	2.13	2.48	2.30	2.01	1.18	2.25	1.12	1.12	2.25	
Nepheline	0	0	0	0	0	0	0	0	0	0	0	
Corundum	0	0	0	0	0	0	0	0	0	0	0	
Diopside	18.76	14.83	21.12	17.93	20.95	32.59	15.24	17.94	23.58	7.8	14.04	
Hypersthene	23.62	25.02	22.56	21.68	4.75	8.77	22.71	3.21	8.41	29.97	18.31	
Olivine	0	0	0	0	16.2	2.95	4.94	17.88	11.16	3.17	0	
Ilmenite	1.71	2.18	2.05	2.49	1.5	2.01	3.27	1.60	2.01	4.06	3.36	
Magnetite	2.39	2.80	2.65	2.91	2.70	2.70	4.00	2.54	2.84	3.99	2.52	
Apatite	0.21	0.23	0.21	0.28	0.12	0.19	0.30	0.14	0.14	0.37	0.25	
Zircon	0.01	0.01	0.01	0.01	0	0.01	0.01	0.01	0.01	0.01	0.01	
Chromite	0.09	0.03	0.04	0.01	0.04	0.04	0.01	0.04	0.06	0.03	0.01	
TOTAL	99.03	98.62	99.14	99.55	99.17	98.77	97.66	99.16	98.43	96.59	99.94	

Abbreviations: CM - Campbell Mtn. Quad. and am - amphibolite

Table 6. Dahlonega gold belt, amphibolite within the Otto Formation: Trace elements.

	DAHLONEGA GOLD BELT — Amphibolites within the Otto Formation											
Sample No.	CM-24	CM-60	CM-62	CM-111	CM-159	CM-266	CM-432	CM-456	CM-526	CM-629	CM-744	
Rock Type	am	am	am	am	am	am	am	am	am	am	am	Detec. Limits (ppm)
Element (ppm)												
Sc*	45	49	46	46	53	46	51	48	50	47	27	1
Be*	nd	nd	nd	nd	nd	nd	nd	nd	nd	nd	nd	1
V	296	360	315	350	307	333	461	280	330	518	159	5
Cr	424	111	197	65	234	175	83	216	250	167	85	20
Co	42	44	43	40	44	41	54	47	51	56	30	1
Ni	155	96	117	75	97	79	78	109	110	99	nd	20
Cu	16	185	111	108	18	11	75	37	55	53	11	10
Zn	95	158	150	158	108	115	155	133	120	177	128	30
Ga	17	19	16	18	15	18	18	14	16	20	23	1
Ge	2	2	2	1	1	1	1	1	1	1	1	1
As	nd	nd	nd	nd	nd	nd	nd	nd	nd	nd	nd	5
Rb	7	10	6	9	4	4	nd	3	3	nd	4	2
Sr	146	100	103	154	119	130	48	70	45	28	274	2
Y	23	30	25	29	26	30	47	23	32	51	30	1
Zr	61	82	71	84	32	50	96	39	54	111	80	5
Nb	nd	2	2	2	nd	nd	nd	nd	nd	2	nd	1
Mo	nd	nd	nd	nd	nd	nd	nd	nd	nd	nd	nd	2
Ag	nd	nd	nd	nd	nd	nd	nd	nd	nd	nd	nd	0.5
In	nd	nd	nd	nd	nd	nd	nd	nd	nd	nd	nd	0.2
Sn	nd	nd	nd	nd	nd	nd	nd	nd	nd	nd	nd	1
Sb	nd	nd	nd	nd	nd	nd	0.6	nd	nd	nd	0.6	0.5
Cs	nd	nd	nd	nd	nd	nd	nd	nd	nd	nd	nd	0.2
Ba	42	49	42	77	93	12	29	30	33	41	47	3
La	7.4	7.6	6.3	6.8	1.2	2.5	4.8	1.3	1.5	5.5	3.8	0.1
Ce	12.6	18.0	14.6	16.3	2.7	5.3	12.0	3.9	4.6	10.6	10.9	0.05
Pr	2.01	2.34	1.91	2.13	0.53	1.09	2.11	0.69	0.85	2.33	1.77	0.05
Nd	9.7	11.4	9.4	10.7	3.5	6.4	12.0	4.4	5.6	13.5	11.5	0.1
Sm	2.7	3.3	2.8	3.0	1.5	2.4	4.1	1.7	2.2	4.9	4.4	0.1
Eu	0.93	1.11	0.93	1.06	0.66	0.94	1.38	0.71	0.94	1.69	1.87	0.05
Gd	3.3	4.2	3.4	3.9	2.6	3.6	5.8	2.7	3.4	6.4	5.1	0.1
Tb	0.6	0.7	0.6	0.7	0.5	0.7	1.1	0.5	0.6	1.2	0.9	0.1
Dy	4.1	5.2	4.3	4.8	4.1	5.0	7.6	3.8	4.8	9.3	5.5	0.1
Ho	0.9	1.1	0.9	1.1	1.0	1.1	1.7	0.9	1.1	2.1	1.1	0.1
Er	2.5	3.2	2.8	3.1	2.9	3.4	5.2	2.7	3.4	6.4	3.0	0.1
Tm	0.36	0.48	0.41	0.48	0.45	0.49	0.75	0.40	0.49	1.01	0.40	0.05
Yb	2.5	3.2	2.7	3.2	3.1	3.3	5.1	2.7	3.3	7.1	2.7	0.1
Lu	0.38	0.51	0.43	0.50	0.48	0.55	0.82	0.45	0.57	1.19	0.38	0.04
Hf	1.7	2.3	2.0	2.4	1.1	1.5	2.8	1.2	1.7	3.5	2.3	0.2
Ta	0.2	0.2	0.2	0.2	nd	nd	nd	nd	nd	0.2	0.1	0.1
W	nd	nd	nd	nd	nd	nd	nd	nd	nd	nd	nd	1
Tl	nd	nd	nd	0.1	nd	nd	nd	nd	nd	nd	0.2	0.1
Pb	11	nd	nd	nd	10	nd	7	nd	nd	nd	11	5
Bi	2.1	nd	nd	nd	nd	nd	nd	nd	nd	nd	nd	0.4
Th	1.0	1.6	1.2	1.4	0.2	nd	0.3	nd	nd	0.5	0.6	0.1
U	0.3	0.4	0.3	0.4	nd	nd	0.2	nd	nd	0.2	0.2	0.1

Abbreviations: CM - Campbell Mtn. Quad. and am - amphibolite

Table 7. Hayesville thrust sheet, amphibolite within the Coweeta Group Coleman River Formation: Major element oxides, normative mineral, and trace elements.

HAYESVILLE THRUST SHEET
Amphibolite within the Coweeta Group Coleman River Formation

Major Oxide and Normative Minerals

Sample Number	CM-283	CM-206	CM-490	Detec.
Rock Type	fg	am (bdn)	am	Limits
Major Oxide (wt. %)				wt. %
SiO_2	49.20	50.13	47.31	0.01
Al_2O_3	14.48	12.70	12.16	0.01
Fe_2O_3	13.70	17.16	19.03	0.01
MnO	0.20	0.26	0.23	0.001
MgO	7.33	5.81	5.37	0.01
CaO	9.50	8.98	11.78	0.01
Na_2O	3.90	0.79	1.14	0.01
K_2O	0.25	0.57	0.31	0.01
TiO_2	0.99	3.32	1.86	0.001
P_2O_5	0.06	0.27	0.15	0.01
LOI	0.77	0.09	0.94	0.01
TOTAL	100.38	100.08	100.28	
Normative Minerals (wt. %)				
Quartz	0	11.48	3.32	
Plagioclase (total)	52.48	36.64	37.39	
Anorthite	21.50	29.87	27.57	
Albite	30.98	6.77	9.82	
Orthoclase	1.48	3.43	1.89	
Nepheline	1.32	0	0	
Corundum	0	0	0	
Diopside	21.33	11.34	25.99	
Hypersthene	0	26.28	22.61	
Olivine	17.96	0	0	
Ilmenite	1.90	6.40	3.59	
Magnetite	3.02	3.78	4.20	
Apatite	0.14	0.63	0.35	
Zircon	0.01	0.04	0.01	
Chromite	0.01	0.01	0.01	
TOTAL	99.65	100.03	99.36	

Abbreviations: CM - Campbell Mtn. Quad., am - amphibolite, and bdn-boudin

Trace Elements

Sample Number	CM-19	CM-206	CM-490	Detec.
Lithology	am	am (bdn)	am	Limits
Element (ppm)				ppm
Sc*	58	37	53	1
Be*	nd	2	nd	1
V	337	507	479	5
Cr	59	84	69	20
Co	54	51	46	1
Ni	110	76	57	20
Cu	131	41	47	10
Zn	147	162	151	30
Ga	15	24	18	1
Ge	1	2	2	1
As	nd	nd	nd	5
Rb	4	10	5	2
Sr	211	106	57	2
Y	31	44	55	1
Zr	46	195	92	5
Nb	nd	15	nd	1
Mo	nd	nd	nd	2
Ag	nd	nd	nd	0.5
In	nd	nd	nd	0.2
Sn	nd	3	nd	1
Sb	nd	nd	nd	0.5
Cs	nd	nd	nd	0.2
Ba	70	150	16	3
La	2.0	15.4	6.9	0.1
Ce	5.1	37.4	12.3	0.05
Pr	0.90	5.16	2.55	0.05
Nd	5.4	25.9	14.6	0.1
Sm	2.2	7.1	4.7	0.1
Eu	0.89	2.45	1.66	0.05
Gd	3.3	8.0	6.8	0.1
Tb	0.7	1.3	1.2	0.1
Dy	5.0	8.1	8.9	0.1
Ho	1.2	1.7	2.0	0.1
Er	3.6	4.4	6.0	0.1
Tm	0.54	0.58	0.89	0.05
Yb	3.6	3.8	5.9	0.1
Lu	0.59	0.51	0.97	0.04
Hf	1.5	5.3	2.9	0.2
Ta	nd	1.2	nd	0.1
W	nd	nd	nd	1
Tl	nd	nd	nd	0.1
Pb	nd	9	nd	5
Bi	nd	nd	nd	0.4
Th	0.4	1.4	0.2	0.1
U	nd	0.7	0.2	0.1

* - INAA

limits, and instrumental neutron activation analyses were obtained for the Cane Creek felsic gneiss samples (i.e., Table 4 versus Table 5). A single powdered whole-rock felsic gneiss sample (CM-283) was chosen for Rb-Sr and Sm-Nd isotopic analyses. P. D. Fullagar at the University of North Carolina-Chapel Hill performed the isotopic analyses using techniques summarized in Fullagar and Butler (1979), Kish (1983), and Fullagar *et al.* (1997).

Approximately 15 kg of fresh sample were collected at the Cane Creek felsic gneiss quarry for ion microprobe (IMP) U-Pb geochronology. Zircons were separated using standard mineral separation techniques, handpicked, mounted with standards in epoxy, polished, and coated with ~10 nm of gold. Before ion probe analyses, the grains were imaged with the JEOL 5600LV scanning electron microscope, equipped with a Hamamatsu photo multiplier tube for cathodoluminescence (CL) imaging, and photographed in reflected and transmitted light at Stanford University. Following the IMP session, the mounted zircons were reimaged with CL and backscattered-electron detectors using the Cameca SX-52 electron microprobe at the University of Tennessee, Knoxville (Figs. 11 and 12). The AS57 (1099 Ma, Paces and Miller, 1993) zircon was used to calibrate the analyses during the SHRIMP session and the techniques outlined in Bacon *et al*. (2000), summarized below, were employed for all analyses. A primary O_2 ion beam at ~15 nA was focused to produce a beam ~ 30 x 40 µm in size (Fig. 11). Analyzed surfaces were rastered for ~4 minutes to remove the gold coat and surface contamination. For each spot, 5 scan cycles were completed for peaks at Zr_2O, ^{204}Pb, background, ^{206}Pb, ^{207}Pb, ^{208}Pb, ^{238}U, ThO, and UO.

GEOCHEMICAL AND SHRIMP RG RESULTS

Major element and normative minerals (Tables 2 - 7) show remarkable similarity within lithologic map units. In addition, chondrite-normalized rare earth element plots (Fig. 13) delineate trends and restricted heavy rare earth element (HREE) ranges within

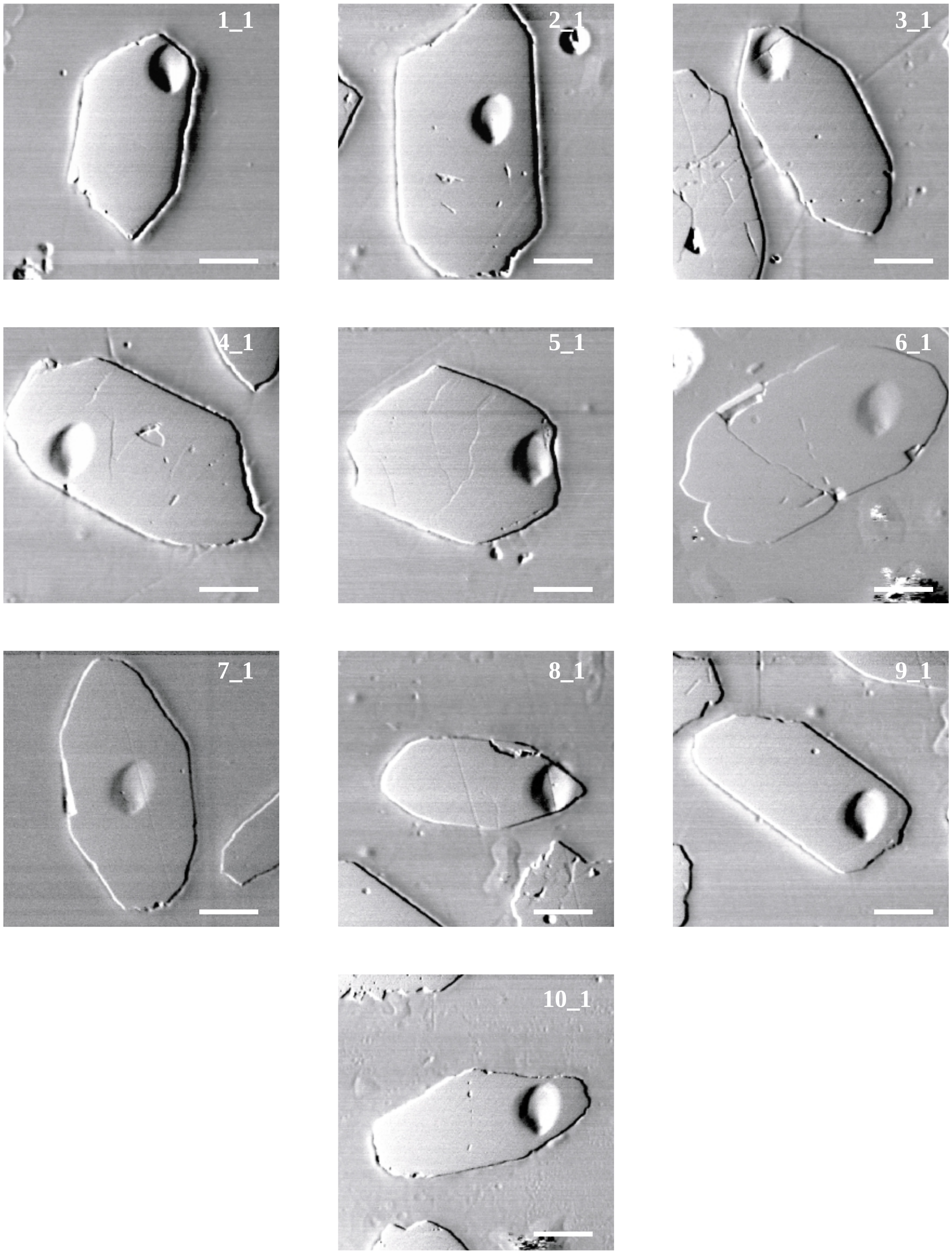

Figure 11. Backscattered electron images of Cane Creek felsic gneiss zircons. Zircons were imaged at the University of Tennessee-Knoxville using a Cameca SX-52 electron microprobe. Scale bar in lower-right corner of each image is 50 µm.

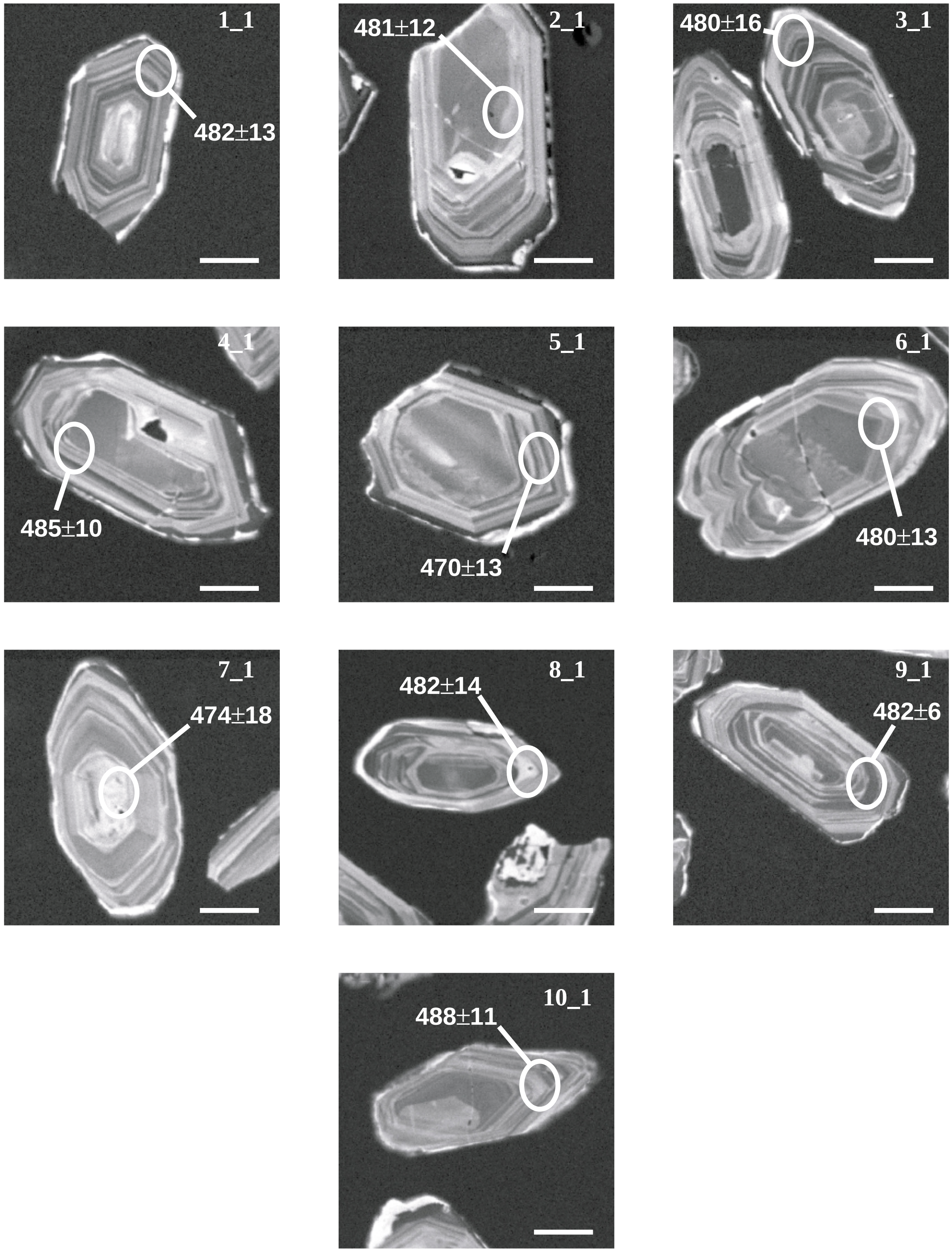

Figure 12. Cathodoluminescence images of Cane Creek felsic gneiss zircons. Zircons were imaged at the University of Tennessee-Knoxville using a Cameca SX-52 electron microprobe. Scale bar in lower-right corner of each image is 50 µm. Ages are $^{206}Pb/^{238}U$ with 2σ errors and reported in Ma. IMP spot size and location were determined from post ablation backscattered electron images of the grains (Fig. 11).

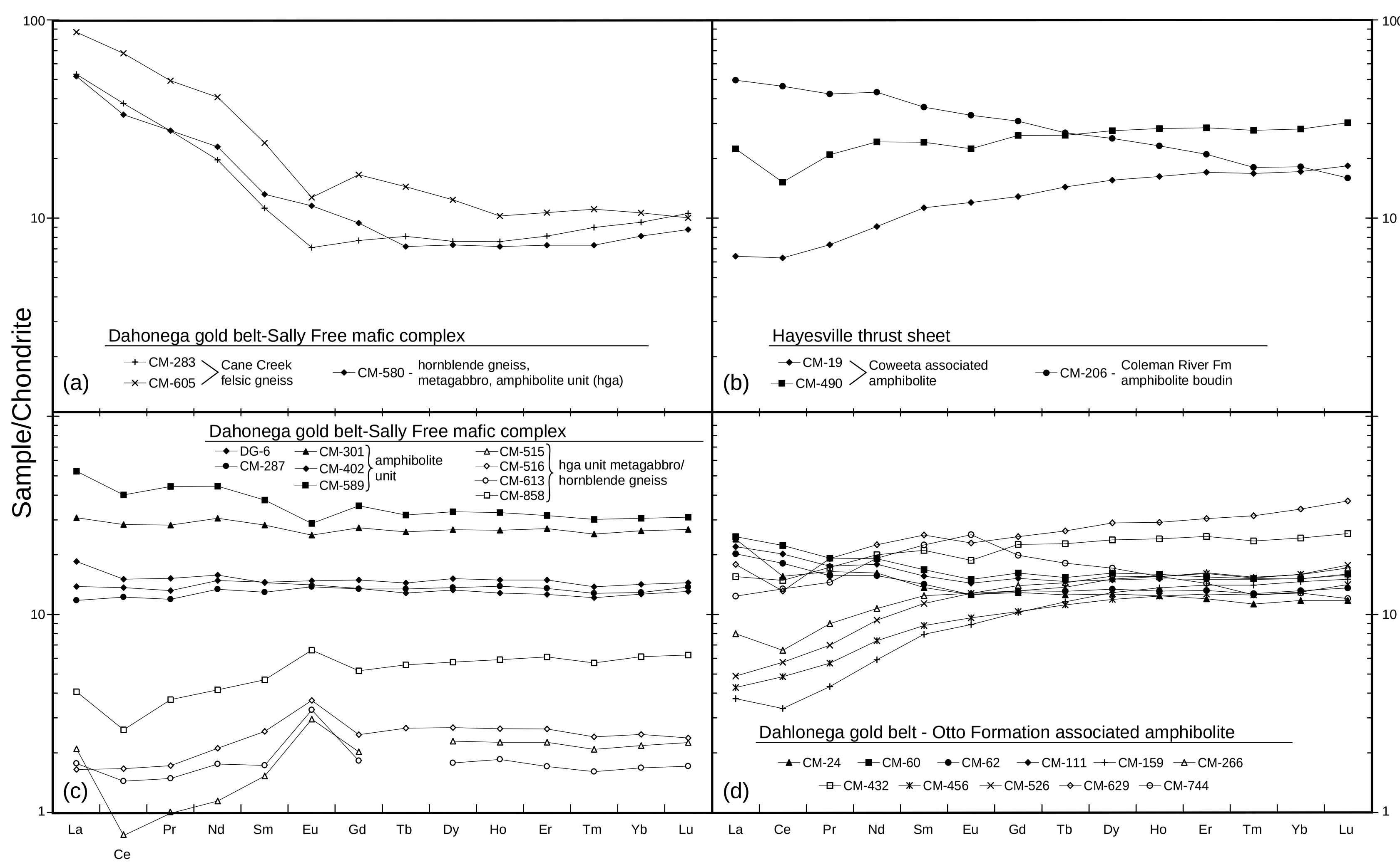

Figure 13. Chondrite normalized REE plots of felsic, intermediate, and mafic samples. Chondrite normalization values are from Boynton (1984). Note that the scale is the same for all plots and that Tb was below the detection limit for samples CM-515 and CM-613. a) Two felsic gneiss samples and a single amphibolite sample from the Sally Free mafic complex. b) Mafic samples from the Hayesville thrust sheet. c) Mafic samples from the Sally Free mafic complex, open symbols are hornblende gneisses and filled symbols are amphibolites. d) Mafic samples from the Dahlonega gold belt.

thrust sheets and between rocks. Amphibolite samples are mostly REE unfractionated, display a wide range of normalized light rare earth element (LREE) concentrations (from 3 to 60x chondrite), and have greater than 10x chondrite values for HREE (from 10 to 40x chondrite). With the exception of a single sample, CM-19, the samples are normative in hypersthene and not nepheline, favoring a tholeiitic basalt protolith for the amphibolites and hornblende gneisses (Yoder and Tilley, 1962). Positive to slightly negative europium anomalies, Eu/Eu*, in most of the mafic samples indicate that plagioclase was possibly not a major cumulative or fractionated phase (note: $Eu/Eu^* = Eu_N/((Sm_N + Gd_N)/2)$, $Eu/Eu^* < 1$ indicates a negative anomaly, $Eu/Eu^* > 1$ indicates a positive anomaly, and N subscript designates chondrite-normalized values).

Trends in covariation diagrams using SiO_2 as a fractionation index are not reliable for the mafic samples (Fig. 14) because of the probability that SiO_2 was mobile during postcrystallization processes. Despite the lack of clear trends in Figure 14, the small range of SiO_2 (~45 to 52%) in the entire suite is apparent. The noticeably lower to non-detectable concentrations of trace elements in the metagabbro-hornblende gneiss unit of the Sally Free mafic complex are evident. Covariation diagrams using the magnesium number ($Mg\# = 100\,[MgO/(MgO + FeO + Fe_2O_3)]$ assuming $Fe^{2+}/Fe^{3+} = 1.5$) as the fractionation index reveal decreasing concentrations of most trace elements (excluding Cr) with increasing Mg#; increasing concentrations of Al_2O_3 and CaO with increasing Mg#, and decreasing concentrations of MnO, TiO_2, and P_2O_5 with increasing Mg# (Fig. 15). The much higher Mg# values and lower trace element concentrations for the metagabbro-hornblende gneiss unit of the Sally Free mafic complex are attributed to its low silica content and possible cumulate nature of this unit as discussed later in the text.

Covariation diagrams using Zr as the fractionation index show trends in the majority of samples with the exception of samples with the lowest and highest concentrations of Zr (metagabbro-hornblende gneiss unit, amphibolite boudin from the Hayesville thrust

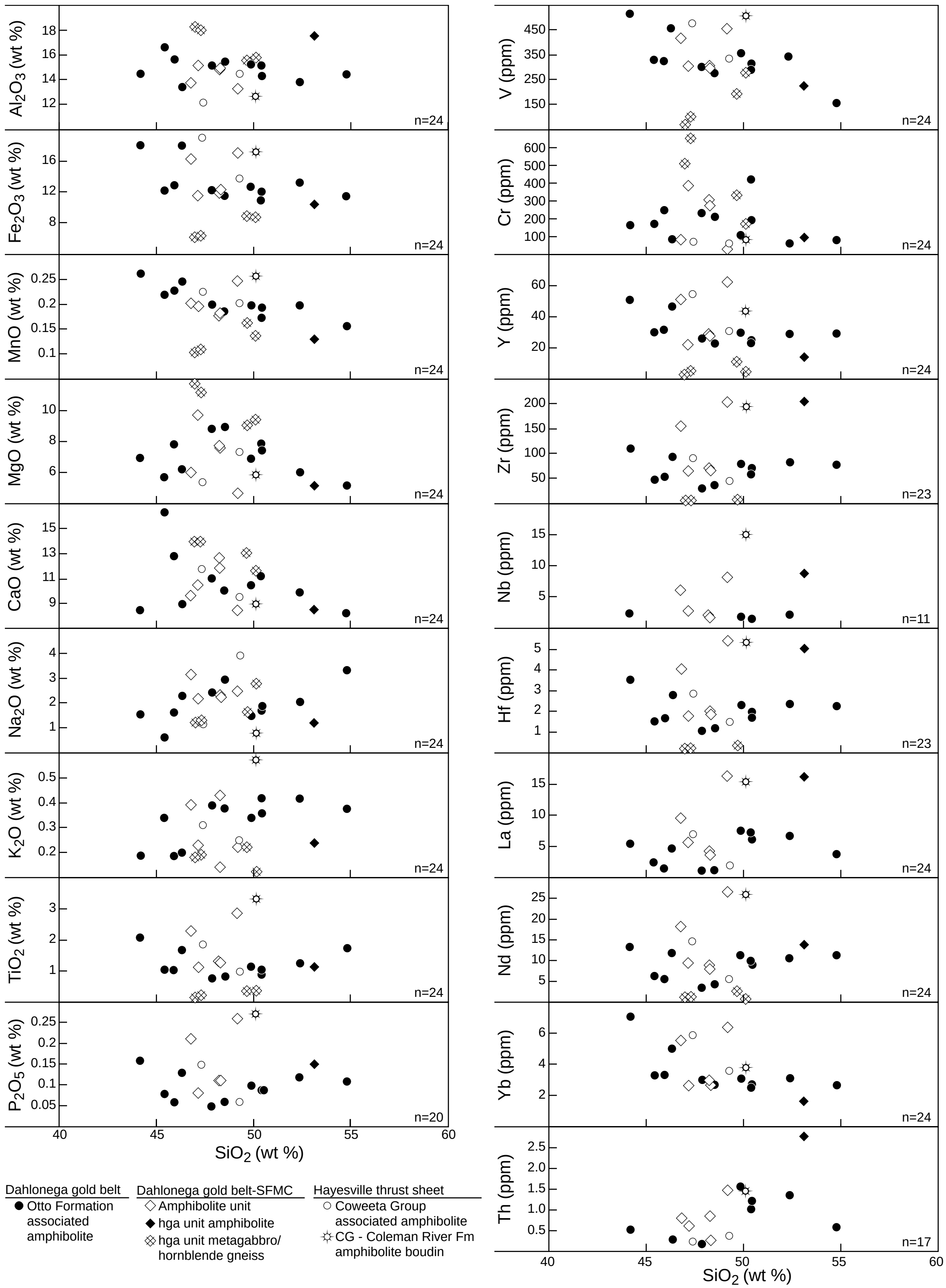

Figure 14. Harker diagrams of major oxides (wt. %) and selected trace elements (ppm) compared to SiO_2 (wt %) for mafic rock types within the Dahlonega gold belt and Hayesville thrust sheet. Refer to Figure 5 for corresponding sample numbers and abbreviations.

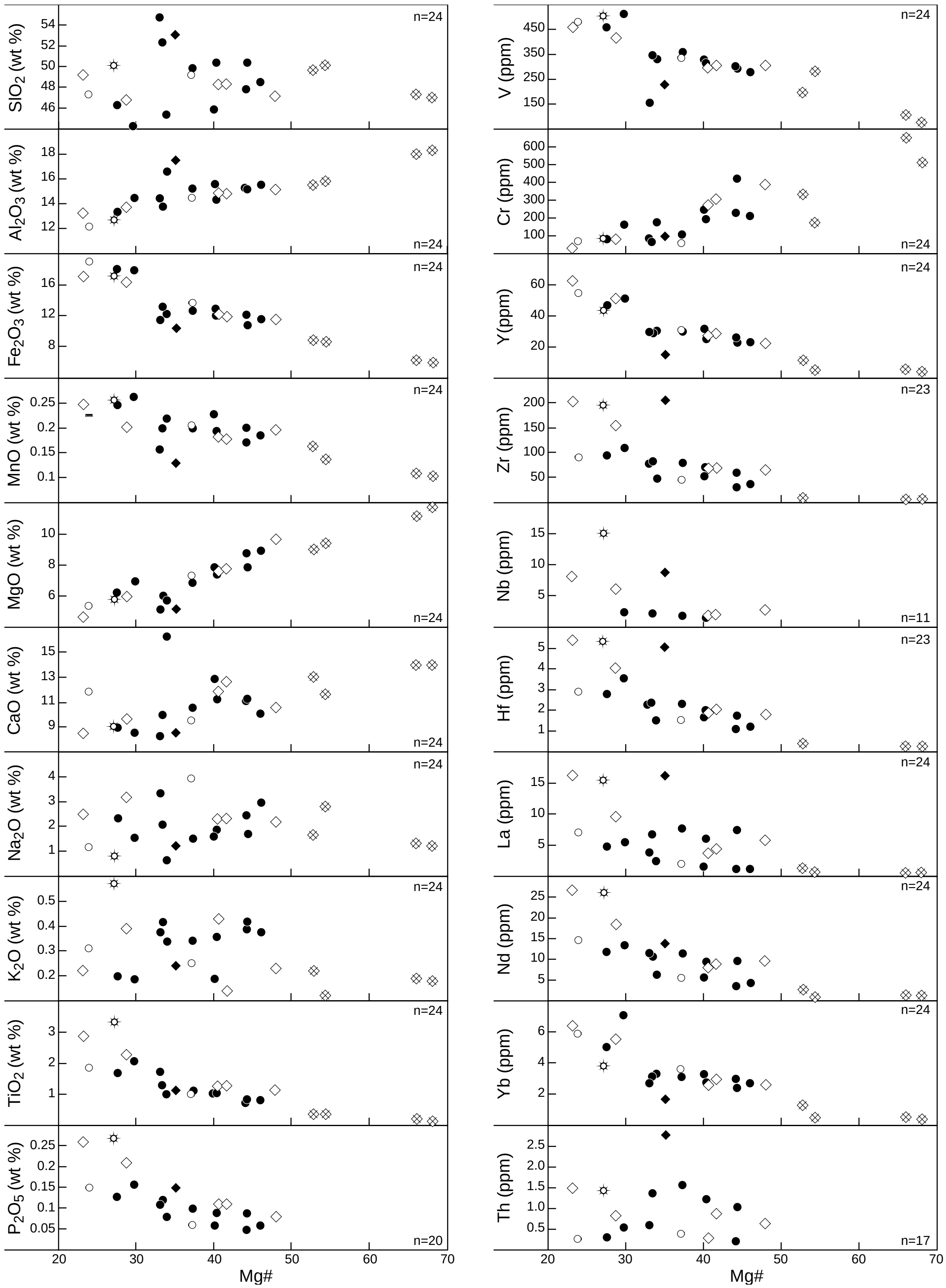

Figure 15. Harker diagrams of major oxides (wt. %) and select trace elements (ppm) compared to the magnesium number (Mg#; wt %) for mafic rock types within the Dahlonega gold belt and Hayesville thrust sheet. Refer to Figure 5 for corresponding sample numbers and abbreviations. Mg# = 100(MgO/(FeO + MnO + $2Fe_2O_3$)); FeO and Fe_2O_3 were calculated assuming Fe^{2+}/Fe^{3+} = 1.5.

sheet, and three amphibolites from the Sally Free mafic complex; Fig 16). The remaining samples show strong correlations with most major oxides and trace elements (excluding SiO_2, Fe_2O_3, MnO, MgO, Na_2O K_2O, Cr, and Th), moderate Zr fractionation, and increasing trace element concentrations with increasing Zr. Systematic variation of several major oxides and trace elements (with the exception of SiO_2, K_2O, and Na_2O) suggests that chemical alteration and element mobility within the samples was minor.

The normative minerals of the Hayesville-Soque River thrust sheet amphibolites are variable but generally dominated by either olivine or hypersthene with little to no nepheline (Table 7). The Hayesville-Soque River thrust sheet amphibolite samples have REE abundances from 6 to 50x chondrite values, show slight HREE enrichment [$(La/Yb)_N$ = 0.4 and 0.8] with the exception of sample CM-206 [$(La/Yb)_N$ = 2.7], and do not have Eu anomalies (Eu/Eu* = 0.89 to 0.99). Dahlonega gold belt amphibolites lack normative nepheline and are mostly olivine or hypersthene normative with variable, but minor, amounts of quartz (up to 7%; Table 4). The Dahlonega gold belt amphibolite samples have REE abundances from 3 to 40x chondrite values and have variable Eu anomalies (Eu/Eu* = 0.85 to 1.19) with most samples displaying slightly negative Eu/Eu* values (Fig. 13). The samples show either HREE [$(La/Yb)_N$ between 0.25 and 0.65] or slight LREE [$(La/Yb)_N$ between 1 and 2] enrichment.

The normative minerals of the Sally Free amphibolites (Table 2) are similar to that of the amphibolites in the Hayesville-Soque River thrust sheet (Table 7) and within the Otto Formation (Table 5). Sally Free complex amphibolites have moderately fractionated REE trends [$(La/Yb)_N$ between 0.91 and 1.73] and lack Eu anomalies (except sample CM-589 Eu/Eu* = 0.8). The REE trends are similar to those of the amphibolites from within the Otto Formation. Samples within the Otto Formation, however, are (as a whole) slightly more LREE enriched than samples in the Sally Free mafic complex (Fig. 13). All Sally Free hornblende gneisses are olivine-, up to 15%, and hypersthene-

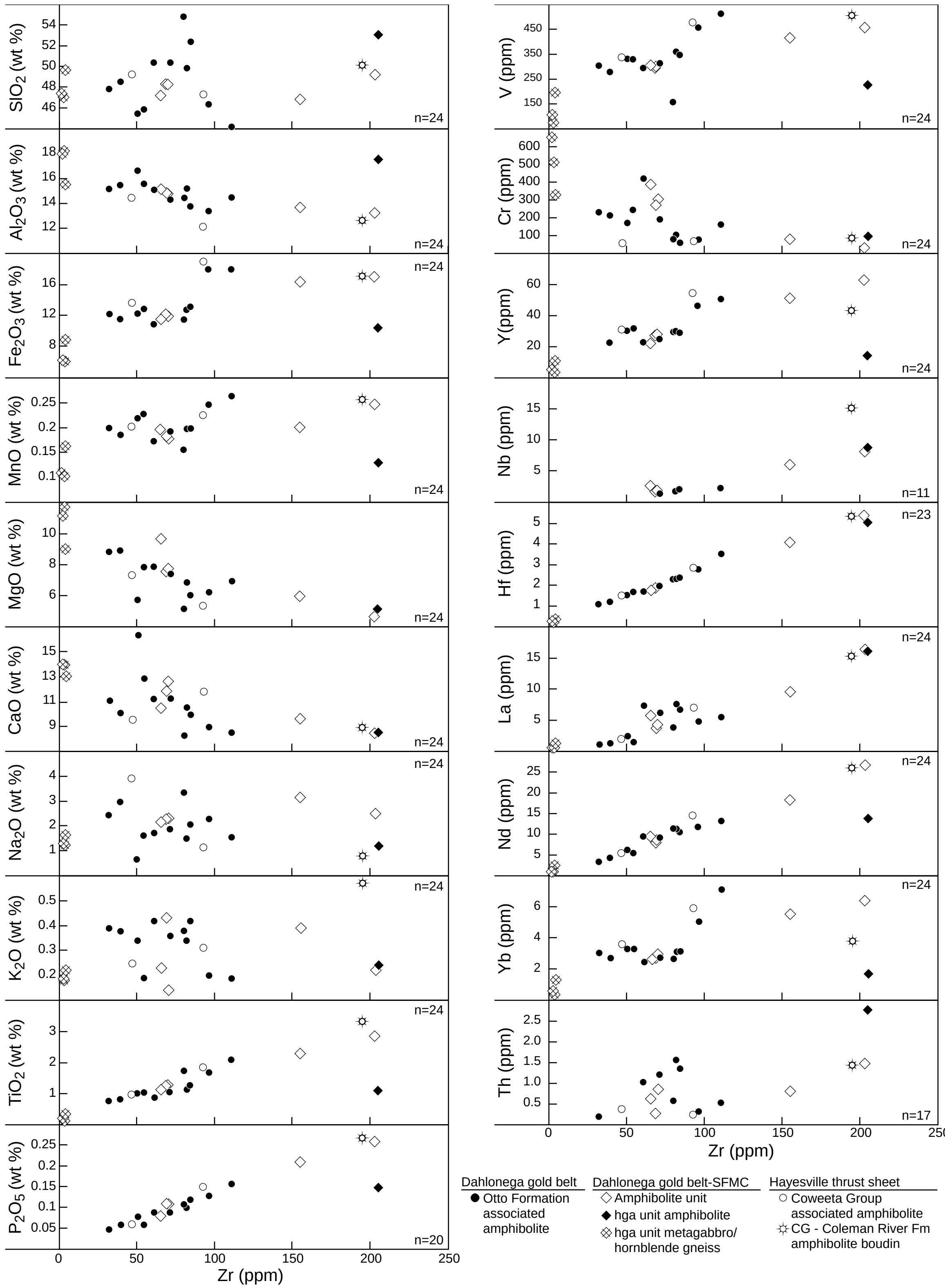

Figure 16. Harker diagrams of major oxides (wt. %) and select trace elements (ppm) compared to Zr (ppm) for mafic rock types within the Dahlonega gold belt and Hayesville thrust sheet. Refer to Figure 5 for corresponding sample numbers and abbreviations.

normative and do not contain normative quartz or nepheline (Table 3). This sample group contains the lowest REE concentrations (all less than 6x chondrite with most around 2x chondrite; Fig. 13), display positive Eu anomalies (Eu/Eu* between 1.02 to 1.85), and are slightly HREE enriched [$(La/Yb)_N$ values not illustrative].

The Cane Creek felsic gness of the Sally Free mafic complex is silica saturated (> 70% SiO_2), metaluminous, and are LREE enriched [(La/Yb_N) = 5.6 and 8.2]. The analyzed samples have low alkaline earth concentrations (Ba < 450 ppm and Sr < 150 ppm), are enriched in several large ion lithophile elements (notably Cs, Rb, K, and Ba) and high field strength elements (except Ti), and have minor negative Eu anomalies (Eu/Eu* = 0.75 and 0.63). The normative minerals of the gneiss are dominated by quartz, albite, and anorthite (Table 4). The relatively high initial $^{87}Sr/^{86}Sr$ of 0.7078 ± 0.0007 suggests that the gneiss was likely derived from upper continental crust. The initial ε_{Nd} value of –3.8 and the T_{DM} of 1410 Ma further suggest a Middle Proterozoic source (Table 8).

Zircons from the Cane Creek felsic gneiss exhibit marked oscillatory zoning (considered magmatic), are euhedral, and approximately 100 - 300 μm in length (Fig. 12). The imaged grains do not show clear evidence of polyphase growth; however, a thin (up to 10 μm wide) dark CL zone is present on some of the grains (i.e., zircon 4 of Fig. 12). These outer zones, possibly metamorphic overgrowths, were not analyzed due to the limiting size of the primary ion beam. SHRIMP analyses were concentrated on areas of maximum zoning to determine the age of magmatic growth. The SHRIMP ion probe

Table 8. Isotopic data for Cane Creek felsic gneiss sample CM-283 from the Sally Free mafic complex. Analyses performed by P. D. Fullagar at the University of North Carolina-Chapel Hill.

Age (Ma)	Rb (ppm)	Sr (ppm)	$^{87}Rb/^{86}Sr$	$^{87}Sr/^{86}Sr$ (± 2σ)†	$^{87}Sr/^{86}Sr^{(i)}$	Sm (ppm)	Nd (ppm)	$^{147}Sm/^{144}Nd$	$^{143}Nd/^{144}Nd$ (± 2σ)†	ε_{Nd}	$\varepsilon_{Nd}^{(i)}$	T_{DM}* (Ma)
481	56.1	84.46	1.925	0.721034 (10)	0.7078	2.430	12.08	0.12449	0.512215 (03)	-8.2	-3.8	1410

$^{(i)}$initial values

*T_{DM} age calculated as in DePaolo (1981)

†2σ errors are reported as last two significant digits

results for individual zircon grains are concordant and yield a single Ordovician $^{206}Pb/^{238}U$ magmatic age of 482 ± 7 Ma (2σ, MSWD = 0.2, n =10) for the Cane Creek felsic gneiss (Table 9 and Fig. 17). Uranium varies in the analyzed spots from 80 to 550 ppm and thorium varies from 25-300 ppm (Table 9).

The complex history and age of these samples greatly increase the probability of postcrystallization alteration or modification, but the mafic samples have relatively low LOI values (< 2.6%), a small SiO_2 range (most samples between 45 –52%) and low Zr/TiO_2 ratios (< 0.1, sample CM-580 = 0.018) which suggest that the samples are not highly altered (Floyd and Winchester, 1978). Several trace element ratios favor a tholeiitic protolith for the mafic samples in the area, including Nb/Y < 0.61 (Winchester and Floyd, 1977) and low sample/chondrite REE values with flat REE patterns (Cullers and Graf, 1984). Although amphibolite occurrence varies in the study area and some textural differences exist within the samples, our field evidence and geochemical data favor a common magmatic source for the amphibolites.

DISCRIMINANT APPROACH

Geochemical discrimination and classification are often used to delimit probable protolith and tectonic setting of analyzed metaigneous rocks. Although such diagrams rarely provide unequivocal confirmation of tectonic setting or protolith for metamorphosed rocks, they do provide (with supporting field data) a reliable approximation of the prior depositional, tectonic, or intrusive environment. An effort is made here to confine discrimination and classification to diagrams using minor and trace elements (Ti, Zr, Nb, Y, Hf, Th, Ta, Yb, and Rb) that are considered relatively immobile during secondary alteration processes such as submarine alteration or metamorphism (Engel and Engel, 1962; Pearce and Cann, 1971; Elliott, 1973; Pearce and Cann, 1973; Field and Elliott, 1974; Winchester and Floyd, 1976; Rollinson, 1993).

Table 9. U/Pb age data Cane Creek felsic gneiss sample CM-283 from the Sally Free mafic complex.

Spot	U (ppm)	Th (ppm)	Th/U	1σ	Pb* (ppm)	204 (ppb)	$^{204}Pb/^{206}Pb$	1σ	UO/U	1σ	$^{208}Pb/^{206}Pb$	1σ	$^{208}Pb/^{232}Th$	1σ
CCFG-1.1	338.8	129.7	0.38	3.1E-03	27	0	3.9E-05	3.8E-05	5.75	2.5E-02	0.12	2.8E-03	2.5E-02	6.9E-04
CCFG-2.1	147.7	51.6	0.35	2.5E-03	12	0	1.0E-05	0	5.49	2.3E-02	0.12	8.0E-03	2.7E-02	1.8E-03
CCFG-3.1	406.3	157.3	0.39	3.9E-03	32	0	2.5E-05	3.7E-05	6.11	4.6E-02	0.12	3.1E-03	2.4E-02	7.7E-04
CCFG-4.1	236.6	84.9	0.36	2.2E-03	19	0	1.0E-05	0	5.35	2.5E-02	0.11	2.5E-03	2.4E-02	6.3E-04
CCFG-5.1	412.5	71.3	0.17	1.6E-03	30	0	1.2E-04	6.9E-05	5.68	3.4E-02	0.05	1.5E-03	2.3E-02	7.5E-04
CCFG-6.1	208.0	68.1	0.33	3.6E-03	16	0	3.1E-05	6.0E-05	5.63	3.5E-02	0.11	3.7E-03	2.5E-02	9.9E-04
CCFG-7.1	80.4	25.2	0.31	3.9E-03	6	0	7.7E-05	1.5E-04	5.66	4.3E-02	0.10	6.5E-03	2.4E-02	1.7E-03
CCFG-8.1	172.3	80.1	0.46	3.6E-03	14	0	7.0E-05	4.9E-05	5.76	3.0E-02	0.15	6.1E-03	2.5E-02	1.1E-03
CCFG-9.1	540.2	277.8	0.51	2.0E-03	44	0	1.0E-05	6.5E-06	5.69	1.3E-02	0.17	2.8E-03	2.5E-02	4.6E-04
CCFG-10.1	197.4	63.9	0.32	2.4E-03	15	0	1.0E-05	1.9E-05	5.49	2.4E-02	0.10	3.5E-03	2.5E-02	9.2E-04

Spot	$^{206}Pb/^{238}U$	1σ	$^{207}Pb/^{235}U$	1σ	$^{207}Pb/^{206}Pb$	1σ	$^{238}U/^{206}Pb$	1σ	$^{235}U/^{207}Pb$	1σ	$^{206}Pb/^{207}Pb$	1σ
CCFG-1.1	7.8E-02	1.1E-03	6.1E-01	1.5E-02	5.7E-02	1.1E-03	12.89	1.8E-01	1.63	3.9E-02	17.47	0.32
CCFG-2.1	7.8E-02	9.8E-04	6.2E-01	2.6E-02	5.8E-02	2.2E-03	12.90	1.6E-01	1.61	6.7E-02	17.22	0.66
CCFG-3.1	7.7E-02	1.3E-03	6.0E-01	1.7E-02	5.6E-02	1.1E-03	12.94	2.2E-01	1.67	4.6E-02	17.76	0.35
CCFG-4.1	7.8E-02	8.6E-04	6.1E-01	2.7E-02	5.6E-02	2.4E-03	12.79	1.4E-01	1.65	7.4E-02	17.76	0.75
CCFG-5.1	7.6E-02	1.1E-03	5.9E-01	1.9E-02	5.6E-02	1.5E-03	13.24	2.0E-01	1.71	5.5E-02	17.78	0.48
CCFG-6.1	7.7E-02	1.1E-03	6.2E-01	2.6E-02	5.8E-02	2.2E-03	12.92	1.9E-01	1.61	6.7E-02	17.15	0.65
CCFG-7.1	7.6E-02	1.5E-03	6.1E-01	3.2E-02	5.8E-02	2.7E-03	13.11	2.6E-01	1.63	8.6E-02	17.15	0.80
CCFG-8.1	7.8E-02	1.1E-03	6.3E-01	2.6E-02	5.9E-02	2.1E-03	12.87	1.9E-01	1.58	6.4E-02	16.94	0.61
CCFG-9.1	7.8E-02	5.2E-04	6.1E-01	9.2E-03	5.7E-02	7.2E-04	12.87	8.6E-02	1.63	2.4E-02	17.49	0.22
CCFG-10.1	7.9E-02	9.6E-04	6.1E-01	1.5E-02	5.7E-02	1.2E-03	12.73	1.6E-01	1.63	4.1E-02	17.69	0.36

Spot	AGE $^{238}U/^{232}Th$ (in Ma)	1σ	AGE $^{206}Pb/^{238}U$ (in Ma)	1σ	AGE $^{207}Pb/^{235}U$ (in Ma)	1σ	AGE $^{207}Pb/^{206}Pb$ (in Ma)	1σ	% Concord-ant
CCFG-1.1	494.19	13.57	481.60	6.32	485.00	9.35	501.14	40.80	96.10
CCFG-2.1	542.47	35.84	481.37	5.88	490.35	16.40	532.52	86.20	90.40
CCFG-3.1	473.22	15.30	479.95	7.83	477.28	10.62	464.49	44.89	103.30
CCFG-4.1	489.00	12.47	485.42	5.14	481.76	17.32	464.42	95.99	104.50
CCFG-5.1	452.25	14.92	469.51	6.73	468.20	12.20	461.82	60.82	101.70
CCFG-6.1	501.73	19.57	480.46	6.65	491.14	16.46	541.28	84.51	88.80
CCFG-7.1	486.92	33.03	473.92	8.91	485.58	20.57	541.02	105.42	87.60
CCFG-8.1	501.41	21.70	482.47	6.78	497.60	15.99	567.80	79.94	85.00
CCFG-9.1	500.68	9.05	482.37	3.11	485.05	5.79	497.75	27.96	96.90
CCFG-10.1	500.52	18.24	487.68	5.74	485.10	9.78	472.93	46.29	103.10

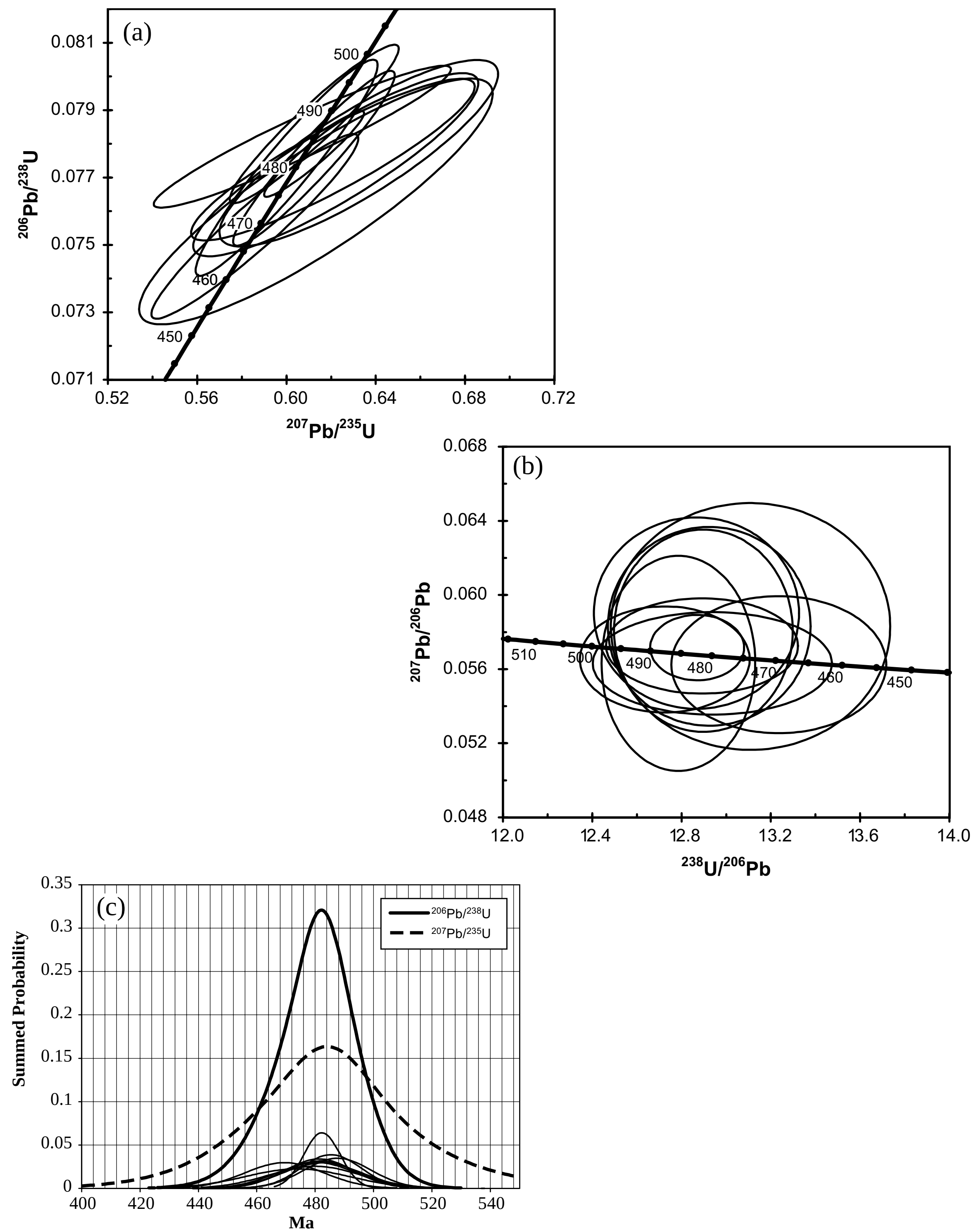

Figure 17. Concordia and age probability plots of Cane Creek felsic gneiss IMP zircon data. a) Conventional concordia plot (Wetherill, 1956). b) Tera-Wasserburg concordia plot (Tera and Wasserburg, 1972). c) Summed age probability plot (smaller curves represent individual 206Pb/238U probability plots for each spot). Note that ISOPLOT v 2.49 written by K. Ludwig was used to create the concordia plots with ratios obtained from Lead 6.5 written by the Ion Probe Group (Stanford University and USGS).

Nine of the twenty amphibolite samples analyzed were excluded from Nb discriminant diagrams because of Nb concentrations below detectable limits. Samples lacking Nb include CM-402 from the Sally Free mafic complex (Table 3); CM-24, -159, -266, -432, -456, -526, and CM-744 from within the Otto Formation (Table 6); and CM-19 and CM-402 from the Hayesville-Soque River thrust sheet (Table 7). Hornblende gneiss/ metagabbro samples CM-515, -516, -613, CM-858 from the Sally Free mafic complex have also been excluded from several diagrams because of low or undetectable concentrations of Nb, Zr, Ti, and Y (Table 3). Low absolute concentrations of these minor and trace elements are attributed to dilution related to the possible cumulate nature of this unit; thus, these samples are inappropriate for discrimination.

Discriminant diagrams of Pearce and Cann (1973) apply to tholeiitic basalts in the compositional range 12% < CaO + MgO < 20%. Four of the twenty amphibolite samples analyzed, including DG-6, CM-402, CM-266, and CM-526, contain MgO+CaO values (20.4, 20.2, 22.1 and 20.7, respectively) greater than the range defined by Pearce and Cann (1973). Data from three of the four samples, excluding CM-266 (CaO+MgO = 22.6), have been plotted on all classification and discriminant diagrams for comparison. The four hornblende gneiss/metagabbro samples discussed previously, considered cumulate, also contain high total MgO+CaO content (21.0 to 25.7).

PROTOLITH

Rocks within the Sally Free mafic complex are considered igneous in origin primarily on the basis of mafic to felsic rock assemblage present. Determining the protoliths of amphibolites within the Otto Formation and Hayesville-Soque River thrust sheet, occurring at various scales from discontinuous pods to distinctive, continuous layers, is more difficult due to the interlayered relationship between amphibolite and thick metasedimentary rock.

The Sally Free mafic complex contains a mixed suite of mafic to felsic rocks with a definable, partially layered, stratigraphy. The complex contains, from west to east, hornblende gneiss/metagabbro (metadiorite/metagabbro), minor intermediate gneiss (andesitic, shallow intrusive?), felsic gneiss (rhyodacitic, shallow intrusive/extrusive), and amphibolite (basalt, shallow intrusive/extrusive; Fig. 2). The metagabbro-hornblende gneiss-amphibolite unit dominating the western limit of the complex (Fig. 2) contains poorly foliated, coarse-grained metagabbro (Fig. 8) considered intrusive in origin. The lack of pervasive deformation within the metagabbro is attributed to a contrast in competency between a relatively dry rigid metagabbro (Fig. 8) composed predominantly of hornblende and the surrounding less competent hornblende gneiss (metadiorite) containing abundant plagioclase (Fig. 7). The massive, poorly foliated metagabbro grades into the more pervasively deformed hornblende gneiss (metagabbro/metadiorite).

The intermediate gneiss unit occurs discontinuously between the hornblende gneiss-metagabbro-amphibolite and the Cane Creek felsic gneiss units (Fig. 2). This unit (not analyzed in this study) contains fine-grained, porphyroclastic, biotite/hornblende gneiss mesosome of intermediate composition surrounded by poorly foliated felsic gneiss leucosome (Fig. 4). The migmatitic nature, relative location (between hornblende and felsic gneiss), and limited occurrence of this intermediate unit could be indicative of a mixed minimum-melt migmatite containing both mafic and felsic constituents of the surrounding units.

The Cane Creek felsic gneiss unit is strongly foliated and lineated (Fig. 5) and contains no relict textures indicating probable protolith. The felsic gneiss most likely represents a shallow intrusive, possibly extrusive, felsite (rhyodacitic). The Cane Creek felsic gneiss unit occurs to the east of, and possibly above, hornblende gneiss/metagabbro and to the west of, and possibly below, the large body of amphibolite. The large amphibolite body, which marks the eastern limit of the complex, is presumed basaltic with possible relict extrusive textures (amygdules?) observed within a very fine-grained amphibolite outcrop at sample locality CM-301 (Figs. 2 and 6). Contacts between the amphibolite and felsic gneiss units are clearly defined and sharp. Although the Sally Free mafic complex has a definable, possibly layered, stratigraphy, it is not considered to be a differentiated, intrusive body.

Ortho- and Paragneiss Discrimination:

Chemical data obtained from the 24 mafic rocks samples analyzed, including the Sally Free mafic complex, Otto Formation associated amphibolites, and amphibolites from the Hayesville-Soque River thrust sheet were plotted on a ortho- and para-amphibolite discriminate diagram after Leake (1964; Fig. 18). The Leake diagram, which defines chemical trends of known ortho- and para-amphibolites, is commonly used to differentiate between igneous and sedimentary amphibolite protolith. The data plotted here closely parallel the trend defined for early to late igneous rocks (Fig. 18).

Volcanic Rock Classification

Data obtained from 11 fine-grained amphibolite samples, presumed to have basalt protoliths, and two Cane Creek felsic gneiss samples, possibly extrusive or shallow intrusive, were plotted on the Zr/TiO_2 – Nb/Y diagram of Winchester and Floyd (1977) to differentiate volcanic composition (Fig. 19). The volcanic rock classification diagram of Winchester and Floyd (1977) provides broad distinctions between degrees of alkalinity (alkaline, subalkaline) and differentiation products (basic, intermediate, acidic) with no distinction made between tholeiitic or calc-alkali suites.

The five samples analyzed from the amphibolite unit located on the eastern limit of the Sally Free mafic complex (DG-6, CM-287, -301, -402, and CM-589) are classified as andesitic/basaltic (Fig. 19). Also, as previously discussed, the hornblende gneiss/ metagabbro appears to be intrusive and thus should be excluded from volcanic rock classification. One sample (CM-580) of fine-grained amphibolite from the hornblende

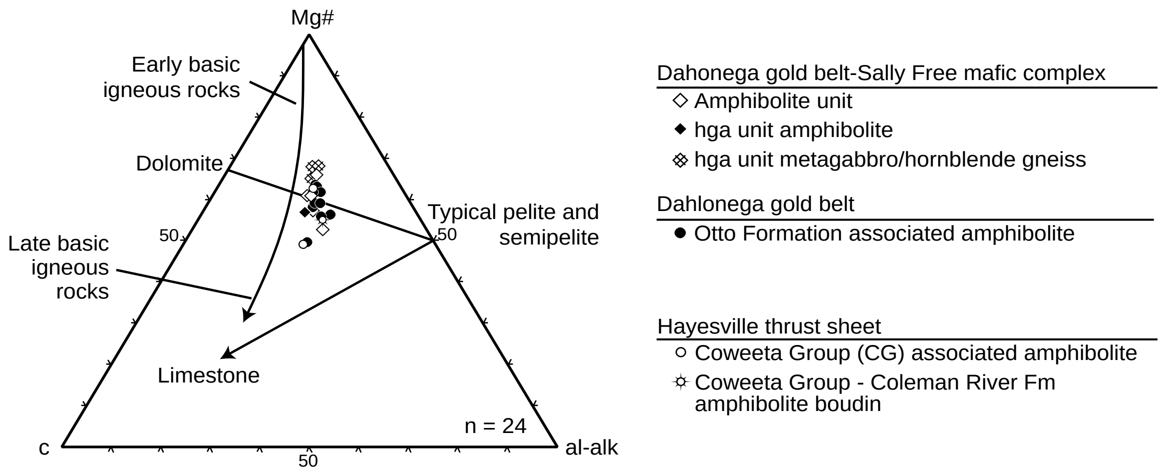

Figure 18. Ortho- and para-amphibolite discrimination diagram after Leake (1964). Amphibolite and metagabbro/hornblende gneiss chemical data from the Dahlonega gold belt and Hayesville thrust sheet plotted. Mg# = 100(MgO/(FeO + MnO + 2Fe_2O_3)); c = CaO; al-alk = Al_2O_3-(K_2O + Na_2O), all in weight percent. Note that FeO and Fe_2O_3 were calculated assuming Fe^{3+}/Fe^{2+} = 0.15; hga - hornblende gneiss-metagabbro-amphibolite.

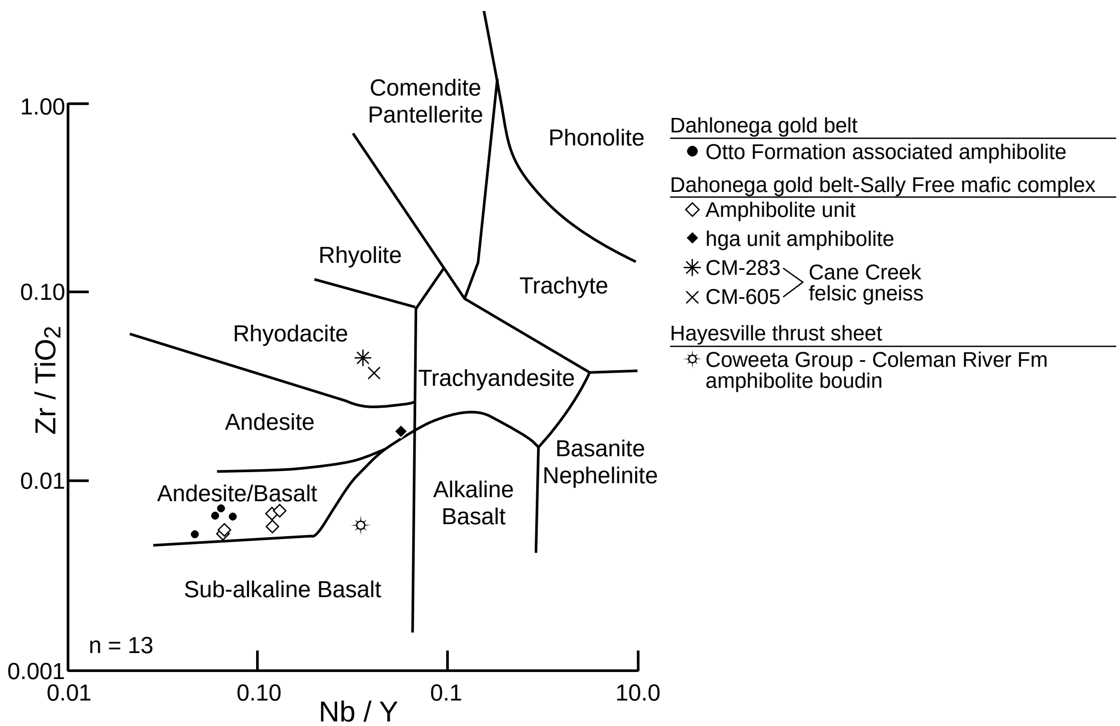

Figure 19. Zr/TiO_2 - Nb/Y volcanic rock classification diagram after Winchester and Floyd (1977). Amphibolite and felsic gneiss chemical data from the Dahlonega gold belt and amphibolite boudin data from within the Hayesville thrust sheet plotted. hga - hornblende gneiss-metagabbro-amphibolite.

gneiss-metagabbro-amphibolite unit contained sufficient Nb and Y for classification here (Table 3 and Fig. 19). Due to higher ratios of Zr/TiO_2 and Nb/Y relative to other analyzed amphibolite samples, sample CM-580 is the only sample to plot within the andesite field on the classification diagram (Fig. 19). The two felsic gneiss samples analyzed from the Cane Creek felsic gneiss unit, CM-283 and CM-605, plotted within the rhyodacite field (Fig. 19).

Similar to the samples from the amphibolite unit within the Sally Free mafic complex, the Otto Formation amphibolite samples (CM-60, -62, -111, and CM-629) plot as andesite/basalt (Fig. 19). According to the classification diagram, sample CM-206, an amphibolite boudin from within the Coweeta Group, Coleman River Formation, is the only sub-alkaline basalt analyzed (Fig. 19). The remaining two Coweeta Group samples (CM-19 and CM-490) lacked detectable concentrations of Nb for classification (Table 7).

Magma Type Discrimination

Amphibolite samples have been further classified with the use of geochemical magma type discrimination diagrams defined by Winchester and Floyd (1976) and Floyd and Winchester (1975). These diagrams primarily provide a distinction between alkali and tholeiitic basalts. The $Nb/Y\text{-}Zr/P_2O_5$ diagram (Floyd and Winchester, 1975; Fig. 20) only provides slight separation between tectonic environments (e.g., continental versus oceanic). Amphibolite samples from both the Dahlonega gold belt and Hayesville-Soque River thrust sheet plot within the tholeiitic field on the $TiO_2\text{-} Zr/P_2O_5$ and $Nb/Y\text{-}Zr/P_2O_5$ diagrams (Floyd and Winchester, 1975; Winchester and Floyd, 1976; Fig. 20).

TECTONOMAGMATIC DISCRIMINATION

Geochemical tectonic discrimination of recent magmas, refined and popularized by Pearce and Cann (1971, 1973) for basaltic chemistry, is commonly used to determine a probable paleotectonic environment of metaigneous rocks (e.g., Winchester and Floyd, 1976; Spell and Norrell, 1990; Misra and Conte, 1991). Basalt, granite, and sedimentary

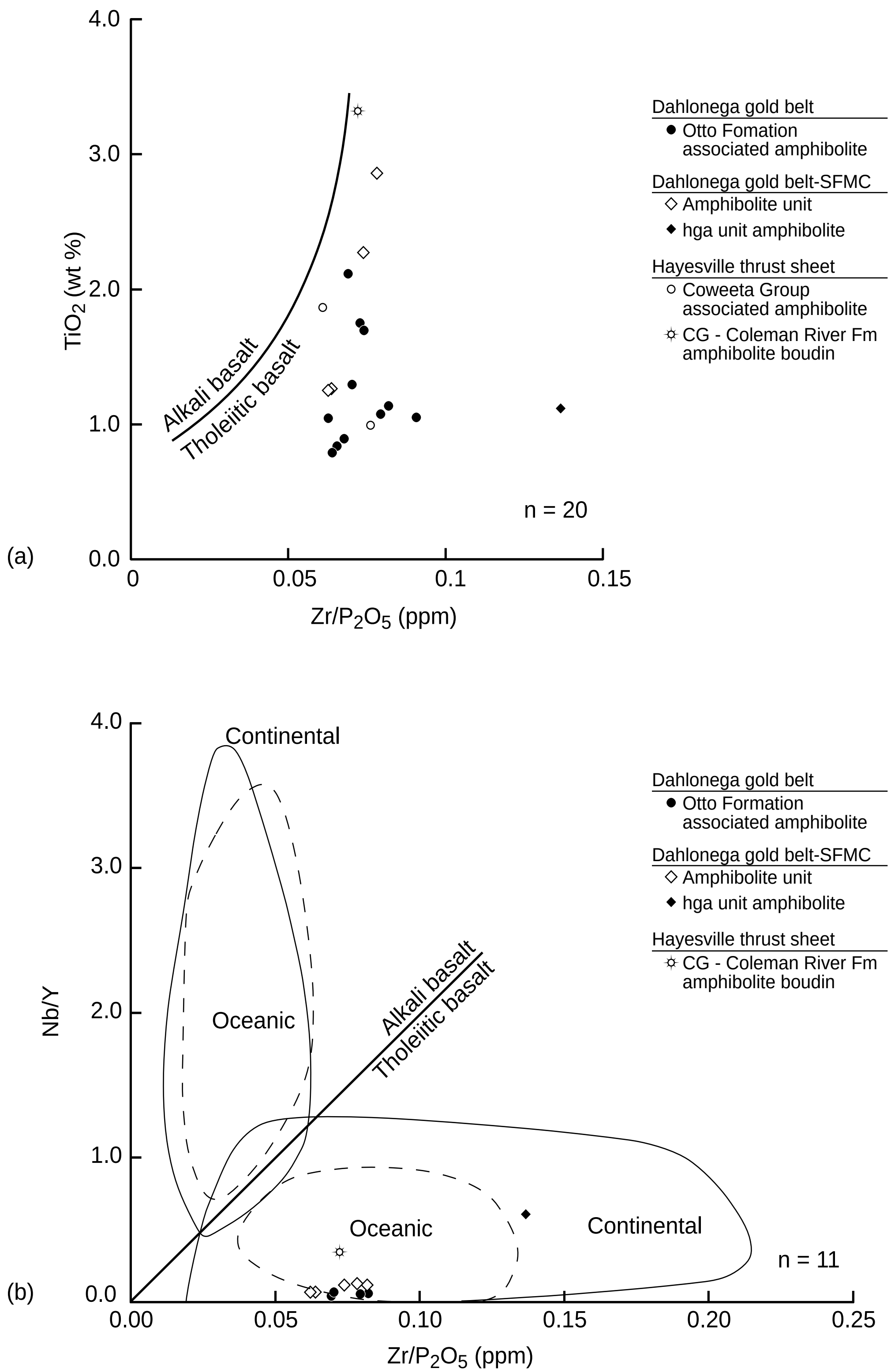

Figure 20. a) TiO_2-Zr/P_2O_5 and (b) Nb/Y-Zr/P_2O_5 magma type discrimination diagrams after Winchester and Floyd (1976) and Floyd and Winchester (1975). Amphibolite (metabasalt) chemical data from the Dahlonega gold belt and Hayesville thrust sheet plotted.

rock discrimination diagrams define numerous tectonic environments including ocean ridges (N- and E-type MORB, incipient spreading center, and fore- and back-arc basin); volcanic arc basalts (active continental margin, tholeiitic and calc-alkali dominant); collisional settings (continent-continent and continent-arc); intraplate settings (intra-continental normal and attenuated crust and ocean-island); and passive continental margins (Rollinson, 1993).

Amphibolite and felsic gneiss minor and trace element chemistry is employed from the Dahlonega gold belt and (in part) the Hayesville-Soque River thrust sheet to delimit the paleotectonic environment of metaigneous rocks in the study area. The use of relatively immobile minor and trace elements (Ti, Zr, Y, Nb, Y, Hf, Th, Ta, Yb, and Rb) provides the most reliable correlation between modern igneous rock signatures with older orogenic metaigneous rocks. Tectonic discrimination diagrams for basalts used here include diagrams after Pearce and Cann (1973; Fig. 21), Pearce and Norry (1979; Fig. 22), Wood (1980; Fig. 23), Pearce (1982, 1983; Figs. 24 and 25), and Meschede (1986; Fig. 26). Discriminant diagrams for felsic rocks (granites) after Pearce *et al.* (1984; Fig. 27) and Harris *et al.* (1986; Fig. 28) are used to define a tectonic environment for the Cane Creek felsic gneiss. Samples from the Sally Free mafic complex hornblende gneiss-metagabbro-amphibolite unit (CM-515, -516, -580, -613, and CM -858), not considered basaltic in origin, have been excluded from the discrimination diagrams.

The use of published data from numerous metaigneous rock occurrences within the southern Appalachian gold belt further delimits the paleotectonic environment of Dahlonega gold belt. An attempt was made to choose published chemical data (including trace elements) of Dahlonega gold belt metaigneous rocks to the southwest (German, 1989; Spell and Norrell, 1990) and northeast (Gillon, 1989; Hopson, 1994) of the study area. Amphibolite and felsic gneiss geochemical data from the Ropes Creek assemblage, near Villa Rica, Georgia (Spell and Norrell, 1990), represent the southwestern-most data

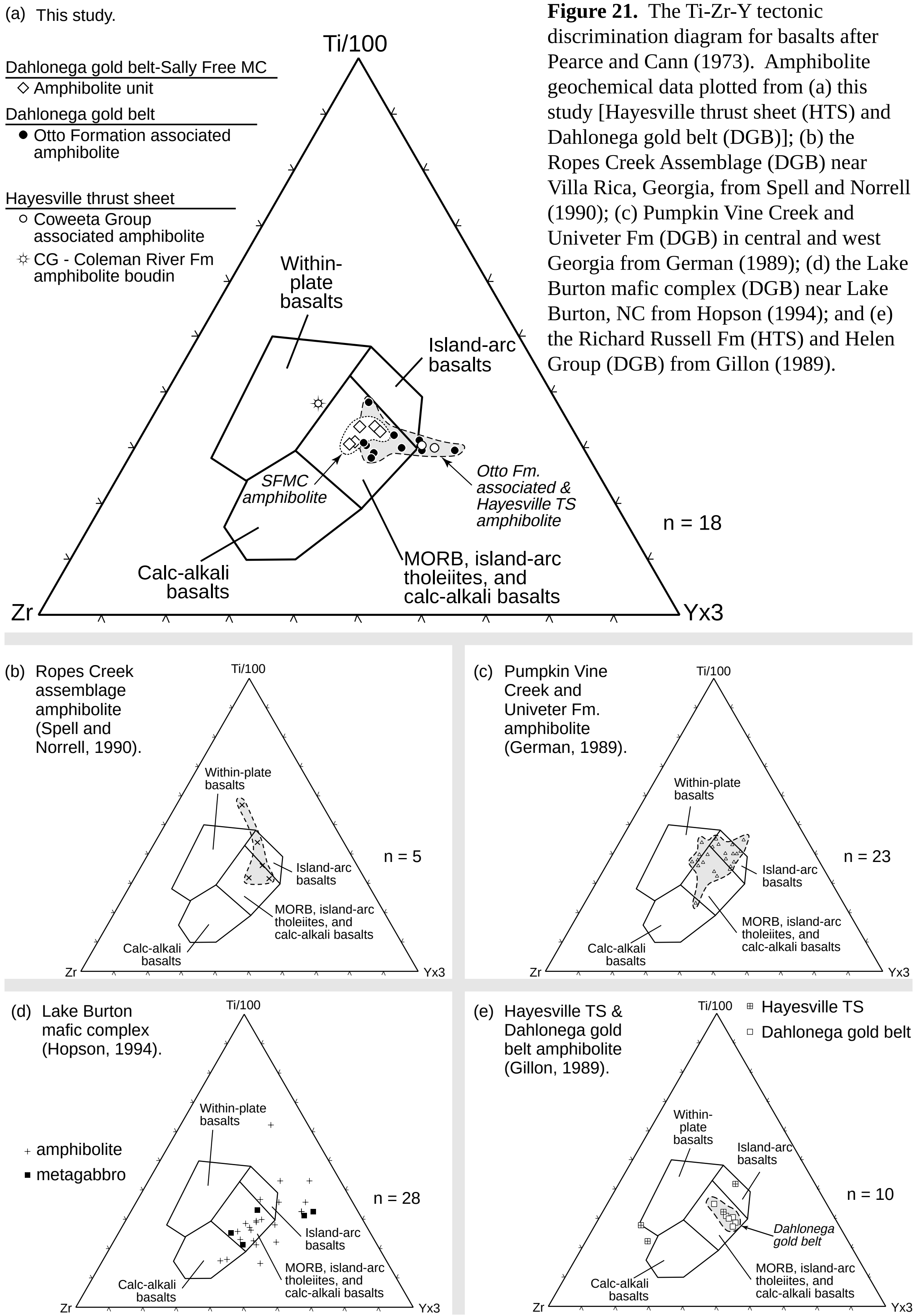

Figure 21. The Ti-Zr-Y tectonic discrimination diagram for basalts after Pearce and Cann (1973). Amphibolite geochemical data plotted from (a) this study [Hayesville thrust sheet (HTS) and Dahlonega gold belt (DGB)]; (b) the Ropes Creek Assemblage (DGB) near Villa Rica, Georgia, from Spell and Norrell (1990); (c) Pumpkin Vine Creek and Univeter Fm (DGB) in central and west Georgia from German (1989); (d) the Lake Burton mafic complex (DGB) near Lake Burton, NC from Hopson (1994); and (e) the Richard Russell Fm (HTS) and Helen Group (DGB) from Gillon (1989).

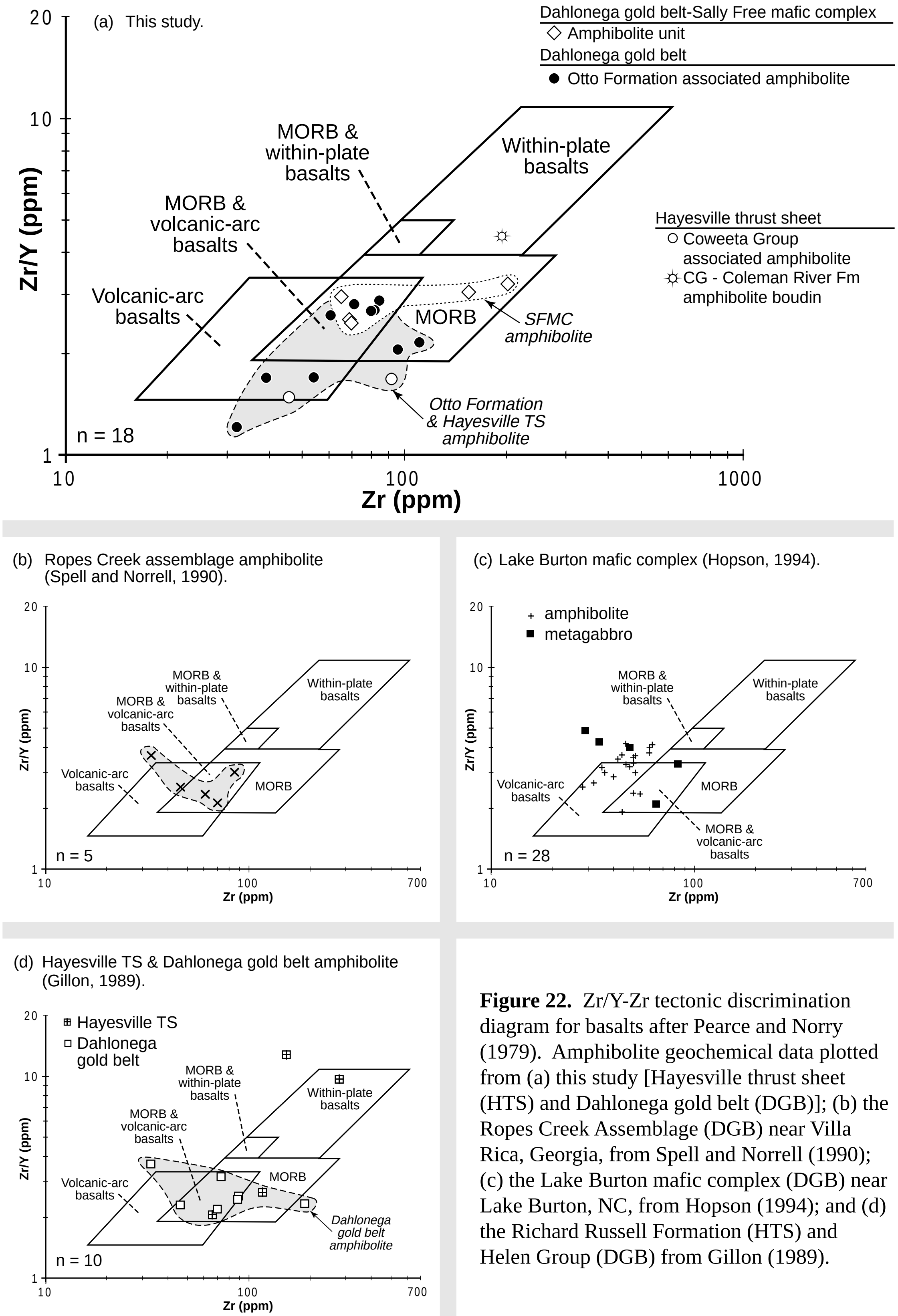

Figure 22. Zr/Y-Zr tectonic discrimination diagram for basalts after Pearce and Norry (1979). Amphibolite geochemical data plotted from (a) this study [Hayesville thrust sheet (HTS) and Dahlonega gold belt (DGB)]; (b) the Ropes Creek Assemblage (DGB) near Villa Rica, Georgia, from Spell and Norrell (1990); (c) the Lake Burton mafic complex (DGB) near Lake Burton, NC, from Hopson (1994); and (d) the Richard Russell Formation (HTS) and Helen Group (DGB) from Gillon (1989).

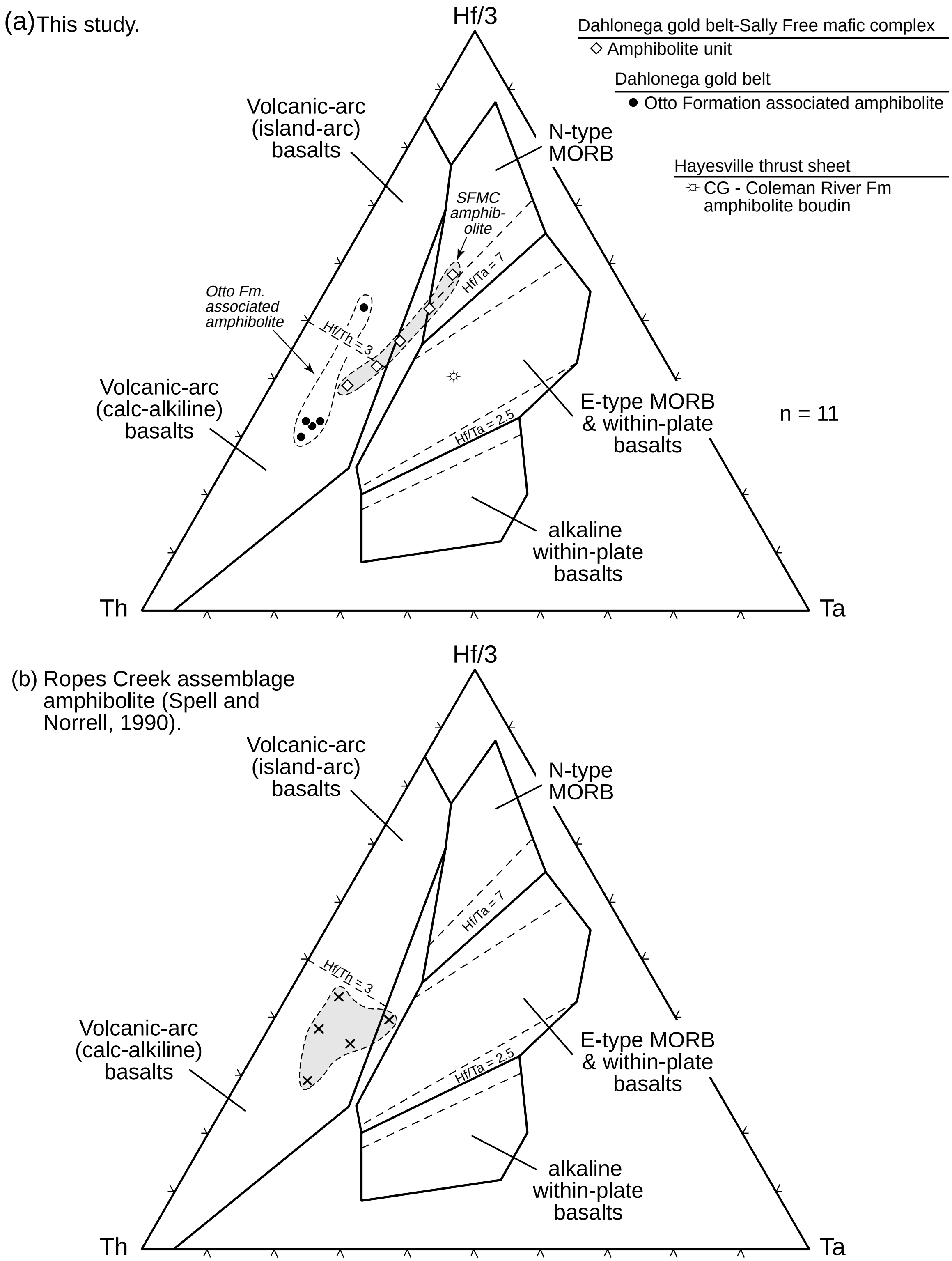

Figure 23. Hf-Th-Ta tectonic discrimination diagram for basalts after Wood (1980). Amphibolite geochemical data plotted from (a) this study [Hayesville thrust sheet (HTS) and Dahlonega gold belt (DGB)]; and (b) the Ropes Creek Assemblage (DGB) near Villa Rica, Georgia, from Spell and Norrell (1990).

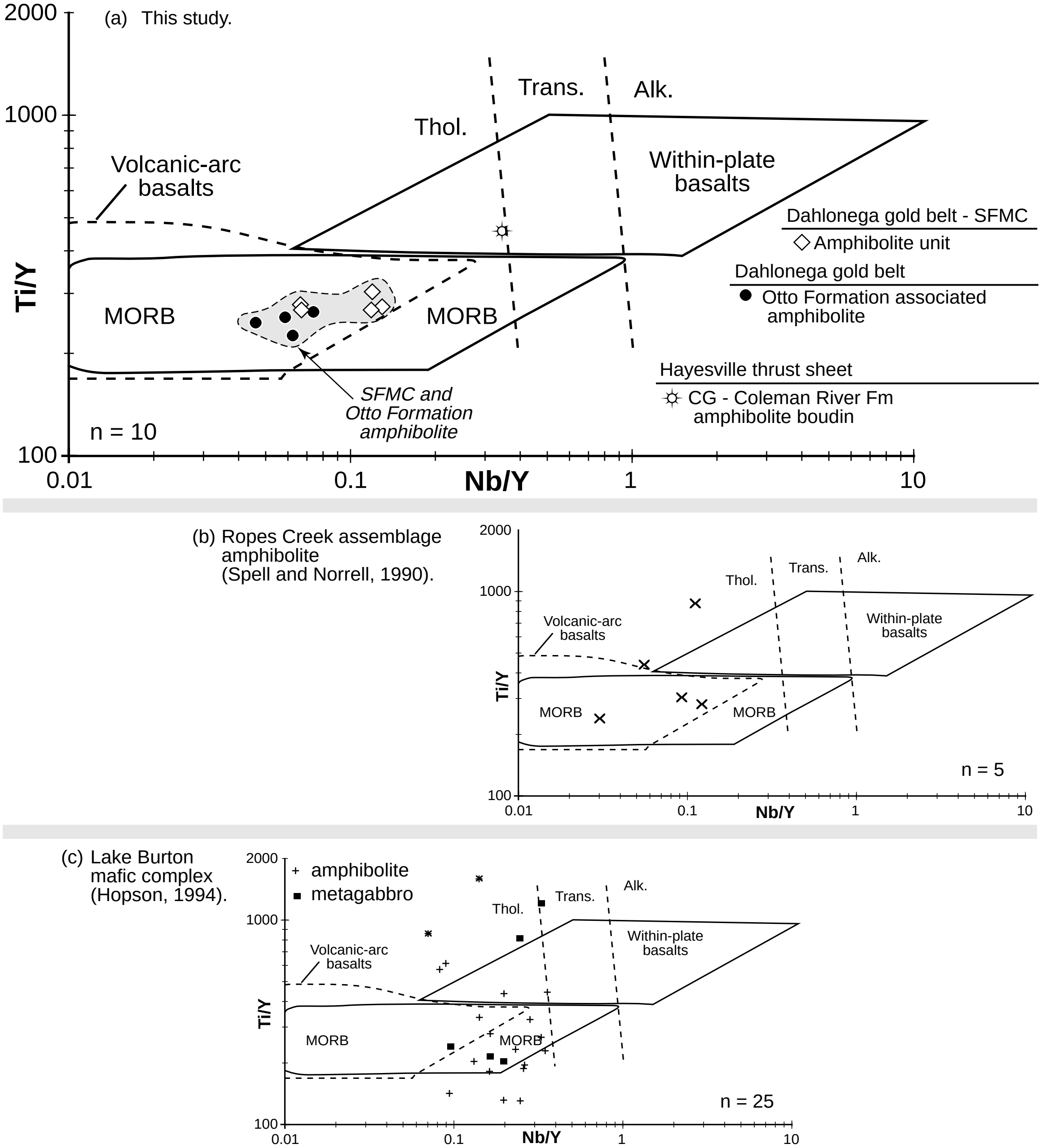

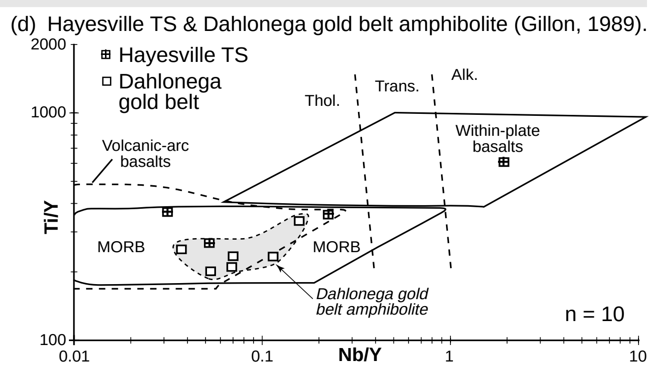

Figure 24. Ti/Y-Nb/Y tectonic discrimination diagram for basalts after Pearce (1982). Amphibolite geochemical data plotted from (a) this study [Hayesville thrust sheet (HTS) and Dahlonega gold belt (DGB)]; (b) the Ropes Creek Assemblage (DGB) near Villa Rica, Georgia, from Spell and Norrell (1990); (c) the Lake Burton mafic complex (DGB) near Lake Burton, NC, from Hopson (1994); and (d) the Richard Russell Formation (HTS) and Helen Group (DGB) from Gillon (1989).

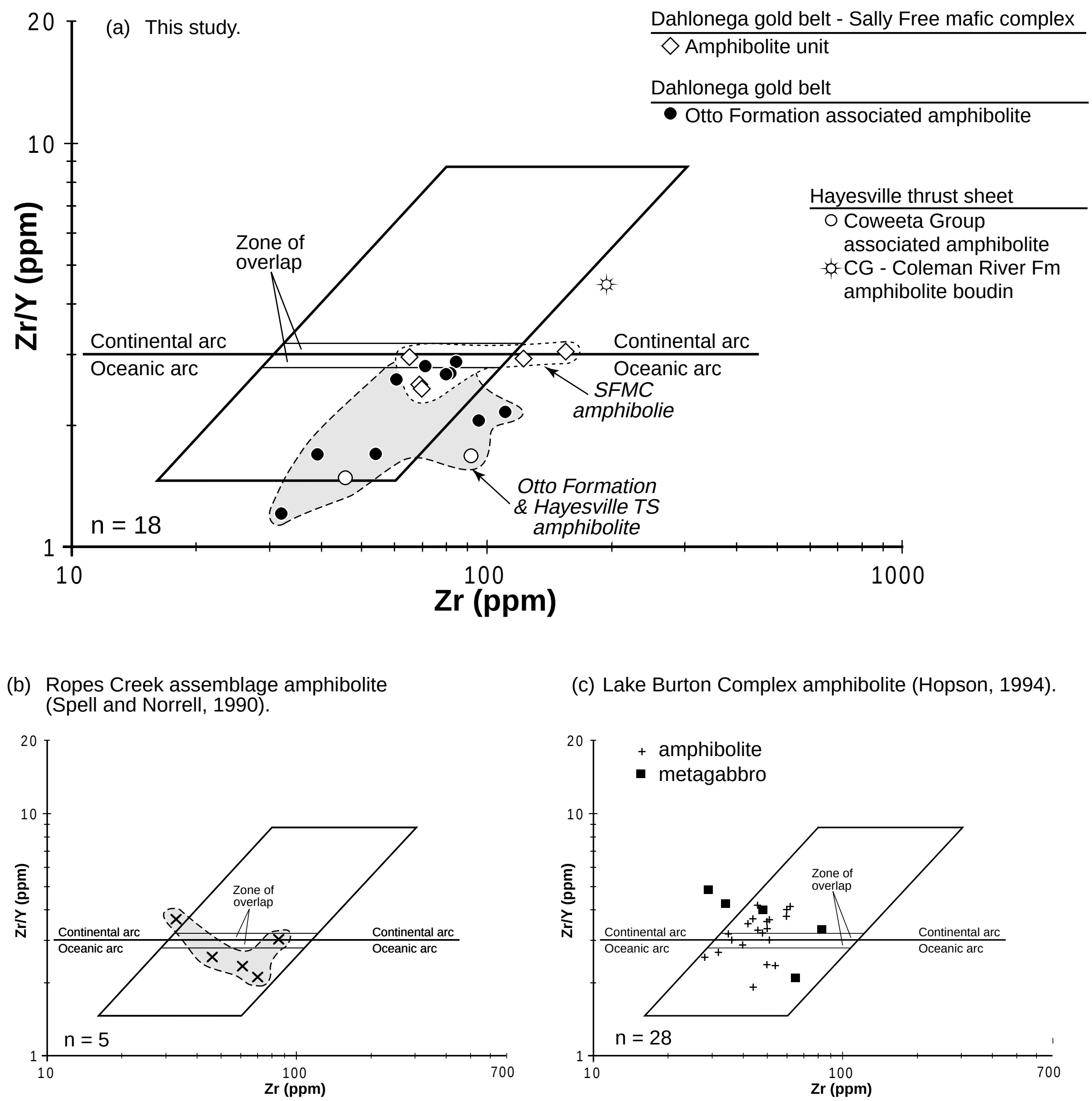

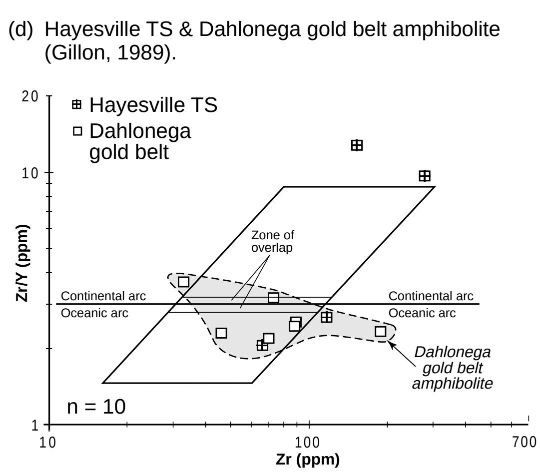

Figure 25. Zr/Y-Zr tectonic discrimination diagram for basalts after Pearce (1983). Fields defined for continental and oceanic-arc basalts, separated on the basis of a Zr/Y value of 3. Field of overlap indicated. Amphibolite geochemical data plotted from (a) this study [Hayesville thrust sheet (HTS) and Dahlonega gold belt (DGB)]; (b) the Ropes Creek Assemblage (DGB) near Villa Rica, Georgia, from Spell and Norrell (1990); (c) the Lake Burton mafic complex (DGB) near Lake Burton, NC, from Hopson (1994); and (d) the Richard Russell Formation (HTS) and Helen Group (DGB) from Gillon (1989).

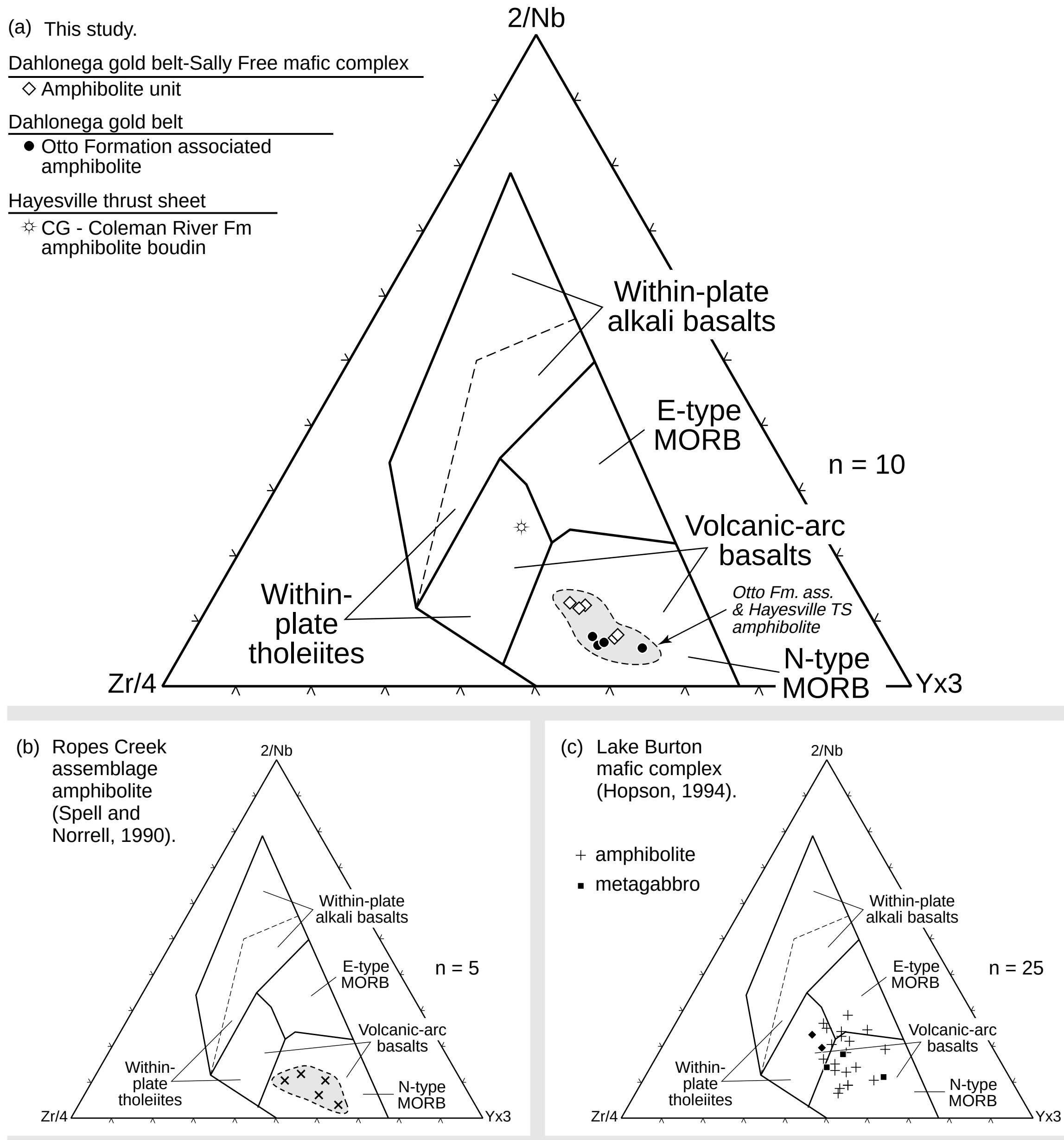

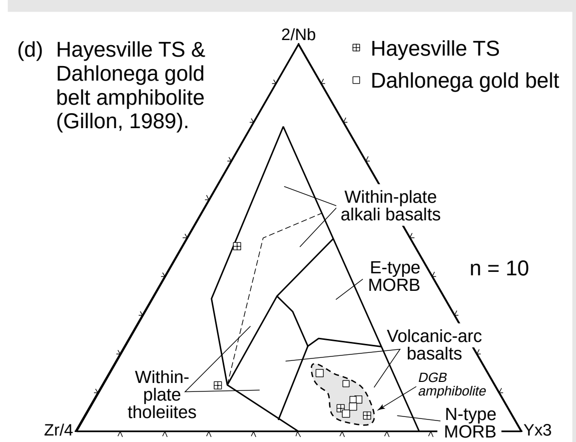

Figure 26. Nb-Zr-Y tectonic discrimination diagram for basalts after Meschede (1986). Amphibolite geochemical data plotted from (a) this study [Hayesville thrust sheet (HTS) and Dahlonega gold belt (DGB)]; (b) the Ropes Creek Assemblage (DGB) near Villa Rica, Georgia, from Spell and Norrell (1990); (c) the Lake Burton mafic complex (DGB) near Lake Burton, NC, from Hopson (1994); and (d) the Richard Russell Formation (HTS) and Helen Group (DGB) from Gillon (1989).

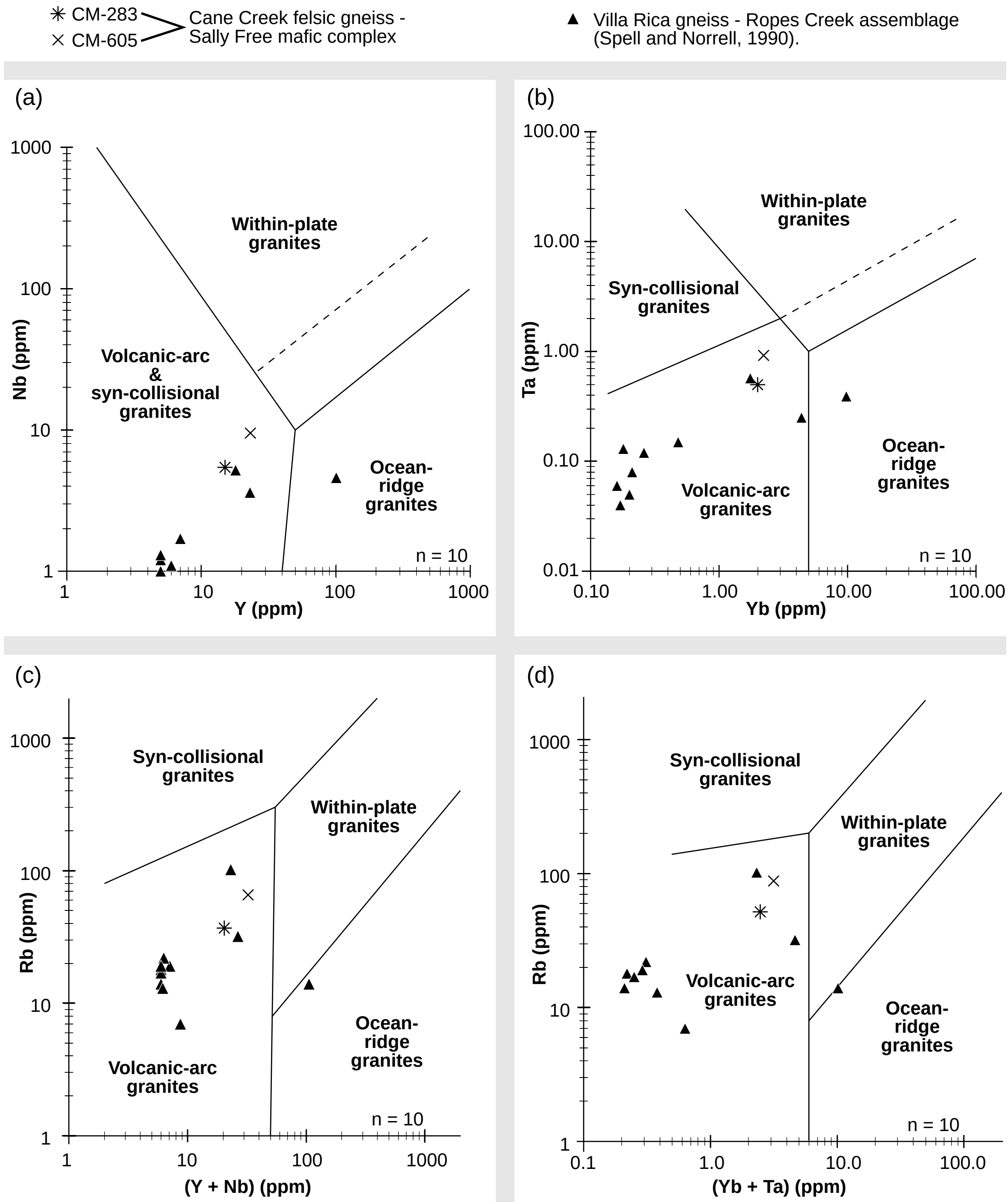

Figure 27. Nb-Y, Ta-Yb, Rb-(Y+Nb), and Rb-(Yb+Ta) tectonic discrimination diagrams (a, b, c, and d, respectively) for granites after Pearce *et al.* (1984). Felsic metaigneous rock geochemical data plotted from the Sally Free mafic complex Cane Creek felsic gneiss (this study) and the Villa Rica gneiss (Spell and Norrell, 1990).

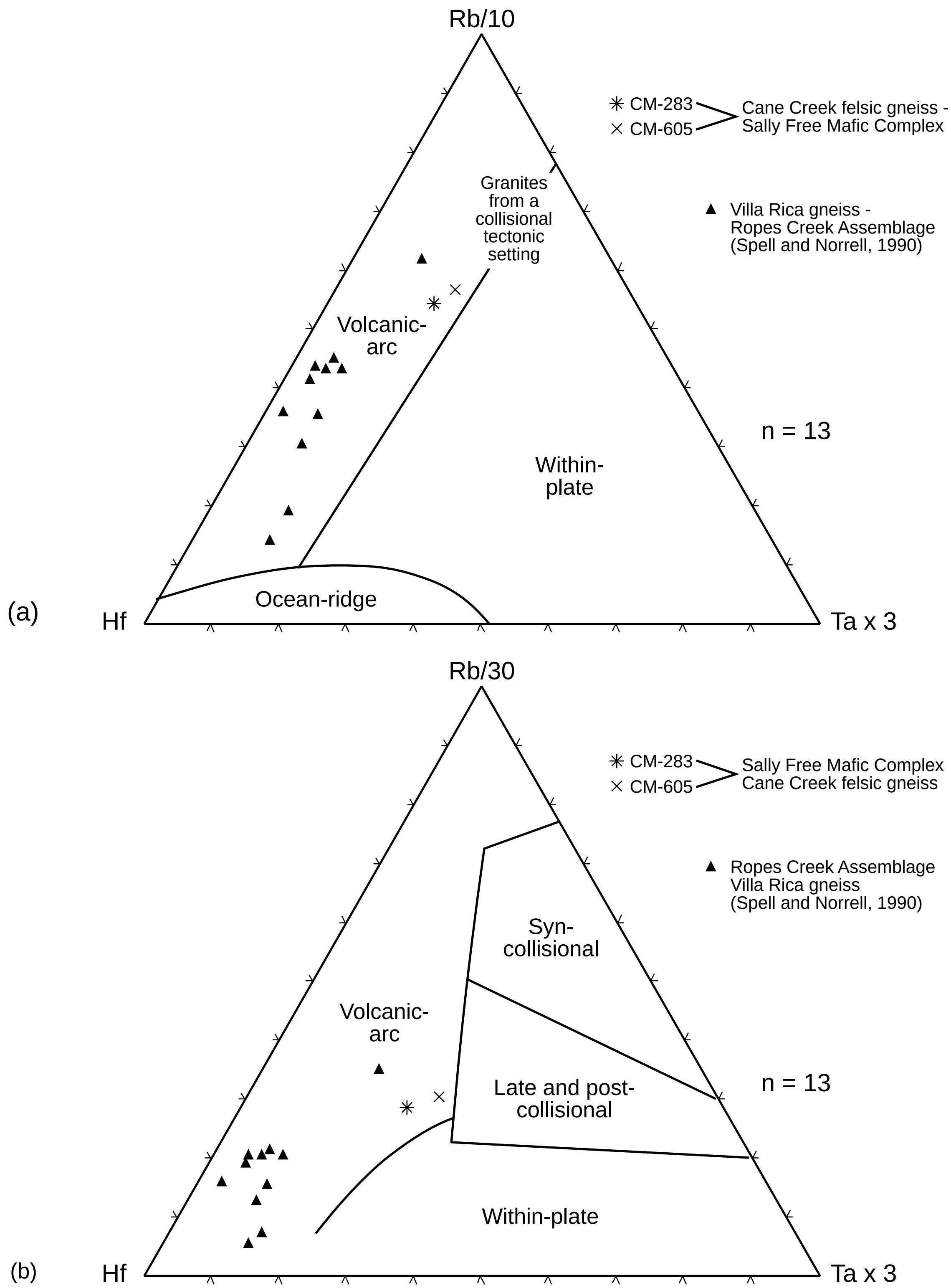

Figure 28. Hf-(Rb/10)-(Tax3) and Hf-(Rb/30)-(Tax3) tectonic discrimination diagrams (a and b, respectively) for granites after Harris *et al.* (1986). Felsic metaigneous rock geochemical data plotted from the Sally Free mafic complex Cane Creek felsic gneiss (this study) and the Villa Rica gneiss (Spell and Norrell, 1990).

used for comparison. Although Spell and Norrell (1990) present geochemical data from both the Dahlonega gold belt (New Georgia and Villa Rica area) and the Inner Piedmont (Woolsey area), data used for comparison is confined to the Dahlonega gold belt, Villa Rica area. Data from this area include 11 sample analyses from the Villa Rica gneiss and five amphibolite analyses (Spell and Norrell, 1990). Ti-Zr-Y discrimination (Pearce and Cann, 1973) of mafic rocks from the Carroll County and Dahlonega gold belts (German, 1989), including the Pumpkin Vine Creek and Univeter Formations, is also presented for comparison.

Amphibolite geochemical data from the Helen area (Gillon, 1989), including four analyses from the Richard Russell Formation (Coleman River Formation, Hayesville-Soque River thrust sheet) and six analyses from the Helen Group (Otto Formation, Dahlonega gold belt), provide a comparison with metaigneous rocks approximately 25 km northeast of the study area. Geochemical data presented by Hopson (1994) for the Lake Burton mafic-ultramafic complex, located approximately 48 km northeast of the study area (near Lake Burton, Georgia), are the northeastern most suite of amphibolite data used in discrimination. A total of 53 analyses were performed on mafic and felsic metaigneous rocks in the Lake Burton area by Hopson (1994). Data used for comparison in this study were confined to 23 amphibolite analyses from the Lake Burton complex central layered sequence (Hopson, 1994) that meet the 12% < CaO + MgO < 20% criteria defined by Pearce and Cann (1973).

Tectonic Discrimination - Dahlonega gold belt

Amphibolites from the Dahlonega gold belt (this study), including the Sally Free mafic complex and the Otto Formation, are tholeiitic, mid-ocean ridge to island-arc basalts based on chemical tectonomagmatic discrimination plots (Figs. 21 to 26). Gold belt samples plotted on the Ti-Zr-Y (Pearce and Cann, 1973), Zr/Y-Zr (Pearce and Norry, 1979), and Ti/Y-Nb/Y (Pearce, 1982) diagrams define a clear overlap between volcanic arc and mid-ocean ridge basalt fields (Figs. 21, 22, and 24, respectively). The Hf-Th-Ta diagram after Wood (1980) depicts a divided distribution with Otto Formation associated amphibolites plotting as calc-alkaline volcanic arc basalts and Sally Free mafic complex samples plotting as calc-alkaline volcanic arc basalt to N-type MORB (Fig. 23). Both Sally Free mafic complex and Otto Formation associated amphibolites plot as volcanic arc to N-type MORB field on the Nb-Zr-Y diagram (Meschede, 1986; Fig. 26). Amphibolite data plotted on the Zr/Y-Zr diagram after Pearce (1983; Fig. 25) support the conclusion that amphibolites from the Dahlonega gold belt are of oceanic-arc rather than continental-arc origin. Felsic metaigneous rock data from the Sally Free mafic complex Cane Creek felsic gneiss and the Villa Rica gneiss (Spell and Norrell, 1990) plot as volcanic arc granites on the Nb-Y, Ta-Yb, Rb-(Yb+Nb), and Rb-(Yb+Ta) diagrams after Pearce *et al.* (1984; Fig. 27) and the Hf-(Rb/10)-(Ta x 3) and Hf-(Rb/30)-(Ta x 3) after Harris *et al.* (1986; Fig. 28).

Chemical data from other mafic rock occurrences within the Georgia central Blue Ridge vary in plotting consistency. The tectonic setting of mafic rocks from the Lake Burton mafic complex, after Hopson (1994), is inconclusive because of excessive scatter of data on discriminant plots (Figs. 21 to 26). Although inconclusive, Lake Burton data plotted on the Ti-Zr-Y diagram after Pearce and Cann (1973) favor the fields defined for island-arc and mid-ocean ridge basalts, thus favoring an oceanic origin (Fig. 21). Amphibolite from the Ropes Creek assemblage (Spell and Norrell, 1990) plot as volcanic arc to mid-ocean ridge basalt on the Ti-Zr-Y (Pearce and Cann, 1973; Fig 21), Zr/Y-Zr (Pearce and Norry, 1979; Fig. 22), and Nb-Zr-Y (Meschede, 1986; Fig. 26) diagrams and as calc-alkaline volcanic arc basalt on the Hf-Th-Ta diagram (Wood, 1980; Fig. 23). Ropes Creek assemblage amphibolite data plotted on the Ti/Y-Nb/Y diagram (Fig. 24; Pearce, 1982) was inconclusive because of excessive scatter. Dahlonega gold belt amphibolite from the Helen area (Gillon, 1989), plotting as volcanic arc to mid-ocean ridge basalt on the Ti-Zr-Y (Pearce and Cann, 1973; Fig. 21), Zr/Y-Zr (Pearce and Norry, 1979; Fig. 22), Ti/Y-Nb/Y (Pearce, 1982; Fig. 24), and Nb-Zr-Y (Meschede, 1986; Fig. 26) diagrams are consistent with data obtained in this study.

Tectonic Discrimination - Hayesville-Soque River thrust sheet

Samples CM-19 and CM-490, collected from amphibolite bodies within the Hayesville-Soque River thrust sheet (Fig. 2), did not plot within a defined tectonic environment on the Ti-Zr-Y (Pearce and Cann, 1973) or Zr/Y-Zr (Pearce and Norry, 1979; Pearce, 1983) diagrams (Figs. 21, 22, and 25, respectively). Samples CM-19 and CM-490 were excluded from the remaining discriminant diagrams (Figs. 23, 24, and 26) due to undetectable Nb and Ta concentrations (Table 7). Sample CM-206, an amphibolite boudin from within the Coleman River Formation (Fig. 10), plots consistently as a within-plate tholeiite (Figs. 21 to 26). Similar to amphibolite data from this study, Hayesville-Soque River thrust sheet amphibolite data from Gillon (1989) do not plot consistently within defined fields on tectonomagmatic discriminant diagrams (Figs. 21 to 26).

DISCUSSION

Field relationships indicate that amphibolite (tholeiitic basaltic-andesite; Figs. 19 and 20) within the Otto Formation, which occurs as large bodies, thin layers, and lenses (CM-526, CM-744, and CM-24, respectively; Fig. 2), either intruded Otto Formation pelitic rocks as hypabyssal mafic sills and/or dikes or formed as extrusive flows and/or ash coeval with sediment deposition. Although no relict abyssal volcanic textures (e.g., pillows, amygdules, etc.) or contact aureoles were observed within Otto Formation associated amphibolite within the study area, negative Ce anomalies in chondrite normalized REE plots (CM-24, -159, -266, and CM-629; Fig. 13) could be indicative of seawater/sediment/magma interaction during crystallization. REE enrichment and negative Ce anomalies are characteristic of hydrothermally altered, seawater sediments and deep sea authigenic phillipsite (Bernat and Church, 1978; Elderfield and Greaves; 1982; Fleet, 1983), which could be secondary components of the extrusive basaltic-andesite (amphibolites) sampled here. Similar anomalies were also observed for Villa Rica area amphibolites from the Ropes Creek assemblage (Fig. 4 in Spell and Norrell, 1990).

The Sally Free mafic complex contains evidence for extrusive and intrusive components. Relict volcanic structures within amphibolite, such as amygdules (Fig. 6) observed along the eastern-limit of the complex (Fig. 2), have been identified throughout the Dahlonega gold belt confirming the volcanic nature of mafic metaigneous rocks (e.g., Hurst and Jones, 1973; McConnell and Abrams, 1984; Higgins *et al.,* 1988; Spell and Norrell, 1990). Metagabbro/metadiorite along the western-limit of the complex (Fig. 2) is considered intrusive based on texture (locally coarse-grained, equigranular, and poorly foliated; Fig. 8) and chemistry (considered cumulate based on rare earth, trace, and minor element depletion; Tables 2 and 3; Fig. 13). The Cane Creek felsic gneiss, considered rhyodacitic (Fig. 19), is likely a shallow intrusive felsite. Confirmation of intrusive emplacement of the well-foliated and strongly lineated felsic gneiss is difficult because of a pervasive metamorphic and deformational overprint (Fig. 5).

Rock types within the island-arc tholeiitic series, also referred to as the low-K tholeiitic series (Pearce and Cann, 1973), typically range from tholeiitic basalt to basaltic andesites and Fe-enriched andesites to dacites and, very rarely, rhyolite (Baker, 1982). Numerous components of the island-arc tholeiitic series are recognized within the gold belt northwest of Dahlonega. Chemical discrimination indicates that amphibolites sampled within the study area are tholeiitic, basaltic-andesite dominant with lesser amounts of andesite and that the Cane Creek felsic gneiss is rhyodacitic (Figs. 19 and 20). Tectonomagmatic discrimination of gold belt amphibolites indicates the presence of both island-arc tholeiites and normal MORB assemblages (Figs 21 to 26). The spatial distribution of mafic rocks suggested by Spell and Norrell (1990) of island-arc tholeiites to island-arc tholeiites + MORB to MORB, spanning the Dahlonega gold belt and extending into the Inner Piedmont from northwest to southeast, was not observed within the gold belt northwest of Dahlonega.

Tectonomagmatic chemical discrimination of amphibolite samples from the Hayesville-Soque River thrust sheet (Coweeta Group, Coleman River Formation) is inconclusive and does not clearly define a paleotectonic setting. Based on our limited study of Hayesville-Soque River thrust sheet amphibolite, it is apparent that a more detailed investigation is necessary before the tectonic setting and petrogenetic history of these amphibolites can be addressed. This is partially attributed to an insufficient number of analyses (3). A more detailed analyses of Hayesville-Soque River thrust sheet mafic metaigneous rocks, including an increased number of spatially distributed samples, is needed. Although only one amphibolite (sub-alkaline basalt; Fig. 19) boudin sample from within the Coleman River Formation (Fig. 10) was analyzed, it appears to be the only within-plate basalt within this study area (Figs. 20 to 26).

The Early Ordovician crystallization age of 482 ± 7 Ma obtained for the Cane Creek felsic gneiss is considered representative of the emplacement age of all metaigneous rocks within the Sally Free mafic complex. Although Dahlonega gold belt amphibolites sampled, including those from within the Otto Formation and the mafic complex, vary in occurrence and texture, our field evidence and geochemical data favor a common magmatic source; thus, the Early Ordovician age obtained for the mafic complex constrains magmatic activity throughout this portion of the gold belt. This also indicates that the Etowah River fault emplacing the Sally Free mafic complex is minor and not crustal-scale. The interlayered relationship of amphibolite and Otto Formation pelitic units northwest of the mafic complex (Fig. 2) also constrains sediment deposition within this portion of the Dahlonega gold belt to Early Ordovician.

CONCLUSIONS

(1) Field observations of hornblende gneiss/metagabbro, felsic gneiss, and amphibolite (from west to east) within the newly delineated, polydeformed, Sally Free mafic complex suggest intrusive, shallow intrusive/extrusive and extrusive igneous protoliths, respectively.

(2) Trace element tectonomagmatic discrimination of amphibolite and felsic gneiss from the Sally Free mafic complex and amphibolite from the Otto Formation indicate an oceanic origin for Dahlonega gold belt metaigneous rocks, which most likely represent an Early Ordovician (Cane Creek felsic gneiss = 482 ± 7 Ma) mixed volcanic arc assemblage (Fig. 29).

(3) The interlayered relationship of Otto Formation metasedimentary rocks and mafic metaigneous rocks; the determined age of 482 ± 7 Ma for igneous activity; combined with the observation of possible extrusive basaltic textures indicates coeval Early Ordovician igneous activity and sediment deposition, possibly within a back-arc basin, for this portion of the Dahlonega gold belt (Fig. 29).

(4) Recently obtained magmatic ages of felsic gneisses throughout the north Georgia Dahlonega gold belt (Villa Rica, Galts Ferry, Barlow, Cane Creek felsic, and Lake Burton gneisses; Thomas, 2001; Thomas *et al.*, 2001; this study) clearly define Early to Middle Ordovician (460 to 490) magmatism and possibly indicate that deformation and metamorphism of the Dahlonega gold belt is Acadian rather than Taconic.

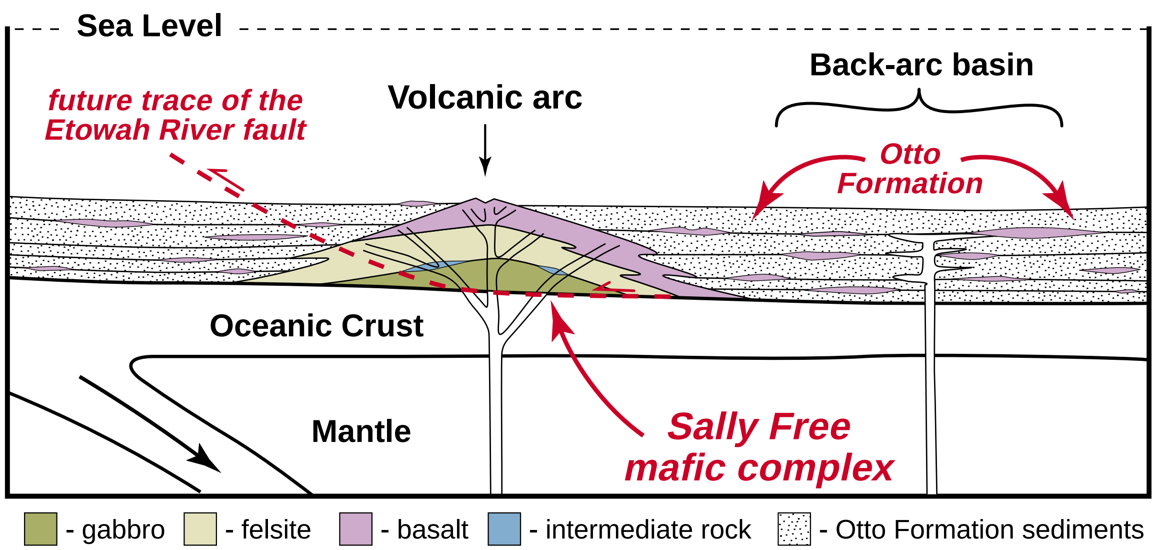

Figure 29. Schematic diagram depicting the probable Early Ordovician paleotectonic volcanic arc/back arc basin setting for the Dahlonega gold belt Sally Free mafic complex and Otto Formation. Probable future trace of the Etowah River fault indicated.

REFERENCES CITED

Albino, G. V., 1989, Shear zone-hosted gold deposits of the Dahlonega Belt, northeast Georgia: Geological Society of America Abstracts with Programs, v. 21, no. 3, p. 1.

Ausburn, M. P., Hatcher, R. D., Jr., Bryan, G., Godfrey, S. C., and Acker, L A., 1998, Geologic map and mineral resources summary of the Topton quadrangle, North Carolina: North Carolina Geologic Survey, Map 6, 1:24,000 scale.

Bacon, C. R., Persing, H. M., Wooden, J. L., and Ireland, T. R., 2000, Late Pleistocene granodiorite beneath Crater Lake caldera, Oregon, dated by ion microprobe: Geology, v. 28, p. 467-470.

Baker, P. E., 1982, Evolution and classification of orogenic volcanic rocks, *in* Thorpe, R. S., ed., Andesites: Norwich, John Wiley and Sons, Ltd., p. 11-23.

Becker, G. F., 1894, Reconnaissance of the gold fields of the southern Appalachians: United States of America 16th Annual Report, pt. 3, p. 251-319.

Bernat, M., and Church, T. M., 1978, Deep sea phillipsite: trace geochemistry and modes of formation, *in* Sand, L. B., and Mumpton, F. A., eds., Natural zeolites: Oxford, United Kingdom, Pergamon Press, p. 259-267.

Blake, W. P., and Jackson, C. T., 1895, Notes and recollections concerning the mineral resources of northern Georgia and western North Carolina: American Institute of Mining Engineers Transactions, v. 25, p. 796-811.

Boynton, W. V., 1984, Cosmochemistry of the rare Earth elements: meterorite studies, *in* Henderson, P., ed., Rare Earth Element Geochemistry: New York, Developments in geochemistry 2, p. 63-114.

Brewer, W. M., 1895, The gold regions of Georgia and Alabama: American Institute of Mining Engineers, v. 25, p. 569-587.

Burnell, J. R., and Cook, R. B., Jr., 1984, The geochemistry of metavolcanic rocks in the Dahlonega district, Lumpkin County, Georgia: Geological Society of America Abstracts with Programs, v. 16, no. 3, p. 127.

Butler, J. R., Age of Paleozoic regional metamorphism in the Carolinas, Georgia, and Tennessee southern Appalachian: American Journal of Science, v. 272, p. 319-333.

Cook, R. B., Jr., and Burnell, J. R., 1985, The trace metal signature of some major lithologic units, Dahlonega district, Lumpkin County, Georgia, *in* Misra, K. C., ed., Volcanogenic sulfide and precious metal mineralization in the southern Appalachians: Geological Society of America, Studies in Geology 16, Knoxville, University of Tennessee, p. 206-219.

Crickmay, G. W., 1952, Geology of the crystalline rocks of Georgia: Georgia Geological Survey Bulletin, v. 58, 54 p.

Cullers, R. L., and Graf, J. L., 1984, Rare earth elements in igneous rocks of the continental crust; predominantly basic and ultrabasic rocks, *in* Henderson, P., ed., Rare earth element geochemistry: New York, Developments in geochemistry 2, p. 63-114.

DePaolo, D., 1981, Neodymium isotopes in the Colorado Front Range and crustal-mantle evolution in the Proterozoic: Nature, v. 291, p. 193-196.

Elderfield, H., and Greaves, M. J., 1982, The rare earth elements of sea water: Nature, v. 296, p. 214-219.

Elliot, R. B., 1973, The chemistry of gabbro/amphibolite transitions in south Norway: Contributions in Mineralogy and Petrology, v. 38, p. 71-79.

Engel, A. E. J., and Engel, C. G., 1962, Progressive metamorphism of amphibolite, northwest Adirondack mountains, New York: Geological Society of America Buddington volume, p. 37-82.

Field, D., and Elliot, R. B., 1974, The chemistry of gabbro/amphibolite transitions in south Norway: trace elements: Contributions in Mineralogy and Petrology, v. 47, p. 63-76.

Fleet, A. J., 1983, Hydrothermal and hydrogenous ferro-manganese deposits: Do they form a continuum? The rare earth element evidence, in Rona, P. A., Bostroem, K., Laubier, L., Smith, K. L., Jr., eds., Hydrothermal processes at seafloor spreading centers: New York, Plenum Press, p. 535-555.

Floyd, P. A., and Winchester, J. A., 1975, Magma-type and tectonic setting discrimination using immobile trace elements: Earth and Planetary Science Letters, v. 27, p. 211-218.

Floyd, P. A., and Winchester, J. A., 1978, Identification and discrimination of altered and metamorphosed volcanic rocks using immobile elements: Chemical Geology, v. 21, p.291-306.

Fullagar, P. D., and Butler, J. R., 1979, 325 to 265 m.y.-old granitic plutons in the Piedmont of the southeastern Appalachians: Geological Society of America Bulletin, v. 82, p. 2845-2862.

Fullagar, P. D., Goldberg, S. A., and Butler, J. R., 1997, Nd and Sr isotopic characterization of crystalline rocks from the southern Appalachian Piedmont and Blue Ridge, North and South Carolina, *in* Sinha, A. K., Whalen, J. B., and Hogan, J. P., eds., The nature of magmatism in the Appalachian 0rogen: Geological Society of America Memoir 191, p. 165-179.

German, J. M., 1985, The geology of the northeastern portion of the Dahlonega gold belt: Georgia Geologic Survey Bulletin, v. 100, 41 p.

German, J. M., 1989, Geologic setting and genesis of gold deposits of the Dahlonega and Carroll County gold belts, Georgia: Economic Geology, v. 84, p. 903-923.

Gillon, K. A., 1982, Stratigraphic, structural, and metamorphic geology of portions of the Cowrock and Helen, Georgia 7.5-minute quadrangles [M.S. thesis]: Athens, University of Georgia, 236 p.

Gillon, K. A., 1989, The geology of eastern Blue Ridge thrust sheets in the vicinity of Helen, Georgia, *in* Fritz, W. J., Hatcher, R. D., Jr., and Hopson, J. L., eds., Geology of the eastern Blue Ridge of northeast Georgia and the adjacent Carolinas: Georgia Geological Society Guidebooks, v. 9, p. 133-169.

Hadley, J. B., 1970, The Ocoee Series and its possible correlatives, *in* Fisher, G. W., Pettijohn, F. J., Reed, J. C., and Weaver, K. N., eds., Studies in Appalachian geology: Central and southern: New York, Wiley Interscience, p. 247-260.

Hadley, J. B., and Nelson, A. E., 1971, Geologic map of the Knoxville quadrangle, North Carolina, Tennessee, and South Carolina: U.S. Geological Survey Miscellaneous Investigations Series Map I-654, scale 1:250,000.

Harris, N. B. W., Pearce, J. A., and Tindle, A. G., 1986, Geochemical characteristics of collision-zone magmatism, *in* Coward, M. P., and Reis, A. C., eds., Collision Tectonics: Boulder, Geological Society of America Special Publication, 19, p. 67-81.

Hatcher, R. D., Jr., 1978, Tectonics of the western Piedmont and Blue Ridge, southern Appalachians: Review and speculation: American Journal of Science, v. 278, p. 276-304.

Hatcher, R. D., Jr., 1988, Bedrock geology and regional geologic setting of Coweeta Hydrologic Laboratory in the eastern Blue Ridge, with some discussion of Quaternary deposits and structural controls of topography, *in* Swank, W. T., and Crossley, D. A., Jr., eds., Coweeta symposium volume 66: New York, Springer–Verlag, p. 81–92.

Hatcher, R. D., Jr., 1989, Tectonic synthesis of the U.S. Appalachians, Chapter 14, *in* Hatcher, R. D., Jr., Thomas, W. A., and Viele, G. W., eds., The Appalachian–Ouachita orogen in the United States: Boulder, Colorado, Geological Society of America, The Geology of North America, v. F–2, p. 511–535.

Hatcher, R. D., Jr., and Goldberg, S. A., 1991, The Blue Ridge geologic province, *in* Horton, J. W., Jr., and Zullo, V. A., eds., The geology of the Carolinas; Carolina Geological Society fiftieth anniversary volume: Knoxville, Tennessee, University of Tennessee Press, p. 11-35.

Higgins, M. W., and McConnell, K. I., 1978, The Sandy Springs Group and related rocks of the Georgia Piedmont – nomenclature and stratigraphy, *in* Sohl, N. F., and Wright, W. B., eds., Changes in stratigraphic nomenclature by the U.S. Geological Survey, 1977: United States Geological Survey Bulletin 1457-A, p. A98-A105.

Higgins, M. W., Atkins, R. L., Crawford, T. J., Crawford, R. F., III, Brooks, R., and Cook, R. B., 1988, The structure, stratigraphy, tectonostratigraphy, and evolution of the southernmost part of the Appalachian orogeny: U. S. Geological Survey Professional Paper 1475, 173 p.

Hopson, J. L., 1994, Geology of part of the eastern Blue Ridge, northeast Georgia and the adjacent Carolinas [PhD Dissertation]: Knoxville, University of Tennessee, 350 p.

Hopson, J. L., Hatcher, R. D., Jr., and Stieve, A. L., 1989, Geology of the eastern Blue Ridge, northeastern Georgia and the adjacent Carolinas, *in* Fritz, W. J., Hatcher, R. D., Jr., and Hopson, J. L., eds., Geology of the eastern Blue Ridge of northeast Georgia and the adjacent Carolinas: Georgia Geological Society Guidebooks, v. 9, p. 1-40.

Horton, J. W., Jr., Drake, A. A., Jr., and Rankin, D. W., 1989, Tectonostratigraphic terranes and their Paleozoic boundaries in the central and southern Appalachians, *in* Terranes in the Circum-Atlantic Paleozoic orogens: Boulder, Geological Society of America Special Paper 230, p. 213-245.

Hurst, V. J., 1955, Stratigraphy, structure, and mineral resources of the Mineral Bluff quadrangle, Georgia: Georgia Geologic Survey, Bulletin 63, 137 p.

Hurst, V. J., 1973, Geology of the southern Blue Ridge belt: American Journal of Science, v. 173, p. 643-670.

Hurst, V. J., and Jones, L, M., 1973, Origin of amphibolites in the Cartersville-Villa Rica area, Georgia: Geological Society of America Bulletin, v. 84, p. 905-911.

Jones, S. P., 1909, Gold deposits of Georgia: Geological Survey of Georgia, Bulletin 19, 283 p.

King, P. B., 1949, The base of the Cambrian in the southern Appalachians: American Journal of Science, v. 247, p. 513-530, 622-645.

Kish, S.A., 1983, A geochronological study of deformation and metamorphism in the Blue Ridge and Piedmont of the Carolinas [Ph.D. dissertation]: Chapel Hill, University of North Carolina, 220 p.

Leake, B. E., 1964, The chemical distinction between ortho- and para-amphibolites: Journal of Petrology, v. 5, p. 238-254.

Mackintosh, J. B., 1879, The gold mining district of Dahlonega, Georgia: Engineering and Mining Journal, v. 72, p. 355-356.

McConnell, K. I., 1980, Origin and correlation of the Pumpkin Vine Creek Formation: a new unit in the Piedmont of northern Georgia: Georgia Geologic Survey Information Circular 52, 19 p.

McConnell, K. I., and Abrams, C. E., 1984, Geology of the Greater Atlanta region: Georgia Geological Survey Bulletin 96, 127 p.

McConnell, K. I., and Costello, J. O., 1980, Guide to geology along a traverse through the Blue Ridge and Piedmont Provinces of North Georgia, *in* Frey, R. W., ed., Excursions in southeastern geology: American Geological Institute, v. 1, p. 241-257.

Meschede, M. 1986, A method of discriminating between different types of mid-ocean ridge basalts and continental tholeiites with the Nb-Zr-Y diagram: Chemical Geology, v. 56, p. 207-218.

Misra, K. C., and Conte, J. A., 1991, Amphibolites of the Ashe and Alligator Back Formations, North Carolina: Samples of Late Preoterozoic-early Paleozoic oceanic crust: Geological Society of America Bulletin, v. 103 , p. 737-750.

Nelson, A. E., 1991, Geologic map of the Campbell Mountain Quadrangle, Lumpkin County, Georgia: U.S. Geological Survey Geologic Quadrangle Map, MF-2148, 1:24,000.

Nelson, A. E., and Gillon, K. A., 1985, Stratigraphic nomenclature in the Richard Russell and Helen thrust sheet, north Georgia, *in* Stratigraphic notes, 1984: U.S. Geological Survey Bulletin, No. 1605-A, p. A59-A62.

Paces, J.B., and Miller, J.D., 1993, U-Pb ages of Duluth complex and related mafic intrusions, northeastern Minnesota: Geochronological insights into physical, petrogenetic, paleomagnetic, and tectonomagmatic processes associated with the 1.1 Ga mid-continent rift system: Journal of Geophysical Research, v. 98, p. 13997-14013.

Pearce, J. A., 1982, Trace element characteristics of lavas from destructive plate boundaries, *in* Thorpe, R. S., ed., Andesites: Norwich, John Wiley and Sons, Ltd., p. 525-548.

Pearce, J. A., 1983, Role of the sub-continental lithosphere in magma genesis at active continental margins, *in* Hawkesworth, C. J., and Norry, M. J., eds., Continental basalts and mantle xenoliths: Shiva, Nantwich, p. 230-249.

Pearce, J. A., and Cann, J. R., 1971, Ophiolite origin investigated by discriminant analysis using Ti, Zr, and Y: Earth and Planetary Science Letters, v. 12, p. 339-349.

Pearce, J. A., and Cann, J. R., 1973, Tectonic setting of basic volcanic rocks determined using trace element analysis: Earth and Planetary Science Letters, v. 19, p. 956-983.

Pearce, J. A., Harris, N. B. W., and Tindle, A. G., 1984, Trace element discrimination diagrams for the tectonic interpretation of granitic rocks: Journal of Petrology, v. 25, p. 956-983.

Pearce, J. A., and Norry, M., J., 1979, Petrogenic implications of Ti, Zr, Y, and Nb variations in volcanic rocks: Contributions to Mineralogy and Petrology, v. 69, p. 33-37.

Pickering, S. M., and Murray, J. B., 1976, Geologic map of Georgia: Georgia Geologic Survey, scale 1:500,000.

Rankin, D. W., 1976, Appalachian salients and recesses: Late Precambrian continental breakup and the opening of the Iapetus Ocean: Journal of Geophysical Research, v. 81, p. 5605-5619.

Rollinson, H., 1993, Using geochemical data: evaluation, presentation, and interpretation: Longman Group UK Limited, 352 p.

Settles, D. J., and Hatcher, R. D., Jr., in progress, The Hayesville–Soque River and Allatoona faults northwest of Dahlonega, Georgia: The central Blue Ridge terrane boundary in northern Georgia.

Spell, T. L., and Norrell, G. T., 1990, The Ropes Creek assemblage: Petrology, geochemistry, and tectonic setting of an ophiolitic thrust sheet in the southern Appalachians: American Journal of Science, v. 290, p. 811-842.

Tera, F., and Wasserburg, G. J., 1972, U-Th-Pb systematics in three Apollo 14 basalts and the problem of initial Pb in lunar rocks: Earth and Planetary Science Letters, v. 14, p. 281-304.

Thomas, C. W., 2001, Origins of mafic-ultramafic complexes of the eastern Blue Ridge province, southern Appalachians: Geochronological and geochemical contraints [MS Thesis]: Nashville, Vanderbilt University, 154 p.

Thomas, C. W., Miller, C. F., Fullagar, P. D., Meschter-McDowell, S. M., Vinson, S. B, and Bream, B. R., 2001, Where is the arc? Discontinuities in Taconian arc magmatism in the southern Appalachians: Geological Society of America, Abstracts with Programs, , v. 23, no. 6, p. 262.

Wetheril, G. W., 1956, Discordant uranium-lead ages: Transactions of the American Geophysical Union, v. 37, p. 320-326.

Williams, H., 1978, Tectonic lithofacies map of the Appalachian orogen: St. Johns, Memorial University of Newfoundland, scale: 1,000,000.

Williams, H., and Hatcher, R. D., Jr., 1983, Appalachian suspect terranes, *in* Hatcher, R. D., Jr., Williams, H., and Zietz, I., eds., Contributions to the tectonics and geophysics of mountain chains: Geological Society of America Memoir 158, p. 33-53.

Winchester, J. A., and Floyd, P. A., 1976, Geochemical magma type discrimination: Application to altered and metamorphosed basic igneous rocks: Earth and Planetary Science Letters, v. 28, p. 459-469.

Winchester, J. A., and Floyd, P. A., 1977, Geochemical discrimination of different magma series and their differentiated products using immobile elements: Chemical Geology, v. 20, p. 325-343.

Wood, D. A., 1980, The application of the Th-Hf-Ta diagram to problems of tectonomagmatic classification and to establishing the nature of crustal contamination of basaltic lavas of the British Tertiary volcanic province: Earth and Planetary Science Letters, v. 50, p. 11-30.

Yeates, W. S., McCallie, S. W., and King, F. P., 1896, A preliminary report on a part of the gold deposits of Georgia: Georgia Geological Survey Bulletin 4-A, 535 p.

Yoder, H. S., and Tilley, C. E., 1962, Origin of basalt magmas: an experimental study of natural and synthetic rock systems: Journal of Petrology, v. 3, p. 342-532.

PART II

The Hayesville–Soque River and Allatoona faults northwest of Dahlonega, Georgia: The central Blue Ridge terrane boundary in northern Georgia

ABSTRACT

The Hayesville-Soque River and Allatoona faults separate three distinct lithostratigraphic assemblages in this area: the Coweeta Group, Great Smoky Group, and Dahlonega gold belt. The gold belt here contains metasandstone, pelitic schist, and abundant mafic rocks of the Otto Formation and the Sally Free mafic complex, while the Great Smoky Group contains metasandstone and pelitic schist with abundant calc-silicate. The abundance of calc-silicate and apparent lack of mafic rocks in the Great Smoky Group versus the apparent lack of calc-silicate and presence of abundant mafic rocks in the gold belt support the delineation of the Allatoona fault. Inequigranular, biotite-dominant (over trace muscovite), commonly migmatitic gneiss and schist of the Coweeta Group, Coleman River Formation, versus two-mica, nonmigmatitic, often equigranular metasandstone and schist of the Great Smoky Group and Otto Formation constitute the principal criteria for the delineation of the Hayesville and Soque River faults. Delineation of the Hayesville and Soque River faults here confirms that they are equivalent, and that the area northwest of Dahlonega marks the southwestern terminus of the Hayesville-Soque River thrust sheet.

Field and petrographic observations indicate that the Dahlonega gold belt within the study area was metamorphosed to a slightly lower grade (middle amphibolite facies, kyanite ± staurolite grade) relative to the adjacent Great Smoky and Coweeta Groups (upper amphibolite facies, sillimanite grade); thus, the Allatoona fault and a portion of the Hayesville-Soque River fault (east of the Allatoona fault intersection) together represent the kyanite-sillimanite isograd in this area.

Fault geometries observed within the study area indicate a pre- to synmetamorphic ancestral Allatoona fault exists, which was later truncated by the pre- to synmetamorphic Hayesville-Soque River fault approximately 10 km west of Dahlonega. Thus, the postmetamorphic Allatoona fault observed to the southwest of the study area possibly

represents reactivation along the ancestral Allatoona fault mapped here. This observation indicates that the Hayesville and Allatoona faults do not represent a continuous Blue Ridge terrane boundary, as previously hypothesized.

INTRODUCTION

The Hayesville/Soque River thrust sheet in northeast Georgia is bounded to the northwest by the Hayesville fault (Fig. 1; Hatcher and Butler, 1979; Shellebarger, 1980; Wooten, 1980) and to the southeast by the Soque River fault (Fig. 1; Gillon, 1982; Hopson *et al.*, 1989; Nelson, 1991). The Hayesville fault places rocks of the Coweeta Group over the Great Smoky Group to the northwest and the Soque River fault places rocks of the Coweeta Group over the Dahlonega gold belt to the southeast (Fig. 1). Nelson (1991) hypothesized that the Hayesville and Soque River faults are equivalent (Hayesville-Soque River) and implied that the area northwest of Dahlonega, Georgia (Campbell Mountain, Nimblewill, and Noontootla 7.5-minute quadrangles), contains the southern terminus of the Hayesville-Soque River thrust sheet. Although regional stratigraphic relationships and fault geometries support this hypothesis (Fig. 1), the southwestern terminus of the Hayesville-Soque River thrust sheet had not been identified. Nelson (1991) also indicated the presence of a third fault west of Dahlonega that juxtaposes rocks of the Dahlonega gold belt in the hanging wall with rocks of the Great Smoky Group in the footwall (Fig 1). Nelson (1991) interpreted this fault to continue southwest of Campbell Mountain into the Talking Rock accretionary complex (Higgins *et al.*, 1988), where it was unmappable. This unnamed fault stratigraphically represents the Allatoona fault, which thrusts rocks of the Dahlonega gold belt (Otto Formation and associated metaigneous rocks) over metasedimentary rocks of the Great Smoky Group in north-central Georgia (Hurst, 1973; German, 1985), and is thus referred to as the Allatoona fault (Fig. 1). Consequently, the central Blue Ridge northwest of Dahlonega contains three distinct lithostratigraphic assemblages, the Great Smoky Group, Coweeta Group, and Dahlonega gold belt, separated by the Hayesville, Soque River, and Allatoona faults. The structural and stratigraphic relationships between these three faults and

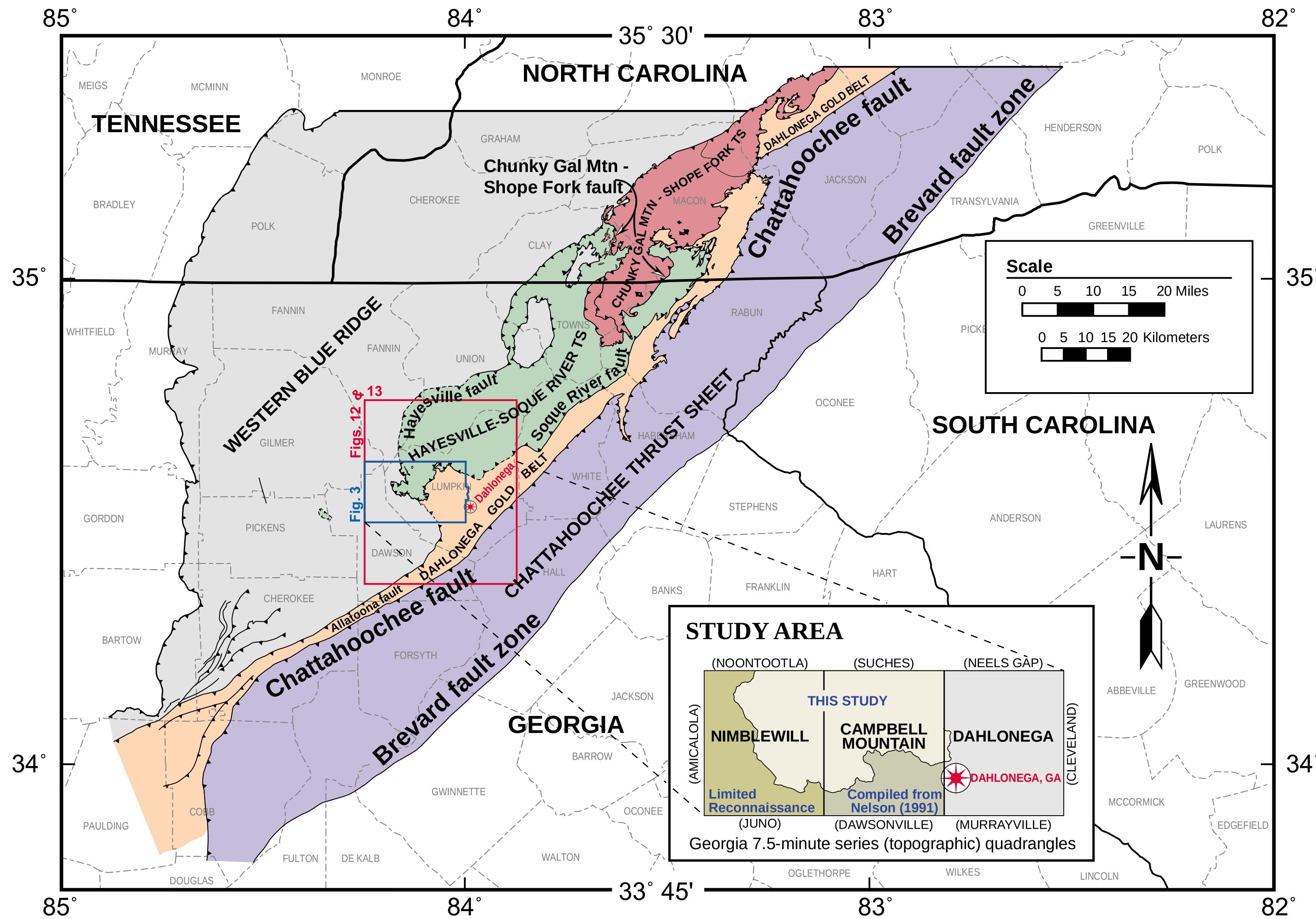

Figure 1. Tectonic divisions within a portion of the southern Appalachian Blue Ridge modified from Gillon (1982) and Hopson *et al.* (1989) including new interpretation of Hayesville-Soque River thrust sheet from the present study. Study area, and location of Figure 3, 13, and 14 indicated. TS - thrust sheet

lithotectonic assemblages provides new information concerning the tectonic evolution of the southern Appalachian Blue Ridge.

Previous investigations have divided the southern Appalachian Blue Ridge province into eastern and western subprovinces along the Allatoona/Hayesville/Gossan Lead fault on the basis of inherent differences between the lithotectonic assemblages present (Fig. 2; Hatcher, 1978; McConnell and Costello, 1980; Hopson *et al.*, 1989; Hatcher and Goldberg, 1991). The western Blue Ridge (Blue-Green-Long axis of Rankin, 1976) is characterized by an assemblage of continentally (Laurentian) derived rifted-margin succession (slope-and-rise) paragneisses (Ocoee Supergroup and Murphy belt; Hatcher, 1978; Hopson *et al*., 1989) resting on Laurentian basement. The western Blue Ridge rocks, containing few mafic and ultramafic rocks, were unconformably deposited on Grenville 1.1 Ga basement (Williams and Hatcher, 1983; Hatcher, 1989; Hopson *et al.*, 1989; Horton *et al.*, 1989) along the Laurentian margin during the Late Proterozoic and early Paleozoic (Rankin, 1976; Hatcher, 1978; Hopson *et al*., 1989). The eastern Blue Ridge is characterized by an assemblage of deep-water, ocean floor, distal slope-and-rise metasedimentary rocks and associated mafic and ultramafic rocks (Hopson *et al*., 1989). Grenville Laurentian basement occurs only in the eastern Blue Ridge as rare isolated massifs (in the Tallulah Falls and Toxaway domes; Hopson *et al*., 1989).

The post-metamorphic Allatoona fault, interpreted as the southwestern segment of the Blue Ridge terrane boundary, extends from central Alabama to north-central Georgia (Fig. 2; Hurst, 1973; Hatcher, 1978; Williams, 1978; McConnell and Costello, 1980; Hatcher *et al*., 1990). The pre- to synmetamorphic Hayesville fault represents the Blue Ridge terrane boundary extending from north-central Georgia northeast into North Carolina and Virginia (Fig. 1; Hatcher, 1978; Hopson *et al.*, 1989; Hatcher and Goldberg, 1991). If the Hayesville and Soque River faults are equivalent and the Hayesville-Soque River thrust sheet terminates northwest of Dahlonega (Fig. 1; Nelson, 1991), questions

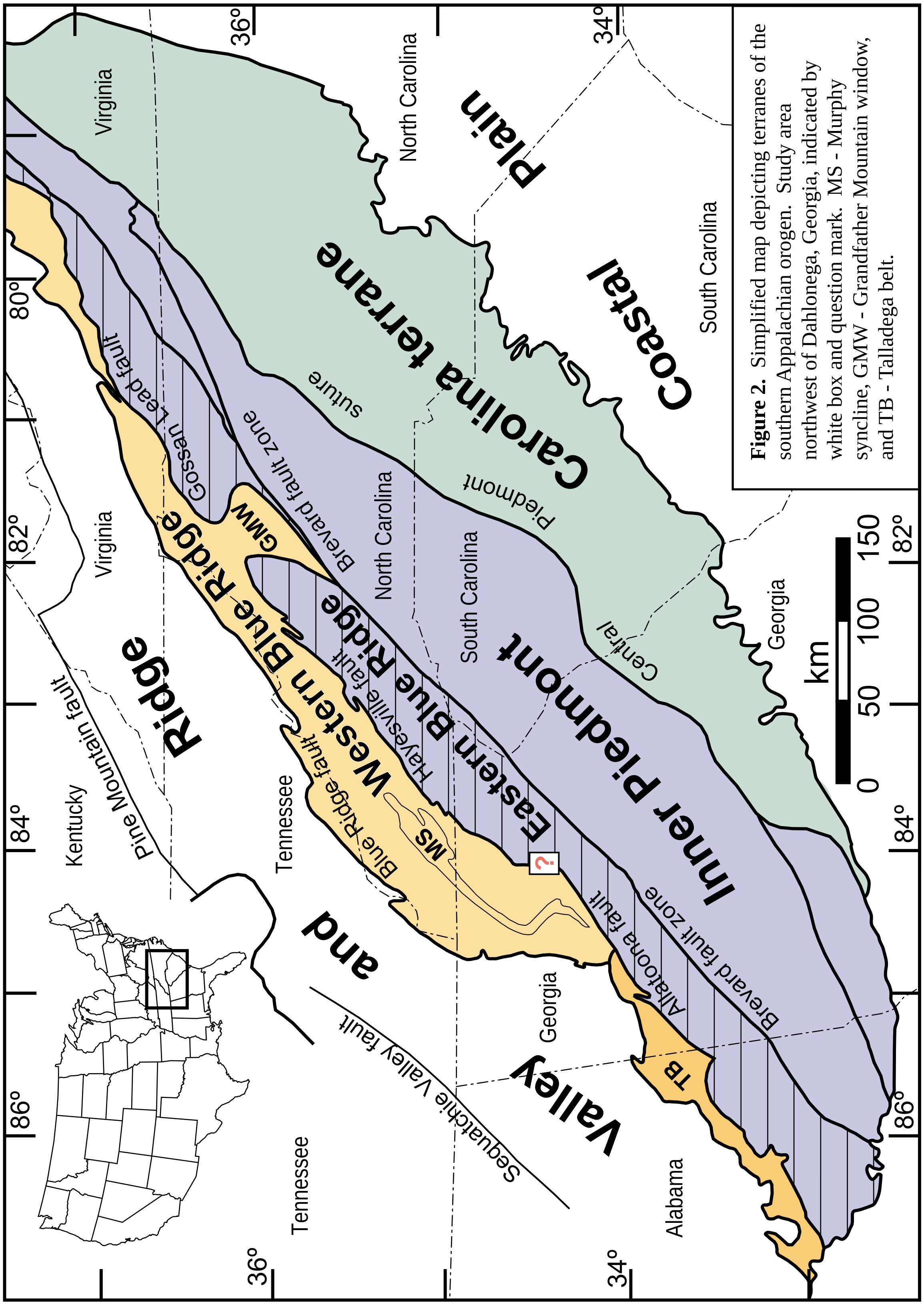

Figure 2. Simplified map depicting terranes of the southern Appalachian orogen. Study area northwest of Dahlonega, Georgia, indicated by white box and question mark. MS - Murphy syncline, GMW - Grandfather Mountain window, and TB - Talladega belt.

remain regarding the relationship between the Hayesville-Soque River and Allatoona faults and the continuation of the Allatoona/Hayesville/Gossan Lead fault as a terrane boundary. Although the regional lithotectonic relationships between the Allatoona and Hayesville faults have been established, dividing the Blue Ridge into eastern and western subprovinces, the actual intersection of the two related faults has not been previously delineated (Fig. 2; Hatcher, 1978; Williams, 1978; McConnell and Costello, 1980; German, 1985; Hatcher *et al*., 1990).

The critical assumption in relating the Allatoona and Hayesville faults is that rocks from both the Hayesville thrust sheet and the Dahlonega gold belt are part of the eastern Blue Ridge. This interpretation is based primarily on the abundance of mafic rocks within the Hayesville/Soque River thrust sheet and the Dahlonega gold belt relative to the western Blue Ridge. Previous authors (Hadley, 1970; Hadley and Nelson, 1971) have also suggested that rocks of the Dahlonega gold belt correlate with rocks of the Great Smoky Group of the western Blue Ridge. This correlation was made despite the lack of abundant mafic rocks in the western Blue Ridge. This interpretation would require a different combination of faults to represent the Blue Ridge terrane boundary (Hayesville/Soque River/Chattahoochee?; Fig. 1) and diminishes the significance of a relationship between the Allatoona and Hayesville faults.

Questions regarding the structural and stratigraphic relationships within the study area addressed here include: (1) Are the Hayesville and Soque River faults equivalent? (2) Does the area northwest of Dahlonega, Georgia, represent the southwestern terminus of the Hayesville/Soque River thrust sheet, as interpreted by Nelson (1991)? (3) What is the relationship (geometry and relative timing) between the Allatoona fault and the Hayesville and Soque River faults? and (4) Does the Allatoona fault represent the southwestern continuation of the Blue Ridge terrane boundary as previously hypothesized by McConnell and Costello (1980)?

Detailed geologic mapping (1:12,000 scale compiled at 1:24,000) of portions of the Nimblewill, Campbell Mountain, and Dahlonega, Georgia, 7.5-minute quadrangles was completed during 1999 and 2000 (Fig. 3). Structural and stratigraphic data were collected at 1550 stations covering approximately 180 km^2. Representative samples were collected to characterize the rock types and lithostratigraphic units (Coweeta Group, Great Smoky Group, and Dahlonega gold belt). Measurements were made of all identifiable structural features to characterize the deformational history of the area. Detailed discussion of metaigneous rocks within the study area, including geochemistry and geochronology, is included in a companion paper by Settles *et al.* (in preparation). Data from the south end of Nelson's (1991) Campbell Mountain quadrangle were compiled here to assess the extent of the Sally Free mafic complex and the geometry of the Allatoona fault.

LITHOLOGIC UNITS

The Hayesville, Soque River, and Allatoona faults separate three lithostratigraphic assemblages within the study area: the Dahlonega gold belt, Coweeta Group of the Hayesville/Soque River thrust sheet, and Great Smoky Group (Fig. 3). The Dahlonega gold belt here contains a mix of metasedimentary and mafic rocks of the Otto Formation (Helen Group of Nelson and Gillon, 1985) and the Sally Free mafic complex. Hatcher (1988) previously defined the Otto Formation near Otto, North Carolina, and the Sally Free mafic complex is defined by Settles *et al.* (in preparation). Hatcher (1979) initially defined the Coweeta Group, including the Coleman River Formation, along the Georgia-North Carolina border. The Great Smoky Group, undivided here, was originally defined and subdivided by King (1949) and later subdivided again by Hurst (1955). A summary of stratigraphic nomenclature used in this and other studies in the north Georgia central Blue Ridge is presented in Table 1. Representative samples were collected from all delineated units to perform petrographic analysis and determine modal mineralogy, which

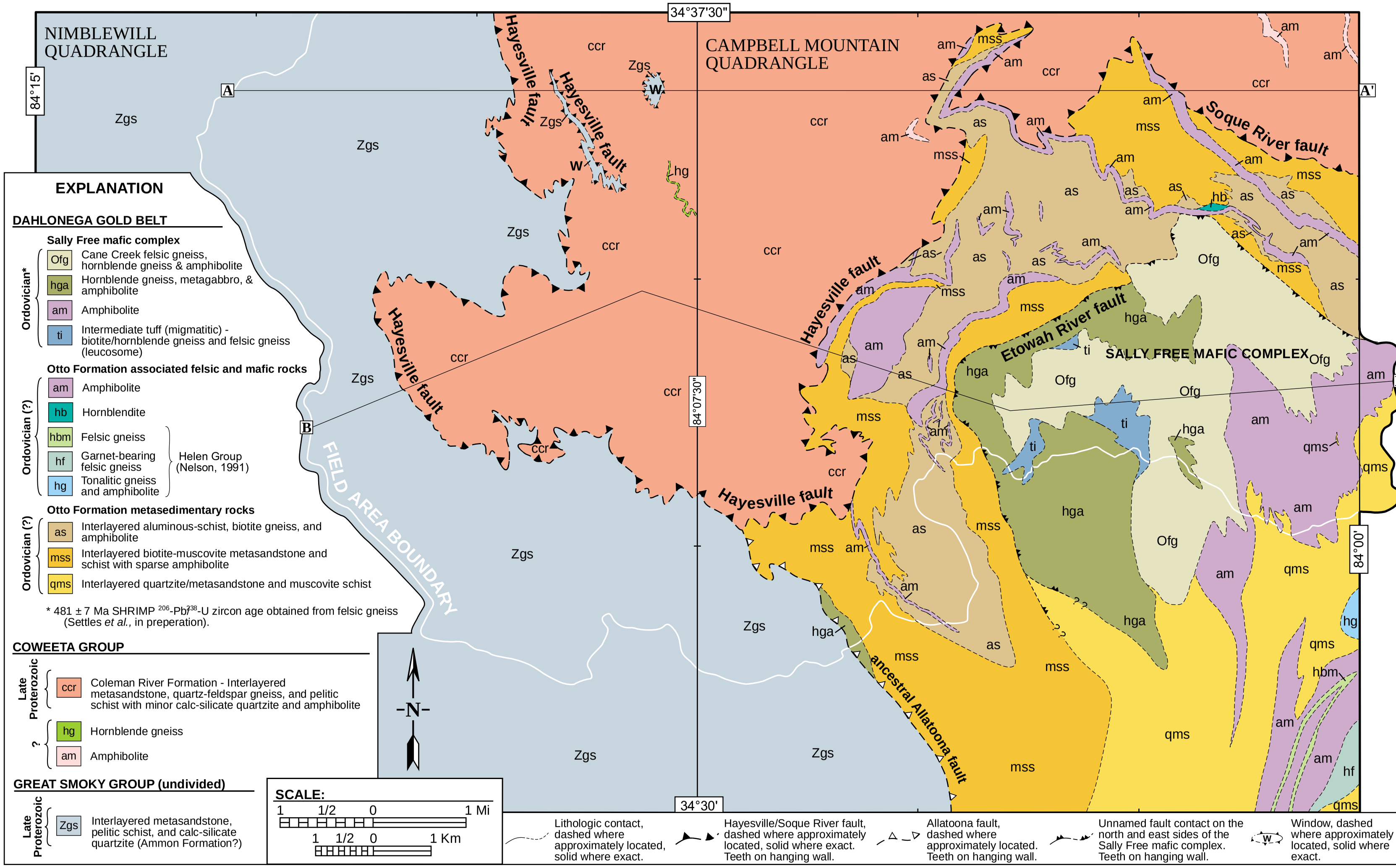

Figure 3. Detailed geologic map of portions of the Nimblewill, Campbell Mountain, and Dahlonega, Georgia, 7.5-minute quadrangles. Geology within the defined boundary was mapped at 1:12,000 scale for this study. Geology outside of the defined area was compiled from Nelson (1991) and limited reconnaissance. Regional location reference indicated on Figure 1.

Table 1. Stratigraphic nomenclature used to define similar lithologic division within the central-eastern Blue Ridge of Georgia and the adjacent Carolinas. Percise correlatives not implied. Stars and bold subdivisions indicate stratigraphic nomenclature used in this study.

GREAT SMOKY THRUST SHEET

King (1949)	Hurst (1955)	Ausburn et al. (1998)	
✴ Great Smoky Group (undivided)	Great Smoky Group	Great Smoky Group	
	+ Dean Fm	+ Dean Fm	+ Wehutty Fm
	+ Hothouse Fm	+ Ammons Fm	+ Copperhill Fm
	+ Hughes Gap Fm	- Horse Branch Mb	
	+ Copper Hill Fm	- Cross-biotite schist unit	
		- Phyllite-metagraywacke unit	
		- metasandstone-schist unit	

HAYESVILLE-SOQUE RIVER THRUST SHEET

Hatcher (1979)	Gillon (1982)	Nelson and Gillon (1985), Nelson (1991, 1992)
✴ Coweeta Group	Richard Russell Fm	Richard Russell Fm
+ Ridgepole Mtn. Fm	+ Rice Cabin mb	
✴ Coleman River Fm		
+ Persimmon Creek Gneiss		

DAHLONEGA GOLD BELT

Higgins and McConnell (1978)	Gillon (1982)	Nelson and Gillon (1985)	Hatcher (1988)
New Georgia Group	Helen Group	Helen Group	✴ Otto Fm
+ Pumpkinvine Creek Fm	+ Unicoi Park Fm	+ Robertstown Fm	
+ Canton Fm	- Andy Mtn. mb	+ Horton	
+ Univeter Fm	+ Chattahoochee Fm	+ Nacoochee Fm	
	- Hamby Mtn. mb		
	+ Nacoochee Fm		

is summarized in Tables 2 (Coweeta and Great Smoky Groups), 3 (Dahlonega gold belt, Otto Formation), and 4 (Dahlonega gold belt and Coweeta Group mafic rocks). Note that mapping here has confirmed that the Hayesville and Soque River faults are equivalent, as hypothesized by Nelson (1991), and the resulting fault has been termed the Hayesville-Soque River fault. A detailed discussion of faults occurs later in the text.

Dahlonega gold belt - Sally Free mafic complex

Rocks within the Sally Free mafic complex are divided into four units: Cane Creek felsic gneiss; hornblende gneiss-metagabbro-amphibolite; amphibolite; and intermediate gneiss (Fig. 3). The Cane Creek felsic gneiss unit, named here for an excellent exposure in a small abandoned quarry 0.5 kilometers northwest of the township of Cane Creek (Lat./Long. - 34° 24’ 33” N / 84° 00’ 59” W), dominates the complex, and contains predominantly felsic gneiss with some hornblende gneiss and amphibolite (Fig. 3; Table 2). Cane Creek felsic gneiss is well foliated, strongly lineated, medium- to coarse-grained (equigranular), and quartzofeldspathic (Table 2). An Early Ordovician, 482 ± 7 Ma, U-Pb ion microprobe age was determined for the Cane Creek felsic gneiss from concordant zircons (Settles *et al*., in preparation).

The hornblende gneiss-metagabbro-amphibolite unit dominates the western edge of the complex (Fig. 3; Table 2). This unit is distinguished from the Cane Creek felsic gneiss unit by the presence of abundant hornblende and only minor quartz. Hornblende gneiss (metadiorite) is well foliated, medium- to coarse-grained with hornblende commonly occurring as porphyroclasts and as distinct bands. Hornblende gneiss is the dominant rock type with sparse poorly foliated metagabbro also present. Metagabbro is poorly foliated, dark green to dark gray, medium grained, and equigranular. Plagioclase is dark blue to gray (calcic) giving fresh rock a dark appearance versus a “salt and pepper” appearance where slightly weathered. Minor, well foliated, amphibolite also occurs throughout the unit.

Table 2. Modes of mafic and felsic metaigneous rock thin sections from the Dahlonega gold belt (Otto Formation and Sally Free mafic complex) and Coweeta Group within the study area. Approximate mineral percentages based on 200 pts. counted across each section.

	Dahlonega gold belt														Hayesville thrust sheet		
	Mafic rocks within the Otto Formation				Sally Free mafic complex										Coweeta Group		
Map Units ->	Amphibolite (am)			Horn-blendite (hb)	Amph-ibolite (am)	Intermediate gneiss (ig)				Felsic gneiss (fg)			Hornblende Gneiss, metagabbro, and amphibolite (hga)		Amphibolite (am)		Hornblende gneiss (hg)
Sample #	CM-60	CM-111	CM-526	CM-563	CM-287	CM-507b	CM-597	CM-611	CM-576	CM-283	CM-543	CM-605	CM-515	CM-516	CM-206	CM-490	NW-258
Rock type	am	am	am	hb	am	leuc	gn/leuc	gn	myl	fg	hbl-gn	fg	hbl-gn	mga	am	am	hg
Plagioclase	18.0	20.5	2.0	–	6.0	23.0	32.0	38.5	43.0	23.5	30.5	25.6	15.0	10.0	10.7	9.0	10.5
% Anorthite	–	38.0	–	–	–	–	–	37.0	–	–	–	–	–	–	–	–	28.0
Hornblende	68.5	65.0	67.0	100.0	77.0	30.5	16.0	15.5	11.0	–	32.0	–	69.5	85.0	47.3	61.5	67.5
Epidote	9.0	5.5	27.0	–	15.0	12.0	6.5	7.5	4.0	7.5	tr	8.0	7.0	5.0	1.3	21.5	4.5
Quartz	1.0	2.5	1.0	–	1.0	32.5	20.5	19.5	18.0	49.5	34.5	36.8	5.5	tr	10.0	3.0	1.0
Sphene	3.5	4.0	1.5	–	tr	–	–	tr	–	–	–	–	tr	tr	1.3	1.0	5.0
Zircon	–	–	–	–	–	–	–	–	–	tr	–	tr	–	–	–	–	–
Garnet	–	–	–	–	–	tr	2.0	3.0	5.5	tr	1.5	–	–	–	14.0	tr	tr
Opaques	tr	1.5	tr	–	tr	0.5	0.5	0.5	1.0	–	tr	–	tr	tr	9.3	4.0	tr
Clinozoisite	–	tr	0.5	–	tr	tr	1.5	0.5	–	1.0	–	1.2	0.5	–	–	tr	0.5
Apatite	–	tr	tr	–	tr	1.5	1.0	tr	tr	tr	–	tr	2.5	–	–	–	–
Biotite	–	0.5	–	–	1.0	–	17.5	15.5	14.5	15.5	1.0	13.2	–	–	3.3	–	–
Muscovite	–	–	–	–	–	tr	3.0	–	3.0	2.5	0.5	15.2	–	–	–	–	–
Sericite	–	0.5	1.0	–	tr	tr	tr	–	tr	tr	–	–	–	–	2.7	–	11.0
Chlorite	–	–	–	–	–	–	–	–	tr	–	–	–	–	–	–	–	–

Abbreviations: am - amphibolite, gn - gneiss, hbl - hornblende, leuc -leucosome, mga - metagabbro, myl - mylonite, sch - schist, CM - Campell Mountain quad., and NW - Nimblewill quad.

Table 3. Modes of metasedimentary rock thin sections from the Dahlonega Gold Belt, Otto Formation, within the study area. Mineral percentages based on 1000 pts. counted across each section. Sections stained for plagioclase are indicated in bold italics.

Otto Formation Metasedimentary Rock Units

Map Units ->	Aluminous Schist (as)				Metasandstone and schist (mss)					Quartzite, Metasandstone, and Schist (qms)
Sample #	***CM-114***	CM-129	CM-586	CM-742	***CM-69***	***CM-324***	***CM-453***	***CM-464***	*CM-530*	DG-10
Rock type	***mgw/sch***	K-sch	sch	K-sch	***mgw/sch***	***mgw***	***sch***	***mgw***	*mgw/sch*	qtzite/mgw
Quartz	42.5	32.6	15.0	23.8	27.7	40.1	19.2	41.0	57.3	27.7
Plagioclase	36.8	3.9	tr	1.6	32.8	34.0	38.2	34.4	14.7	32.8
% Anorthite	5.0	–	–	–	1.0	4.0	–	12.0	12.0	–
Biotite	13.9	5.9	0.3	4.4	19.8	22.6	21.0	13.0	9.9	19.8
Muscovite	2.2	39.3	66.3	55.2	15.9	2.4	2.1	7.2	15.4	15.9
Chlorite	—	—	5.8	1.0	—	—	—	—	—	—
Sericite	—	—	1.6	—	—	—	—	—	0.1	—
Epidote	1.3	—	—	—	0.5	—	—	0.6	0.2	0.5
Clinozoisite	—	—	—	—	—	—	—	—	—	—
Kyanite	—	4.0	—	2.0	—	—	4.0	—	—	—
Sillimanite	—	—	—	—	—	—	tr	—	—	—
Garnet	1.2	9.9	6.1	7.4	1.8	tr	7.4	0.9	0.8	1.8
Staurolite	—	3.3	—	2.8	—	0.1	0.3	—	—	—
Sphene	—	—	—	—	—	0.3	—	—	—	—
Apatite	—	—	—	—	—	—	4.6	—	—	—
Opaques	2.1	1.1	4.9	1.8	1.5	0.5	5.7	2.9	1.6	1.5

Abbreviations: mgw - metagraywacke, sch - schist, qtzite - quartzite, K - kyanite, CM - Campbell Mountain quad., and DG - Dahlonega quad.

Table 4. Modes of metasedimentary rock thin sections from the Coweeta Group, Coleman River Formation, and Great Smoky Group within the study area. Mineral percentages based on 1000 pts. counted across each section. Sections stained for plagioclase are indicated in bold italics.

	Coweeta Group								Great Smoky Group					
	Coleman River Formation								Great Smoky Group (undivided)					
Sample #	***CM-484***	NW-11	***NW-31***	NW-62	NW-270a	NW-270b	***NW-349***	NW-523	NW-19	NW-122	NW-149	***NW-191***	NW-224	NW-343
Rock type	***mgw***	mgw	***mgw***	sch	sch	mgw	***mgw***	mgw	mgw	mgw	mgw	***mgw***	mgw/peg	mgw
Quartz	37.0	41.6	38.0	17.2	34.8	36.8	47.7	30.6	32.0	65.0	56.7	50.2	50.8	46.8
Plagioclase	24.2	26.2	32.0	14.4	33.0	37.0	30.4	56.2	33.4	18.4	14.4	32.0	18.8	31.8
% Anorthite	11.0	13.5	19.0	–	12.0	13.0	8.0	–	14.0	–	8.0	–	11.0	–
Biotite	27.8	25.4	25.8	24.0	23.0	21.2	20.5	7.6	25.4	15.1	26.5	16.9	28.0	21.0
Muscovite	0.4	1.0	3.6	30.2	8.6	3.2	—	5.6	9.2	0.4	2.2	—	2.4	—
Chlorite	tr	—	—	—	—	—	—	—	—	—	—	—	—	—
Sericite	8.0	5.4	—	6.2	0.4	0.2	—	—	—	—	—	—	—	—
Epidote	tr	0.4	—	—	tr	tr	tr	—	—	tr	tr	tr	tr	0.4
Clinozoisite	—	—	—	—	—	—	—	—	—	—	—	—	—	—
Kyanite	—	—	—	—	—	—	—	—	—	—	—	—	—	—
Sillimanite	—	—	—	—	—	—	—	—	—	—	—	—	—	—
Garnet	tr	—	—	7.0	—	tr	1.2	—	—	—	—	—	—	—
Staurolite	—	—	—	—	—	—	—	—	—	—	—	—	—	—
Sphene	—	—	—	—	—	—	—	—	—	—	—	0.7	—	—
Apatite	—	—	—	—	—	—	—	—	—	—	—	—	—	—
Opaques	2.6	—	0.6	1.0	0.2	0.8	0.2	tr	—	1.1	0.2	0.2	tr	tr

Abbreviations: mgw - metagraywacke, sch - schist, peg - pegmatite, CM - Campbell Mountain quad., and NW - Nimblewill quad.

A large amphibolite body marks the eastern edge of the mafic complex (Fig. 3; Table 2). The amphibolite is dark gray to black, well foliated, medium- to fine-grained. Outcrops are defined by extensive jointing and a prominent foliation parallel to compositional layering.

The intermediate gneiss unit is locally migmatitic and contains both fine-grained biotite/hornblende gneiss and coarse-grained felsic gneiss leucosome (Fig. 4; Table 2). Biotite/hornblende gneiss is dark gray, fine- to medium-grained, porphyroclastic, and inequigranular. Felsic gneiss (leucosome) is moderately foliated, coarse grained, and inequigranular with elliptical porphyroclastic augen, composed predominantly of quartz with some plagioclase. Although petrographic analysis revealed biotite/hornblende gneiss of intermediate composition, outcrops resemble dark metagraywacke and augen gneiss (Fig. 4).

Key outcrops at Rock Acres Farm (Lat./Long. - 34° 33' 39" N / 84° 02' 56" W) depict a complex highly sheared migmatite containing felsic leucosome and intermediate paleosome (Fig. 4) with limited occurrences of thinly layered biotite gneiss xenoliths within the leucosome. Intermediate gneiss observed along the western limit of the mafic complex, resembling garnet schist in outcrop, has a mylonitic texture indicating a local

Figure 4. Highly sheared, migmatitic, intermediate gneiss outcrop (Sally Free mafic complex) at Rock Acres Farm depicting felsic leucosome and intermediate paleosome.

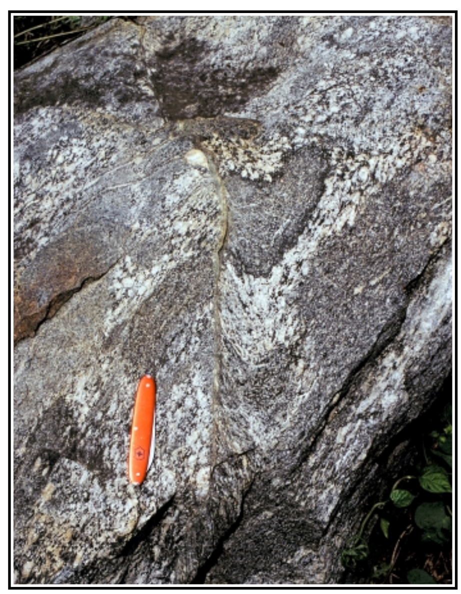

zone of shearing. Biotite/hornblende and felsic gneiss are interlayered/intermixed and occur in limited exposure as migmatitic enclaves within the Sally Free mafic complex.

Dahlonega gold belt - Otto Formation

Rocks within the Otto Formation are divided into five units: aluminous schist; metasandstone and schist; quartzite/metasandstone and schist; amphibolite, and hornblendite (Fig. 3; Tables 2 and 3). The distinction between the aluminous schist, and the metasandstone and schist units is based on the dominance of kyanite bearing muscovite schist (Fig. 5) within the aluminous schist unit. The aluminous schist unit contains pelitic schist, metasandstone, and quartzite, with variable amounts of amphibolite. Schist is light gray to silver (fresh) and fine- to coarse-grained containing abundant muscovite and quartz and locally abundant kyanite and staurolite (Fig. 5; Table 3). Opaque minerals, often slightly magnetic, are abundant (1 to 5%) and characteristic in outcrop (Fig. 5; Table 3). Schistose outcrops typically weather tan to orange (Fig. 6). Metasandstone is medium- to dark-gray, fine- to medium-grained and typically weathers dark red, occurring predominantly as thin layers (cm to m) within the schist-dominant unit. Amphibolite commonly occurs within the aluminous schist unit with thicknesses ranging from < 1 meter to hundreds of meters (Figs. 3 and 7). Amphibolite is well foliated, dark green to black (Fig. 6), and fine- to medium-grained similar to amphibolite previously described within the mafic complex.

The metasandstone and schist unit contains biotite-muscovite schist and metasandstone, with sparse amphibolite. Schist is silver to gray (fresh) and fine- to coarse-grained containing locally abundant kyanite and trace amounts of staurolite. Metasandstone is commonly gneissic, light- to dark-gray, fine- to medium-grained, and quartz dominant with locally abundant staurolite. A trace amount of sillimanite was observed in one of five thin sections from the metasandstone and schist unit. Metasandstone and schist are variably interlayered with both thin layers of metasandstone

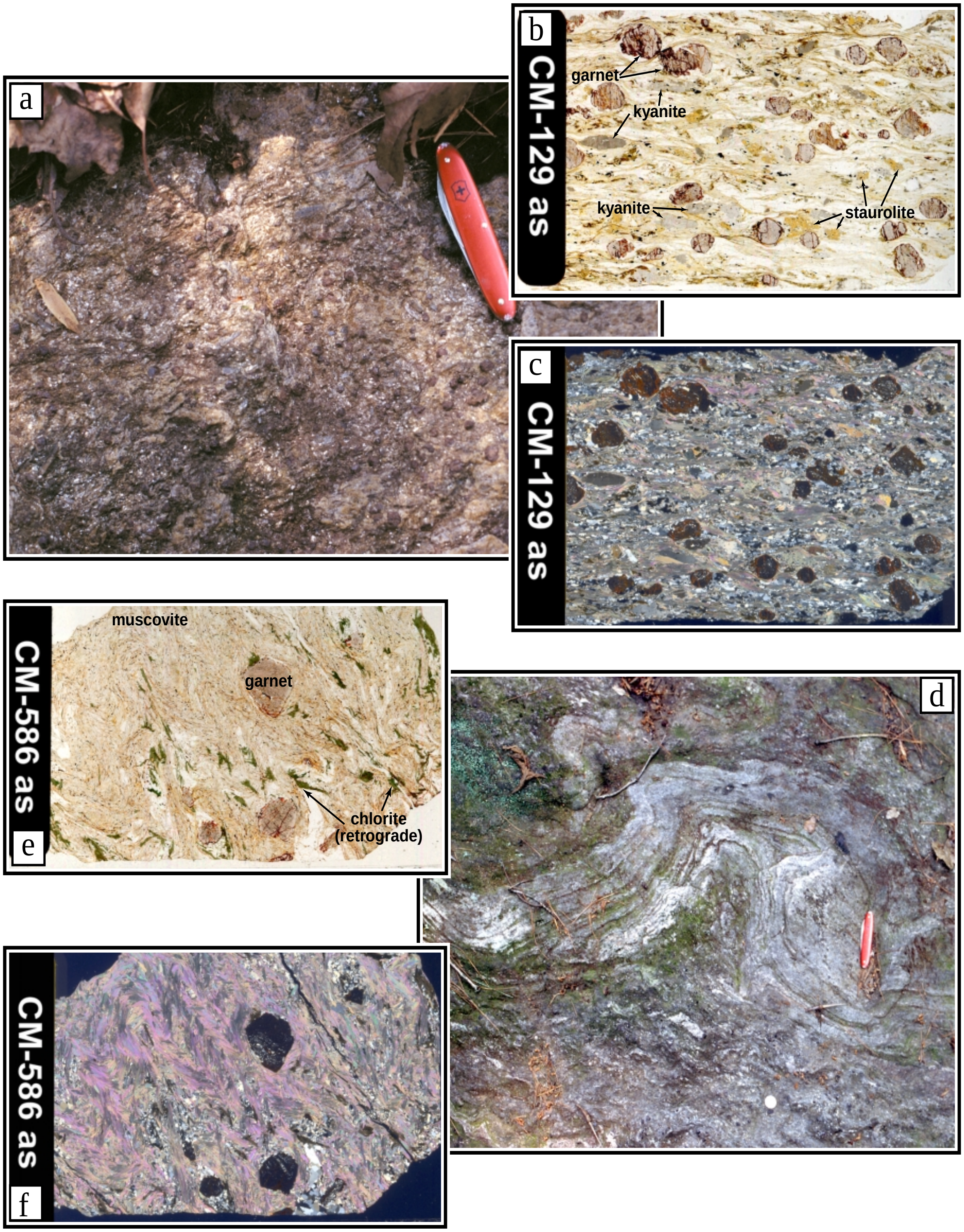

Figure 5. Dahlonega gold belt, Otto Formation, aluminous schist unit. a) Kyanite-bearing aluminous schist outcrop at station CM-129 accompanied by both plane-polarized (b) and cross-polarized (c) thin section images. d) Sheath fold within a highly crenulated aluminous schist outcrop at station CM-586 accompanied by both plane-polarized (e) and cross-polarized (f) thin section images. Long axis of thin section images = 3.4 cm.

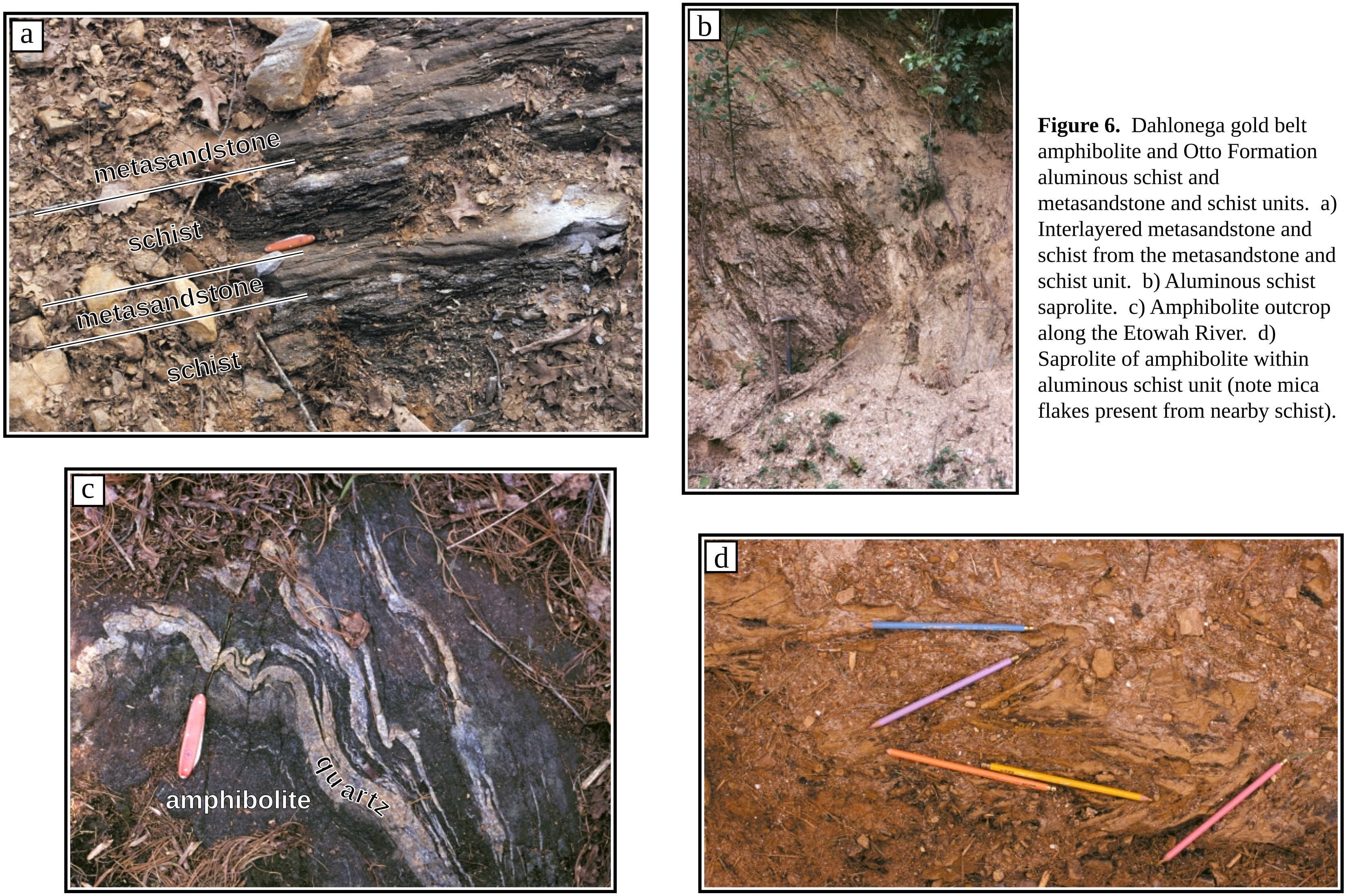

Figure 6. Dahlonega gold belt amphibolite and Otto Formation aluminous schist and metasandstone and schist units. a) Interlayered metasandstone and schist from the metasandstone and schist unit. b) Aluminous schist saprolite. c) Amphibolite outcrop along the Etowah River. d) Saprolite of amphibolite within aluminous schist unit (note mica flakes present from nearby schist).

within schist and thin layers of schist within metasandstone (Fig. 6a). Amphibolite occurs as sparse localized layers of varying thicknesses (< 1 meter to hundreds of meters). Amphibolite texture and composition is similar to amphibolite previously described within the mafic complex. The quartzite/metasandstone and schist unit predominantly contains fine-grained, light to medium gray, quartzite/metasandstone with locally abundant muscovite schist. The saprolite for the quartzite/metasandstone and schist unit is characteristically orange-brown to tan to light lavender to pink.

A small, localized occurrence of hornblendite exists near the north end of the Sally Free mafic complex (Fig. 3). The hornblendite is dark green, fine- to medium-grained, slightly weathered, discontinuous, and massive. The relationship between the hornblendite and the surrounding metasedimentary rocks of the Otto Formation and the adjacent Sally Free mafic complex is unclear.

Coweeta Group

Rocks of the Coweeta Group (Hayesville-Soque River thrust sheet) within the study area have been divided into three units: Coleman River Formation, amphibolite, and hornblende gneiss (Fig. 3). The Coleman River Formation consists of metasandstone, quartz-feldspar gneiss, pelitic schist, minor calc-silicate quartzite, and amphibolite. Metasandstone is well-foliated, medium to dark gray, fine- to medium-grained, inequigranular (Fig. 7; Table 4). Metasandstone layers range from centimeters to meters thick and are typically separated by pelitic schist of varying thickness (Fig. 7). Gneiss, similar in composition to the previous metasandstone, is fine- to medium-grained and inequigranular (Fig. 7d). Gneissic texture (common to the Coleman River Formation) is produced by a combination of partial migmatization (minimum melt conditions) and thin biotite-dominant schistose interlayers (Fig. 7).

Schists are well-foliated, gray to silver (fresh) and medium- to coarse-grained. Thicknesses of schist layers vary from thin interlayers within metasandstone to several

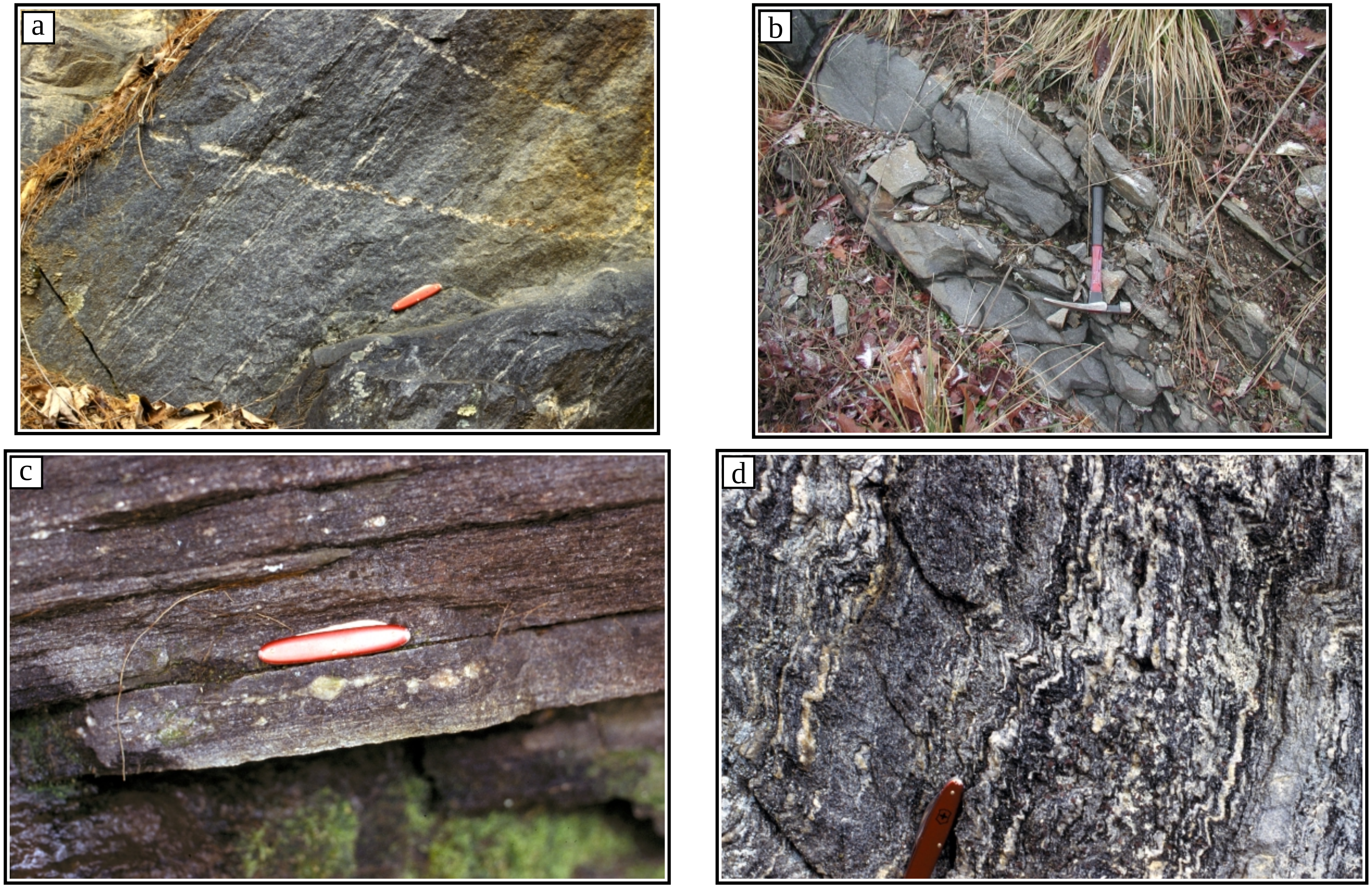

Figure 7. Coweeta Group, Coleman River Formation, from within the Hayesville thrust sheet. a) and (b) Dark, massive metasandstone. c) Inequagranular texture common to Coleman River Formation metasandstone. d) Gneissic texture produced by a combination of partial migmatization and thin biotite-dominant schistose interlayers.

meters. Calc-silicate quartzite occurs throughout the Coweeta Group in massive, poorly foliated layers, as much as 25 cm thick. Metasandstone, gneiss, and schist are moderately to well foliated with crenulations common in mica-rich zones (Fig. 7). The Coleman River Formation weathers red-brown to characteristic dark red-brown due to biotite dominance.

Amphibolite, similar in composition and texture to those previously discussed within the Dahlonega gold belt, occurs locally as sparse thin layers throughout the Coweeta Group. Garnet-bearing amphibolite boudins have also been observed infrequently. Highly weathered hornblende gneiss was delineated in limited saprolite exposures and as float along the border between the Campbell Mountain and Nimblewill quadrangles (Fig. 3). The origin of the hornblende gneiss and its relationship to the surrounding Coleman River Formation are unclear.

Great Smoky Group

The Great Smoky Group within the study area contains metasandstone, muscovite-biotite schist, and abundant calc-silicate quartzite (Fig. 8). Metasandstone is moderately- to well-foliated, medium gray, fine- to medium-grained, dominantly equigranular and is typically massive but can occur as thin layers with muscovite-biotite schist (Table 4; Fig. 8). Muscovite-biotite schist is well foliated, gray to silver, medium grained and is commonly thinly layered separating both thin and massive metasandstone layers (Fig. 8). Abundant macroscopic sillimanite was locally observed in outcrops of muscovite-biotite schist (Fig. 8d). Calc-silicate quartzite is abundant and occurs in massive, poorly foliated layers (Fig. 8). The Great Smoky Group here is moderately to well foliated and typically weathers red-brown to brown to tan.

PROTOLITHS

Modes of metasedimentary rocks from the Dahlonega gold belt (Otto Formation), Coweeta Group (Coleman River Formation), and Great Smoky Group (undivided) were

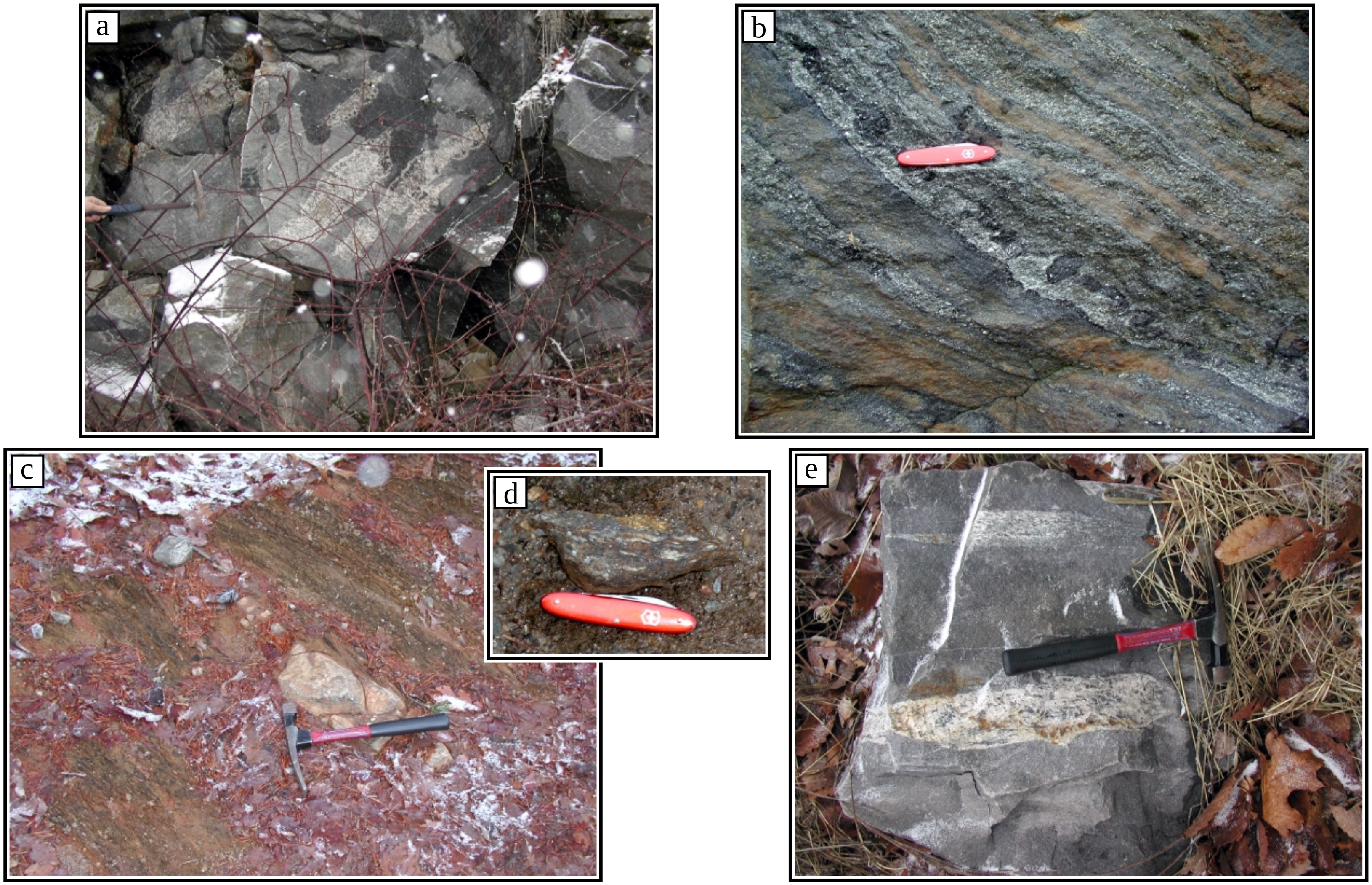

Figure 8. Great Smoky Group metasandstone and schist. a) Massive metasandstone containing pods of calc-silicate quartzite. b) Interlayered metasandstone and schist. c) Calc-silicate within sillimanite-bearing pelitic schist. d) Locally abundant sillimanite within previous (c) pelitic schist. e) Calc-silicate quartzite within dark, massive metasandstone.

plotted on modified sandstone classification ternary diagram from Pettijohn (1949) to determine probable protolith (Fig. 9). The classification diagrams, originally used for unmetamorphosed sandstones by Pettijohn (1949), are used here with the following assumptions previously outlined by McClellan (1988): mica represents metamorphosed clay (Hadley and Goldsmith, 1963); quartz and feldspar reactions are minimal; quartz and feldspar are present in their original abundances; and volume change is negligible. Protoliths for the Coleman River Formation here consist predominantly of graywacke with some arkose. The Great Smoky Group here is also dominantly graywacke with some arkose and feldspathic sandstone. Protoliths for the Otto Formation vary from shale to subgraywacke to graywacke to arkose, indicative of the variety of metasedimentary rocks within the Dahlonega gold belt.

Rocks within the Sally Free mafic complex are considered igneous of both plutonic and volcanic origin (Settles *et al,* in preparation). Mineralogy and texture of rocks within the hornblende gneiss-metagabbro-amphibolite unit indicate gabbroic to dioritic protoliths, which appear intrusive in origin. Key outcrops of the amphibolite unit along the eastern side of the complex contain possible relict extrusive basaltic igneous textures, such as amygdules (Settles *et al.*, in preparation). Pervasive shearing, transposition, and alteration related to intense deformation and metamorphism of rocks within the Sally Free mafic complex complicate accurate determination of possible protoliths.

METAMORPHISM

The Blue Ridge comprises a large portion of the southern Appalachian metamorphic core. Metamorphic grade in the western Blue Ridge ranges from lower greenschist facies (chlorite grade) along the Blue Ridge front to upper amphibolite facies (sillimanite grade) within the western-central Blue Ridge Great Smoky Group (Drake *et al.*, 1989). The central-eastern Blue Ridge is dominantly amphibolite facies reaching as high as granulite facies (second sillimanite) within portions of the central Blue Ridge (Winding Stair Gap

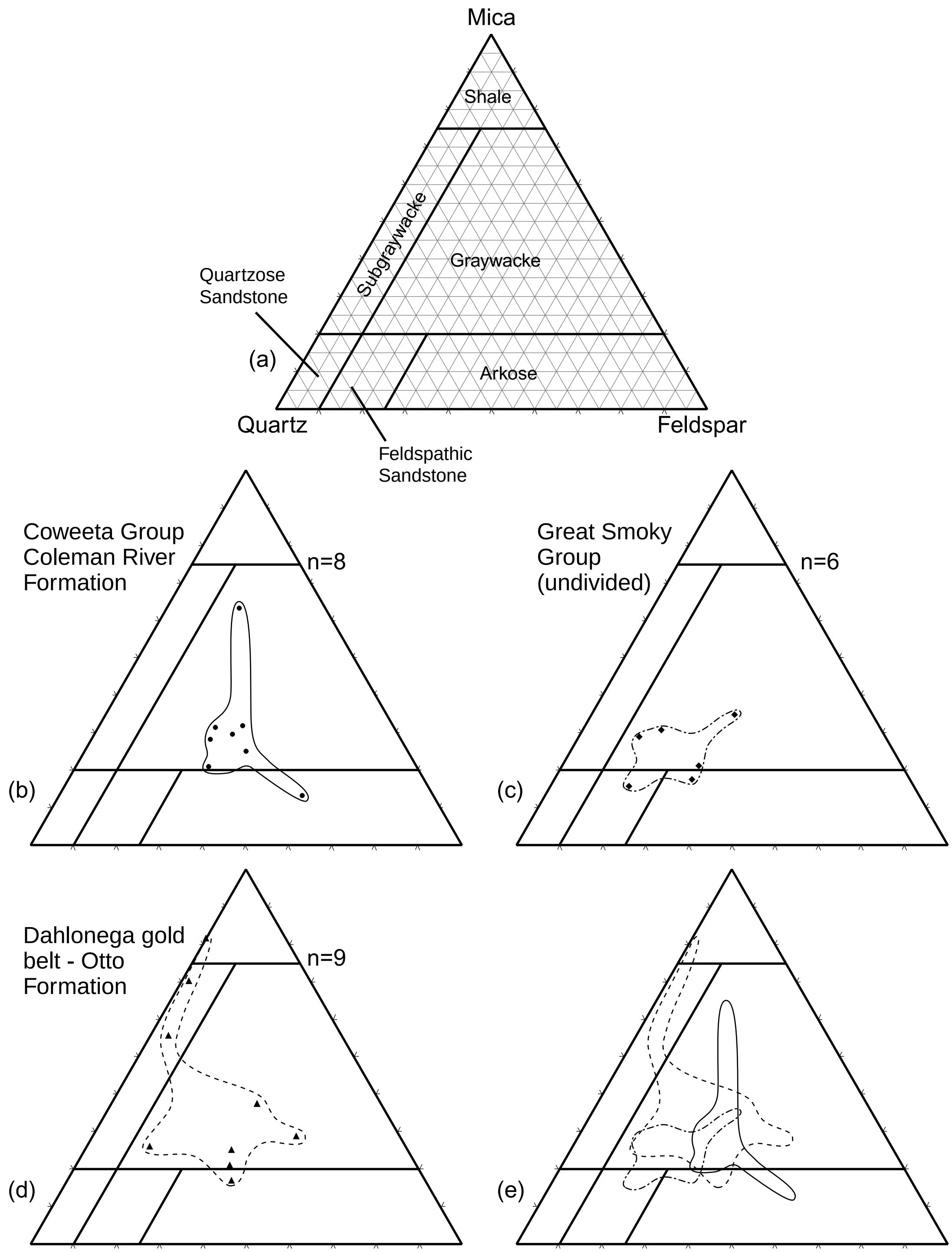

Figure 9. Quartz-feldspar-mica ternary diagrams comparing the composition of metasedimentary rocks from the the Coweeta Group, Coleman River Formation, Great Smoky Group (undivided), and the Dahlonega gold belt-Otto Formation. a) Modifed sandstone classification from Pettijohn (1949). b) Coweeta Group, Coleman River Formation. c) Great Smoky Group (undivided). d) Dahlonega gold belt, Otto Formation. e) Composite field diagram of b, c, and d.

and the Wayah granulite facies metamorphic core; Force, 1976; Absher and McSween, 1985; Eckert *et al.*, 1989). Metamorphism of Great Smoky Group rocks within the study area (Fig. 3) occurred under upper amphibolite facies conditions indicated by observed sillimanite in both outcrop (Fig. 8) and thin section. Rocks of the Coweeta Group, Coleman River Formation, within the Hayesville-Soque River thrust sheet, locally have a prominent gneissic texture (Fig. 7d) resulting from metatexis and metamorphic segregation. The metamorphic grade of these rocks are also believed to be upper amphibolite facies.

Abundant garnet, staurolite, and kyanite observed in numerous thin sections from Dahlonega gold belt, Otto Formation, aluminous schist unit (e.g., sample CM-129 on Fig. 5) indicate middle amphibolite facies metamorphism, which is a lower metamorphic grade relative to the adjacent Great Smoky and Coweeta Groups (Fig 10). Several workers have also noted a lower metamorphic grade within the gold belt relative to the surrounding thrust sheets (Fig. 10; Gillon, 1982; McConnell and Abrams, 1984; German, 1985). Equilibrium metamorphic conditions within the Dahlonega gold belt produced kyanite as the dominant aluminum silicate mineral rather than sillimanite, which is prominent in other units of the study area. Evidence of incomplete retrogression to chlorite grade is pervasive within the study area and throughout the central-eastern Blue Ridge (Butler, 1972; Hatcher, 1978). Chlorite frequently replaces biotite and, to a lesser extent, garnet (Fig. 5) and sericite replaces plagioclase in numerous thin sections.

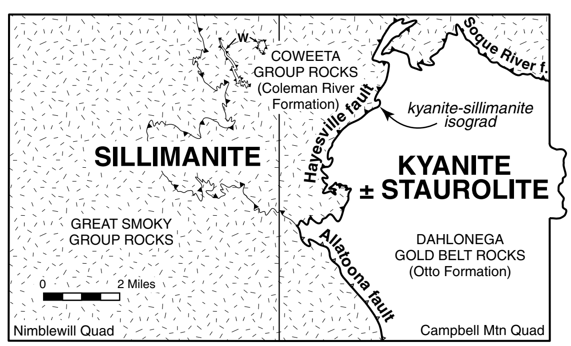

Figure 10. Metamorphic grade based on index minerals observed in the study area. Kyanite-sillimanite isograd follows the trace of the Hayesville-Soque River fault in the northern and northwestern parts of the Campbell Mountain quadrangle and the Allatoona fault in southwestern part of the Campbell Mountain quadrangle.

Numerous studies have broadly defined timing of peak metamorphism within the Blue Ridge as Early Paleozoic, Taconian. Recent U-Pb zircon age dating by Moecher and Miller (2000) of post-kinematic leucosomes that crosscut the dominant foliation at Winding Stair Gap defines an age of 470 Ma for youngest melting and peak metamorphism. The timing of high-grade Ordovician metamorphism has also been age dated at 461 ± 4 Ma with U-Pb analyses of metamorphic zircon from the Bakersville, North Carolina eclogite (Miller *et al.,* 2000). Quinn (written comm., 2001) determined an age of 460 Ma for metamorphic monazite from within the Hayesville thrust sheet near Sylva, North Carolina, further supporting a Middle Ordovician age of Taconian metamorphism within the central Blue Ridge. Numerous other isotopic studies have broadly defined a 480 to 440 Ma range for Blue Ridge Taconian metamorphism (Dallmeyer, 1975; Kish *et al.*, 1976; Kish, 1982).

Over 50 metamorphic monazite age determinations by Kohn (2001) of amphibolite facies Great Smoky Group rocks yielded a strong ~370 Ma age peak and no ages older than 425 Ma or younger than 320 Ma for metamorphism within the Great Smoky Mountains. Kohn (2001) interpreted this younger age to be indicative of arc terrane accretion during the Acadian rather than the Taconian orogeny and that southeastern Laurentia, including the western Blue Ridge Great Smoky Group, was unaffected by earlier Taconian-age events. $^{40}Ar/^{39}Ar$ isotopic studies by Dallmeyer (1988) of eastern Blue Ridge rocks in the vicinity of Tallulah Falls Dome and within the Dahlonega gold belt have yielded considerably younger 320 and 330 Ma ages providing the closest estimate of the minimum age of uplift in the eastern Blue Ridge.

DEFORMATION

Penetrative polyphase deformation within the southern Appalachian central/eastern Blue Ridge has been well documented by numerous authors (summarized in Table 5). Most workers have identified at least four episodes of deformation and folding although

Table 5. Compilation from select previous studies of deformation and folding within the central/eastern Blue Ridge modified from Hopson (1994).

this study	D_1 Early S_1 foliation preserved with isoclinal, recumbent F_2 folded amphibolite boudins	D_2 F_2 - isoclinal with axial planar S_2 penetrative schistosity and gneissic banding (dominant)	D_3 F_3 - tight to isoclinal; S_3 - nonpenetrative axial planar cleavage	D_4 F_4 - crenulations and chevron folds; S_4 - crenulation cleavage	D_5 F_5 - open, upright folding of all previous structures	D_6 Not Recognized
Hatcher (1977)	F_0 suggested that macroscopic structure of the Toxaway dome required pre-F_1 folds, thus F_0	F_1 isoclinal, E to NE trending fold axes, recumbent; S_1 - dominant foliation	F_2 isoclinal to open, NE trending, upright	F_3 crenulations. NE trending, upright; S_4 - crenulation cleavage	F_4 open, flexural folds, NE trending, upright	F_5 open, flexural folds, NW trending, upright
Hatcher and Butler (1979)	F_1 isoclinal, EW to NE trending axes, recumbent, observed in amphibolite boudins and as intrafolial folds	F_2 isoclinal, EW to NW trending fold axes, recumbent; S_1 - dominant foliation	F_3 isoclinal to open, NE trending, upright	F_4 crenulations. NE trending, upright; crenulation cleavage	F_5 open, NE trending, upright	F_6 open, NW trending, upright
Shellebarger (1980)	D_1 recumbent, flowage folds; S_1 - non-penetrative	D_2 isoclinal, NE trending fold axes, upright to overturned; S_1 - penetrative foliation	D_3 F_2 - crenulations, N-NE trending, axial surfaces upright to overturned; S_3 - nonpenatrative crenulation cleavage	D_4 tight to open folds and crenulations, E-W trending; S_4 - locally developed crenulation cleavage	Not Recognized	Not Recognized
Wooten (1980)	Not Recognized	D_1 isoclinal, NE trending fold axes, overturned; S_1 - dominant foliation	D_2 F_2 - crenulations, N-NE trending, axial surfaces upright to overturned; S_3 - nonpenatrative crenulation cleavage	Not Recognized	D_3 regional warping of all structures, E-W crenulations	Not Recognized
Eckert (1984)	Not Recognized	F_1 isoclinal, E to NE trending fold axes, upright; S_1 - dominant foliation	F_2 tight to isoclinal, NE trending, upright	F_3 open to tight folds and crenulations, NE trending	F_4 upright, crenulations	Not Recognized
Nelson (1988)	F_1 rootless, isoclinal, NE trending fold axes, recumbent to reclined	Not Recognized	F_2 isoclinal, NE trending, steep to recumbent; S_3 - rarely well developed	F_2 crenulations, upright; S_3 - crenulation cleavage observed in schists	F_4 gentle warps, ENE to NNE, upright	Not Recognized
McClellan (1988)	D_1 F_1 - not observed; S_1 - pinstripes	F_2 isoclinal, rootless, intrafolial, recumbent; S_2 - dominant foliation	D_2 F_3 - tight to isoclinal, NE trending, recumbent; S_3 - locally observed	D_3 F_4 - tight to open upright folds or kink folds, NNE trending; S_4 - locally observed	D_4 F_5 - open to chevron folds, NW to NNW trending, upright to overturned	D_6 open, NW trending, upright to recumbent
Gillon (1989)	F_1 rootless, NE to WNW trending fold axes, recumbent	Not Recognized	F_2 isoclinal, NE trending, upright	F_3 crenulations; S_3 - crenulation cleavage locally observed	F_4 open upright folds produce dome and basin interference pattern	Not Recognized
Hopson (1994)	D_1 F_1 - intrafoliol folds, orientation unknown; S_1 - includes pinstriping and gneissic banding	D_2 F_2 - NE trending, recumbent to upright due to later folding by F_3; S_2 - dominant foliation, penetrative schistosity and gneissic banding	D_3 F_3 - tight to isoclinal, NE trending, axial surfaces upright to steeply dipping; S_3 - nonpenatrative	D_4 F_4 - crenulations and chevron folds, NE to NW trending (orientation depends on rotation of surface folded) subhorizontal to gently dipping axial surfaces; S_4 - crenulation cleavage	D_5 F_5 - open, NE to EW trending, upright	D_6 F_6 - open, N to NW trending, upright

as many as six phases have been recognized, producing complex interference patterns at both meso- and macroscopic scales (Table 5; Hatcher, 1977; Hatcher and Butler, 1979; Wooten, 1980; Shellebarger, 1980; Eckert, 1984; McClellan, 1988; Nelson, 1988; Gillon, 1989; Hopson *et al.*, 1989; Hopson, 1994). The identification of multiple deformational events in the study area is limited by the lack of large, well exposed, outcrops with overprinting relationships such as observed at Woodal Shoals (Chattahoochee thrust sheet), South Carolina and Georgia (Hatcher, 1976, 1977), and Sill Vinson's Rock (Dahlonega gold belt) near Otto, North Carolina (Hatcher, 1980). As a result, the identification of deformational events is based on observed macro-, meso-, and microscale structures within the study area and comparison with other studies within the Blue Ridge (Table 5).

Evidence of D_1 deformation within the study area is limited to F_2 (D_2) rootless recumbent isoclinal folds of an older S_1 (D_1) foliation within amphibolite boudins of the Coleman River Formation. Rootless intrafolial folds and axial-planar recumbent folds (within boudins) observed in other parts of the Blue Ridge are considered F_1 and related to D_1 deformation (Table 5; Hatcher and Butler, 1979; Hopson, 1994). S_2 penetrative foliation, related to the D_2 event, is deflected around amphibolite boudins. No evidence of D_1 deformation has been observed within either the Dahlonega gold belt or Great Smoky Group within the study area.

Pervasive D_2 deformation within the study area is characterized by F_2 tight to isoclinal, subhorizontal to recumbent, folds and a penetrative axial planar S_2 foliation. Near complete transposition of the S_1 foliation surface occurred during D_2 with the exception of the amphibolite boudins. S_2 is the dominant foliation in the central/eastern Blue Ridge and is primarily defined by parallel alignment of platy minerals, schistosity, and compositional banding consisting of alternating quartzofeldspathic (minimum melt) layers with muscovite/biotite rich layers (Fig. 7). The S_2 surface is further characterized by the preferred orientation of micas within interlayered metagraywacke and muscovite/biotite schist (graywacke and shale protoliths, respectively?), possibly related to original S_0 depositional layering of incomplete (finer fraction) Bouma sequences (Figs. 6 and 7), which have survived D_1 deformation.

S_2 measurements from the study area are divided into four structural domains on the basis of structural trends (Fig. 11). Domain analysis is complicated by trend modification due to later folding events (F_3 to F_6?). Yet, equal-area stereonet scatter and Kamb plots of poles to S_2 foliation within domains I, III, and IV show polar concentrations and slight variations in mean foliation trends (345º, 317º, and 322º, respectively; Fig. 11). Domain II contains considerable interference and is less clear. The S_2 surface dips moderately with amounts varying from shallow to steep (mean = 38.5º) with 60 percent occurring between 20 and 45 degrees (Fig. 11).

D_3 deformation is characterized by F_3 folding of the previous S_2 foliation and the development of an S_3 axial planar, nonpenetrative, cleavage. F_3 flexural flow folds are tight to isoclinal, upright to reclined, and commonly have attenuated limbs and thickened hinges. Less common, disharmonic and sheath folds (Fig. 6c and 5d, respectively) are also considered to be F_3. D_4 deformation is characterized by S_4 crenulation cleavage and chevron folds (Figs. 6d and 7d, respectively) that occur sporadically in the study area. D_5 deformation is characterized by regional warping of all structures producing open upright folds.

FAULTS

Faulting occurs within the study area as both early pre- to syn-metamorphic crustal-scale (Hayesville-Soque River and Allatoona faults) and minor thrust faults (Etowah River fault). The presence of mylonites and contact cut offs along the northwestern perimeter of the Sally Free mafic complex indicates fault emplacement (thrust) to the northwest over the metasandstone-and-schist and aluminous-schist units of the Otto

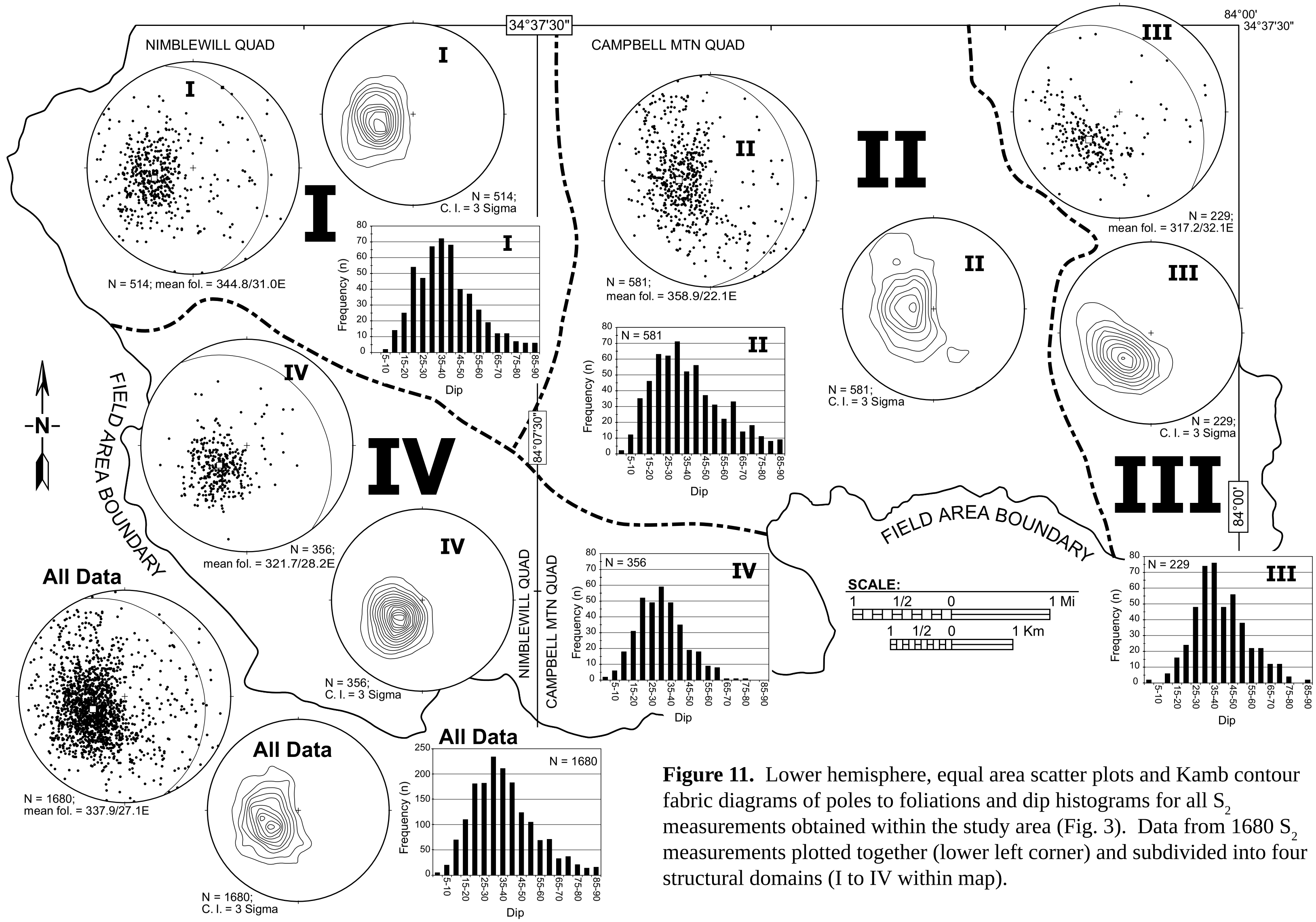

Figure 11. Lower hemisphere, equal area scatter plots and Kamb contour fabric diagrams of poles to foliations and dip histograms for all S_2 measurements obtained within the study area (Fig. 3). Data from 1680 S_2 measurements plotted together (lower left corner) and subdivided into four structural domains (I to IV within map).

Formation (Figs. 3 and 12). Detailed mapping for this study only defines the northern and western fault contacts of the Sally Free mafic complex; thus, it is unclear whether this fault, termed the Etowah River fault, bounds the complex as a klippe or continues to the south and east into the Dahlonega gold belt (Fig. 3). Compilation of the southern portion of the Campbell Mountain quadrangle from Nelson (1991) with mapping from this study and careful observation of published geologic maps of the Dahlonega (east of Campbell Mountain; Nelson, 1991) and Dawsonville (south of Campbell Mountain; German, 1985) 7.5-minute quadrangles does not clearly indicate a fault relationship to the south and/or east of the complex (Fig. 3). The contact between the Sally Free mafic complex and the Otto Formation quartzite/metasandstone along the southern perimeter of the complex is more sinuous than the northern contact of the Etowah River fault (Fig. 3; section B-B' on Fig. 12). This observation is interpreted to mean the complex is not fault bounded.

Hayesville-Soque River fault

Detailed geologic mapping and tracing of the Hayesville fault contact between the Coweeta Group (hanging wall) and Great Smoky Group (footwall) from the northwest and the Soque River fault contact between the Coweeta Group (HW) and Dahlonega gold belt (FW) from the northeast into the study area (Figs. 1, 3, and 13) confirms that the Hayesville and Soque River faults bound different sides of the same thrust sheet and are the same fault, as hypothesized by Nelson (1991). This also confirms Nelson's (1991) hypothesis that the area west-northwest of Dahlonega, Georgia, marks the southwestern terminus of the Hayesville-Soque River thrust sheet (Figs. 3, 12, and 13). Inequigranular, biotite-dominant (over trace muscovite), often migmatitic gneiss and schist of the Coleman River Formation (Coweeta Group) versus two-mica, nonmigmatitic, often equigranular metasandstone and schist of the Great Smoky Group and Otto Formation (Dahlonega gold belt) are the principal characteristics for delineation of the Hayesville-

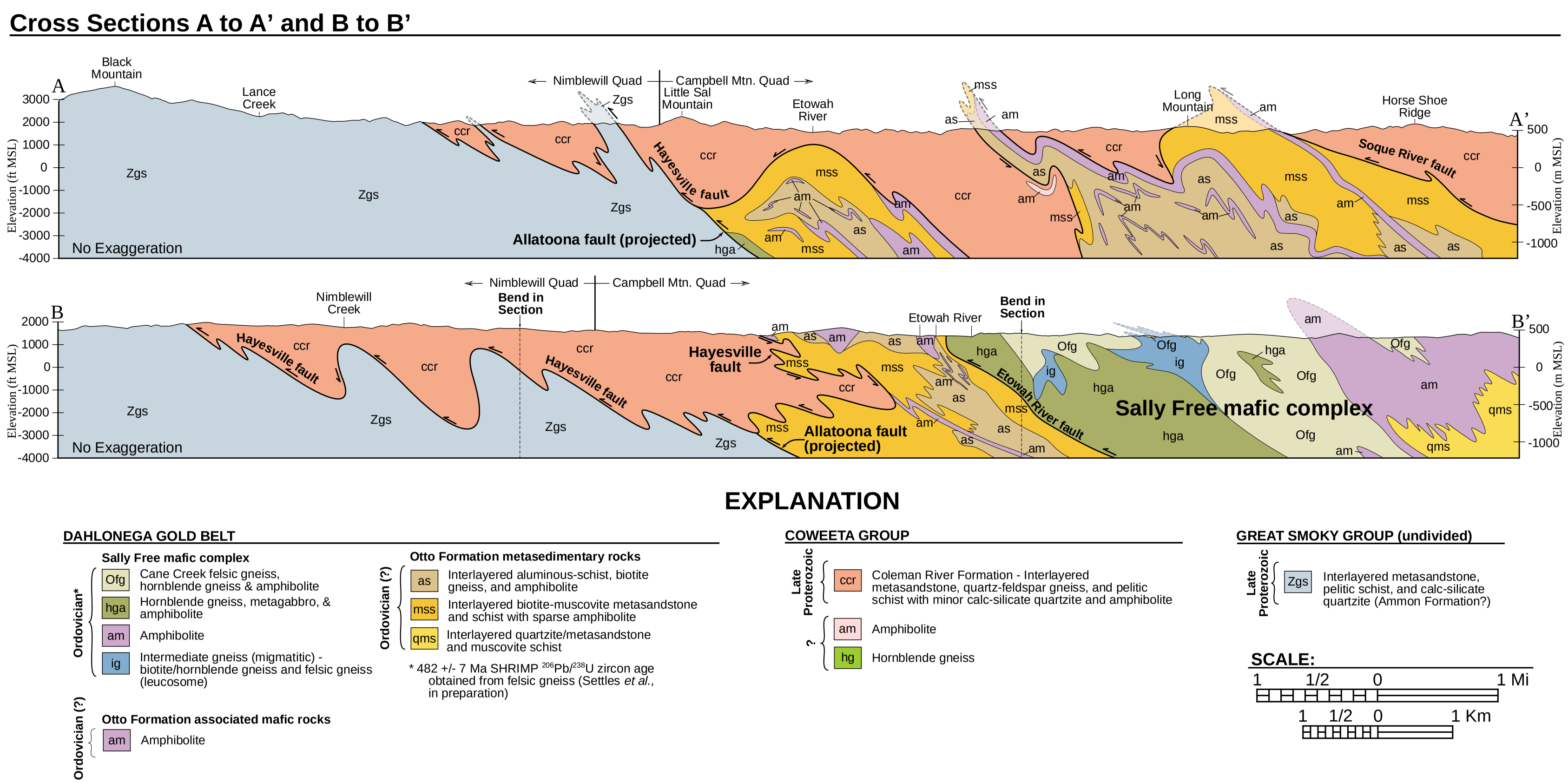

Figure 12. Cross sections A-A' and B-B' across the study area. Sections lines referenced on Figure 3.

Scale: 1:250,000

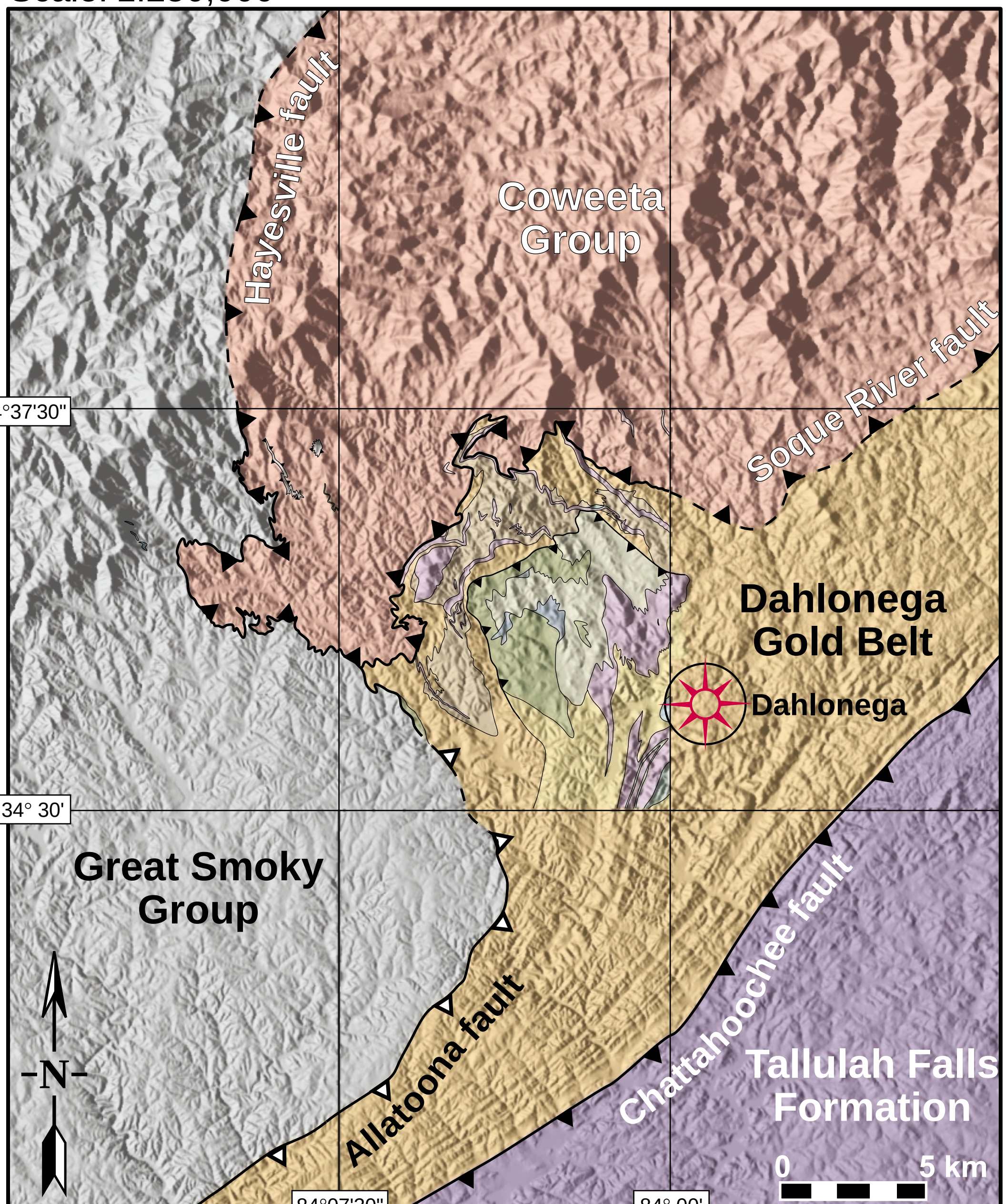

Figure 13. Geologic shaded relief map of the central Blue Ridge in the vacinity of Dahlonega, Georgia. Geology compiled from Gillon (1982), German (1985), Nelson (1991, 1992), and this study. Regional location reference indicated on Figure 1.

Soque River fault here. The premetamorphic Hayesville-Soque River fault within the study area is highly folded (F_3), locally overturned, and considered to predate D_3 deformation (Figs. 3, 12, and 13). The premetamorphic nature of the Hayesville fault is based on observed folding (Figs. 3 and 12) and the relationship of the fault to uninterrupted metamorphic isograds observed in numerous parts of the southern Appalachian Blue Ridge (Hatcher, 1978; Wooten, 1980; Eckert, 1984, 1988; Eckert *et al.*, 1989).

Tight to isoclinal F_3 folding of the Hayesville-Soque fault is evident in map pattern (Fig. 3) and within cross sections through the study area (Fig. 12). Fold interference produces two Hayesville-Soque river fault windows exposing Great Smoky Group paragneiss within Hayesville-Soque River thrust sheet (section A-A' on Figs. 3 and 12). Costello (per comm.) has also identified a Hayesville-Soque River klippe of Coleman River Formation paragneiss, tentatively referred to as the Burnt Mountain klippe, in the southwestern corner of the Amicalola quadrangle, approximately 13 km west of the study area (Fig. 1). The Burnt Mountain klippe is also the result of fold interference and possibly represents an erosional remnant of a northeastward retreating Hayesville-Soque River thrust sheet.

Allatoona fault

Hurst (1973) first named the Allatoona fault for a major fault traceable from Paulding to Dawson County, Georgia, separating rocks of the Ashland Group (Dahlonega gold belt) to the southeast from rocks of the Great Smoky Group and Talladega belt to the northwest (Fig 1). This major fault has since been continued from central Alabama into Lumpkin County, Georgia, where it enters the study area (Fig. 2; Hatcher, 1978; Williams, 1978; McConnell and Costello, 1980; German, 1985; Hatcher *et al.*, 1990). The Allatoona fault is interpreted as post-peak metamorphic within Paulding, Cherokee, and Dawson Counties, Georgia (McConnell and Costello, 1980; German, 1985). German

(1985) identified postmetamorphic movement along the Allatoona fault approximately 20 km southwest of Dahlonega based on the truncation of the northwestern limb of the Auraria antiform within Dawson County, Georgia (Fig. 14).

No evidence of postmetamorphic movement along the Allatoona fault was observed within the study area west of Dahlonega (Fig. 3). The fault boundary here, which separates the Dahlonega gold belt (hanging wall) from the Great Smoky Group (footwall), appears to be pre- to synmetamorphic and to predate the Hayesville-Soque River fault (Figs. 12 and 14). Although the intersection of the Hayesville-Soque River and Allatoona faults was not observed in outcrop, it appears the Hayesville-Soque River fault truncates the Allatoona fault approximately 11 km west of Dahlonega, Georgia (Figs. 3, 12, 13, and 14). The previous interpretation that the Hayesville and Soque River faults are equivalent requires that the Allatoona fault terminate here (Figs. 4 and 14).

DISCUSSION

The Allatoona fault appears to have a complex history of pre- to synmetamorphic movement followed by later reactivation; thus, the fault delineated within the Campbell Mountain quadrangle for this study, termed the ancestral Allatoona fault (Fig. 3), was later reactivated as the postmetamorphic Allatoona fault extending from Dawson County, Georgia (German, 1985) to the southwest (Fig. 14). Hurst (1973) suggested decreasing displacement along the postmetamorphic Allatoona fault to the northeast from Paulding County to Dawson County, Georgia (Fig. 1). Considering this observation, it can be suggested that reactivation along the ancestral Allatoona fault, producing the postmetamorphic Allatoona fault recognized by German (1985) in Dawson County, only continued to a point approximately 8 km southwest of Dahlonega (Fig. 14). At this point, the ancestral Allatoona fault continues to the northwest, approximately 90 degrees from the original northeast trend (Fig. 14), where it terminates into, and is cut off by, the Hayesville-Soque River fault. Postmetamorphic displacement was possibly transferred

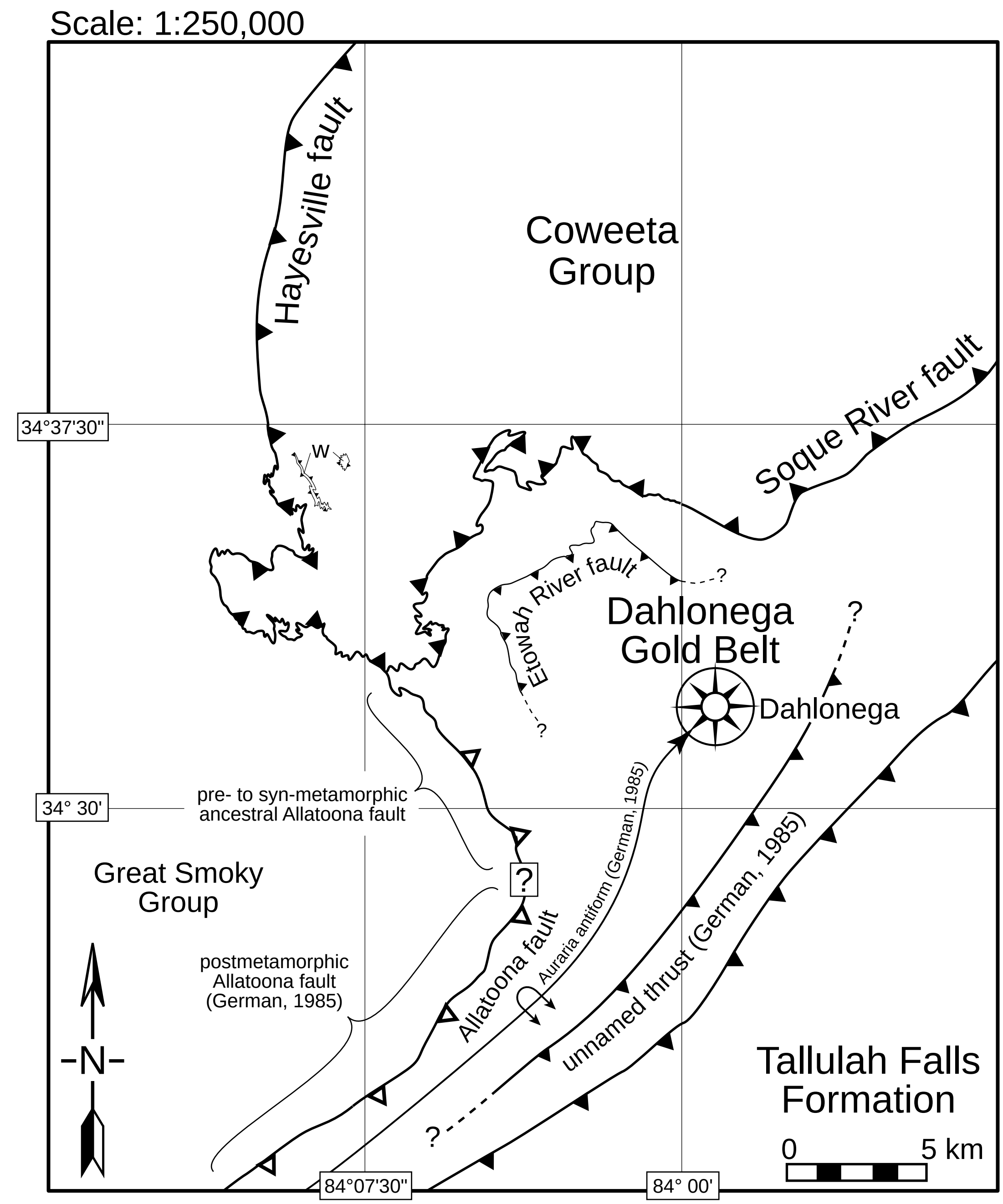

Figure 14. Tectonic map of the central Blue Ridge in the vacinity of Dahlonega, Georgia. Geology and structure compiled from Gillon (1982), German (1985), Nelson (1991, 1992), and this study. Blue Ridge location reference indicated on Figure 1.

from the Allatoona fault to internal faulting within the Dahlonega gold belt (Fig. 14). This interpretation is further supported by the delineation of an internal thrust south-southwest of Dahlonega by German (1985), which parallels the original northeast trend of the reactivated postmetamorphic Allatoona fault (Fig. 14).

Confirmation that the Hayesville and Soque River faults are equivalent indicates that the Hayesville-Soque River fault trends southwest along the northwest side of the thrust sheet (Coweeta Group over Great Smoky Group) into Lumpkin County, Georgia, at which point the trace turns 180 degrees and trends northeast along the southeast side of the thrust sheet (Coweeta Group over Dahlonega gold belt; Figs. 1, 4, and 14). It is uncertain along which fault, if any, the Hayesville-Soque River fault returns to the southwest (Fig. 1). Despite unresolved issues concerning relative timing between the Hayesville-Soque River fault (premetamorphic) and the Chattahoochee fault (postmetamorphic), similarities in stratigraphy indicate that the Chattahoochee fault may also be part of the Hayesville-Soque River fault system, continuing the fault to the southwest (Fig. 1). Both thrust sheets contain dark, biotite dominant, often migmatitic, upper-amphibolite facies, metasandstone and schist.

TECTONIC IMPLICATIONS

The previous interpretation that the Allatoona fault represents the southwestern continuation of the Hayesville-Gossan Lead terrane boundary requires significant reconsideration due to observed fault geometries within this study. Resolution of this problem requires careful consideration of regional fault geometries and the Dahlonega gold belt, its current tectonic position, and its role in the tectonic evolution of the southern Appalachians. Previous hypotheses defining the Allatoona-Hayesville thrust and terrane boundary in North Georgia interpreted rocks of the Hayesville-Soque River, Dahlonega gold belt, and Chattahoochee thrust sheets to be part of a collective eastern Blue Ridge assemblage. This association is made despite obvious differences between the gold belt and the adjacent eastern Blue Ridge thrust sheets (Hayesville-Soque River and Chattahoochee).

A recently obtain U/Pb 482 ± 7 Ma magmatic age for the Cane Creek felsic gneiss within the Sally Free Mafic complex constrains volcanic arc related igneous activity, and possibly sediment deposition, for this portion of the Dahlonega gold belt to the Early Ordovician (Settles *et al.*, in preparation). This interpretation is further supported by Early to Middle Ordovician (460 to 490) magmatic ages of felsic gneisses throughout the north Georgia Dahlonega gold belt (Villa Rica, Galts Ferry, Barlow, and Lake Burton gneisses; Thomas, 2001; Thomas *et al.*, 2001). Timing of igneous activity and sediment deposition within the gold belt significantly conflicts with timing of Early to Middle Ordovician Taconian metamorphism, recently dated at 470 Ma and 460 Ma within the central/eastern Blue Ridge at Winding Stair Gap (Moecher and Miller, 2000), and near Bakersville and Sylva, North Carolina (Miller *et al.*, 2000; Quinn written comm., 2001), respectively.

The observation that gold belt volcanic arc related igneous activity and sediment deposition occurred coeval with Taconian metamorphism within other parts of the eastern Blue Ridge (Hayesville-Soque River, Chunky Gal Mountain, and Chattahoochee thrust sheets?) and new data suggesting the lack of Taconian metamorphism in the western Blue Ridge (Kohn, 2001) suggest that the eastern Blue Ridge, not including the gold belt, underwent high grade Ordovician metamorphism east of the Dahlonega gold belt and presumably outboard of Laurentia. This requires that arc terrane (gold belt) and eastern Blue Ridge accretion along the ancestral Allatoona and Hayesville-Soque River-Chattahoochee (?) faults, respectively, occurred during an extensive Acadian event rather than during the Taconic orogeny.

CONCLUSIONS

(1) Detailed geologic mapping confirms the hypothesis of Nelson (1991) that the Hayesville and Soque River faults are parts of the same thrust sheet and that the area immediately west-northwest of Dahlonega marks the southwestern terminus of the Hayesville-Soque River thrust sheet.

(2) Field and petrographic observations indicate that the Dahlonega gold belt within the study area was metamorphosed to a slightly lower grade (middle amphibolite facies, kyanite ± staurolite grade) relative to the adjacent Great Smoky and Coweeta Groups (upper amphibolite facies, sillimanite grade); thus, the Allatoona fault and a portion of the Hayesville-Soque River fault (east of the Allatoona fault intersection) together represent the kyanite-sillimanite isograd in this area.

(3) A pre- to synmetamorphic ancestral Allatoona fault exists, which was later truncated and cut off by the pre- to synmetamorphic Hayesville-Soque River fault west of Dahlonega; thus, the postmetamorphic Allatoona fault observed to the southwest (German, 1980) possibly represents reactivation along the ancestral Allatoona fault mapped here.

(4) Regional and local fault geometries indicate that the Dahlonega gold belt was thrust northwestward over the western Blue Ridge Great Smoky Group along the ancestral Allatoona fault and later overridden by the Hayesville-Soque River and Chattahoochee faults (Acadian?); thus, the Allatoona and Hayesville faults do not represent a continuous terrane boundary.

(5) The interpreted Early Ordovician age for both igneous activity and sediment deposition for the Dahlonega gold belt (Settles *et al.*, in preparation) implies that faulting (Hayesville-Soque River and Allatoona), metamorphism, and deformation within this portion of the southern Appalachian Blue Ridge is related to the Acadian rather than the Taconic orogeny.

REFERENCES CITED

Absher, B. S., and McSween, H. Y., Jr., 1985, Granulites at Winding Stair Gap, North Carolina: The thermal axis of Paleozoic metamorphism in the southern Appalachians: Geological Society of America Bulletin, v. 96, p. 647-654.

Ausburn, M. P., Hatcher, R. D., Jr., Bryan, G., Godfrey, S. C., and Acker, L. A., 1998, Geologic map and mineral resources summary of the Topton quadrangle, North Carolina: North Carolina Geologic Survey Map 6, 1:24,000 scale.

Butler, J. R., Age of Paleozoic regional metamorphism in the Carolinas, Georgia, and Tennessee southern Appalachian: American Journal of Science, v. 272, p. 319-333.

Dallmeyer, R. D., 1975, Incremental $^{40}Ar/^{39}Ar$ ages of biotite and hornblende from retrograded basement gneisses of the southern Blue Ridge: Their bearing on the age of Paleozoic metamorphism: American Journal of Science, v. 275, p. 440-460.

Dallmeyer, R. D., 1988, Polymetamorphic evolution of the western Blue Ridge allochthon: Evidence from $^{40}Ar/^{39}Ar$ mineral ages, *in* Fritz, W. J., and La Tour, T. E., eds., Geology of the Murphy Belt and related rocks, Georgia and North Carolina: Georgia Geological Society Guidebooks, v. 8, p. 111-134.

Drake, A. A., Jr., Sinha, A. K., Laird, J., and Guy, R. E., 1989, The Taconic orogen, *in* Hatcher, R. D., Jr., Thomas, W. A., and Viele, G. W., eds., The Appalachian–Ouachita orogen in the United States: Boulder, Colorado, Geological Society of America, The Geology of North America, v. F–2, p. 101-177.

Eckert, J. O., Jr., 1984, Stratigraphy, structure, and metamorphism in the east half of the Wayah Bald quadrangle, North Carolina: Key to Paleozoic granulite facies metamorphism in the southern Appalachians [M.S. thesis]: Columbia, University of South Carolina, 411 p.

Eckert, J. O., Jr., 1988, Petrology and tectonic implications of the transition from the staurolite-kyanite zone to the Wayah granulite facies metamorphic core, southwest Noth Carolina Blue Ridge: Including quantitative analysis of mineral homogeneity [Ph.D. dissertation]: College Station, Texas A&M University, 337 p.

Eckert, J. O., Hatcher, R. D., Jr., and Mohr, D. W., 1989, The Wayah granulite-facies metamorphic core, southwestern North Carolina: High-grade culmination of Taconian metamorphism in the southern Blue Ridge: Geological Society of America Bulletin, v. 101, p. 1434-1447.

Force, E. R., 1976, Metamorphic source rocks of titanium placer deposits—a geochemical cycle: U.S. Geolgical Survey Professional Paper 959-B, 13 p.

German, J. M., 1985, The geology of the northeastern portion of the Dahlonega gold belt: Georgia Geologic Survey Bulletin, v. 100, 41 p.

Gillon, K. A., 1982, Stratigraphic, structural, and metamorphic geology of portions of the Cowrock and Helen, Georgia 7.5-minute quadrangles [M.S. thesis]: Athens, University of Georgia, 236 p.

Gillon, K. A., 1989, The geology of eastern Blue Ridge thrust sheets in the vicinity of Helen, Georgia, *in* Fritz, W. J., Hatcher, R. D., Jr., and Hopson, J. L., eds., Geology of the eastern Blue Ridge of northeast Georgia and the adjacent Carolinas: Georgia Geological Society Guidebooks, v. 9, p. 133-169.

Hadley, J. B., 1970, The Ocoee Series and its possible correlatives, *in* Fisher, G. W., Pettijohn, F. J., Reed, J. C., and Weaver, K. N., eds., Studies in Appalachian geology: central and southern: New York, Wiley Interscience, p. 247-260.

Hadley, J. B., and Goldsmith, R., 1963, Geology of the eastern Great Smoky Mountains, North Carolina and Tennessee: U.S. Geological Survey Professional Paper 349-B, 118 p.

Hadley, J. B., and Nelson, A. E., 1971, Geologic map of the Knoxville quadrangle, North Carolina, Tennessee, and South Carolina: U.S. Geological Survey Miscellaneous Investigations Series Map I-654, scale 1:250,000.

Hatcher, R. D., Jr., 1976, Introduction to the geology of the eastern Blue Ridge of the Carolinas and nearby Georgia: Carolina Geological Society Guidebook, 53 p.

Hatcher, R. D., Jr., 1977, Macroscopic polyphase folding illustrated by the Toxaway dome, eastern Blue Ridge, South Carolina-North Carolina: Geological Society of America Bulletin, v. 89, p. 1678-1688.

Hatcher, R. D., Jr., 1978, Tectonics of the western Piedmont and Blue Ridge: Review and speculation: American Journal of Science, v. 278, p. 276-304.

Hatcher, R. D., Jr., 1979, The Coweeta Group and Coweeta syncline: major feature of the North Carolina-Georgia Blue Ridge: Southeastern Geology, v. 21, no. 1, p. 17-29.

Hatcher, R. D., Jr., 1980, Geologic map and mineral resources of the Prentiss quadrangle, North Carolina: North Carolina Geological Survey, GM 167–SW, scale 1:24,000.

Hatcher, R. D., Jr., 1988, Bedrock geology and regional geologic setting of Coweeta Hydrologic Laboratory in the eastern Blue Ridge, with some discussion of Quaternary deposits and structural controls of topography, *in* Swank, W. T., and Crossley, D. A., Jr., eds., Coweeta Symposium Volume 66: New York, Springer–Verlag, p. 81–92.

Hatcher, R. D., Jr., 1989, Tectonic synthesis of the U.S. Appalachians, Chapter 14, *in* Hatcher, R. D., Jr., Thomas, W. A., and Viele, G. W., eds., The Appalachian–Ouachita orogen in the United States: Boulder, Colorado, Geological Society of America, The Geology of North America, v. F–2, p. 511–535.

Hatcher, R. D., Jr., and Butler, J. R., 1979, Guidebook for southern Appalachian field trip in the Carolinas, Tennessee, and northeastern Georgia: International Geologic Correlation Program-Caledonide Orogen Project 27, University of North Carolina, Chapel Hill, 117 p.

Hatcher, R. D., Jr., Osberg, P. H., Robinson, P., and Thomas, W. A., 1990, Tectonic map of the U.S. Appalachians: Plate 1, *in* Hatcher, R. D., Jr., Thomas, W. A., and Viele, G. W., eds., The Appalachian–Ouachita orogen in the United States: Boulder, Colorado, Geological Society of America, The Geology of North America, v. F–2, scale 1:2,500,000.

Higgins, M. W., and McConnell, K. I., 1978, The Sandy Springs Group and related rocks of the Georgia Piedmont – nomenclature and stratigraphy, *in* Sohl, N. F., and Wright, W. B., eds., Changes in stratigraphic nomenclature by the U.S. Geological Survey, 1977: United States Geological Survey Bulletin 1457-A, p. A98-A105.

Higgins, M. W., Crawford, R. F., III, Nelson, A. E., and Crawford, T. J., 1988, The Talking Rock Complex: An ancient accretionary complex, northern Georgia and southern North Carolina: Geological Society of America Abstracts with Programs, v. 20, no. 4, p. 270.

Hopson, J. L., 1994, Geology of part of the eastern Blue Ridge, northeast Georgia and the adjacent Carolina [unpublished M.S. thesis]: Knoxville, University of Tennessee, 350 p.

Hopson, J. L., Hatcher, R. D., Jr., and Stieve, A. L., 1989, Geology of the eastern Blue Ridge, northeastern Georgia and the adjacent Carolinas, *in* Fritz, W. J., Hatcher, R. D., Jr., and Hopson, J. L., eds., Geology of the eastern Blue Ridge of northeast Georgia and the adjacent Carolinas: Georgia Geological Society Guidebooks, v. 9, p. 1-40.

Horton, J. W., Jr., Drake, A. A., Jr., and Rankin, D. W., 1989, Tectonostratigraphic terranes and their Paleozoic boundaries in the central and southern Appalachians: Geological Society of America Special Paper 230, p. 213-245.

Hurst, V. J., 1955, Stratigraphy, structure, and mineral resources of the Mineral Bluff quadrangle, Georgia: Georgia Geologic Survey, Bulletin 63, 137 p.

Hurst, V. J., 1973, Geology of the southern Blue Ridge belt: American Journal of Science, v. 273, p. 643-670.

King, P. B., 1949, The base of the Cambrian in the southern Appalachians: American Journal of Science, v. 247, p. 513-530, 622-645.

Kish, S. A., 1982, The application of potassium-argon dating of slates to the study of the metamorphic history of the southern Appalachian Piedmont and Blue Ridge: Geological Society of America Abstracts with Programs, v. 14, p. 31.

Kish, S. A., Fullagar, P. D., and Dabbagh, A. E., 1976, Paleozoic plutonic activity in the Blue Ridge of North Carolina: Geological Society of America Abstracts with Programs, v. 8, p. 211-212.

Kohn, M. J., 2001, Timing of arc accrection in the southern Appalachians: Perspectives from the Laurentian margin: Geological Society of America Abstracts with Programs, v. 33, no. 6, p. 262.

McClellan, E. A, 1988, Geologic history of a portion of the eastern Blue Ridge, southern Appalachians: Tray Mountain and Macedonia 7 1/2' quadrangles, Georgia [unpublished M.S. thesis]: Knoxville, University of Tennessee, 179 p.

McConnell, K. I., and Abrams, C. E., 1984, Geology of the Greater Atlanta region: Georgia Geological Survey Bulletin 96, 127 p.

McConnell, K. I., and Costello, J. O., 1980, Guide to geology along a traverse through the Blue Ridge and Piedmont Provinces of North Georgia, *in* Frey, R. W., ed., Excursions in southeastern geology: American Geological Institute, v. 1, p. 241-257.

Miller, B. V., Stewart, K. G., Miller, C. F., and Thomas, C. W., 2000, U-Pb ages from the Bakersville, North Carolina eclogite: Taconian eclogite metamorphism followed by Acadian and Alleghanian cooling: Geological Society of America Abstracts with Programs, v. 32, no. 2, p. A62.

Moecher, D. P., and Miller, C. F., 2000, Percise age for peak granulite facies metamorphism and melting in the eastern Blue Ridge from SHRIMP U-Pb analysis of zircon: Geological Society of America Abstracts with Programs, v. 32, no. 7, p. A113.

Nelson, A. E., 1988, Structure and chemistry of the metasedimentary and metavolcanic rocks of the Helen terrane in the Blue Ridge structural province of northeast Georgia: Geological Society of America Abstracts with Programs, v. 20, p. 307.

Nelson, A. E., 1991, Geologic map of the Campbell Mountain quadrangle, Lumpkin County, Georgia: U.S. Geological Survey Miscellaneous Field Studies Map MF-2148, 1:24,000 scale.

Nelson, A. E., 1992, Geologic map of the Dahlonega Quadrangle, Lumpkin and White Counties, Georgia: U.S. Geological Survey Geological Quadrangle Map GQ-1705, 1:24,000 scale.

Nelson, A. E., and Gillon, K. A., 1985, Stratigraphic nomenclature in the Richard Russell and Helen thrust sheet, north Georgia, *in* Contributions to Stratigraphy, 1984: U.S. Geological Survey Bulletin No. 1605-A, p. A59-A62.

Pettijohn, F. J., 1949, Sedimentary rocks: New York, Harper and Brothers, 526 p.

Rankin, D. W., 1976, Appalachian salients and recesses: Late Precambrian continental breakup and the opening of the Iapetus ocean: Journal of Geophysical Research, v. 81, p. 5605-5619.

Settles, D. J., Bream, B. R., and Hatcher, R. D., Jr., in preparation, The Sally Free mafic complex and associated mafic rocks of the Dahlonega gold belt: Evidence of Ordovician arc volcanism and intrusion northwest of Dahlonega, Georgia.

Shellebarger, J. E., 1980, Geology of portions of the Jacks Gap and Coosa Bald 7.5-minute quadrangles, northeast Georgia [M.S. thesis]: Athens, University of Georgia, 209 p.

Thomas, C. W., 2001, Origins of mafic-ultramafic complexes of the eastern Blue Ridge province, southern Appalachians: Geochronological and geochemical contraints [MS Thesis]: Nashville, Vanderbilt University, 154 p.

Thomas, C. W., Miller, C. F., Fullagar, P. D., Meschter-McDowell, S. M., Vinson, S. B, and Bream, B. R., 2001, Where is the arc? Discontinuities in Taconian arc magmatism in the southern Appalachians: Geological Society of America, Abstracts with Programs, , v. 23, no. 6, p. 262.

Williams, H., 1978, Tectonic lithofacies map of the Appalachian orogen: St. Johns, Memorial University of Newfoundland, scale 1:1,000,000.

Williams, H., and Hatcher, R. D., Jr., 1983, Appalachian suspect terranes, *in* Hatcher, R. D., Jr., Williams, Harold, and Zietz, Isidore, eds., Contributions to the tectonics and geophysics of mountain chains: Geological Society of America Memoir 158, p. 33-53.

Wooten, R. M., 1980, Stratigraphy, structure, and metamorphism in portions of the Hayesville and Hiawassee 7.5-minute quadrangles, North Carolina-Georgia [M.S. thesis]: Athens, University of Georgia, 276 p.

APPENDICES

APPENDIX A

Structural Domain Analysis Methodology

Structural measurements, including 1701 foliation, 35 lineation, 52 fold, and 201 joint measurements were taken from 1550 stations covering approximately 70 mi^2 (Plate 1 and 2). In an attempt to simplify structural analysis, the field area was divided into 4 domains based on structural trends and map patterns (Plate 2). Domains I, III, and IV were derived based on relative dominance of NNW, WNW, and NNW trends respectively. Domain II, located in the center of the field area, contains measurements of various structural trends with an overall NW dominance. Structural analysis was performed with the use of Adobe® Illustrator (AI), Microsoft® Excel (Excel), and Stereonet® PPC 6.0.2. The method used to produce plots and analytical results of the measured structural data is summarized below:

STEP I (ADOBE ILLUSTRATOR):

Upon map completion, domains can be defined manually using the pen-tool in AI. With separate layers for domain boundaries and stations, station numbers can manually be selected, copied, pasted into a new AI document, and exported as text to be used in Excel for data sorting.

1. Manually define domain boundaries (in a new AI layer) based on observed structural trends and map patterns.
2. With the domain boundaries defined and locked, and using a copy of the station layer, check along the boundaries to assure station numbers are not offset into an incorrect domain. Stations will be manually selected and exported, thus maintaining original map position is not necessary. Ensuring that station numbers are located within their correct domains is the only concern.
3. Manually select (holding shift) and copy all station numbers within a domain (e.g.. Domain 1) and paste into a new AI document. NOTE: Station numbers typically coincide with an individual quadrangle meaning that numbers may be repeated across a field area where more than one quadrangle is used (e.g. the number 1 is used on several quadrangles covering a large area). If numerous quadrangles are used across a large field area, care must be taken not to repeat numbers. Domains must be divided by domain boundaries and quadrangle boundaries.
4. Export the new document as a text file. e.g. NW_dom1.txt (Nimblewill quadrangle-domain 1).

STEP II (MICROSOFT EXCEL):

Text files created in AI can be opened in Excel in a tabular format. These numbers with their corresponding domains can be used define the domains within a spread sheet database of structural data.

1. Open each text files created with AI into Excel and move each individual sheet into the main database file (containing all structural data). Within the structural database, name each text file according to their corresponding domains. Remember the domain sheets should correspond to domain number and quadrangle. Example pictured below:

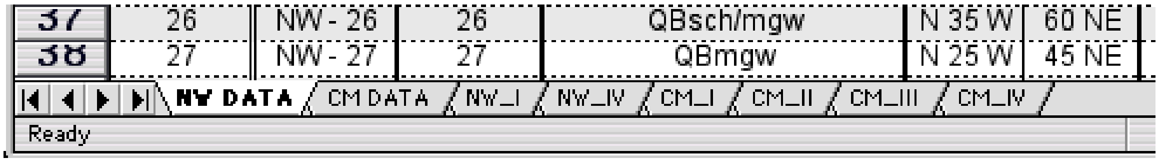

37	26	NW - 26	26	QBsch/mgw	N 35 W	60 NE
38	27	NW - 27	27	QBmgw	N 25 W	45 NE

NW DATA / CM DATA / NW_I / NW_IV / CM_I / CM_II / CM_III / CM_IV /

Ready

1) cont. Note that two quadrangles of data are present, Campbell Mountain (CM) and Nimblewill (NW) with sheets corresponding to the different domains located within each quadrangle.

2) An Excel formula can now be used to correlate the quadrangle station numbers to there defined domains using the following methodology:

a) Create two new columns adjacent to the column of defined station numbers within one of the quadrangle structural data sheet. One of these columns will contain number values corresponding to the station numbers (without text) and the second column will contain the formula for defining domains. Pictured Adjacent ------>

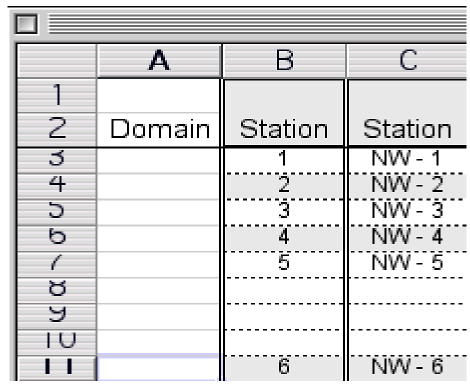

	A	B	C
1			
2	Domain	Station	Station
3		1	NW - 1
4		2	NW - 2
5		3	NW - 3
6		4	NW - 4
7		5	NW - 5
8			
9			
10			
11		6	NW - 6

b) The column created to contain station numbers without text (column B in the above figure) can easily be created using the find and replace function in Excel. Copy and paste the station number (Column C in the above figure) and use [Edit -> Replace] to remove text.

c) The following formula written for the data processed here (Cell A9) can be modified to any database.

=IF(ISBLANK(B9),A8,IF((COUNTIF(NW_I!A$1:A$469,B9)>0), "I", IF((COUNTIF(NW_IV!A$1:A$200,B9)>0), "IV", "NA")))

The formula is written to correlate station numbers listed with their corresponding number within one of the listed domain sheets and return a domain number (figure below).

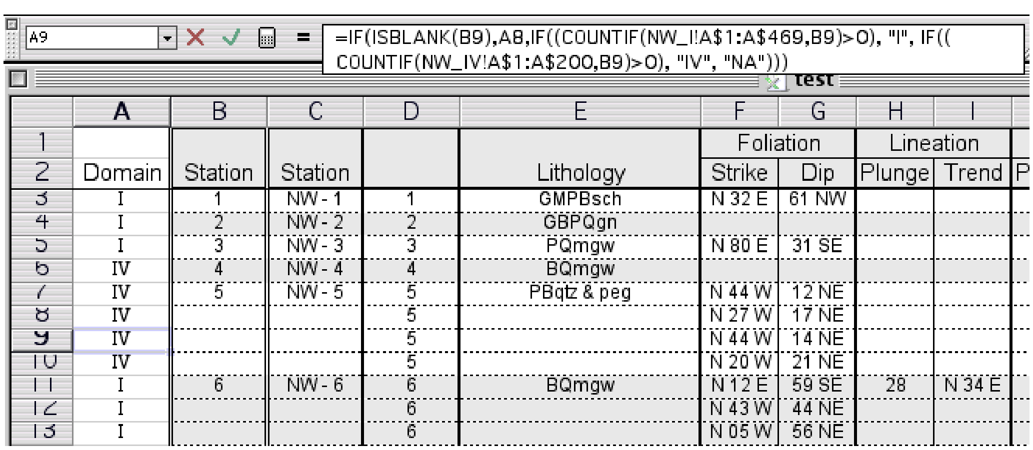

A9 =IF(ISBLANK(B9),A8,IF((COUNTIF(NW_I!A$1:A$469,B9)>0), "I", IF((COUNTIF(NW_IV!A$1:A$200,B9)>0), "IV", "NA")))

test

	A	B	C	D	E	F	G	H	I
1						Foliation		Lineation	
2	Domain	Station	Station		Lithology	Strike	Dip	Plunge	Trend
3	I	1	NW - 1	1	GMPBsch	N 32 E	61 NW		
4	I	2	NW - 2	2	GBPQgn				
5	I	3	NW - 3	3	PQmgw	N 80 E	31 SE		
6	IV	4	NW - 4	4	BQmgw				
7	IV	5	NW - 5	5	PBqtz & peg	N 44 W	12 NE		
8	IV			5		N 27 W	17 NE		
9	IV			5		N 44 W	14 NE		
10	IV			5		N 20 W	21 NE		
11	I	6	NW - 6	6	BQmgw	N 12 E	59 SE	28	N 34 E
12	I			6		N 43 W	44 NE		
13	I			6		N 05 W	56 NE		

c) cont. The [ISBLANK] function is used to avoid problems where blank cells are present below a station number, such as depicted above. The [COUNTIF] function returns "true" values when a corresponding station number is located in one of the domain sheets (depicted at the top of the previous page). The "NA" will be returned if the station number your processing is not located within any of the domain sheets, which indicates a problem either with the original station map or the defined domains. Although this formula is highly specialized, it can be modified to process data in any spread sheet database. The formula should only search for numbers in sheets corresponding to the quadrangle sheet where the formula is written (NW quadrangle in this example). Note the formula displayed above is written for cell A9.

d) Once the domains have been defined the database can be sorted by the Domain column and the data can be easily separated and analyzed with a stereonet program.

APPENDIX B-1

Structural and rock type data for the Nimblewill quadrangle

Note: Stations correspond to locations within the Nimblewill quadrangle presented on Plate II: Station numbers, sample locations, and structural domains within portions of the Nimblewill, Campbell Mountain, and Dahlonega, Georgia 7.5-minute quadrangles.

ABBREVIATIONS:

Note: Lithology indicated by lower case lettering and minerals indicated by UPPER case lettering.

Lithologies

amp	-	amphibolite
c-si	-	calc-silicate
gn	-	gneiss
hgn	-	hornblende gneiss
mgr	-	metagabbro
mgw	-	metagraywacke
peg	-	pegmatite
qtz	-	quartzite
sch	-	schist

Other

aug	-	augen
bd	-	boudin
blk	-	black
Iso	-	isoclinal
myl	-	mylonitic
sap	-	saprolite
zen	-	zenolith

Minerals

B	-	biotite
C	-	chlorite
E	-	epidote
F	-	feldspar
G	-	garnet
H	-	hornblende
K	-	kyanite
M	-	muscovite
P	-	plagioclase
S	-	sillimanite

Map Unit

Zgs	-	Great Smoky Group
CG	-	Coweeta Group
ccr	-	Coleman River Formation
GB	-	Gold Belt
am	-	amphibolite
as	-	aluminous schist
hb	-	hornblendite
hg	-	Hornblende gneiss
hga	-	hornblende gneiss, metagabbro, & amphibolite
mss	-	metasandstone and schist
Ofg	-	felsic gneiss
qms	-	quartzite, metasandstone, & schist
ig	-	intermediate gneiss

Station	Lithology	Foliation		Lineation		Fold Axis		Axial Surface		IL	Amp.	Fold	Joint		Map	Dom-
		Strike	Dip	Plunge	Trend	Plunge	Trend	Strike	Dip	Angle	(m)	Verg.	Strike	Dip	Unit	ain
CM - 1	amp														am/mss	II
CM - 2	GMQsch	N 35 E	45 SE												mss	II
CM - 3	Msch	N 20 E	51 SE												as	II
CM - 4	amp & MQmgw	N 30 E	45 SE												am/mss	II
CM - 5	GMQsch	N 40 W	55 NE												as	III
CM - 6	mgw	N 87 E	34 NW												as	III
		N 12 E	58 NW													III
CM - 7	mgw & MQsch	N 46 E	28 NW												ccr	III
		N 73 E	30 NW													III
CM - 8	Bmgw	N 23 W	28 NE												ccr	III
CM - 9	mgw	N 27 W	26 NE												ccr	III
CM - 10	mgw	N 37 W	78 NE												ccr	III
CM - 11	mgw	N 12 W	48 NE												ccr	III
CM - 12	mgw					16	S 52 E	N 53 W	43 SW	90		NE			ccr	III
CM - 13	mgw	N 62 E	68 SE												ccr	III
CM - 14	mgw	N 62 W	37 NE												ccr	III
CM - 15	mgw	N 47 W	56 SW												ccr	III
CM - 16	mgw					19	S 63 E	N 63 E	24 NW	75		NE			ccr	III
CM - 17	mgw	N 07 E	54 NW												ccr	III
		N 54 W	86 NE													III
CM - 18	mgw	N 67 W	47 NE												ccr	III
CM - 19	amp	N 87 W	37 NE			7	S 19 E	N 24 W	24 NE	75		SW			amp-CG	III
		N 47 W	37 NE													III
CM - 20	amp														amp-CG	III
CM - 21	mgw	N 29 W	34 NE												ccr	III
CM - 22	MBsch & mgw	N 63 W	24 NE												ccr	III
		N 73 E	66 SW													III
CM - 23	sch & mgw	N 11 W	72 SW												ccr	III
CM - 24	amp & PQBMsch	N 12 E	36 SE												am/as	II
CM - 25	gn	N 76 W	42 NE												ccr	II
CM - 26	Msch	N 58 W	31 NE												ccr	II
CM - 27	GBQMsch & BPQmgw	N 37 W	31 NE												ccr	II
CM - 28	GBmgw	N 44 W	54 NE												ccr	II
CM - 29	mgw	N 11 E	42 SE												ccr	II
CM - 30	GKMsch	N 19 E	33 SE												as	II
CM - 31	GKMsch w/ c-si	N 66 E	22 SE												as	II
CM - 32	KGMsch	N 59 E	43 SE												as	II
CM - 33	KGMsch	N 43 E	62 SE												as	II
CM - 34	KGMsch	N 72 E	70 SE	21	N 74 E								N 25 W	68 SW	as	II
CM - 35	Ksch & mgw	N 30 E	26 SE												as	II
CM - 36	GKMsch	N 38 E	51 SE												as	II
CM - 37	GKMsch	N 13 E	37 SE												as	II
CM - 38	GKMsch & MEQmgw/qtz	N 38 W	04 NE												as	II
CM - 39	KGMsch	N 09 W	31 NE												as	II
		N 37 W	18 NE													II
CM - 40	amp	N 47 E	82 SE												am-GB	II
CM - 41	amp	N 22 E	62 NW												am-GB	II
CM - 42	amp	N 56 E	49 NW												am-GB	II
CM - 43	amp	N 77 E	74 NW												am-GB	II
CM - 44	amp	N 67 W	43 NE												am-GB	II
CM - 45	amp	N 84 E	58 NW												am-GB	II
CM - 46	amp	N 84 E	62 NW												am-GB	II
CM - 47	GKMsch	N 75 E	71 SE												as	II
CM - 48	GKMsch	N 88 E	72 SE												as	II
CM - 49	amp	N 18 W	51 SW												am-GB	II
CM - 50	amp	N 34 E	36 NW												am-GB	II
CM - 51	GKMsch	N 74 E	14 SE												as	II
CM - 52	GKMsch	N 73 E	46 NW												as	II
CM - 53	KGQMsch	N 68 E	33 SE												as	II
CM - 54	GBMEqtz & GMsch	N 32 E	27 SE												as	II
	amp-float															II
CM - 55	GMBPQmgw & GMsch	N 78 E	46 SE												as	II
CM - 56	GMsch & mgw	N 52 E	49 SE												as	II
CM - 57	GBmgw	N 52 E	31 SE												as	II
	amp-float															II
CM - 58	GPBMQmgw & MBsch	N 52 E	39 SE			15	S 80 E	N 3 E	17 SE	160	0.02 - 0.05				as	II
CM - 59	amp	N 20 W	19 NE												am-GB	II
CM - 60	amp	N 32 E	42 SE												am-GB	II
CM - 61	amp	N 14 E	21 SE												am-GB	II
CM - 62	amp	N 77 E	41 SE										N 25 W	63 SW	am-GB	II
		N 72 E	89 SE										N 14 E	90		II
													N 32 W	89 SW		II
CM - 63	amp					34	N 8 W	N 65 E	28 NW	45	0.05 - 0.15	SW			am-GB	II
CM - 64	amp	N 60 E	64 SE												am-GB	II
CM - 65	amp	N 40 W	35 NE													II
CM - 66	amp	N 35 W	26 NE													II
CM - 67	GQBMsch & amp	N 34 W	24 NE										N 48 E	90	mss	II
		N 56 W	11 NE										N 09 W	62 NE	am-GB	II
													N 55 W	52 NE		II
													N 64 E	88 NW		II
CM - 68	GQBMsch& mgw	N 81 E	34 NW												mss	II
CM - 69	GPQBMsch	N 60 E	28 SE										N 29 W	56 SW	mss	II
													N 40 E	51 NW		II
													N 12 W	50 SW		II
													N 41 W	59 NE		II
CM - 70	GBMQsch\mgw	N 32 E	24 SE												mss	II
CM-71	GMBPQmgw	N 23 E	12 SE										N 34 E	71 SE	mss	II
													N 18 E	85 NW		II
													N 42 W	90		II
CM - 72	MBsch	N 18 W	24 NE												ccr	II
CM - 73	BQmgw & sch	N 58 W	18 NE												ccr	II
CM - 74	BQmgw & sch	N 63 W	19 NE												ccr	II
CM - 75	GMBPQmgw/sch	N 60 W	29 NE												ccr	II
CM - 76	BQPmgw	N 65 W	29 NE												ccr	II
CM - 77	BQmgw	N 72 E	49 NW												ccr	II

Station	Lithology	Foliation		Lineation		Fold Axis		Axial Surface		IL	Amp.	Fold	Joint		Map	Dom-
		Strike	Dip	Plunge	Trend	Plunge	Trend	Strike	Dip	Angle	(m)	Verg.	Strike	Dip	Unit	ain
NW - 77	PQMBsch/mgw	N 11 E	28 SE												Zgs	I
NW - 78	PQBsch/mgw	N 11 E	25 SE												Zgs	I
NW - 79	PQBmgw	N 34 E	36 SE												Zgs	I
NW - 80	MQBsch	N 03 E	38 SE												Zgs	I
NW - 81	MQBsch	N 16 E	44 SE												Zgs	I
NW - 82	QMBsch	N 14 E	41 SE												Zgs	I
NW - 83	PQMBmgw	N 11 E	46 SE												Zgs	I
NW - 84	PBQmgw	N 38 E	22 SE												Zgs	I
NW - 85	PBQmgw & MBsch	N 22 W	40 NE												Zgs	I
NW - 86	QMBsch & mgw	N 18 E	36 SE												Zgs	I
NW - 87	Bsch	N 29 E	37 SE												Zgs	I
NW - 88	QBsch	N 15 E	30 SE												Zgs	I
NW - 89	QPBsch	N 43 W	85 NE	23	S 65 E										Zgs	I
NW - 90	QBsch	N 27 E	44 SE												Zgs	I
NW - 91	PQBmgw	N 49 W	34 NE												ccr	I
NW - 92	PQBmgw												N 29 W	74 NE	ccr	I
													N 33 E	68 SE		I
NW - 93	QMBsch														ccr	I
NW - 94	PQBmgw	N 54 W	34 NE												ccr	IV
		N 59 W	05 NE													IV
NW - 95	QPBmgw & MBsch	N 35 W	61 NE			15	S 45 E	N 4 W	37 NE	100	0.5 - 0.75	NE			ccr	IV
		N 06 W	46 NE			19	S 45 E	N 32 W	28 NE	25		SW				IV
		N 03 E	43 SE			4	S 34 E	N 18 W	36 NE	70	0.45	SW				IV
		N 35 W	61 NE													IV
NW - 96	QBmgw	N 54 E	61 SE												ccr	I
NW - 97	PQBmgw & sch	N 33 E	24 SE												ccr	I
NW - 98	PQBmgw	N 16 W	17 NE												ccr	I
NW - 99	GPQMBsch	N 43 W	43 NE												ccr	IV
NW - 100	QBmgw	N 45 W	22 NE												ccr	IV
NW - 101	QBmgw	N 81 E	26 SE												ccr	IV
NW - 102	QBmgw	N 27 E	37 SE												ccr	I
NW - 103	QBmgw	N 53 E	25 SE												ccr	I
NW - 104	MBsch	N 21 W	12 NE												ccr	I
NW - 105	MBsch & QBmgw	N 46 E	11 NW												ccr	I
NW - 106	PQBmgw	N 18 E	16 SE												ccr	I
NW - 107	PQBmgw	N 34 W	14 NE												ccr	I
		N 00 E	19 SE													I
NW - 108	PQBmgw	N 05 W	34 NE												ccr	IV
NW - 109	PQBmgw	N 79 W	80 NE			30	N 54 W	N 24 W	50 NE	160	0.15				ccr	IV
						24	S 64 E	N 24 W	36 NE	80	?	NE				IV
NW - 110	QMBsch	N 85 W	38 NE												ccr	IV
NW - 111	QMBsch	N 36 W	45 NE	16	N 45 W										ccr	IV
NW - 112	PQBmgw & Bsch	N 21 W	46 NE												ccr	IV
NW - 113	PQBmgw	N 73 E	34 NE												ccr	IV
NW - 114	QMBsch	N 28 E	22 SE												Zgs	I
NW - 115	PQBmgw	N 72 W	20 SW												Zgs	I
NW - 116	PQBmgw	N 5 W	20 NE												Zgs	I
NW - 117	Bsch	N 01 W	24 NE												Zgs	I
NW - 118	PQMBsch	N 52 W	54 NE												Zgs	I
NW - 119	MBsch	N 59 E	52 SE	39	S 71 E										Zgs	I
NW - 120	MBsch	N 00 E	41 SE	41	S 58 E										Zgs	I
NW - 121	QPMgn	N 33 W	31 NE												Zgs	IV
NW - 122	QPBgn	N 30 W	21 NE	16	S 81 E								N 01 W	81 SW	Zgs	IV
		N 32 W	34 NE													IV
NW - 123	Msch	N 08 E	35 SE												Zgs	IV
NW - 124	PQBMmgw/gn & Bsch														Zgs	IV
NW - 125	QPBgn/mgw & Bsch	N 07 W	39 NE	44	S 55 E										Zgs	IV
NW - 126	QPBmgw & Bsch	N 02 E	35 SE	50	N 85 E										Zgs	IV
NW - 127	QPBgn/mgw	N 01 E	34 SE												Zgs	IV
NW - 128	GPQBsch	N 43 W	34 NE												ccr	IV
NW - 129	PGQMBsch	N 75 W	25 NE										N 45 W	90	ccr	IV
		N 50 W	25 NE												ccr	IV
NW - 130	PQBmgw	N 50 W	44 NE												ccr	IV
NW - 131	GPQBsch	N 16 W	44 NE												ccr	IV
NW - 132	PQBMsch	N 10 E	33 SE												ccr	IV
NW - 133	PQCMBsch	N 45 E	58 SE												ccr	IV
NW - 134	GPQBsch/mgw	N 20 W	26 NE												ccr	IV
		N 38 W	54 NE													IV
NW - 135	PQmgw	N 16 W	29 NE	23	N 78 W										ccr	IV
NW - 136	PQmgw	N 10 E	26 SE												ccr	IV
NW - 137	PQmgw	N 36 W	45 NE										N 38 E	70 SE	ccr	IV
													N 86 W	52 SW		IV
NW - 138	GBsch	N 35 W	31 NE												ccr	IV
NW - 139	Bsch	N 62 W	25 SW												ccr	IV
NW - 140	Bsch	N 51 W	51 NE												ccr	IV
NW - 141	QPBsch	N 19 W	57 NE												Zgs	I
NW - 142	PBQmgw	N 16 W	31 NE												Zgs	I
NW - 143	PQBmgw/sch	N 43 W	40 NE												Zgs	I
		N 42 W	31 NE												Zgs	I
NW - 144	PQBmgw/sch	N 35 W	25 NE												Zgs	I
		N 17 W	31 NE			30	N 68 E	N 66 E	76 SE	160	0.1 - 0.25					I
NW - 145	PBQmgw	N 05 W	30 NE													I
NW - 146	PBQmgw	N 13 W	32 NE										N 28 E	87 SE	Zgs	I
													N 71 E	90		I
NW - 147	PBQmgw	N 24 E	32 SE													I
NW - 148	PQBmgw & Bsch	N 22 W	32 NE			12	S 66 E	N 62 W	80 NE	120	0.1 - 0.2	SW	N 66 W	81 SW	Zgs	I
		N 17 W	43 NE													I
		N 31 W	33 NE													I
		N 40 W	46 NE													I
		N 21 W	41 NE													I
NW - 149	PBQmgw & PQBsch	N 08 W	49 NE	51	S 34 E								N 43 E	84 SE	Zgs	I

Station	Lithology	Foliation		Lineation		Fold Axis		Axial Surface		IL	Amp.	Fold	Joint		Map	Dom-
		Strike	Dip	Plunge	Trend	Plunge	Trend	Strike	Dip	Angle	(m)	Verg.	Strike	Dip	Unit	ain
		N 23 W	55 NE										N 53 W	56 SW		I
													N 65 E	59 NW		I
NW - 150	PBQmgw	N 24 W	21 NE										N 46 E	76 SE	Zgs	I
NW - 151	PBQmgw	N 44 W	25 NE												Zgs	I
NW - 152	PBQmgw	N 15 E	49 SE												Zgs	I
NW - 153	PBQmgw	N 33 E	51 SE												Zgs	I
NW - 154	PBQmgw	N 10 W	54 NE												Zgs	I
NW - 155	PBQmgw	N 25 E	54 SE												Zgs	I
NW - 156	mgw & sch	N 06 W	34 NE												Zgs	I
NW - 157	PBQmgw	N 12 E	11 SE												Zgs	I
NW - 158	PQBmgw	N 16 E	31 SE												Zgs	I
NW - 159	PQBsch & PBQmgw	N 32 W	39 NE												Zgs	I
NW - 160	mgw	N 38 W	70 NE												Zgs	I
		N 46 W	85 NE													I
		N 62 W	68 SW													I
NW - 161	PQBsch/mgw	N 10 E	31 SE												Zgs	I
NW - 162	QBsch	N 04 W	40 NE												Zgs	I
NW - 163	BQmgw	N 46 W	51 NE												Zgs	I
NW - 164	PBQmgw	N 38 W	41 NE			25	S 55 E	N 58 W	90	90	1				Zgs	I
NW - 165	PQBmgw	N 16 E	31 SE												Zgs	I
NW - 166	BQmgw	N 17 W	26 NE												Zgs	I
NW - 167	mgw & sch	N 16 W	36 NE	15	S 55 E	21	S 57 E	N 35 W	34 NE	160	0.05				Zgs	I
NW - 168	PQBmgw	N 55 W	59 NE												Zgs	I
NW - 169	PQBmgw	N 07 W	44 NE												Zgs	I
		N 22 W	56 NE													I
NW - 170	PQBmgw	N 30 W	68 NE												Zgs	I
NW - 171	PBQmgw	N 64 W	56 NE												Zgs	I
NW - 172	PBQmgw	N 34 W	71 NE												Zgs	I
NW - 173	PBQmgw	N 32 W	68 NE												Zgs	I
NW - 174	PBQmgw	N 43 W	74 NE												Zgs	I
NW - 175	mgw & sch	N 29 W	69 NE												Zgs	I
NW - 176	PBQmgw	N 19 W	73 NE												Zgs	I
NW - 177	PBQmgw	N 33 W	64 NE												Zgs	I
NW - 178	PBQmgw	N 29 E	33 SE												Zgs	I
NW - 179	PBQmgw	N 68 W	50 NE												Zgs	I
NW - 180	GQPmgw	N 21 W	62 SW												cc	I
NW - 181	mgw	N 14 E	75 SE												ccr	I
NW - 182	mgw	N 09 E	42 SE												ccr	I
		N 28 W	44 NE													I
NW - 183	PHgn	N 44 W	40 NE												gha	I
NW - 184	PQBmgw	N 48 E	29 NW												ccr	I
NW - 185	PQBmgw	N 20 W	21 NE												ccr	I
		N 35 W	36 NE													I
NW - 186	mgw	N 04 W	45 NE												ccr	I
		N 14 W	39 NE													I
		N 04 W	36 NE													I
NW - 187	mgw	N 08 E	45 SE												ccr	I
NW - 188	GPQMBsch & PBQmgw	N 06 W	31 NE			16	S 38 E	N 02 E	20 SE				N 35 W	76 NE	ccr	I
		N 24 W	40 NE										N 32 E	51 NW		I
		N 10 W	36 NE										N 65 W	71 SW		I
		N 40 E	33 SE													I
NW - 189	GPQMBsch & PBQmgw	N 33 W	20 NE												ccr	I
		N 22 W	30 NE													I
		N 30 W	43 NE													I
NW - 190	PMBQsch & MPBQmgw	N 45 W	63 NE												Zgs	I
NW - 191	PBQmgw	N 02 W	38 NE												Zgs	I
NW - 192	PBQmgw	N 18 W	40 NE												Zgs	I
NW - 193	QMBsch & PBQmgw	N 35 W	38 NE												Zgs	I
NW - 194	MPBQmgw	N 08 W	45 NE												Zgs	I
NW - 195	BQmgw	N 08 W	63 NE	18	S 15 E										Zgs	I
NW - 196	BQmgw & MBsch	N 35 E	24 SE	44	S 68 E										Zgs	I
NW - 197	BQmgw & MBsch	N 04 E	48 SE												Zgs	I
NW - 198	BQmgw & MBsch	N 04 E	48 SE												Zgs	I
NW - 199	BQmgw & MBsch	N 08 W	34 NE												Zgs	I
NW - 200	BQmgw	N 01 E	24 SE												Zgs	I
NW - 201	BQmgw	N 04 W	56 NE												Zgs	I
NW - 202	BQmgw	N 10 E	38 SE												Zgs	I
NW - 203	PMBQmgw	N 02 W	44 NE												Zgs	I
NW - 204	PMBQmgw	N 22 W	26 NE												Zgs	I
NW - 205	PMBQmgw & MBS	N 34 W	60 NE												Zgs	I
NW - 206	PMBQmgw	N 23 W	40 NE												Zgs	I
NW - 207	mgw & sch	N 27 W	43 NE												Zgs	I
NW - 208	PBQmgw	N 06 W	34 NE	30	S 84 E										Zgs	I
NW - 209	PBQmgw	N 46 W	29 NE												Zgs	I
NW - 210	GPBQmgw & Bsch	N 44 W	32 NE												Zgs	I
NW - 211	GPBQmgw & MBsch	N 06 E	25 SE												Zgs	I
NW - 212	MBsch	N 25 E	48 SE												Zgs	I
		N 20 E	56 SE													I
NW - 213	PBQmgw	N 06 W	42 NE												Zgs	I
NW - 214	MBsch					25	S 45 E	N 5 E	32 SE	100	0.15	NW			Zgs	I
NW - 215	MBsch	N 25 W	61 SE												Zgs	I
NW - 216	MBsch & MPBQmgw	N 15 W	50 SE												Zgs	I
NW - 217	MBsch & BQmgw	N 05 W	55 NE	45	S 58 E										Zgs	I
NW - 218	PQBmgw	N 20 E	54 SE												Zgs	I
NW - 219	PQBmgw	N 16 E	44 SE												Zgs	I
NW - 220	PBQmgw	N 46 W	65 NE												Zgs	I
NW - 221	PBQmgw	N 32 W	35 NE												Zgs	I
NW - 222	PBQmgw	N 41 E	25 SE												Zgs	I
		N 25 E	39 SE													I
NW - 223	BQmgw	N 12 E	36 SE												Zgs	I
NW - 224	BQmgw	N 16 E	31 SE												Zgs	I

Station	Lithology	Foliation Strike	Foliation Dip	Lineation Plunge	Lineation Trend	Fold Axis Plunge	Fold Axis Trend	Axial Surface Strike	Axial Surface Dip	IL Angle	Amp. (m)	Fold Verg.	Joint Strike	Joint Dip	Map Unit	Dom-ain
NW - 225	BQmgw	N 25 E	20 SE												Zgs	I
NW - 226	BQmgw	N 11 W	34 NE												Zgs	I
NW - 227	BQmgw	N 10 E	42 SE												Zgs	I
NW - 228	BQmgw	N 02 W	48 NE												Zgs	I
NW - 229	BQmgw	N 05 E	80 SE												Zgs	I
NW - 230	BQmgw	N 18 E	37 SE												Zgs	I
NW - 231	BQmgw	N 35 E	44 SE												Zgs	I
NW - 232	MBsch	N 70 W	40 NE												Zgs	I
NW - 233	MBsch	N 32 E	21 SE												Zgs	I
NW - 234	mgw	N 15 W	40 NE												Zgs	I
NW - 235	MBsch	N 65 E	42 SE												Zgs	I
		N 78 W	40 NE													I
NW - 236	MBsch	N 31 W	37 NE												Zgs	I
NW - 237	MBsch & BQmgw	N 37 W	34 NE										N 70 W	89 NE	Zgs	I
NW - 238	MBsch	N 60 E	41 SE												Zgs	I
NW - 239	MBsch	N 05 E	52 SE												Zgs	I
NW - 240	MBsch	N 06 W	71 NE												Zgs	I
NW - 241	MBsch	N 28 E	28 SE												Zgs	I
NW - 242	MBsch/mgw	N 19 E	24 SE										N 55 W	61 SW	Zgs	I
NW - 243	MBsch & PBQmgw	N 28 E	16 SE										N 06 E	84 SE	Zgs	I
													N 89 E	88 NW		I
NW - 244	PBQmgw	N 23 W	57 NE												Zgs	I
		N 19 W	70 NE													I
		N 46 E	18 SE													I
NW - 245	BQmgw & MBQmgw	N 59 W	35 NE												Zgs/ccr	I
		N 14 W	46 NE													I
NW - 246	GMPBQmgw														ccr	I
NW - 247	MBsch	N 01 E	45 SE												ccr	I
		N 25 E	55 SE													I
NW - 248	MBsch & BQmgw	N 32 E	15 SE												ccr	I
NW - 249	PBQmgw & sch	N 23 E	35 SE												ccr	I
NW - 250	QBmgw & sch	N 31 W	50 NE												ccr	I
NW - 251	BQmgw	N 34 E	24 SE										N 40 W	63 SW	ccr	I
													N 58 E	71 NW		I
NW - 252	BQmgw	N 03 W	22 NE										N 29 W	76 SW	ccr	I
													N 53 E	84 NW		I
NW - 253	BQmgw	N 04 E	11 SE										N 64 W	84 NE	ccr	I
													N 16 E	80 NW		I
NW - 254	QBmgw	N 20 W	11 NE										N 13 E	72 NW	ccr	I
													N 48 E	85 SE		I
NW - 255	PBQmgw	N 10 W	19 NE												ccr	I
NW - 256		N 03 W	14 NE												ccr	I
NW - 257	BQmgw	N 37 W	24 NE												ccr	I
NW - 258	Hgn - float														hgn-CG	I
NW - 259	orange-brn to tan sap														ccr	I
NW - 260	BQmgw	N 56 W	34 NE												ccr	I
NW - 261	BQmgw - Float														ccr	I
NW - 262	PMBQmgw	N 77 W	24 NE												ccr	I
NW - 263	PBQmgw & Bsch	N 66 W	24 NE												ccr	I
NW - 264	PBQmgw	N 60 W	41 NE												ccr	I
NW - 265	PBQmgw	N 05 W	41 NE												ccr	I
		N 02 E	43 SE													I
NW - 266	PQBmgw	N 76 W	50 NE	28	N 85 E										ccr	I
NW - 267	PBQmgw	N 20 E	41 SE												ccr	I
NW - 268	PQBmgw	N 22 E	41 SE												ccr	I
NW - 269	drk red sap	N 80 W	90												ccr	I
NW - 270	PBQmgw/qzt & QMBsch	N 23 W	26 NE	26	N 78 E										ccr	I
NW - 271	PBQmgw & GQMBsch	N 09 W	31 NE												ccr	I
NW - 272	PBQmgw	N 13 W	51 NE												ccr	I
NW - 273	PBQmgw & MBsch	N 32 W	32 NE										N 45 E	53 SE	ccr	I
		N 40 W	28 NE													I
		N 26 W	26 NE													I
NW - 274	PBQmgw & MBsch	N 40 W	35 NE												ccr	I
NW - 275	PMBQmgw	N 30 W	28 NE												ccr	I
NW - 276	mgw	N 30 W	30 NE												ccr	I
NW - 277	BQmgw	N 28 W	24 NE												ccr	I
NW - 278	PBQmgw & MBsch	N 27 E	15 SE	21	S 86 E								N 55 W	80 SW	ccr	I
		N 25 E	21 SE										N 51 E	74 NW		I
													N 82 W	45 SW		I
NW - 279	PBQmgw & MBsch	N 30 E	15 SE										N 75 E	42 NW	ccr	I
NW - 280	PBMQmgw	N 56 E	29 NW												Zgs	I
NW - 281	PMBQmgw	N 13 E	46 NW										N 76 W	60 NE	Zgs	I
NW - 282	PMBQmgw	N 04 E	33 SE												ccr	I
NW - 283	MPBQmgw	N 63 E	24 SE												ccr	I
NW - 284	PBQmgw	N 40 E	34 SE												ccr	I
NW - 285	PBQmgw	N 46 W	08 NE												ccr	I
NW - 286	PMBQmgw	N 68 E	16 NW												ccr	I
NW - 287	PMBmgw	N 63 E	45 SE												ccr	I
NW - 288	BQmgw	N 25 W	24 NE												ccr	IV
		N 06 E	36 SE													IV
NW - 289	PyriteQMBsch	N 12 W	29 NE												ccr	IV
NW - 290	GQMBsch	N 36 W	25 NE												ccr	IV
NW - 291	MBsch	N 31 W	59 NE												ccr	IV
NW - 292	GQMBsch	N 08 W	39 NE												Zgs	IV
NW - 293	PMBQmgw & MBsch	N 05 E	26 SE												Zgs	IV
		N 18 W	27 NE													IV
NW - 294	MBsch	N 44 W	09 NE												Zgs	IV
NW - 295	MBsch	N 08 W	32 NE												Zgs	IV
NW - 296	MBsch	N 16 W	31 NE												Zgs	IV
NW - 297	MBsch	N 22 E	38 SE										N 68 W	64 NE	Zgs	IV
													N 45 E	90		IV

Station	Lithology	Foliation Strike	Foliation Dip	Lineation Plunge	Lineation Trend	Fold Axis Plunge	Fold Axis Trend	Axial Surface Strike	Axial Surface Dip	IL Angle	Amp. (m)	Fold Verg.	Joint Strike	Joint Dip	Map Unit	Dom-ain
NW - 298	MQPpeg	N 50 E	76 SE												Zgs	I
NW - 299	MPBQmgw & MBsch	N 37 W	36 NE												Zgs	I
NW - 300	BQmgw	N 46 E	30 SE												Zgs	I
NW - 301	BQmgw	N 13 E	28 SE												Zgs	I
NW - 302	PMBQmgw	N 36 E	34 SE												Zgs	I
NW - 303	PBQmgw	N 58 E	35 SE												Zgs	I
		N 10 E	22 SE													I
NW - 304	PMBQmgw	N 62 E	34 SE												Zgs	I
NW - 305	PMBQmgw	N 40 E	49 SE												Zgs	I
NW - 306	PMBQmgw	N 4 W	48 NE												Zgs	I
NW - 307	PMBQmgw & MBsch	N 08 E	34 SE												Zgs	I
		N 55 E	36 SE													I
NW - 308	PMBQmgw	N 08 W	81 NE												ccr	I
NW - 309	PMBQmgw	N 50 W	38 NE												ccr	I
NW - 310	PMBQmgw	N 10 W	36 NE			27	N 88 E	N 26 W	32 NE	50	0.13 - 0.15				ccr	I
		N 05 W	37 NE													I
NW - 311	PMBQmgw	N 65 E	31 SE												ccr	I
NW - 312	GQPMBsch	N 34 W	39 NE	32	N 31 W										ccr	I
NW - 313	GQPMBsch					19	N 00 S	N 16 W	40 NE	65	0.15	NW			ccr	I
NW - 314	GPMBQmgw	N 90 E	45 NW												ccr	I
NW - 315	GPMBQmgw	N 37 W	31 NE												ccr	I
NW - 316	GBQPMsch/mgw	N 40 W	31 NE												ccr	I
NW - 317	PQMBsch	N 64 W	30 NE												ccr	I
NW - 318	MBsch & BQmgw	N 51 W	29 NE												ccr	I
NW - 319	MPBQmgw & MBsch	N 46 W	31 NE												ccr	I
NW - 320	MPBQmgw & MBsch	N 48 W	40 NE												ccr	I
NW - 321	GPQMBsch	N 22 W	24 NE												ccr	I
NW - 322	GPQMBsch	N 24 W	26 NE												ccr	I
NW - 323	PMBQmgw	N 16 W	33 NE												ccr	I
NW - 324	MPBQmgw	N 7 W	41 NE										N 80 W	29 SW	ccr	I
NW - 325	GMBQmgw	N 24 W	24 NE												ccr	I
NW - 326	GPBQmgw	N 15 W	24 NE										N 54 E	72 SE	ccr	I
NW - 327	BQmgw	N 01 W	44 NE												ccr	I
NW - 328	QPBMsch	N 43 W	27 NE										N 72 W	64 SW	Zgs	NA
													N 72 E	65 NW		NA
NW - 329	PQMBsch	N 30 W	64 NE												Zgs	NA
NW - 330	PQMBsch	N 80 W	62 NE										N 22 E	78 NW	Zgs	NA
NW - 331	sch & mgw												N 56 W	84 NE	Zgs	NA
NW - 332	PQBmgw & MBsch	N 56 E	44 SE												Zgs	NA
NW - 333	PQBmgw & MBsch	N 80 W	33 SE												Zgs	NA
		N 87 E	86 NW													NA
NW - 334	MBsch	N 45 W	44 NE	34	N 85 E										Zgs	NA
NW - 335	MBsch - float														Zgs	NA
NW - 336	MBsch	N 62 W	38 NE												Zgs	NA
NW - 337	MBsch	N 38 W	42 NE												Zgs	NA
NW - 338	MBsch	N 82 E	47 SE												Zgs	NA
NW - 339	MBmgw/sch	N 20 W	63 NE												Zgs	NA
NW - 340	Msch	N 30 W	10 NE												Zgs	NA
NW - 341	Msch	N 26 W	55 NE												Zgs	NA
NW - 342	BMPQgn	N 46 E	39 SE												Zgs	I
NW - 343	MBQPmgw	N 39 W	24 NE												Zgs	I
NW - 344	PMBQmgw														Zgs	I
NW - 345	PMBQmgw														Zgs	I
NW - 346	PMBQmgw	N 07 W	28 NE												Zgs	I
NW - 347	PMBQmgw	N 08 W	31 NE												Zgs	I
NW - 348	PMBQmgw	N 06 E	31 SE												Zgs	I
NW - 349	PBQmgw	N 34 W	26 NE												ccr	I
NW - 350	PBQmgw	N 82 W	29 NE										N 50 E	90	ccr	I
NW - 351	PBQmgw	N 24 E	21 SE												ccr	I
NW - 352	PBQmgw	N 07 W	38 NE												ccr	I
NW - 353	MBmgw	N 20 W	75 NE												ccr	I
NW - 354	MPBQmgw	N 30 W	31 NE												ccr	I
NW - 355	BQmgw	N 27 W	66 NE												ccr	I
NW - 356	PMBQmgw - Float														ccr	I
NW - 357	PMBQmgw	N 06 E	45 SE												ccr	I
NW - 358	PBQmgw	N 38 W	37 NE	21	S 64 E										ccr	I
NW - 359	PBQmgw	N 06 W	37 NE												ccr	I
NW - 360	GPBQmgw	N 09 W	19 NE												ccr	I
NW - 361	GPBQmgw	N 21 W	22 NE										N 20 E	82 SE	ccr	I
		N 03 E	41 SE										N 01 W	75 SW		I
NW - 362	GPBQmgw	N 15 W	41 NE												ccr	I
NW - 363	PBQmgw & MBsch					24	N 64 E	N 63 W	31 NE	135	0.01 - 1.6	SE			ccr	I
						26	N 65 E			155	0.02	SE			ccr	I
NW - 364	PMBmgw	N 24 W	22 NE												ccr	I
NW - 365		N 42 W	85 SW												ccr	I
NW - 366	MPBQmgw	N 51 W	33 NE			5	S 47 E	N 23 W	28 SE	50	1.0	NW			ccr/Zgs	I
						1	S 43 E	N 43 W	43 SW	150	1.0	NE				I
						31	N 20 W	N 89 E	39 NW	100	0.5	NE				I
NW - 367	PBQmgw	N 05 W	34 NE												ccr	I
NW - 368	PBQmgw	N 15 E	38 SE										N 70 W	41 SW	ccr	I
		N 00 E	47 SE										N 35 W	90		I
NW - 369		N 05 W	24 NE										N 53 W	69 SW	ccr	I
NW - 370	PBQmgw & MBsch	N 09 W	34 NE												ccr	I
NW - 371	MBsch	N 42 W	20 NE													I
NW - 372	PMBQmgw	N 18 E	39 SE													I
NW - 373	MBsch	N 04 W	38 NE												Zgs	I
NW - 374	PMBQmgw	N 04 W	31 NE										N 36 W	71 SW	ccr	I
		N 05 W	39 NE													I
NW - 375	PMBQmgw	N 20 W	29 NE												ccr	I
NW - 376	MBsch	N 32 W	63 NE												ccr	I
NW - 377	MBsch	N 35 W	23 SW												ccr	I

Station	Lithology	Foliation		Lineation		Fold Axis		Axial Surface		IL	Amp.	Fold	Joint		Map	Dom-
		Strike	Dip	Plunge	Trend	Plunge	Trend	Strike	Dip	Angle	(m)	Verg.	Strike	Dip	Unit	ain
NW - 378	MBsch	N 35 W	34 SW			27	N 52 W	N 57 W	21 NE	80	0.05 - 0.07				ccr5	I
NW - 379	PMBQmgw	N 58 E	42 NW												ccr	I
NW - 380	PMBQmgw	N 10 E	22 SE												ccr	I
NW - 381	MPQmgw & Msch	N 20 E	22 SE												Zgs	I
NW - 382	mgw	N 25 W	50 NE												ccr	I
NW - 383	PMBQmgw & MBsch	N 25 W	39 NE										N 60 W	71 SW	Zgs	I
		N 24 W	35 NE										N 40 W	73 SW		I
		N 32 W	35 NE										N 53 E	48 NW		I
NW - 384	PMBmgw														ccr	I
NW - 385	BQmgw	N 22 W	28 NE												ccr	I
NW - 386	BQmgw & BMsch	N 10 E	51 SE												ccr	I
NW - 387	mgw	N 23 W	45 NE												Zgs	I
NW - 388	mgw	N 23 W	45 NE												Zgs	I
NW - 389	mgw	N 45 W	22 NE	20	N 78 E										Zgs	I
NW - 390	MPBQmgw	N 37 W	58 NE												ccr	I
NW - 391	BMsch &mgw	N 25 E	76 SE												ccr	I
NW - 392	GPBQmgw	N 58 E	56 NW												ccr	I
NW - 393	PQMBsch	N 15 W	32 NE												ccr	I
NW - 394	MBPQmgw	N 24 W	54 NE												ccr	I
NW - 395	BQmgw	N 17 W	56 NE												ccr	I
NW - 396	GPBQmgw & GMBsch	N 32 W	20 NE			34	N 62 E	N 22 W	34 NE	35	1.0	NW			ccr	I
NW - 397	MBsch	N 12 E	44 SE												ccr	I
NW - 398	MBsch	N 30 E	86 NW												ccr	I
NW - 399	MBsch	N 35 E	87 SE												ccr	I
NW - 400	GMBsch	N 55 E	55 NW												ccr	I
NW - 401	GMBsch	N 05 E	64 NW												ccr	I
NW - 402	BPQmgw & BMsch	N 08 W	48 NE												ccr	I
NW - 403	MBsch	N 00 E	47 SE												ccr	I
NW - 404	MBPQmgw & MBsch	N 15 W	48 NE	34	S 70 E	34	N 80 E	N 10 W	34 NE	40	0.3	SW			ccr	I
						5	N 00 S	N 05 E	33 SE	30	1	NW				I
NW - 405	MBPQmgw & MBsch	N 18 W	45 NE												ccr	I
		N 12 E	48 NE													I
NW - 406	MBPQmgw & MBsch	N 22 W	54 NE												ccr	I
NW - 407	BPQmgw	N 18 W	37 NE												ccr	I
NW - 408	BPQmgw	N 20 W	33 NE												ccr	I
NW - 409	BPQmgw	N 04 W	28 NE												ccr	I
NW - 410	KMBsch	N 42 E	34 SE												ccr	I
NW - 411	MBPQmgw	N 12 W	40 NE												ccr	I
NW - 412	MBsch	N 17 E	51 SE												ccr	I
NW - 413	PQBmgw	N 12 W	29 NE												Zgs	I
NW - 414	PQMBmgw	N 10 W	36 NE												Zgs	I
NW - 415	MBPQmgw	N 16 W	44 NE												Zgs	I
NW - 416	MBPQmgw	N 00 E	54 SE												Zgs	I
NW - 417	MBsch	N 08 W	73 NE												Zgs	I
NW - 418	GMBQsch	N 25 W	43 NE												ccr	I
NW - 419	GMBsch	N 65 E	64 SE												ccr	I
NW - 420	GMBsch & BQPgn	N 32 W	39 NE												ccr	I
NW - 421	BQPmgw\gn	N 10 W	34 NE												ccr	I
NW - 422	GBQPmgw & CSAMsch?	N 04 E	41 SE												ccr	I
NW - 423	MBsch & BQPmgw	N 05 W	56 NE												ccr	I
NW - 424	PMsch	N 35 W	45 NE												Zgs	I
NW - 425	PMsch	N 33 W	24 NE												Zgs	I
NW - 426	PMsch	N 18 W	35 NE												Zgs	I
NW - 427	Msch & mgw	N 39 W	52 NE												Zgs	I
NW - 428	MBPQmgw	N 10 E	36 SE												Zgs	I
NW - 429	BMsch & mgw	N 18 W	34 NE												Zgs	I
NW - 430	BMsch & mgw	N 65 W	39 NE												ccr	I
NW - 431	MBsch & mgw	N 40 W	39 NE												Zgs	IV
NW - 432	MBPQmgw	N 20 W	40 NE												Zgs	IV
NW - 433	MBPQmgw & Msch	N 29 W	33 NE												Zgs	IV
		N 45 W	28 NE													IV
NW - 434	mgw	N 44 E	33 SE												ccr	I
NW - 435	mgw	N 73 W	24 SW												ccr	I
NW - 436	mgw	N 60 E	40 NW												ccr	I
		N 64 E	29 NW													I
NW - 437	mgw	N 73 W	16 NE												ccr	IV
NW - 438	Msch	N 38 W	46 SW												Zgs	IV
NW - 439	MBsch	N 11 E	55 SE												ccr	I
NW - 440	PQMBsch	N 36 W	46 NE												Zgs	I
NW - 441	MBQPmgw , MBsch, & c-si	N 32 W	46 NE												Zgs	I
NW - 442	MBsch	N 12 W	14 NE												Zgs	I
NW - 443	MBsch & c-si	N 19 W	63 NE												Zgs	I
NW - 444	BMsch & MBPQmgw/sch	N 22 E	39 NE												Zgs	I
NW - 445	QMBsch	N 11 E	49 SE												Zgs	I
NW - 446	mgw/sch	N 16 W	53 NE												Zgs	I
NW - 447	BPQmgw/sch	N 28 W	49 NE												Zgs	I
NW - 448	MBPQsch	N 32 W	21 NE												Zgs	I
NW - 449	GQBMsch	N 26 E	29 SE												Zgs	I
NW - 450	MBQPmgw	N 23 E	21 SE												Zgs	I
		N 37 E	45 SE													I
NW - 451	QMBsch & MBPQmgw	N 18 W	57 NE												Zgs	I
NW - 452	MPQBsch & BPQmgw	N 48 W	54 SW												Zgs	I
NW - 453	TMQPpeg w/ MBQPmgw-zen														Zgs	I
																I
NW - 454	MBsch	N 51 W	46 NE												Zgs	I
NW - 455	MBsch	N 59 W	42 SW												Zgs	I
NW - 456	MBsch & BPQmgw	N 58 W	72 NE												Zgs	I
NW - 457	MBsch & BPQmgw	N 47 W	61 NE												Zgs	I
NW - 458	MBsch & BPQmgw	N 58 W	32 NE												Zgs	I
NW - 459	peg & veinQ	N 59 W	28 NE												Zgs	I
NW - 460	BMsch	N 49 W	25 NE												Zgs	I

Station	Lithology	Foliation Strike	Foliation Dip	Lineation Plunge	Lineation Trend	Fold Axis Plunge	Fold Axis Trend	Axial Surface Strike	Axial Surface Dip	IL Angle	Amp. (m)	Fold Verg.	Joint Strike	Joint Dip	Map Unit	Dom-ain
		N 13 W	39 NE													I
NW - 461	BPQmgw & MBsch	N 23 W	81 NE												Zgs	I
NW - 462	BPQmgw & c-si	N 81 E	21 SE												Zgs	I
NW - 463	BMsch	N 45 W	56 SW												Zgs	I
NW - 464	mgw & c-si	N 07 E	49 SE												Zgs	I
NW - 465	MBsch	N 41 W	69 NE												Zgs	I
NW - 466	mgw & MBsch	N 55 W	41 SW												Zgs	I
NW - 467	mgw & MBsch	N 25 E	21 NW												Zgs	I
NW - 468	MBsch	N 32 W	29 NE												Zgs	I
NW - 469	MBPQmgw &	N 24 W	58 NE												Zgs	I
	MBsch	N 33 W	51 NE													I
NW - 470	MBPQsch/gn	N 38 W	36 NE												Zgs	I
NW - 471	BPQmgw & MBsch	N 40 W	65 NE												Zgs	I
NW - 472	MBsch & c-si	N 31 W	66 NE												Zgs	I
NW - 473	mgw & sch	N 36 W	76 SW												Zgs	I
NW - 474	MBPQmgw & MBsch	N 38 W	62 NE												Zgs	I
NW - 475	mgw	N 84 E	51 NW												Zgs	I
		N 51 W	51 NE													I
NW - 476	BPQmgw	N 53 W	76 NE												Zgs	I
NW - 477	MBsch & mgw	N 18 W	41 NE												Zgs	I
NW - 478	MBsch & c-si	N 31 E	44 SE												Zgs	I
NW - 479	MBPQsch/mgw	N 57 W	52 NE												Zgs	I
NW - 480	MBPQsch/mgw	N 44 W	56 NE												Zgs	I
NW - 481	mgw & MBsch	N 42 W	59 NE												Zgs	I
NW - 482	mgw	N 26 W	44 NE												Zgs	I
NW - 483	BMPmgw	N 76 W	18 NE												Zgs	I
NW - 484	mgw	N 80 W	49 NE												Zgs	I
NW - 485	mgw & BMsch	N 31 W	69 NE												Zgs	I
NW - 486	BPQmgw	N 38 E	61 SE												Zgs	I
NW - 487	mgw & BMsch	N 10 W	68 NE												Zgs	I
NW - 488	QMBsch	N 13 E	37 SE												Zgs	I
NW - 489	MBPQmgw	N 19 E	45 SE												Zgs	I
NW - 490	MBPQmgw	N 27 W	49 SE												Zgs	I
NW - 491	BQPMsch & mgw	N 85 W	17 NE												Zgs	I
NW - 492	MBPmgw & BMsch	N 37 W	46 NE												Zgs	I
NW - 493	MBPmgw & BMsch	N 26 W	44 NE												Zgs	I
NW - 494	MBPmgw & BMsch	N 39 W	24 NE												Zgs	I
NW - 495	QPMBsch	N 00 E	21 SE												Zgs	I
NW - 496	BPQmgw	N 16 E	38 SE												Zgs	I
NW - 497	MBPQmgw	N 85 W	34 NE												Zgs	I
NW - 498	GBMsch	N 32 E	40 SE												Zgs	I
NW - 499	mgw	N 55 E	37 SE										N 51 E	69 NW	Zgs	I
													N 18 W	90		I
NW - 500	mgw	N 85 E	26 SE												Zgs	I
NW - 501	BPQmgw	N 27 E	45 SE												Zgs	I
NW - 502	MBPQmgw	N 68 E	28 SE												Zgs	I
NW - 503	GBPQmgw														Zgs	I
NW - 504	MBQPmgw	N 38 W	38 NE												Zgs	I
NW - 505	MBQPmgw & sch	N 52 W	25 NE												Zgs	I
		N 79 E	49 NW													I
NW - 506	MBQPmgw & sch	N 83 W	34 NE												Zgs	I
NW - 507	MBQPsch	N 33 W	29 NE												Zgs	I
NW - 508	MBQPmgw	N 36 E	45 SE												Zgs	I
NW - 509	GMBsch	N 22 E	26 SE												Zgs	I
		N 16 E	28 SE													I
NW - 510	MBQPmgw	N 03 W	17 NE												Zgs	I
NW - 511	BPQmgw	N 33 W	44 NE												Zgs	I
NW - 512	MBQPmgw	N 38 E	29 SE												Zgs	I
NW - 513	MBQPmgw	N 19 W	16 NE												Zgs	I
NW - 514	Bqtz/mgw	N 11 E	18 SE												ccr	I
NW - 515	Bqtz/mgw	N 18 E	20 SE												ccr	I
NW - 516	Bqtz/mgw	N 53 W	10 NE												ccr	I
NW - 517	Bqtz/mgw	N 42 W	31 NE												ccr	I
NW - 518	Bqtz/mgw	N 59 E	18 SE												ccr	I
NW - 519	Bqtz/mgw	N 90 E	11 SE												ccr	I
NW - 520	BPQmgw	N 09 E	34 SE												ccr	I
NW - 521	MBsch & mgw-sap	N 37 W	66 NE												ccr	I
NW - 522	MBsch & mgw-sap	N 26 W	36 NE												ccr	I
NW - 523	mgw & MBsch	N 47 W	38 NE												ccr	I
NW - 524	mgw & MBsch	N 32 W	38 NE												ccr	I
NW - 525	mgw & MBsch	N 10 E	36 SE												ccr	I
NW - 526	MBsch	N 17 E	54 SE												Zgs	I
NW - 527	mgw	N 12 W	46 NE												Zgs	I
NW - 528	MBsch & mgw	N 03 E	39 NE												ccr	I
NW - 529	mgw	N 27 W	56 NE												ccr	IV
NW - 530	mgw & MBsch	N 46 W	13 NE												ccr	IV
NW - 531	MBsch	N 48 E	54 SE												ccr	IV
NW - 532	MBsch	N 28 E	17 SE												ccr	IV
NW - 533	mgw	N 83 W	23 NE												ccr	IV
NW - 534	MBsch & mgw	N 71 E	23 NW												Zgs	IV
NW - 535	MBPQmgw & BMsch	N 54 W	24 NE												Zgs	IV
NW - 536	MBsch & mgw	N 37 W	36 NE												Zgs	IV
NW - 537	BMsch & mgw	N 62 W	37 NE												Zgs	IV
NW - 538	BMsch & mgw	N 44 W	26 NE												Zgs	IV
		N 53 W	28 NE													IV
		N 77 W	41 NE													IV
		N 58 W	26 NE													IV
NW - 539	mgw	N 67 W	37 NE												Zgs	IV
NW - 540	mgw	N 48 W	38 NE												Zgs	IV
		N 67 W	37 NE													IV
NW - 541	sch & mgw-sap	N 48 W	59 NE												Zgs	IV

Station	Lithology	Foliation Strike	Foliation Dip	Lineation Plunge	Lineation Trend	Fold Axis Plunge	Fold Axis Trend	Axial Surface Strike	Axial Surface Dip	IL Angle	Amp. (m)	Fold Verg.	Joint Strike	Joint Dip	Map Unit	Dom-ain
NW - 542	sch & mgw	N 52 W	38 NE	23	N 47 E										Zgs	IV
NW - 543	GBMsch	N 05 E	63 SE												Zgs	IV
NW - 544	GBMsch	N 58 W	52 NE										N 36 W	46 SW	Zgs	IV
													N 17 E	79 SE		IV
													N 57 W	44 SW		IV
NW - 545	GBMsch	N 57 W	41 NE												Zgs	IV
NW - 546	mgw & sch	N 58 W	39 NE												Zgs	IV
NW - 547	BMsch & mgw	N 66 W	12 NE												Zgs	IV
NW - 548	mgw-sap	N 09 W	36 NE												Zgs	IV
		N 37 E	28 SE													IV
NW - 549	MBsch	N 13 W	13 NE												Zgs	IV
NW - 550	mgw-sap	N 27 E	43 SE												Zgs	IV
NW - 551	MBsch & mgw	N 33 W	22 NE												Zgs	IV
NW - 552	mgw-sap	N 42 W	24 NE												Zgs	IV
NW - 553	mgw-sap	N 73 W	22 NE												Zgs	IV
NW - 554	MBsch & mgw-sap	N 41 E	31 SE												Zgs	IV
NW - 555	MBQPmgw & MBsch	N 81 W	38 NE												Zgs	IV
NW - 556	mgw-sap	N 23 W	14 NE	22	N 51 E										Zgs	IV
		N 59 W	58 NE													IV
NW - 557	mgw-sap	N 52 W	44 NE												Zgs	IV
NW - 558	BMsch	N 54 W	29 NE												ccr	IV
NW - 559	mgw-sap	N 68 W	18 SW												ccr	IV
NW - 560	MBsch & mgw-sap	N 44 W	22 NE												ccr	IV
NW - 561	MBsch & mgw-sap	N 26 W	17 NE												ccr	IV
		N 12 E	14 NE													IV
NW - 562	MBsch & mgw-sap	N 48 W	28 NE												ccr	IV
NW - 563	MBsch & mgw-sap	N 30 W	39 NE												ccr	IV
NW - 564	MBsch & mgw-sap	N 50 W	38 NE												ccr	IV
NW - 565	MBsch & mgw-sap	N 51 W	37 NE												ccr	IV
NW - 566	mgw-sap	N 44 W	48 NE												ccr	IV
NW - 567	MBsch & mgw-sap	N 13 W	24 NE												ccr	IV
NW - 568	mgw-sap	N 28 W	12 NE												ccr	IV
NW - 569	MBsch & mgw-sap	N 24 W	33 NE												ccr	IV
NW - 570	MBsch & mgw-sap	N 58 W	36 NE												ccr	IV
NW - 571	MBsch & mgw-sap	N 43 W	34 NE												ccr	IV
NW - 572	MBsch & mgw-sap	N 22 E	36 SE												Zgs	IV
NW - 573	MBsch & mgw-sap	N 06 E	41 SE												Zgs	IV
NW - 574	MBsch & mgw-sap	N 04 E	39 SE												Zgs	IV
NW - 575	MBsch, mgw-sap, & c-si	N 08 W	24 NE												Zgs	IV
NW - 576	MBsch & mgw-sap	N 61 W	28 SW												Zgs	IV
NW - 577	MBsch & mgw-sap	N 28 W	24 NE												ccr	IV
NW - 578	MBsch & mgw-sap	N 24 W	29 NE												ccr	IV
NW - 579	MBsch & mgw-sap	N 44 W	14 NE												ccr	IV
NW - 580	MBsch & mgw-sap	N 54 W	48 NE												ccr	IV
NW - 581	MBsch & mgw-sap	N 42 W	34 NE												ccr	IV
NW - 582	MBsch & mgw-sap	N 54 W	34 NE												ccr	IV
NW - 583	MBsch & mgw-sap	N 44 W	29 NE												ccr	IV
NW - 584	MBsch & mgw-sap	N 86 W	21 NE												Zgs	IV
NW - 585	MBsch & mgw-sap	N 26 W	23 NE												Zgs	IV
NW - 586	MBsch & mgw-sap	N 33 W	21 NE												Zgs	IV
NW - 587	MBsch & mgw-sap	N 12 W	27 NE												Zgs	IV
NW - 588	MBsch & mgw-sap	N 28 W	17 NE												Zgs	IV
NW - 589	MBsch & mgw-sap	N 16 W	33 NE												ccr	IV
NW - 590	mgw-sap	N 08 W	29 NE												ccr	IV
NW - 591	mgw-sap	N 24 W	33 NE												ccr	IV
NW - 592	mgw-sap	N 06 E	22 SE												ccr	IV
NW - 593	MBsch & mgw-sap	N 32 W	34 NE												Zgs	IV
NW - 594	MBsch & MBQPmgw	N 04 E	18 SE												ccr	IV
NW - 595	MBsch & MBQPmgw	N 19 E	18 SE												ccr	IV
NW - 596	MBsch & mgw-sap	N 76 W	24 NE												ccr/Zgs	IV
NW - 597	MBsch & mgw-sap	N 07 E	11 SE												ccr	IV
NW - 598	mgw-sap	N 39 W	64 NE												Zgs	IV
NW - 599	mgw	N 17 W	57 NE												Zgs	IV
NW - 600	BPQmgw	N 24 W	45 NE												Zgs	IV
		N 38 W	67 NE													IV
NW - 601	mgw & MBsch	N 61 W	51 NE												Zgs	IV
NW - 602	mgw & MBsch	N 11 W	43 NE												Zgs	IV
NW - 603	MBsch	N 17 E	13 SE												Zgs	IV
NW - 604	BPQmgw	N 38 W	37 NE												Zgs	IV
NW - 605	BPQmgw & MBsch	N 5 E	19 SE												Zgs	IV
NW - 606	mgw	N 51 W	63 NE												Zgs	IV
NW - 607	mgw & MBsch	N 53 W	54 NE												Zgs	IV
NW - 608	mgw & MBsch	N 66 E	56 SE												Zgs	IV
NW - 609	mgw & MBsch	N 58 W	43 NE												Zgs	IV
NW - 610	mgw-sap	N 74 W	38 NE												Zgs	IV
NW - 611	MBsch & mgw	N 44 W	46 NE												Zgs	IV
NW - 612	MBsch & mgw	N 26 W	48 NE												Zgs	IV
NW - 613	Msch & mgw-sap	N 49 W	64 NE												Zgs	IV
NW - 614	mgw-sap	N 14 W	39 NE												Zgs	IV
NW - 615	mgw-sap	N 44 W	31 NE												Zgs	IV
NW - 616	MBQPmgw	N 43 W	34 NE												Zgs	IV
NW - 617	BMsch & mgw-sap	N 83 W	32 NE												ccr	IV
NW - 618	MBPQmgw-sap	N 31 W	24 NE												Zgs	IV
NW - 619	mgw	N 71 W	43 NE												Zgs	IV
NW - 620	mgw	N 84 W	40 NE												Zgs	IV
NW - 621	MBPQmgw	N 41 W	38 NE												Zgs	IV
NW - 622	BMsch & mgw	N 38 W	42 NE												Zgs	IV
		N 51 W	29 NE													IV
NW - 623	BMsch & mgw	N 42 W	22 NE												Zgs	IV
NW - 624	BMsch & mgw	N 10 W	42 NE												Zgs	IV
NW - 625	BMsch & mgw	N 10 W	42 NE												Zgs	IV

Station	Lithology	Foliation		Lineation		Fold Axis		Axial Surface		IL	Amp.	Fold	Joint		Map	Dom-
		Strike	Dip	Plunge	Trend	Plunge	Trend	Strike	Dip	Angle	(m)	Verg.	Strike	Dip	Unit	ain
NW - 626	BMsch & mgw	N 07 W	38 NE												Zgs	IV
NW - 627	BMsch & mgw	N 13 W	73 NE												Zgs	IV
NW - 628	BMsch	N 36 W	54 NE												Zgs	IV
NW - 629	BMsch & mgw	N 48 W	31 NE												Zgs	IV
NW - 630	BMsch & mgw	N 27 W	38 NE												Zgs	IV
NW - 631	BMsch & mgw	N 51 W	63 NE												Zgs	IV
NW - 632	BMsch & mgw	N 33 W	26 NE												Zgs	IV
NW - 633	mgw	N 22 W	18 NE												Zgs	IV
NW - 634	QPMBsch	N 43 W	33 NE												Zgs	IV
NW - 635	mgw & BMsch	N 64 W	23 NE												Zgs	IV
NW - 636	MBPQmgw/sch	N 68 W	20 NE												Zgs	IV
NW - 637	MBPQmgw/sch	N 63 W	16 NE												Zgs	IV
NW - 638	GBPQmgw	N 46 W	22 NE												Zgs	IV
NW - 639	BPQmgw	N 39 W	23 NE												Zgs	IV
NW - 640	mgw	N 58 W	50 NE												Zgs	IV
NW - 641	mgw	N 76 W	04 NE												Zgs	IV
NW - 642	BPQmgw/qtz	N 64 W	11 NE												Zgs	IV
NW - 643	BMsch & mgw-sap	N 53 W	27 NE												Zgs	IV
NW - 644	BMsch	N 64 W	24 NE												Zgs	IV
NW - 645	BMsch	N 38 W	64 NE												Zgs	IV
NW - 646	mgw-sap	N 74 W	18 NE												Zgs	IV
NW - 647	BMsch	N 26 W	14 NE												Zgs	IV
NW - 648	MBQPmgw & BMsch	N 36 E	26 SE												Zgs	IV
NW - 649	MBQPmgw	N 58 W	38 NE												Zgs	IV
NW - 650	BM/MBsch	N 39 W	31 NE												Zgs	IV
NW - 651	mgw & BMsch	N 31 W	31 NE												Zgs	IV
NW - 652	MBsch & mgw	N 16 W	39 NE												Zgs	IV
NW - 653	MBsch & mgw	N 04 W	41 NE												Zgs	IV
NW - 654	MBsch & mgw-sap	N 53 W	49 NE												Zgs	IV
		N 76 W	46 SW													IV
NW - 655	MBsch & mgw-sap	N 48 W	43 NE												Zgs	IV
NW - 656	Msch & mgw	N 21 W	22 NE												Zgs	IV
NW - 657	MBsch & mgw	N 51 W	41 NE												Zgs	IV
NW - 658	mgw	N 54 W	55 NE												Zgs	IV
NW - 659	mgw	N 51 W	31 NE												Zgs	IV
NW - 660	MBsch & mgw	N 36 W	29 NE												Zgs	IV
NW - 661	MBsch & mgw	N 48 W	27 NE												Zgs	IV
NW - 662	MBsch & mgw w/ c-si	N 54 W	25 NE												Zgs	IV
NW - 663	mgw	N 66 W	41 NE												Zgs	IV
NW - 664	mgw	N 71 W	56 NE												Zgs	IV
NW - 665	BMsch & mgw-sap	N 46 W	55 NE												Zgs	IV
NW - 666	MBsch & mgw	N 54 W	32 NE												Zgs	IV
NW - 667	MBQPmgw	N 61 W	55 NE												Zgs	IV
NW - 668	MBsch & mgw	N 34 W	18 NE												Zgs	IV
NW - 669	MBsch & mgw	N 58 W	33 NE												Zgs	IV
NW - 670	MBsch & mgw	N 14 W	33 NE												Zgs	IV
NW - 671	MBsch & mgw w/ c-si	N 44 W	49 NE												Zgs	IV
NW - 672	MBsch & mgw	N 41 W	29 NE												Zgs	IV
NW - 673	MBsch & mgw	N 66 W	44 NE												Zgs	IV
NW - 674	MBsch & mgw	N 36 W	28 NE												Zgs	IV
NW - 675	MBsch & mgw-sap	N 38 W	39 NE												Zgs	IV
NW - 676	mgw	N 64 W	31 NE										N 49 W	61 SW	Zgs	IV
NW - 677	MBsch	N 37 W	41 NE										N 23 W	50 SW	Zgs	IV
NW - 678	MBsch & mgw-sap	N 52 W	31 NE												Zgs	IV
NW - 679	MBsch & mgw-sap	N 88 E	24 NW												Zgs	IV
NW - 680	MBsch & mgw-sap	N 46 W	54 NE												Zgs	IV

APPENDIX B-2

Structural and rock type data for the Campbell Mountain quadrangle

Note: Stations correspond to locations within the Campbell Mountain quadrangle presented on Plate II: Station numbers, sample locations, and structural domains within portions of the Nimblewill, Campbell Mountain, and Dahlonega, Georgia 7.5-minute quadrangles.

ABBREVIATIONS:

Note: Lithology indicated by lower case lettering and minerals indicated by UPPER case lettering.

Lithologies

- amp - amphibolite
- c-si - calc-silicate
- gn - gneiss
- hgn - hornblende gneiss
- mgr - metagabbro
- mgw - metagraywacke
- peg - pegmatite
- qtz - quartzite
- sch - schist

Other

- aug - augen
- bd - boudin
- blk - black
- Iso - isoclinal
- myl - mylonitic
- sap - saprolite
- zen - zenolith

Minerals

- B - biotite
- C - chlorite
- E - epidote
- F - feldspar
- G - garnet
- H - hornblende
- K - kyanite
- M - muscovite
- P - plagioclase
- S - sillimanite

Map Unit

- Zgs - Great Smoky Group

- CG - Coweeta Group
- ccr - Coleman River Formation

- GB - Gold Belt
- am - amphibolite
- as - aluminous schist
- hb - hornblendite
- hg - Hornblende gneiss
- hga - hornblende gneiss, metagabbro, & amphibolite
- mss - metasandstone and schist
- Ofg - felsic gneiss
- qms - quartzite, metasandstone, & schist
- ig - intermediate gneiss

Station	Lithology	Foliation Strike	Foliation Dip	Lineation Plunge	Lineation Trend	Fold Axis Plunge	Fold Axis Trend	Axial Surface Strike	Axial Surface Dip	IL Angle	Amp. (m)	Fold Verg.	Joint Strike	Joint Dip	Map Unit	Dom-ain
CM - 1	amp														am/mss	II
CM - 2	GMQsch	N 35 E	45 SE												mss	II
CM - 3	Msch	N 20 E	51 SE												as	II
CM - 4	amp & MQmgw	N 30 E	45 SE												am/mss	II
CM - 5	GMQsch	N 40 W	55 NE												as	III
CM - 6	mgw	N 87 E	34 NW												as	III
		N 12 E	58 NW													III
CM - 7	mgw & MQsch	N 46 E	28 NW												ccr	III
		N 73 E	30 NW													III
CM - 8	Bmgw	N 23 W	28 NE												ccr	III
CM - 9	mgw	N 27 W	26 NE												ccr	III
CM - 10	mgw	N 37 W	78 NE												ccr	III
CM - 11	mgw	N 12 W	48 NE												ccr	III
CM - 12	mgw					16	S 52 E	N 53 W	43 SW	90		NE			ccr	III
CM - 13	mgw	N 62 E	68 SE												ccr	III
CM - 14	mgw	N 62 W	37 NE												ccr	III
CM - 15	mgw	N 47 W	56 SW												ccr	III
CM - 16	mgw					19	S 63 E	N 63 E	24 NW	75		NE			ccr	III
CM - 17	mgw	N 07 E	54 NW												ccr	III
		N 54 W	86 NE													III
CM - 18	mgw	N 67 W	47 NE												ccr	III
CM - 19	amp	N 87 W	37 NE			7	S 19 E	N 24 W	24 NE	75		SW			amp-CG	III
		N 47 W	37 NE													III
CM - 20	amp														amp-CG	III
CM - 21	mgw	N 29 W	34 NE												ccr	III
CM - 22	MBsch & mgw	N 63 W	24 NE												ccr	III
		N 73 E	66 SW													III
CM - 23	sch & mgw	N 11 W	72 SW												ccr	III
CM - 24	amp & PQBMsch	N 12 E	36 SE												am/as	II
CM - 25	gn	N 76 W	42 NE												ccr	II
CM - 26	Msch	N 58 W	31 NE												ccr	II
CM - 27	GBQMsch & BPQmgw	N 37 W	31 NE												ccr	II
CM - 28	GBmgw	N 44 W	54 NE												ccr	II
CM - 29	mgw	N 11 E	42 SE												ccr	II
CM - 30	GKMsch	N 19 E	33 SE												as	II
CM - 31	GKMsch w/ c-si	N 66 E	22 SE												as	II
CM - 32	KGMsch	N 59 E	43 SE												as	II
CM - 33	KGMsch	N 43 E	62 SE												as	II
CM - 34	KGMsch	N 72 E	70 SE	21	N 74 E								N 25 W	68 SW	as	II
CM - 35	Ksch & mgw	N 30 E	26 SE												as	II
CM - 36	GKMsch	N 38 E	51 SE												as	II
CM - 37	GKMsch	N 13 E	37 SE												as	II
CM - 38	GKMsch & MEQmgw/qtz	N 38 W	04 NE												as	II
CM - 39	KGMsch	N 09 W	31 NE												as	II
		N 37 W	18 NE													II
CM - 40	amp	N 47 E	82 SE												am-GB	II
CM - 41	amp	N 22 E	62 NW												am-GB	II
CM - 42	amp	N 56 E	49 NW												am-GB	II
CM - 43	amp	N 77 E	74 NW												am-GB	II
CM - 44	amp	N 67 W	43 NE												am-GB	II
CM - 45	amp	N 84 E	58 NW												am-GB	II
CM - 46	amp	N 84 E	62 NW												am-GB	II
CM - 47	GKMsch	N 75 E	71 SE												as	II
CM - 48	GKMsch	N 88 E	72 SE												as	II
CM - 49	amp	N 18 W	51 SW												am-GB	II
CM - 50	amp	N 34 E	36 NW												am-GB	II
CM - 51	GKMsch	N 74 E	14 SE												as	II
CM - 52	GKMsch	N 73 E	46 NW												as	II
CM - 53	KGQMsch	N 68 E	33 SE												as	II
CM - 54	GBMEqtz & GMsch	N 32 E	27 SE												as	II
	amp-float															II
CM - 55	GMBPQmgw & GMsch	N 78 E	46 SE												as	II
CM - 56	GMsch & mgw	N 52 E	49 SE												as	II
CM - 57	GBmgw	N 52 E	31 SE												as	II
	amp-float															II
CM - 58	GPBMQmgw & MBsch	N 52 E	39 SE			15	S 80 E	N 3 E	17 SE	160	0.02 - 0.05				as	II
CM - 59	amp	N 20 W	19 NE												am-GB	II
CM - 60	amp	N 32 E	42 SE												am-GB	II
CM - 61	amp	N 14 E	21 SE												am-GB	II
CM - 62	amp	N 77 E	41 SE										N 25 W	63 SW	am-GB	II
		N 72 E	89 SE										N 14 E	90		II
													N 32 W	89 SW		II
CM - 63	amp					34	N 8 W	N 65 E	28 NW	45	0.05 - 0.15	SW			am-GB	II
CM - 64	amp	N 60 E	64 SE												am-GB	II
CM - 65	amp	N 40 W	35 NE													II
CM - 66	amp	N 35 W	26 NE													II
CM - 67	GQBMsch & amp	N 34 W	24 NE										N 48 E	90	mss	II
		N 56 W	11 NE										N 09 W	62 NE	am-GB	II
													N 55 W	52 NE		II
													N 64 E	88 NW		II
CM - 68	GQBMsch& mgw	N 81 E	34 NW												mss	II
CM - 69	GPQBMsch	N 60 E	28 SE										N 29 W	56 SW	mss	II
													N 40 E	51 NW		II
													N 12 W	50 SW		II
													N 41 W	59 NE		II
CM - 70	GBMQsch\mgw	N 32 E	24 SE												mss	II
CM-71	GMBPQmgw	N 23 E	12 SE										N 34 E	71 SE	mss	II
													N 18 E	85 NW		II
													N 42 W	90		II
CM - 72	MBsch	N 18 W	24 NE												ccr	II
CM - 73	BQmgw & sch	N 58 W	18 NE												ccr	II
CM - 74	BQmgw & sch	N 63 W	19 NE												ccr	II
CM - 75	GMBPQmgw/sch	N 60 W	29 NE												ccr	II
CM - 76	BQPmgw	N 65 W	29 NE												ccr	II
CM - 77	BQmgw	N 72 E	49 NW												ccr	II

Station	Lithology	Foliation Strike	Foliation Dip	Lineation Plunge	Lineation Trend	Fold Axis Plunge	Fold Axis Trend	Axial Surface Strike	Axial Surface Dip	IL Angle	Amp. (m)	Fold Verg.	Joint Strike	Joint Dip	Map Unit	Dom-ain
CM - 78	mgw & sch	N 05 E	57 SE												ccr	II
CM - 79	mgw	N 02 E	38 SE												ccr	II
CM - 80	mgw	N 78 E	41 SE												ccr	II
CM - 81	mgw & sch	N 64 E	24 SE												ccr	II
CM - 82	mgw	N 68 E	23 SE												ccr	II
CM - 83	mgw	N 70 E	35 SE												ccr	II
CM - 84	BPQmgw	N 19 E	28 SE												ccr	II
CM - 85	BPQmgw	N 10 E	18 SE												ccr	II
CM - 86	mgw	N 22 E	42 SE												ccr	II
		N 34 E	42 SE													II
CM - 87	mgw	N 23 E	32 SE												ccr	II
CM - 88	mgw	N 10 W	24 NE												ccr	II
CM - 89	mgw	N 33 E	20 SE										N 34 W	68 NE	ccr	II
													N 38 W	90		II
													N 28 E	67 SE		II
													N 24 W	59 NE		II
CM - 90	mgw	N 03 E	24 SE										N 51 E	90	ccr	II
CM - 91	mgw	N 03 W	28 NE												ccr	II
CM - 92	mgw	N 04 E	37 SE												ccr	II
CM - 93	BQPmigmatite	N 38 E	27 SE												ccr	II
CM - 94	mgw	N 35 E	15 SE												ccr	II
CM - 95	mgw	N 07 E	17 SE												ccr	II
CM - 96	mgw	N 07 E	17 SE												ccr	II
CM - 97	amp	N 44 E	25 SE												am-GB	II
CM - 98	mgw/sch	N 3 W	38 NE												ccr	II
CM - 99	mgw	N 27 E	27 SE												ccr	II
CM - 100	mgw	N 04 E	15 SE												ccr	II
CM - 101	mgw	N 34 E	18 SE												ccr	II
CM - 102	mgw	N 38 E	35 SE												ccr	II
		N 75 E	31 SE													II
CM - 103	mgw	N 29 E	40 SE												ccr	II
CM - 104	mgw	N 42 E	34 SE												ccr	II
CM - 105	mgw	N 18 E	40 SE												ccr	II
CM - 106	mgw	N 26 E	34 SE												ccr	II
CM - 107	mgw	N 34 E	32 SE												ccr	II
CM - 108	mgw	N 24 E	08 SE												ccr	II
CM - 109	mgw	N 11 E	29 SE												ccr	II
CM - 110	mgw	N 03 E	40 SE												ccr	II
CM - 111	amp	N 18 E	26 SE										N 48 E	46 NW	am-GB	II
CM - 112	BPQmgw	N 18 W	14 NE												as	II
CM - 113	K?GMsch	N 07 E	28 SE												as	II
CM - 114	K?GMsch & BPQmgw	N 04 E	27 SE										N 15 E	63 NW	as	II
CM - 115	BQmgw/qtz	N 04 E	45 SE												as	II
		N 07 E	26 SE													II
CM - 116	amp	N 35 W	44 NE												am-GB	II
CM - 117	amp	N 62 E	24 SE												am-GB	II
CM - 118	BPQmgw	N 04 E	10 SE												as	II
CM - 119	mgw	N 54 E	42 SE												as	II
CM - 120	amp	N 54 E	54 NW												am-GB	II
CM - 121	KGMsch	N 07 E	28 SE												as	II
CM - 122	PBQmgw & MBsch	N 19 E	14 SE												as	II
CM - 123	amp & MBsch	N 64 W	62 NE												as	II
CM - 124	amp	N 38 W	22 NE												am-GB	II
CM - 125	Msch	N 36 W	18 NE												as	II
CM - 126	amp	N 16 W	60 SW												am-GB	II
CM - 127	Msch	N 08 W	30 NE												as	II
CM - 128	amp	N 06 W	50 SW												am-GB	II
CM - 129	KGMsch & mgw	N 28 W	49 NE												as	II
		N 54 W	25 NE	12	N 80 E											II
CM - 130	KGMsch & mgw	N 05 W	34 NE												as	II
CM - 131	GMsch	N 32 W	41 NE												as	II
CM - 132	KGMsch	N 22 W	49 NE												as	II
CM - 133	KGMsch	N 04 E	27 SE												as	II
CM - 134	KGMsch	N 02 W	26 NE												as	II
CM - 135	GMsch	N 13 E	31 SE												as	II
CM - 136	GMsch	N 28 W	28 NE												as	II
CM - 137	K?GMsch	N 15 E	14 SE												as	II
CM - 138	GMsch	N 40 W	29 NE										N 35 W	84 SW	as	II
CM - 139	K?GMsch & mgw	N 05 E	28 SE												as	II
CM - 140	GMsch	N 32 E	33 SE										N 46 W	85 SW	as	II
CM - 141	amp & GMsch	N 43 E	85 SE												as/am	II
CM - 142	GQMsch & amp	N 35 E	44 SE												as	II
CM - 143	PQBmgw & sch	N 64 E	72 SE												mss	II
CM - 144	BMsch	N 57 E	68 SE												mss	II
CM - 145	BMsch	N 60 E	90												mss	II
CM - 146	MQmgw	N 09 W	49 NE												as	II
CM - 147	Msch	N 58 W	15 NE												as	II
CM - 148	amp	N 68 E	75 SE												am-GB	II
CM - 149	amp	N 71 W	31 NE												am-GB	II
CM - 150	amp	N 38 W	26 NE			46	N 75 E	N 63 W	62 NE	45	0.05 - 0.1				am-GB	II
CM - 151	BPQmgw, MBsch, & amp	N 54 E	22 SE												as	II
CM - 152	mgw & sch	N 85 W	34 NE												as	II
CM - 153	GMBsch	N 85 W	34 NE												as	II
CM - 154	mgw	N 06 W	22 NE												as	II
CM - 155	GMBsch	N 70 W	24 NE										N 48 E	67 SE	as	II
													N 27 W	62 SW		II
													N 45 W	64 SW		II
													N 02 W	72 SW		II
CM - 156	GMBsch	N 35 W	21 NE												as	II
CM - 157	K?GMsch	N 26 E	41 SE												as	II
CM - 158	K?GMSsch	N 32 W	34 NE												as	II
CM - 159	amp	N 70 E	34 SE												am-GB	II
CM - 160	BQPmgw	N 64 E	49 SE												mss	II
CM - 161	MBsch & mgw	N 60 E	76 SE												mss	II
CM - 162	GMsch	N 75 E	72 SE												as	II

Station	Lithology	Foliation		Lineation		Fold Axis		Axial Surface		IL	Amp.	Fold	Joint		Map	Dom-
		Strike	Dip	Plunge	Trend	Plunge	Trend	Strike	Dip	Angle	(m)	Verg.	Strike	Dip	Unit	ain
CM - 163	amp	N 52 E	64 SE												am-GB	II
CM - 164	amp & BMsch	N 43 E	72 SE												as/am	II
CM - 165	Mqtz aver amp	N 44 E	63 SE												as/am	II
CM - 166	amp over Msch	N 65 E	76 SE												as/am	II
CM - 167	BQPmgw	N 63 E	48 SE												mss	II
CM - 168	mgw	N 42 E	73 SE												ccr	II
CM - 169	mgw & sch	N 47 E	88 SE												ccr	II
CM - 170	QBsch	N 43 E	41 SE												ccr	II
CM - 171	GBPQmgw/gn	N 50 E	39 SE												ccr	II
CM - 172	GBPQgn					21	N 47 E	N 49 E	56 SE	45	0.05 - 0.07	NW			ccr	II
CM - 173	BPQmgw & MBsch	N 66 E	34 NW												ccr	II
CM - 174	GBMsch	N 66 E	34 NW												ccr	II
CM - 175	Bmgw & sch	N 05 E	34 NW												ccr	II
		N 68 E	49 NW													II
CM - 176	Bmgw & sch	N 63 W	46 NE												ccr	III
CM - 177	BPQgn	N 72 W	51 NE												ccr	III
CM - 178	gn sap	N 25 W	40 NE												mss	III
CM - 179	MBsch	N 28 W	51 NE												ccr	III
CM - 180	Bmgw	N 89 E	26 NW												ccr	II
CM - 181	GBQPmgw/gn	N 89 E	26 NW												ccr	II
CM - 182	mgw	N 82 E	21 NW												ccr	II
CM - 183	BQPmgw/gn	N 89 E	26 NW												ccr	II
CM - 184	BQPmgw	N 74 E	44 NW												ccr	II
CM - 185	mgw	N 44 E	49 NW												ccr	II
CM - 186	mgw & peg	N 28 E	14 SE												ccr	II
CM - 187	GBQPmgw/gn	N 34 E	56 SE												ccr	II
CM - 188	BQPmgw/gn	N 64 E	14 SE												ccr	II
CM - 189	BQPmgw/gn	N 61 W	29 NE												ccr	II
CM - 190	BQPmgw/gn	N 07 E	69 SE												ccr	II
CM - 191	BQPmgw/gn	N 14 W	54 NE												ccr	II
CM - 192	BQPmgw/gn	N 58 W	08 NE												ccr	II
CM - 193	mgw	N 53 W	57 NE												ccr	II
CM - 194	mgw	N 33 W	26 NE												ccr	II
CM - 195	mgw	N 05 E	34 NW												ccr	II
CM - 196	mgw	N 01 W	61 NE												ccr	II
CM - 197	mgw	N 39 W	44 NE												ccr	II
CM - 198	mgw	N 04 E	47 SE												ccr	II
CM - 199	mgw	N 03 W	35 NE												ccr	II
CM - 200	amp	N 28 W	34 NE												am-CG	II
CM - 201	mgw	N 18 W	49 NE												ccr	II
CM - 202	BPQmgw	N 32 E	65 SE												ccr	II
		N 25 E	43 SE													II
CM - 203	BPQmgw	N 37 E	25 SE												ccr	II
CM - 204	BPQmgw	N 62 E	13 SE										N 35 W	52 NE	ccr	II
CM - 205	BPQmgw/gn	N 34 E	17 SE										N 62 E	81 NW	ccr	II
													N 71 W	68 SW		II
CM - 206	BPQmgw/gn w/ amp bd	N 27 W	16 NE										N 62 E	81 NW	ccr	II
													N 71 W	68 SW		II
CM - 207	BPQmgw/gn	N 61 W	22 NE												ccr	II
CM - 208	BPQmgw/gn	N 15 E	14 SE												ccr	II
		N 34 W	26 NE													II
CM - 209	BPQmgw/gn	N 03 W	11 NE										N 39 W	85 SW	ccr	II
													N 53 E	78 NW		II
CM - 210	BPQmgw & MBsch	N 03 E	39 SE												ccr	II
CM - 211	BPQmgw & MBsch	N 09 E	24 SE												ccr	II
CM - 212	BPQmgw & MBsch	N 53 W	42 NE												ccr	II
CM - 213	MBsch	N 04 E	30 SE												ccr	II
CM - 214	mgw	N 04 W	11 NE												ccr	II
CM - 215	mgw/gn	N 23 W	20 NE												ccr	II
CM - 216	mgw/gn	N 44 W	21 NE												ccr	II
CM - 217	mgw/gn	N 08 W	13 NE												ccr	II
CM - 218	GMBsch	N 26 W	19 NE												ccr	II
CM - 219	MBPQmgw/sch	N 54 W	49 NE												mss	II
CM - 220	mgw & sch	N 44 W	27 NE												ccr	II
CM - 221	mgw & sch	N 19 W	58 NE												ccr	II
CM - 222	BQPmgw	N 33 E	26 SE										N 44 E	84 NW	ccr	II
		N 08 E	31 SE										N 39 W	54 SW		II
CM - 223	MBPQmgw	N 07 E	17 SE												mss	II
CM - 224	MBQPgn	N 32 E	16 SE												mss	II
CM - 225	BMQPgn/sch	N 22 W	35 NE												mss	II
CM - 226	BMQPgn	N 44 W	16 NE												mss	II
CM - 227	MBQPsch/gn	N 22 W	16 NE												mss	II
CM - 228	MBsch	N 28 W	40 NE												mss	II
CM - 229	MBQPgn	N 74 E	22 NW												mss	II
CM - 230	PQBsch/mgw					24	S 69 E	N 6 W	18 NE	Iso.	0.15 - 0.20	SW			ccr	II
CM - 231	MBPQgn/sch	N 55 E	26 SE												ccr	II
CM - 232	GMBPQgn	N 37 E	12 SE												ccr	II
CM - 233	GMBPQmgw/sch	N 58 E	10 SE										N 66 W	83 NE	ccr	II
CM - 234	K?GBMsch	N 85 E	65 SE												mss	II
CM - 235	GPQBMsch	N 42 W	23 NE												mss	II
CM - 236	GBPQmgw	N 54 W	14 NE												ccr	II
CM - 237	MBQPgn	N 67 E	21 SE												mss	II
CM - 238	MBQPgn	N 28 E	16 SE												mss	II
CM - 239	BPQmgw	N 85 W	07 NE												ccr	II
		N 34 W	20 NE													II
CM - 240	MBsch	N 75 E	04 NW												ccr	II
CM - 241	BQPmgw & MBsch														ccr	II
CM - 242	MBQPmgw	N 36 W	43 NE	26	N 79 E								N 14 W	60 NE	mss	II
CM - 243	MBQPmgw	N 04 E	44 SE												mss	II
CM - 244	MBQPmgw	N 23 W	38 NE	36	N 85 E										mss	II
CM - 245	BMsch	N 69 E	28 SE												mss	II
CM - 246	K?GMsch & amp	N 19 W	35 NE												mss/am	II
CM - 247	amp & Msch	N 14 W	46 NE												mss/am	II
CM - 248	K?GMsch, amp, & BPQmgw	N 15 E	33 SE										N 27 W	65 SW	mss/am	II
													N 17 E	75 NW		II

Station	Lithology	Foliation Strike	Foliation Dip	Lineation Plunge	Lineation Trend	Fold Axis Plunge	Fold Axis Trend	Axial Surface Strike	Axial Surface Dip	IL Angle	Amp. (m)	Fold Verg.	Joint Strike	Joint Dip	Map Unit	Dom-ain
													N 12 W	59 SW		II
CM - 249	MBsch & amp	N 80 E	29 NW												mss/am	II
	BPQmgw	N 34 W	25 NE												mss	II
CM - 250	BMsch & mgw-sap	N 42 W	27 NE												mss	II
CM - 251	amp	N 17 E	30 SE												am-GB	II
CM - 252	amp	N 44 E	48 NW												am-GB	II
CM - 253	amp	N 31 W	32 NE										N 17 E	60 NW	am-GB	II
CM - 254	amp	N 44 W	34 NE												am-GB	II
CM - 255	MBPQgn	N 04 E	54 SE												as	II
CM - 256	MBPQmgw & MBsch	N 03 E	44 SE												as	II
CM - 257	GMBPQmgw & MBsch	N 03 E	43 SE												as	II
		N 06 E	46 SE													II
CM - 258	KGBQMsch & MBPQmgw	N 65 W	62 NE												as	II
CM - 259	KGQMsch	N 09 W	46 NE												as	II
CM - 260	KBMS & MBPQmgw					44	S 64 E	N 41 W	65 NE	Iso.	0.10 - 0.15	SW			mss	II
CM - 261	GMBPQgn	N 26 W	51 NE												mss	II
CM - 262	amp														am-GB	II
CM - 263	MBQPgn	N 75 E	26 SE												mss	II
CM - 264	MBQPgn	N 16 E	22 SE												mss	II
CM - 265	BQPmgw/gn	N 58 W	08 SW												ccr	II
CM - 266	amp	N 24 E	39 SE												am-GB	II
CM - 267	amp	N 33 E	32 SE												am-GB	II
CM - 268	MBPQgn	N 10 W	23 NE												mss	II
CM - 269	MBPQgn	N 23 W	11 NE												mss	II
CM - 270	MBPQgn	N 55 W	19 NE												mss	II
CM - 271	amp	N 14 E	33 SE			9	N 88 E	N 65 W	33 NE	90	?	SW			am-GB	II
CM - 272	amp	N 59 E	59 NW												am-GB	II
		N 50 E	78 NW													II
CM - 273	amp	N 62 E	64 NW												am-GB	II
CM - 274	amp	N 68 E	79 NW												am-GB	II
CM - 275	amp	N 71 E	72 SE												am-GB	II
CM - 276	K?GMsch	N 7 W	34 NE												as	II
CM - 277	amp	N 36 W	23 NE												am-GB	II
CM - 278	mgw & Msch	N 47 E	43 SE												as	II
CM - 279	MBQPmgw & Msch	N 44 E	38 SE												as	II
CM - 280	MBQPmgw & Msch	N 07 E	49 SE												as	II
CM - 281	MBPQmgw/sch	N 23 E	66 SE												as	II
CM - 282	amp	N 12 W	51 NE												am-GB	II
CM - 283	EGQBH?Pgn	N 44 W	25 NE	26	N 23 E										Ofg	III
		N 46 W	30 NE													III
CM - 284	Fgn-sap	N 55 W	44 NE												Ofg	III
CM - 285	Fgn-sap	N 07 E	44 SE												Ofg	III
CM - 286	Fgn & amp w/ blk G	N 10 W	33 SW												Ofg	III
CM - 287	amp	N 32 W	26 NE										N 34 W	84 SW	am-GB	III
		N 66 W	31 NE										N 73 E	81 NW		III
		N 70 W	31 NE										N 42 E	33 SE		III
		N 62 W	26 NE										N 41 W	90		III
		N 47 W	46 NE										N 26 W	78 SW		III
		N 43 W	61 NE										N 90 E	73 SE		III
													N 41 W	80 SW		III
													N 88 E	62 SE		III
													N 9 W	78 NE		III
													N 43 W	45 SW		III
													N 18 E	77 NW		III
													N 42 W	80 SW		III
													N 28 W	53 SW		III
													N 39 W	54 SW		III
CM - 288	amp	N 30 W	36 NE												am-GB	III
CM - 289	amp	N 58 W	54 NE										N 37 W	39 SW	am-GB	III
		N 30 W	33 NE													III
CM - 290	amp	N 20 W	39 NE												am-GB	III
CM - 291	amp	N 18 W	29 NE										N 62 W	57 NE	am-GB	III
		N 25 W	53 NE										N 35 W	90		III
CM - 292	amp	N 54 W	32 NE												am-GB	III
CM - 293	amp	N 23 W	40 NE												am-GB	III
CM - 294	amp	N 34 W	56 NE												am-GB	III
CM - 295	amp	N 22 W	28 NE												am-GB	III
CM - 296	amp	N 57 W	48 NE												am-GB	III
CM - 297	amp	N 31 W	41 NE												am-GB	III
CM - 298	amp	N 31 W	44 NE												am-GB	III
CM - 299	GBQMsch	N 32 W	43 NE												qms	III
CM - 300	amp	N 13 W	64 NE												am-GB	III
CM - 301	EPamp	N 5 W	44 NE										N 48 W	41 SW	am-GB	III
CM - 302	EPamp	N 18 W	45 NE										N 43 W	66 SW	am-GB	III
CM - 303	amp	N 02 E	56 SE												am-GB	III
CM - 304	amp	N 12 W	42 NE										N 48 W	51 SW	am-GB	III
													N 37 E	85 NW		III
CM - 305	Fgn-sap														Ofg	III
CM - 306	Fgn-float														Ofg	III
CM - 307	amp	N 72 E	30 NE										N 66 w	58 SW	am-GB	III
													N 12 W	36 NE		III
													N 55 W	55 SW		III
													N 09 E	80 NW		III
CM - 308	amp	N 34 W	21 NE												am-GB	III
CM - 309	GQMsch, MPQmgw, &	N 42 W	43 NE										N 65 E	88 SE	as	III
	amp	N 32 W	64 NE												am-GB	III
		N 42 W	63 NE													III
CM - 310	GQMsch, MPQmgw, &	N 24 W	63 NE												as	III
	amp														am-GB	III
CM - 311	Fgn	N 14 W	55 NE												Ofg	III
CM - 312	amp	N 17 W	74 SW												am-GB	III
CM - 313	amp	N 14 E	56 SE												am-GB	III
CM - 314	amp & Msch	N 08 E	64 SE												as/am	III
CM - 315	Msch	N 15 E	51 SE												as	III
CM - 316	BQPmgw-sap & Msch	N 64 W	38 NE												as	III

Station	Lithology	Foliation Strike	Foliation Dip	Lineation Plunge	Lineation Trend	Fold Axis Plunge	Fold Axis Trend	Axial Surface Strike	Axial Surface Dip	IL Angle	Amp. (m)	Fold Verg.	Joint Strike	Joint Dip	Map Unit	Dom-ain
CM - 317	BPQmgw & BMsch	N 52 W	41 NE												ccr	III
CM - 318	MBsch	N 79 W	33 NE												ccr	III
CM - 319	BQPmgw	N 82 W	11 NE												mss	III
CM - 320	GQBMsch	N 46 W	41 NE												mss	III
		N 33 W	52 NE													III
CM - 321	GQBMsch	N 74 w	42 NE												mss	III
CM - 322	BMQPmgw	N 62 W	46 NE												mss	III
CM - 323	GBMsch	N 86 W	25 NE										N 44 W	90	mss	III
													N 35 W	69 SW	mss	III
CM - 324	BQPmgw	N 83 W	44 NE												mss	III
CM - 325	BMsch	N 66 W	35 NE												mss	III
CM - 326	BQPgn	N 82 W	38 NE										N 41 W	46 SW	mss	III
													N 31 E	84 SE		III
CM - 327	BQPgn & MBsch	N 57 W	38 NE												mss	III
CM - 328	MBQPmgw	N 69 W	36 NE												mss	III
CM - 329	BMsch	N 76 W	39 NE												mss	III
CM - 330	BMQpmgw & BMsch	N 69 W	41 NE												mss	III
CM - 331	BQPmgw	N 85 E	50 NW												mss	III
CM - 332	MBsch	N 63 W	52 NE												mss	III
CM - 333	MBQPmgw	N 83 W	51 NE												mss	III
CM - 334	BPQmgw	N 17 E	19 NW												ccr	III
CM - 335	BPQmgw	N 34 W	29 NE												ccr	III
CM - 336	BPQmgw	N 43 W	21 NE												ccr	III
CM - 337	BPQmgw	N 65 W	35 NE												ccr	III
CM - 338	BMPQgn/mgw & MBsch	N 62 W	25 NE												mss	III
CM - 339	BMPQgn/mgw & GMBsch	N 71 W	25 NE												mss	III
CM - 340	BMPQgn/mgw & GMBsch	N 58 W	25 NE												mss	III
CM - 341	mgw & sch - sap	N 49 W	61 NE												mss	III
CM - 342	amp	N 52 W	05 NE												am-GB	III
		N 68 W	25 SW													III
CM - 343	amp	N 56 W	24 NE												am-GB	III
CM - 344	amp	N 03 W	37 SW												am-GB	III
CM - 345	amp	N 77 W	31 NE												am-GB	III
CM - 346	amp	N 79 W	46 NE												am-GB	III
CM - 347	amp	N 06 E	67 NW												am-GB	III
CM - 348	MBsch & BPQmgw	N 12 E	14 NW												ccr	III
CM - 349	MBsch & BPQmgw	N 58 W	30 NE										N 42 W	68 SW	ccr	III
CM - 350	MBsch	N 78 E	34 NW												ccr	III
CM - 351	BPQmgw & MBsch	N 34 W	41 NE												ccr	III
CM - 352	BPQmgw	N 03 W	48 NE												ccr	III
CM - 353	BPQmgw	N 78 E	29 NW												ccr	III
CM - 354	BPQmgw	N 84 E	53 NW												ccr	III
CM - 355	BPQmgw	N 75 E	17 NW												ccr	III
CM - 356	BPQmgw & Mbsch	N 10 E	36 NW												ccr	III
CM - 357	BPQmgw	N 86 E	59 NW												ccr	III
CM - 358	BPQmgw	N 32 W	33 NE												ccr	III
CM - 359	BPQmgw	N 61 W	32 NE												ccr	III
CM - 360	MBPQmgw	N 70 W	12 NE												mss	III
CM - 361	MBPQmgw	N 23 E	62 NW												mss	III
CM - 362	BPQmgw	N 34 W	35 NE												ccr	III
CM - 363	BPQmgw	N 56 W	17 NE												ccr	III
CM - 364	BPQmgw	N 41 W	29 NE												ccr	III
CM - 365	BPQmgw	N 69 W	27 NE												ccr	III
CM - 366	BPQmgw	N 48 W	26 NE												ccr	III
CM - 367	BPQmgw	N 51 W	31 NE												ccr	III
CM - 368	BPQmgw	N 71 W	27 NE												ccr	III
CM - 369	BPQmgw	N 38 E	28 NW												ccr	III
CM - 370	amp & Msch	N 71 W	27 NE												am/mss	III
CM - 371	amp	N 38 W	42 NE												am-GB	III
CM - 372	amp	N 40 W	43 NE												am-GB	III
		N 44 W	67 NE													III
		N 61 W	51 NE													III
CM - 373	amp	N 46 W	38 NE												am-GB	III
CM - 374	BMsch	N 58 W	37 NE												mss	III
CM - 376	MBQP/gn	N 74 W	19 NE												mss	III
CM - 377	MBQP/gn	N 52 W	39 NE												mss	III
CM - 378	MBsch & MBQPmgw	N 80 W	37 NE												mss	III
CM - 379	amp & MBsch	N 65 W	44 NE												am/ccr	II
CM - 380	amp	N 63 W	53 NE												am-GB	II
CM - 381	amp	N 17 W	39 NE												am-GB	II
CM - 382	BMsch	N 41 W	55 NE												mss	II
CM - 383	BMsch	N 00 E	34 SE												mss	II
CM - 384	amp	N 41 E	59 SE												am/GB	II
CM - 385	MBsch	N 42 E	57 SE												ccr	II
CM - 386	Bsch & mgw	N 00 E	63 SE												ccr	II
CM - 387	amp	N 32 W	36 NE												am-GB	II
CM - 388	S?GQMBsch	N 37 E	61 SE												ccr	II
		N 56 E	39 SE													II
CM - 389	S?BMsch & mgw	N 56 E	86 SE			34	N 09 W	N 04 W	67 NE	40	?	SW			ccr	II
CM - 390	BMsch	N 53 E	34 SE												ccr	II
CM - 391	BMsch & mgw	N 43 E	64 SE												ccr	II
CM - 392	BMsch & mgw	N 43 E	64 SE										N 42 W	51 SW	ccr	II
CM - 393	MBsch	N 22 E	62 SE												ccr	II
CM - 394	MBsch	N 81 W	27 NE												ccr	II
CM - 395	MBsch	N 09 E	37 SE												ccr	II
CM - 396	Fgn-sap	N 06 W	74 NE												Ofg	III
CM - 397	Fgn-sap	N 18 E	36 SE												Ofg	III
CM - 398	Fgn-sap	N 13 W	39 NE												Ofg	III
CM - 399	Fgn-sap & amp	N 76 W	24 NE												Ofg	II
CM - 400	Fgn/amp-sap														Ofg	II
CM - 401	Fgn, amp, & mgr	N 68 W	37 NE												Ofg	II
CM - 402	MBsch & Hgn	N 11 W	51 NE												qms/am	III
CM - 403	MQPmgw/sch	N 62 W	47 NE												qms	III
CM - 404	Mmgw/sch & amp	N 18 W	49 NE												qms/am	III
		N 21 E	33 SE													III

Station	Lithology	Foliation Strike	Foliation Dip	Lineation Plunge	Lineation Trend	Fold Axis Plunge	Fold Axis Trend	Axial Surface Strike	Axial Surface Dip	IL Angle	Amp. (m)	Fold Verg.	Joint Strike	Joint Dip	Map Unit	Dom-ain
CM - 405	amp	N 12 W	49 NE										N 38 E	73 SE	am-GB	III
													N 40 W	34 SW		III
CM - 406	Msch	N 19 W	34 NE												qms	III
CM - 407	BMPQmgw/qtz	N 03 W	36 NE												qms	III
CM - 408	amp	N 55 W	54 NE												am-GB	III
CM - 409	amp	N 22 W	54 NE												am-GB	III
CM - 410	amp	N 32 E	68 SE												am-GB	III
CM - 411	amp &	N 60 W	48 NE										N 45 W	50 SW	qms	III
	BQPmgw	N 02 E	44 SE													III
CM - 412	mgw/sch	N 39 W	38 NE												qms	III
CM - 413	amp	N 27 W	46 NE												am-GB	III
CM - 414	amp	N 22 W	48 NE												am-GB	III
CM - 415	amp	N 29 W	48 NE												am-GB	III
CM - 416	Fgn?	N 72 W	36 NE												Ofg	II
CM - 417	Fgn-sap	N 15 E	08 SE												Ofg	II
CM - 418	amp	N 53 W	31 NE												am-GB	III
CM - 419	amp	N 14 W	33 NE										N 28 E	53 SE	am-GB	III
													N 32 W	56 SW		III
CM - 420	amp	N 62 W	49 NE										N 37 W	48 SW	am-GB	III
		N 32 W	37 NE										N 19 W	48 SW		III
		N 36 W	36 NE										N 30 W	48 SW		III
CM - 421	amp	N 36 W	32 NE												am-GB	III
CM - 422	amp	N 28 W	31 NE												am-GB	III
CM - 423	amp	N 44 W	28 NE												am-GB	III
CM - 424	amp	N 22 W	37 NE												am-GB	III
CM - 425	amp	N 35 W	46 NE												am-GB	III
CM - 426	amp	N 44 W	31 NE												am-GB	III
CM - 427	amp	N 43 W	51 NE												am-GB	III
CM - 428	amp	N 49 W	34 NE												am-GB	III
CM - 429	amp	N 46 W	30 NE												am-GB	III
CM - 430	amp	N 01 W	37 NE												am-GB	III
CM - 431	amp	N 36 W	34 NE												am-GB	III
CM - 432	amp	N 44 W	44 NE												am-GB	III
CM - 433	Bmgw	N 14 W	46 NE												ccr	III
	MBPQmgw & GBMsch	N 67 W	43 NE												mss	III
CM - 434	mgw & sch	N 68 W	40 NE												ccr	III
CM - 435	amp	N 34 W	26 NE												ccr	III
CM - 436	amp & mgw/sch	N 68 W	44 NE												ccr & am-GB	II
CM - 437	Bmgw														ccr	II
CM - 438	PQMsch	N 67 E	54 NW												ccr	II
CM - 439	MBPQmgw	N 12 W	34 SW												ccr	II
CM - 440	MBsch	N 88 E	31 SE												ccr	II
CM - 441	MBsch	N 32 E	62 NW												ccr	II
CM - 442	mgw	N 66 E	74 NW												ccr	II
CM - 443	mgw	N 44 E	75 NW												ccr	II
		N 58 E	80 SE													II
CM - 444	mgw	N 47 E	79 SE										N 27 W	69 SW	ccr	II
CM - 445	mgw	N 46 E	75 SE										N 46 W	54 SW	ccr	II
		N 48 E	76 SE													II
CM - 446	mgw	N 33 E	36 SE												ccr	II
CM - 447	mgw	N 42 E	32 NW												ccr	II
CM - 448	BQPmgw	N 76 W	44 NE												ccr	II
CM - 449	MBsch	N 65 E	90												ccr	II
CM - 450	MBPQmgw & Msch	N 53 E	81 SE												ccr	II
CM - 451	BMQPmgw & MBsch	N 42 E	86 NW												mss	II
CM - 452	BMQPmgw & MBsch	N 39 W	42 NE												mss	II
CM - 453	GMBPQmgw & GMBsch	N 57 W	36 NE												mss	II
CM - 454	GBMQPmgw & sch	N 28 W	41 NE	31	N 83 E										mss	II
CM - 455	amp	N 58 E	59 NW												am-GB	II
		N 25 E	75 NW													II
		N 15 W	29 NE													II
CM - 456	amp	N 87 W	80 NE												am-GB	II
CM - 457	amp	N 74 W	26 NE												am-GB	II
CM - 458	amp	N 41 W	19 NE												am-GB	II
CM - 459	KGPQMsch	N 36 E	71 SE												as	II
CM - 460	KGPQMsch	N 13 E	43 SE												as	II
CM - 461	BQmgw & peg	N 24 W	21 NE												as	II
CM - 462	GMBPQmgw	N 74 E	31 NW												as	II
CM - 463	MBPQmgw	N 12 W	49 NE												mss	II
CM - 464	MBPQgn/sch	N 83 W	43 NE										N 46 E	58 SE	mss	II
CM - 465	MBPQmgw/sch	N 80 E	66 NW												mss	II
		N 14 W	26 NE													II
CM - 466	MBsch	N 34 E	34 SE												mss	II
CM - 467	MBsch	N 30 W	48 NE			34	S 70 E	N 44 E	35 SE	100	0.05	NE			mss	II
CM - 468	PBQmgw	N 63 E	52 NW												mss	II
CM - 469	PBQmgw	N 66 E	30 NW												mss	II
CM - 470	PBQmgw	N 74 E	34 NW												mss	II
CM - 471	MBPQmgw	N 34 W	44 NE												mss	II
CM - 472	K?GBMQsch	N 54 W	43 NE												mss	II
CM - 473	mgw	N 18 W	49 NE												mss	III
CM - 474	MBPQmgw	N 03 E	25 SE												mss	III
CM - 475	MBPQmgw	N 44 E	65 NW												mss	II
CM - 476	BPQmgw	N 61 E	41 NW												mss	II
CM - 477	mgw	N 57 E	51 NW										N 14 E	78 SE	mss	II
													N 34 W	72 SW		II
CM - 478	GBPQmgw/sch	N 44 E	39 SE												ccr	II
CM - 479	GKBPQsch	N 87 W	31 NE												ccr	II
		N 3 W	44 NE													II
		N 24 W	29 NE													II
		N 26 W	26 NE													II
		N 06 W	26 NE													II
		N 31 W	45 NE													II
CM - 480	GKBPQsch	N 37 W	24 NE												ccr	II
CM - 481	GKBPQsch	N 37 W	32 NE												ccr	II
CM - 482	GBPQmgw & GKBPQsch	N 68 W	35 NE												ccr	II

Station	Lithology	Foliation Strike	Foliation Dip	Lineation Plunge	Lineation Trend	Fold Axis Plunge	Fold Axis Trend	Axial Surface Strike	Axial Surface Dip	IL Angle	Amp. (m)	Fold Verg.	Joint Strike	Joint Dip	Map Unit	Dom-ain
CM - 483	GBQPmgw & MBsch	N 55 W	42 NE												ccr	II
CM - 484	MBPQmgw & MBsch	N 11 W	16 NE			32	S 89 E	N 83 W	55 SW	55	0.05-0.07	NE	N 34 W	76 SW	ccr	II
						33	N 78 E	N 46 E	46 SW	90	0.1	NW	N 78 E	73 SW		II
CM - 485	MBsch	N 16 W	61 NE			48	N 79 E	N 7 E	53 SE	30	0.03-0.05	?			ccr	II
CM - 486	BQmgw	N 11 W	36 NE			24	N 83 E	N 25 E	48 SE	25-Iso.	> 9.0		N 45 E	63 SE	ccr	II
		N 43 W	42 NE										N 32 W	75 SW		II
		N 21 E	38 SE													II
		N 25 E	48 SE													II
		N 17 E	52 SE													II
CM - 487	mgw	N 19 W	32 NE												ccr	II
CM - 488	MBsch	N 83 E	38 SE												ccr	II
CM - 489	BQPmgw & MBsch	N 44 E	74 SE												ccr	II
CM - 490	Hgn/amp	N 64 W	40 NE												am-CG	II
CM - 491	BPQmgw	N 86 W	32 NE												ccr	II
CM - 492	mgw	N 43 E	61 SE												ccr	II
CM - 493	MBsch & mgw	N 46 W	39 NE												ccr	II
CM - 494	BQPmgw	N 31 W	34 NE												ccr	I
CM - 495	mgw	N 08 E	23 SE												ccr	I
CM - 496	QPMBsch	N 06 W	47 NE												ccr	I
CM - 497	mgw	N 33 W	46 NE												ccr	I
CM - 498	BQPmgw	N 67 W	43 NE												ccr	I
CM - 499	mgw	N 83 E	43 SE										N 58 W	68 SW	ccr	I
CM - 500	mgw & peg	N 31 E	88 SE												ccr	I
CM - 501	mgw	N 85 E	90												ccr	I
		N 66 E	59 SE													I
CM - 502	mgw	N 43 E	19 NW												ccr	I
CM - 503	mgw	N 56 E	74 NW												ccr	I
CM - 504	mgw	N 14 W	66 NE												ccr	II
CM - 505	mgw	N 78 W	39 NE												ccr	II
CM - 506	mgw & peg	N 12 E	41 SE												ccr	II
CM - 507	GBHPQaug-gn	N 73 w	43 NE												ig	II
CM - 508	aug-gn sap	N 08 E	48 SE												ig	II
CM - 509	Fgn-sap	N 62 W	18 NE										N 26 W	41 SW	Ofg	II
		N 47 W	39 NE										N 27 W	44 SW		II
CM - 510	mgr & Hgn	N 83 W	24 NE										N 24 W	36 NE	hga	II
CM - 511	mgr & Hgn	N 53 W	51 NE												hga	II
CM - 512	PHgn/mga	N 79 W	69 NE												hga	II
CM - 513	Hgn	N 69 E	61 SE												hga	II
CM - 514	Hgn/mga	N 66 W	60 NE												hga	II
CM - 515	Hgn/amp	N 74 W	62 NE										N 52 E	60 NW	hga	II
CM - 516	mga	N 64 E	39 NE										N 38 E	81 SE	hga	II
													N 71 W	82 SW		II
CM - 517	BPQaug-gn & BPQmgw	N 41 E	20 SE										N 11 E	76 NW	ig	II
CM - 518	Fgn	N 45 W	27 NE												Ofg	II
CM - 519	Fgn	N 16 W	36 NE												Ofg	II
CM - 520	Fgn & amp	N 63 W	23 NE												Ofg	II
		N 85 W	42 NE													II
		N 57 E	33 SE													II
		N 78 W	29 NE													II
CM - 521	mga/Hgn	N 55 E	80 SE												hga	II
CM - 522	GMBQPsch	N 61 E	83 SE												mss	II
CM - 523	amp														hga	II
CM - 524	Fgn														hga	II
CM - 525	MBQPmgw/sch	N 52 E	81 SE												mss	II
CM - 526	amp	N 77 W	19 NE												am-GB	II
CM - 527	GBMQPmgw/sch	N 32 E	49 SE	25	N 62 E										mss	II
CM - 528	GBMQPmgw/sch	N 32 E	41 SE												mss	II
CM - 529	MBsch	N 73 E	68 SE												mss	II
CM - 530	MBsch & GMBPQmgw/qtz	N 86 E	18 NW			13	N 66 E	N 79 E	26 NW	140	0.03-0.05	SE	N S	81 W	mss	II
		N 86 W	29 NE										N 29 W	76 SW		II
		N 48 W	22 NE										N 12 E	90		II
													N 74 W	79 SW		II
CM - 531	GBPQmgw/gn & MBsch	N 88 E	21 NW												mss	II
CM - 532	amp	N 72 E	11 SE												am-GB	II
	BQPmgw	N 67 W	21 NE												mss	II
CM - 533	K?GBPQMsch	N 28 E	28 SE												as	II
CM - 534	GMBsch	N 22 W	08 NE												mss	II
CM - 535	QHPgn	N 48 E	79 NW										N 36 W	75 SW	hga	II
CM - 536	QHPgn	N 05 W	36 NE												hga	II
CM - 537	QHPgn	N 43 W	56 NE												hga	II
CM - 538	mgw	N 76 E	52 NW												mss	II
CM - 539	amp	N 36 W	78 NE												am-GB	II
CM - 540	K?GBMsch	N 36 W	14 NE												as	II
CM - 541	BMPQmgw	N 67 W	40 NE												as	II
CM - 542	GH?BQPgn	N 80 W	48 NE												Ofg	II
CM - 543	EBH?QPgn	N 28 W	60 NE												Ofg	II
CM - 544	EBH?QPgn														Ofg	II
CM - 545	Hgn/amp	N 18 E	32 SE												hga	III
CM - 546	Hgn	N 53 W	44 NE												hga	II
CM - 547	Hgn	N 38 E	47 SE												hga	II
CM - 548	MBsch	N 76 E	36 NW												as	III
CM - 549	BQPmgw	N 68 W	48 SW												as	III
CM - 550	amp	N 71 E	73 NW												am-GB	III
CM - 551	mgw	N 68 W	38 NE												as	III
CM - 552	mgw	N 79 W	31 NE												as	III
CM - 553	mgw & MBsch	N 78 W	46 NE												as	III
CM - 554	amp	N 78 E	33 NW												am-GB	III
CM - 555	GPQBMsch & peg	N 21 W	45 NE												mss	III
CM - 556	GMBPQmgw & MBsch	N 49 W	46 NE												mss	III
CM - 557	GQMBsch	N 53 W	57 NE												mss	III
CM - 558	Msch & BQPmgw	N 84 W	44 NE												as	III
CM - 559	BQPmgw	N 62 W	31 NE												mss	III
CM - 560	GMBPQmgw/gn	N 47 W	22 NE										N 43 W	58 SW	mss	III
CM - 561	Bqtz & BPQmgw/sch	N 43 W	26 NE												mss	III
CM - 562	MBQPgn	N 50 W	31 NE												mss	III

Station	Lithology	Foliation Strike	Foliation Dip	Lineation Plunge	Lineation Trend	Fold Axis Plunge	Fold Axis Trend	Axial Surface Strike	Axial Surface Dip	IL Angle	Amp. (m)	Fold Verg.	Joint Strike	Joint Dip	Map Unit	Dom-ain
CM - 563	Asch	N 73 E	21 SE												hb	II
		N 08 W	35 NE													II
CM - 564	GH?BQPgn	N 03 E	25 NW												Ofg	II
CM - 565	amp	N 86 E	24 NW										N 41 E	82 NW	am-GB	II
													N 32 W	76 SW		II
CM - 566	amp	N 76 W	55 NE												am-GB	II
		N 82 E	54 NW													II
CM - 567	GQMsch	N 46 W	51 NE												as	II
CM - 568	GMBQPmgw/sch	N 63 W	36 NE												mss	III
		N 53 W	40 NE													III
CM - 569	GBQPmgw & MBsch	N 25 W	34 NE												mss	III
CM - 570	GBQPmgw & MBsch	N 54 W	58 NE												mss	III
CM - 571	mgw	N 42 W	66 NE												mss	III
CM - 572	mgw	N 30 W	20 NE												mss	III
CM - 573	BAPmgw	N 34 W	38 NE												mss	III
CM - 574	HPgn-sap	N 36 W	48 NE												hga	II
CM - 575	Hgn-sap	N 20 E	64 SE										N 42 W	56 SW	hga	II
		N 88 W	45 SW													II
		N 56 E	65 SE													II
		N 60 E	69 SE													II
		N 81 W	51 SW													II
CM - 576	GMQHBPmyl-gn	N 13 W	68 NE	51	S 86 E								N 27 W	42 SW	Ofg	II
		N 8 W	58 NE													II
CM - 577	GMQHBPmyl-gn sap	N 3 W	36 NE												Ofg	II
		N 54 E	57 SE													II
		N 28 E	57 SE													II
CM - 578	GBQPMmyl-sch	N 09 W	39 NE												Ofg	II
		N 03 E	49 SE													II
CM - 579	GBQPMmyl-sch	N 16 E	51 SE												Ofg	II
CM - 580	GEPHgn	N 28 E	31 SE										N 18 W	69 SW	hga	II
CM - 581	GMH?BPgn	N 85 E	89 SE												Ofg	II
CM - 582	Hgn	N 03 W	49 SW												hga	II
CM - 583	GQBHPgn	N 41 E	71 SE												Ofg	II
		N 27 W	65 NE													II
CM - 584	GBPQMsch	N 62 W	24 NE												as	II
CM - 585	GMBPQmgw					32	N 52 E	N 53 E	81 SE	90	0.05-0.1				as	II
CM - 586	GBMQPmgw & GMCQsch	N 23 E	52 SE			84	N 80 E	N 76 E	71 NW	Iso.	0.08				as	II
		N 31 E	60 SE													II
		N 61 E	48 NW													II
		N 34 E	55 SE													II
		N 72 E	63 SE													II
CM - 587	GMBQPmgw, Bqtz/mgw, &	N 05 E	31 SE										N 38 W	73 NE	as	II
	GCMsch	N 28 W	19 NE													II
		N 32 E	60 SE													II
		N 39 E	64 SE													II
CM - 588	GMsch & mgw	N 61 E	56 SE												as	II
		N 65 E	90													II
CM - 589	amp	N 21 E	61 SE												am-GB	III
		N 16 E	60 SE													III
CM - 590	amp	N 13 E	73 SE												am-GB	III
CM - 591	QHPgn	N 64 W	38 NE										N 48 W	42 SW	Ofg	III
		N 38 W	36 NE													III
CM - 592	GMH?BPQgn &	N 16 E	17 SE												ig	II
	BPQaug-gn w/ zen?															II
CM - 593	GQPHgn	N 39 E	18 SE												ig	II
CM - 594	BPQgn & BPQaug-gn	N 86 E	25 SE										N 59 W	56 NE	ig	II
		N 58 E	25 SE													II
CM - 595	BPQgn & BPQaug-gn	N 28 E	18 SE												ig	II
CM - 596	BHQPgn	N 76 E	23 SE												ig	II
CM - 597	GBH?PQmgw &														ig	II
	BPQaug-gn															II
CM - 598	GBH?PQmgw &	N 73 W	36 SW												ig	II
	BPQaug-gn															II
CM - 599	MH?BQPgn	N 02 W	36 NE												Ofg	II
CM - 600	Fgn	N 09 E	28 SE												Ofg	II
CM - 601	Fgn	N 03 E	41 SE												Ofg	II
CM - 602	Fgn	N 13 W	24 NE												Ofg	II
		N 24 W	22 NE													II
CM - 603	Fgn	N 30 W	31 NE										N 79 W	48 SW	Ofg	II
		N 11 W	36 NE													II
CM - 604	Fgn	N 24 W	32 NE												Ofg	II
		N 06 W	35 NE													II
CM - 605	GMBQPgn	N 13 E	36 SE												Ofg	II
		N 22 E	31 SE													II
CM - 606	Fgn	N 16 W	41 NE												Ofg	II
CM - 607	Hgn														hga	II
CM - 608	Fgn	N 61 E	81 SE										N 28 E	61 SW		II
CM - 609	Fgn	N 27 E	35 SE												Ofg	II
CM - 610	Fgn	N 03 E	20 SE												Ofg	II
CM - 611	GMBQPgn	N 66 E	61 SE												ig	II
CM - 612	amp	N 44 E	31 SE												ig	II
CM - 613	PEHgn	N 28 E	90												hga	II
CM - 614	amp	N 54 W	64 SW												am-GB	II
		N 38 E	10 SE													II
CM - 615	MBPQmgw & MBsch	N 04 W	31 NE			19	N 62 E	N 62 E	90	120	0.3				mss	II
	above amp	N 66 W	18 NE													II
CM - 616	mgw &	N 41 W	28 NE												mss	II
	amp	N 19 W	28 NE												am-GB	II
CM - 617	BPQmgw/qtz	N 00 E	42 SE										N 31 W	62 SW	mss	II
CM - 618	QPHgn	N 10 E	81 NW												hga	II
CM - 619	GPHamp	N 31 E	68 NW												hga	II
CM - 620	GQPHamp	N 05 W	37 NE												hga	II
		N 30 E	20 SE													II
CM - 621	amp	N 44 E	48 NW												hga	II
CM - 622	BQHPmgr	N 58 E	52 SE												hga	II

Station	Lithology	Foliation		Lineation		Fold Axis		Axial Surface		IL	Amp.	Fold	Joint		Map	Dom-
		Strike	Dip	Plunge	Trend	Plunge	Trend	Strike	Dip	Angle	(m)	Verg.	Strike	Dip	Unit	ain
CM - 623	PHgn	N 64 E	66 SE												hga	II
CM - 624	GQPHgn	N 54 W	14 NE												hga	II
CM - 625	peg/veinQ												N 69 W	80 NE	hga	II
													N 13 W	54 SW		II
													N 11 W	46 NE		II
CM - 626	PHgn	N 22 E	82 SE												hga	II
CM - 627	GQPHgn	N 53 E	74 NW												hga	II
CM - 628	GQPHgn	N 62 E	68 SE												hga	II
CM - 629	amp	N 75 E	34 NW												am-GB	III
		N 86 E	33 NW													III
		N 71 E	32 NW													III
CM - 630	amp	N 26 W	59 NE												am-GB	III
CM - 631	BMsch, Bmgw, & amp	N 73 W	39 NE												as	III
CM - 632	QPBMsch & amp	N 61 E	38 NE												as	III
CM - 633	MBsch	N 61 W	38 NE												as	III
CM - 634	MBsch & BPQmgw w/ c-si	N 53 W	46 NE												ccr	III
CM - 635	MPQBsch	N 19 E	48 SE										N 89 E	68 SE	ccr	III
		N 07 E	46 SE													III
CM - 636	BPqtz	N 07 E	78 SE												ccr	III
CM - 637	mgw & sch	N 11 E	61 SE												ccr	III
CM - 638	MBQPmgw & sch	N 07 E	60 SE												ccr	III
CM - 639	MBsch	N 46 W	17 NE												ccr	III
CM - 640	MBQPmgw & sch	N 10 W	31 NE												ccr	III
CM - 641	MBsch & BQPmgw	N 06 E	44 SE												ccr	III
CM - 642	BQPgn	N 31 W	19 NE												ccr	III
CM - 643	BQPgn	N 12 W	54 NE												ccr	III
CM - 644	BQPmgw & MBsch	N 10 E	28 SE												ccr	III
CM - 645	amp	N 16 W	34 NE												am-CG	III
CM - 646	amp	N 46 W	44 NE												am-GB	II
CM - 647	Msch & Bmgw-sap	N 14 W	33 NE												am-GB	II
CM - 648	MBsch & mgw-sap	N 06 W	42 NE												as	II
CM - 649	MBsch & amp	N 23 E	54 SE												as-am	II
CM - 650	amp	N 20 W	35 NE												am-GB	II
CM - 651	amp	N 22 E	38 SE												am-GB	II
CM - 652	MBsch, mgw, & amp	N 50 E	38 SE												as-am	II
CM - 653	BPQmgw	N 37 E	21 SE												ccr	II
CM - 654	mgw/gn	N 59 E	18 NW												ccr	II
CM - 655	mgw/gn	N 29 E	26 SE												ccr	II
CM - 656	mgw/gn	N 28 E	19 SE										N 12 E	71 NW	ccr	II
		N 04 E	19 SE										N 36 W	89 NE		II
CM - 657	mgw/gn	N 08 E	22 SE												ccr	II
CM - 658	mgw/gn	N 53 E	27 SE										N 54 W	79 SW	ccr	II
		N 44 E	26 SE													II
CM - 659	mgw/gn	N 29 E	12 SE												ccr	II
CM - 660	mgw/gn	N 77 E	23 SE												ccr	II
CM - 661	mgw/gn	N 18 E	12 SE												ccr	II
CM - 662	mgw/gn	N 13 E	14 SE												ccr	II
CM - 663	mgw/gn	N 13 W	20 NE												ccr	II
CM - 664	mgw/gn	N 71 E	61 SE												ccr	II
CM - 665	mgw/gn	N 21 W	12 NE												ccr	II
CM - 666	MBQPmgw/gn	N 12 E	18 SE										N 63 E	85 SE	ccr	II
													N 20 E	56 SE		II
CM - 667	MBQPmgw/gn	N 88 W	9 NE												ccr	II
CM - 668	mgw/gn	N 68 W	15 NE										N 53 W	62 SW	ccr	II
		N 82 W	16 NE													II
CM - 669	mgw/gn	N 86 E	37 SE												ccr	II
CM - 670	MBQPmgw/gn	N 56 E	10 SE												ccr	II
CM - 671	mgw/gn	N 05 E	24 SE												ccr	II
CM - 672	mgw/gn	N 15 W	24 NE												ccr	II
CM - 673	BPQmgw	N 53 E	25 SE												ccr	II
CM - 674	BPQmgw/qtz	N 48 E	27 SE												ccr	II
CM - 675	BPQmgw/qtz	N 43 E	14 SE												ccr	II
CM - 676	BPQmgw/qtz	N 48 E	22 SE										N 17 W	76 NE	ccr	II
		N 12 W	33 NE													II
CM - 677	mgw/gn	N 12 W	13 NE												ccr	II
CM - 678	BPQmgw/qtz	N 13 E	13 SE												ccr	II
		N 21 W	33 NE													II
CM - 679	BPQmgw/qtz	N 56 W	28 NE												ccr	II
		N 26 W	40 NE													II
		N 16 W	31 NE													II
CM - 680	mgw/gn	N 33 W	25 NE												ccr	II
CM - 681	BPQmgw/qtz	N 62 W	25 NE												ccr	II
CM - 682	BPQmgw/qtz	N 51 E	21 SE												ccr	II
CM - 683	mgw/gn	N 71 W	12 NE												ccr	II
CM - 684	mgw/gn	N 03 E	19 SE												ccr	II
CM - 685	mgw/gn	N 61 E	25 SE												ccr	II
CM - 686	mgw/gn	N 06 W	26 NE												ccr	II
CM - 687	mgw/gn	N 48 W	34 NE												ccr	II
CM - 688	mgw/gn	N 31 W	28 NE												ccr	II
CM - 689	mgw/gn	N 16 E	18 SE												ccr	II
CM - 690	mgw/gn	N 02 E	47 SE										N 50 W	68 SW	ccr	II
CM - 691	mgw/gn	N 74 E	38 SE												ccr	II
CM - 692	mgw & MBsch	N 14 W	28 NE												Zgs	IV
CM - 693	mgw & sch	N 63 W	19 NE												Zgs	IV
CM - 694	MBsch & mgw-sap	N 38 E	31 SE												mss	IV
CM - 695	mgw-sap	N 03 W	34 NE												mss	IV
CM - 696	MBsch & BQPmgw	N 07 E	29 SE												mss	IV
CM - 697	mgw & MBsch	N 36 W	27 NE												mss	IV
CM - 698	Qpeg & K?GMsch	N 63 W	35 SW												as	IV
		N 03 E	12 NW													IV
CM - 699	K?QBMsch	N 73 W	13 NE												as	IV
CM - 700	K?QBMsch	N 36 W	56 NE												as	IV
CM - 701	aug-gn, Hgn, & Bgn	N 67 W	73 SW												ig	II
CM-701.5	BPQmgw	N 18 W	29 SW												mss	IV
CM - 702	BPQmgw & MBsch	N 24 W	14 SW												mss	IV

Station	Lithology	Foliation		Lineation		Fold Axis		Axial Surface		IL Angle	Amp. (m)	Fold Verg.	Joint		Map Unit	Dom-ain
		Strike	Dip	Plunge	Trend	Plunge	Trend	Strike	Dip				Strike	Dip		
CM - 703	BPQmgw & MBsch	N 31 E	16 SE												mss	IV
CM - 704	mgw/qtz	N 12 E	26 SE												mss	IV
CM - 705	BPQmgw	N 22 E	27 SE												mss	IV
CM - 706	amp	N 24 W	28 NE												am-GB	IV
		N 08 W	44 NE													IV
CM - 707	mgw	N 36 W	37 NE												mss	IV
		N 44 W	40 SW													IV
CM - 708	amp	N 28 W	46 NE												am-GB	IV
CM - 709	amp & veinQ	N 19 W	54 NE												am-GB	IV
CM - 710	mgw	N 54 W	17 NE										N 32 W	73 SW	mss	IV
		N 24 W	08 NE													IV
CM - 711	mgw	N 18 W	31 NE												mss	IV
CM - 712	mgw	N 06 E	39 SE												mss	IV
CM - 713	QBMsch	N 07 W	38 NE												as	IV
CM - 714	mgw & BMsch	N 03 E	31 SE												as	IV
CM - 715	mgw	N 28 W	18 NE										N 11 W	77 SW	mss	IV
CM - 716	mgw	N 59 W	6 NE												mss	IV
CM - 717	mgw	N 33 W	22 NE												mss	IV
CM - 718	mgw-sap & BMsch	N 48 W	16 NE												as	IV
CM - 719	mgw	N 57 W	39 NE												mss	IV
CM - 720	Bmgw/qtz	N 22 E	43 NW												mss	IV
CM - 721	mgw	N 49 W	22 NE												mss	IV
CM - 722	PQMBsch	N 09 W	29 NE												mss	IV
CM - 723	amp/Hgn	N 49 E	69 SE												am-GB	II
CM - 724	GKMsch w/ c-si	N 73 W	63 NE												as	II
CM - 725	GKMsch	N 03 E	54 NW												as	II
CM - 726	mgw	N 58 W	41 NE												ccr	II
CM - 727	mgw	N 53 W	48 NE												ccr	II
CM - 728	MBsch & mgw	N 74 W	59 NE												ccr	II
CM - 729	mgw	N 53 W	24 NE												ccr	II
CM - 730	mafic-sap	N 64 E	52 SE												am-GB	II
CM - 731	Msch & mgw-sap	N 49 W	53 NE												as	IV
CM - 732	Msch & mgw-sap	N 22 E	22 SE												as	IV
		N 44 W	26 NE													IV
		N 64 W	21 NE													IV
CM - 733	Msch & mgw-sap	N 29 W	24 NE												as	IV
CM - 734	Msch & mgw-sap	N 08 W	26 NE												as	IV
CM - 735	GBMsch & mgw-sap	N 48 W	18 NE												as	IV
		N 00 E	15 SE													IV
CM - 736	GBMsch & mgw-sap	N 28 W	33 NE												as	IV
CM - 737	GBMsch & mgw-sap	N 54 E	38 NW												as	IV
CM - 738	GBMsch & mgw-sap	N 62 W	36 NE												as	IV
CM - 739	PQBMsch & MBsch	N 54 W	54 NE												as	IV
CM - 740	PQBMsch & MBsch	N 51 W	44 NE												as	IV
CM - 741	K?GQBMsch	N 49 W	39 NE												as	IV
CM - 742	KGPQBMsch	N 36 W	44 NE										N 45 W	37 SW	as	IV
CM - 743	sch	N 56 W	34 NE												as	IV
CM - 744	Hgn & MBsch	N 52 W	46 NE												as/am-GB	IV
CM - 745	BMsch & mgw-sap	N 69 W	54 NE												as	IV
CM - 746	MBsch & BQmgw/qtz	N 56 W	47 NE												as	IV
	Hgn float	N 87 W	33 NE													IV
		N 65 W	47 NE													IV
CM - 747	MBsch & BQmgw/qtz	N 23 W	34 NE												as	IV
CM - 748	GPBMsch, mgw, & Hgn	N 48 W	49 NE												as/am-GB	IV
CM - 749	GPBMsch & mgw	N 70 W	39 NE												as	IV
CM - 750	MBQPgn	N 62 W	40 NE												as	IV
		N 54 W	28 NE													IV
CM - 751	MBQPgn	N 34 W	29 NE												as	IV
CM - 752	MBsch	N 53 W	22 NE												mss	IV
CM - 753	MBsch & mgw	N 81 W	28 NE												mss	IV
CM - 754	MBQPgn	N 14 W	43 NE												mss	IV
CM - 755	K?GPQBMsch & Bmgw	N 22 W	40 NE												as	IV
CM - 756	PQBmgw	N 43 W	24 NE												mss	IV
CM - 757	PQBmgw	N 31 w	51 NE												mss	IV
CM - 758	PQBmgw	N 48 W	24 NE												mss	IV
CM - 759	mgw	N 53 W	35 NE												mss	IV
CM - 760	mgw	N 66 W	8 NE										N 29 W	62 SW	mss	IV
CM - 761	mgw	N 62 W	23 NE										N 36 W	64 SW	mss	IV
CM - 762	mgw	N 83 E	26 NW										N 45 E	65 SE	mss	IV
CM - 763	mgw	N 44 W	22 NE												mss	IV
CM - 764	mgw	N 56 W	34 NE												mss	IV
CM - 765	mgw	N 36 W	22 NE												mss	IV
CM - 766	BPQmgw & MBsch	N 00 E	18 SE												Zgs	IV
CM - 767	BPQmgw	N 36 W	34 NE												Zgs	IV
		N 37 w	28 NE												Zgs	IV
CM - 768	mgw	N 32 W	18 NE												Zgs	IV
CM - 769	BPQmgw & BQPmgw	N 65 W	31 NE												Zgs	IV
CM - 770	BPQmgw	N 74 W	26 NE												Zgs	IV
CM - 771	MBPQmgw & MBsch	N 71 W	21 NE												Zgs	IV
CM - 772	BPQmgw	N 38 E	24 NE												Zgs	IV
CM - 773	BPQmgw	N 26 W	39 NE												Zgs	IV
CM - 774	BPQmgw	N 32 W	25 NE												Zgs	IV
CM - 775	M?BPQmgw	N 83 E	31 NW												Zgs	IV
CM - 776	MBPQmgw	N 68 W	52 NE												Zgs	IV
CM - 777	mgw	N 83 W	33 NE												Zgs	IV
CM - 778	mgw	N 68 W	25 NE												Zgs	IV
CM - 779	mgw	N 48 W	33 NE												Zgs	IV
CM - 780	mgw	N 22 W	22 NE												Zgs	IV
CM - 781	mgw	N 49 W	16 NE												Zgs	IV
CM - 782	MBsch & mgw	N 57 W	18 NE												Zgs	IV
CM - 783	MBsch & mgw	N 38 W	48 NE												Zgs	IV
CM - 784	MBsch	N 57 W	49 NE												Zgs	IV
CM - 785	MBQPmgw/gn	N 43 W	21 NE												Zgs	IV
CM - 786	MBQPmgw/gn	N 36 E	18 NW												Zgs	IV
CM - 787	mgw-sap	N 10 W	23 NE												Zgs	IV

Station	Lithology	Foliation		Lineation		Fold Axis		Axial Surface		IL	Amp.	Fold	Joint		Map	Dom-
		Strike	Dip	Plunge	Trend	Plunge	Trend	Strike	Dip	Angle	(m)	Verg.	Strike	Dip	Unit	ain
CM - 788	mgw-sap	N 11 E	29 NW												Zgs	IV
CM - 789	mgw & MBsch	N 39 W	41 NE												Zgs	IV
CM - 790	BPQmgw	N 86 E	37 NW												Zgs	IV
CM - 791	MBsch & mgw-sap	N 49 W	32 NE												Zgs	IV
CM - 792	BMsch	N 82 W	30 NE												Zgs	IV
CM - 793	MBsch & mgw-sap	N 53 W	43 NE												Zgs	IV
CM - 794	MBsch & mgw-sap	N 73 W	19 NE												Zgs	IV
CM - 795	MB/BMsch	N 26 W	37 NE												Zgs	IV
CM - 796	MBQPmgw	N 31 W	10 NE												Zgs	IV
CM - 797	BMsch & gmw	N 57 W	49 NE												Zgs	IV
CM - 798	BMsch & gmw	N 46 W	18 NE												Zgs	IV
CM - 799	BMsch & MBQPmgw	N 59 W	36 NE												Zgs	IV
CM - 800	MBsch & mgw-sap	N 18 W	23 NE												Zgs	IV
CM - 801	GPQBMsch	N 25 W	34 NE												Zgs	IV
CM - 802	MBsch & MBPQmgw	N 61 W	39 NE												Zgs	IV
CM - 803	BMsch	N 62 W	33 NE												Zgs	IV
CM - 804	MBPQmgw	N 76 W	42 NE												Zgs	IV
CM - 805	BMsch	N 86 W	42 NE												Zgs	IV
CM - 806	BMsch	N 03 E	33 SE												Zgs	IV
CM - 807	BMsch & mgw	N 11 E	26 SE												mss	IV
CM - 808	BMsch & mgw-sap	N 34 W	28 NE												Zgs	IV
CM - 809	BMsch & mgw-sap	N 14 W	38 NE												Zgs	IV
CM - 810	BPQmgw & BMsch	N 58 W	18 NE												Zgs	IV
CM - 811	mgw & MBsch	N 48 W	41 NE												Zgs	IV
		N 37 W	33 NE													IV
CM - 812	MBsch	N 86 W	18 NE												Zgs	IV
CM - 813	MBsch w/ c-si	N 32 W	28 NE												Zgs	IV
CM - 814	BPQmgw	N 53 W	18 NE												Zgs	IV
CM - 815	mgw	N 59 W	32 NE												Zgs	IV
CM - 816	mgw	N 88 e	31 NW												Zgs	IV
CM - 817	mgw	N 86 W	14 NE												Zgs	IV
CM - 818	mgw	N 88 E	10 NW												Zgs	IV
CM - 819	mgw	N 22 W	28 NE												Zgs	IV
CM - 820	MBsch & mgw	N 48 E	18 SE												ccr	IV
CM - 821	K?GPQMsch	N 74 W	24 NE												as	II
CM - 822	K?GPQMsch	N 53 E	23 SE												as	II
CM - 823	K?GPQMsch	N 76 E	41 SE												as	II
CM - 824	K?GPQMsch	N 26 E	09 SE												as	II
CM - 825	MBsch & Hgn	N 52 W	39 NE												as/am-GB	II
CM - 826	mgw	N 84 E	36 SE												ccr	II
CM - 827	mgw	N 64 E	24 SE												ccr	II
CM - 828	mgw					11	N 88 E	N 88 E	90	120	1.5-3.0	?			ccr	II
CM - 829	mgw	N 43 E	23 SE												ccr	II
CM - 830	mgw	N 56 E	18 SE												ccr	II
CM - 831	mgw & MBsch	N 66 E	31 SE												ccr	II
CM - 832	mgw	N 51 E	28 SE												ccr	II
CM - 833	mgw	N 65 E	41 SE												ccr	II
CM - 834	BMsch & amp	N 62 E	16 SE												as/am-GB	II
CM - 835	amp	N 12 E	40 SE												am-GB	II
CM - 836	MBsch	N 17 E	23 SE												as	II
CM - 837	K?GBMsch	N 81 E	28 SE												as	II
CM - 838	BPQmgw/qtz, Hgn, &	N 85 W	53 NE												mss	II
	GPQCMsch/MBsch															II
CM - 839	GMBPgn & MBsch	N 86 W	15 SE												mss	II
CM - 840	amp/Hgn	N 88 E	15 SE										N 86 W	15 SE	am-GB	II
CM - 841	GMBPgn & MBsch	N 88 E	41 SE												mss	II
CM - 842	GBMPQgn & MBsch	N 46 W	56 SW												mss	II
CM - 843	GBMPQgn & MBsch	N 86 E	46 SE												mss	II
CM - 844	GBMPQgn & MBsch	N 84 E	36 SE												mss	II
CM - 845	amp	N 16 W	50 NE												am-GB	II
CM - 846	BMsch	N 06 W	42 NE												as	IV
CM - 847	BMsch	N 19 E	17 SE												as	II
CM - 848	mgw & sch	N 16 W	18 NE												as	II
		N 35 W	33 NE													II
CM - 849	mgw & sch	N 42 W	14 NE												as	II
CM - 850	GBMPQgn & MBsch	N 14 W	34 NE												as	II
CM - 851	BMsch, mgw-sap, & amp	N 34 W	12 NE												as/am-GB	II
CM - 852	BMsch, mgw-sap, & amp	N 56 W	59 NE												as/am-GB	II
CM - 853	BMsch & amp	N 38 W	52 NE												as/am-GB	II
CM - 854	BMsch & amp	N 38 W	52 NE												as/am-GB	II
CM - 855	MBsch & mgw-sap	N 46 W	54 NE												Zgs	IV
CM - 856	MBsch & mgw-sap	N 34 w	24 NE												Zgs	IV
CM - 857	MBsch w/ c-si	N 39 W	31 NE												Zgs	IV
CM - 858	PHgn	N 87 W	65 NE												hga	II

APPENDIX B-3

Structural and rock type data for the Dahlonega duadrangle

Note: Stations correspond to locations within the Campbell Mountain quadrangle presented on Plate II: Station numbers, sample locations, and structural domains within portions of the Nimblewill, Campbell Mountain, and Dahlonega, Georgia 7.5-minute quadrangles.

ABBREVIATIONS:

Note: Lithology indicated by lower case lettering and minerals indicated by UPPER case lettering.

Lithologies

- amp - amphibolite
- c-si - calc-silicate
- gn - gneiss
- hgn - hornblende gneiss
- mgr - metagabbro
- mgw - metagraywacke
- peg - pegmatite
- qtz - quartzite
- sch - schist

Other

- aug - augen
- bd - boudin
- blk - black
- Iso - isoclinal
- myl - mylonitic
- sap - saprolite
- zen - zenolith

Minerals

- B - biotite
- C - chlorite
- E - epidote
- F - feldspar
- G - garnet
- H - hornblende
- K - kyanite
- M - muscovite
- P - plagioclase
- S - sillimanite

Map Unit

- Zgs - Great Smoky Group

- CG - Coweeta Group
- ccr - Coleman River Formation

- GB - Gold Belt
- am - amphibolite
- as - aluminous schist
- hb - hornblendite
- hg - Hornblende gneiss
- hga - hornblende gneiss, metagabbro, & amphibolite
- mss - metasandstone and schist
- Ofg - felsic gneiss
- qms - quartzite, metasandstone, & schist
- ig - intermediate gneiss

		Foliation		Lineation		Fold Axis		Axial Surface		IL	Amp.	Fold	Joint		Map	Dom-
Station	Lithology	Strike	Dip	Plunge	Trend	Plunge	Trend	Strike	Dip	Angle	(m)	Verg.	Strike	Dip	Unit	ain
DG - 1	amp	N 86 W	53 NE												am-GB	III
DG - 2	amp	N 55 W	42 NE												am-GB	III
DG - 3	amp	N 40 W	39 NE										N 47 W	59 SW	am-GB	III
DG - 4	amp	N 34 E	46 SE												am-GB	III
DG - 5	amp	N 65 W	20 NE										N 17 W	67 SW	am-GB	III
													N 85 E	79 SE		III
DG - 6	amp	N 78 W	74 NE												am-GB	III
DG - 7	Msch & QPMmgw	N 07 W	34 NE												qms	III
		N 14 E	46 SE													III
DG - 8	Msch & amp	N 80 E	37 NW												qms/am-GB	NA
DG - 9	MBQPmgw & BMsch	N 68 W	57 NE													NA
DG - 10	BMPQmgw/qtz	N 24 E	62 SE												qms	III
DG - 11																NA
DG - 12																NA

VITA

David Jonathan Settles was born and raised in Albany, Georgia, where he spent the majority of his youth. Many summer weeks and weekends throughout the year around were spent at his grandparents home in Edison, Georgia, (a small farming town west of Albany) where he began his love for rocks by collecting druse quartz, also known as "Sugar Rock", with his grandfather Archie Coleman (deceased). Moving to Carrollton, Georgia, in 1987, David attended Carrollton High School, where he performed as a percussionist in the marching band. After graduating from Carrollton High School in 1992, David continued his love for music and marched for the State University of West Georgia, the Atlanta Olympic Band, and Escape Percussion. While pursuing recreational interests at West Georgia, David remained undecided about career direction for two years. Upon the realization that percussion would not pay the bills, David began soul searching for a major and career. With a general interest in rocks and the outdoors, David took Geology 101 in 1995 at which point he put down his drum sticks and picked up a rock hammer to begin his career in geology. Upon the completion of his bachelor's degree in geology from the State University of West Georgia, David worked as a geotechnical consultant in Atlanta, Georgia. David returned to graduate school at the University of Tennessee–Knoxville (UTK) in the Fall of 1998 to continue learning and gaining more experience in field geology. After struggling through his first fall semester at UTK, David began his research in the beautiful north Georgia mountains near Dahlonega, Georgia, under the supervision of his advisor and friend Bob Hatcher. For three years David has devoted the majority of his time and effort to his research and has provided new information and ideas concerning the tectonic setting and evolution of the north Georgia central Blue Ridge via structural, stratigraphic, and geochemical studies. David received his Master's degree in geology from the University of Tennessee in December, 2001.